UTM
UNIVERSITI TEKNOLOGI MALAYSIA
Faculty of
Electrical Engineering

Proceedings of 2017 Electrical Engineering Symposium (EES2017) - Vol. 1

PROCEEDINGS OF 2017 ELECTRICAL ENGINEERING SYMPOSIUM (EES2017)

VOLUME 1

First Edition 2017

Diterbitkan oleh: Fakulti Kejuruteraan Elektrik, Universiti Teknologi Malaysia, 81310 Johor Bahru Johor, Malaysia

PREFACE

This book introduces several research works from final year undergraduate project till the level of master project by taught course. The projects have been evaluated by industries as well as academician to ensure that its fulfill the standard of each level before it can be published. The text emphasizes the combination of the research material in different field of engineering generally in power, electronic, communication, control and mechatronic which hampered by three main program offered by Faculty of Electrical Engineering.

This book is generally suitable as an accompaniment to students and researchers that generally involved with different field of study including modeling and control design for various example of application. There are also research on hardware design implementation which integrate both for simulation and experimental study as well as laboratory sessions available at a particular institution.

Mohamad Kamal A. Rahim
Md. Pauzi Abdullah
Faculty of Electrical Engineering
Universiti Teknologi Malaysia

2017 ELECTRICAL ENGINEERING SYMPOSIUM COMMITTEE

GENERAL CHAIR

PROFESSOR DR. MOHAMAD KAMAL A. RAHIM

CO-CHAIR

IR. DR. MD. PAUZI ABDULLAH

2017 ELECTRICAL ENGINEERING SYMPOSIUM MEMBERS

DR. KAMALUDIN MOHD. YUSOF

DR. SHAHARIN FADZLI ABD. RAHMAN

DR. YUSMEERAZ YUSOF

DR. MOHD. HAFIZI AHMAD

DR. NURUL EZAILA ALIAS

DR. ZULKARNAIN AHMAD NOORDEN

DR. MOHD. AFZAN OTHMAN

DR. MOHD. AMRI MD. YUNUS

DR. MOHD. RASHIDI SALIM

2017 ELECTRICAL ENGINEERING SYMPOSIUM SECRETARIAT STAFF

SABRINA ZAINAL ABIDIN

AZLINA MOHD. LAZIM

Solar Powered Fertigation System

Nabilah Afiah binti Mohd Isa, Salinda Buyamin*
Faculty of Electrical Engineering
Universiti Teknologi Malaysia
Johor Bahru, Malaysia.
nabilah_isa@yahoo.com, *salinda@utm.my**

Norzanah Rosmin, Mohamad Shukri Zainal Abidin
Faculty of Electrical Engineering
Universiti Teknologi Malaysia
Johor Bahru, Malaysia.
norzanah@utm.my, *shukri@utm.my*

***Abstract*— This paper proposes a solar powered system that could be installed in a conventional fertigation plant. The main objectives of this proposed system is to manage the amount of plants watering by benefitting the free source of solar energy from the sun, besides increasing the plants yield. To be a reliable system, two batteries (Sealed Lead Acid, 12V, 7.2Ah) were used to store the solar energy and then used as the battery backup for the later use. The energy management algorithm of this system is controlled using an Arduino Mega circuit, equipped with a data logging shield for the data recording purpose. As the results of the experimental study, it was found that during sunny day, battery can be charged up to 75% in eight hours, when one PV panel (12V, 20W) was used. It was also shown that the proposed system can be operated successfully. As an implication, a low-cost and reliable solar powered system for fertigation plant was successfully developed and operated automatically.**

Keywords— Solar powered; solar energy; fertigation; photovoltaic (PV); battery backup; Arduino.

I. INTRODUCTION

Solar energy from the sun is a free power source, clean-green renewable energy (RE), high reliability, low maintenance and has long life span [1-2]. Our country, Malaysia is situated at the equatorial region and receives an average of solar radiation between 400-600 MJ/m2 per month. Fig. 1 shows the average solar radiation zones in Malaysia. Due to this, the usage of photovoltaic (PV) in generating electricity is quite efficient. In addition, Malaysia has a constant weather condition throughout the year (hot and wet) [1]. PV panel uses an ultraviolet from sunlight to generate electricity [3]. In PV panel, semiconductor materials are installed to enable the electricity conductivity, reliable to generate input voltage, and therefore, able to control the current flow through its natural electronic process [1][3,4]. There are various types of PV that widely used in the market such as monocrystalline silicon, polycrystalline silicon, thick-film silicon and amorphous silicon. Since PV markets are growing rapidly nowadays, the PV usage is economically viable as the cost of the PV panels keep reducing from year to year [2].

Since Malaysia has hot and wet climate throughout the year, agricultural has becomes one of the popular activities that promising incomes to its population. Through agricultures in our own lands, foods and raw materials can be supplied easier, cheaper and faster. Demands on these items become increasing with increment of population. Hence, nowadays, traditional agriculture becomes not really practical for massive productions. Presently, there are numerous agronomic plants are operated automatically using diesel generator, either by individual installation or utility company. However, since solar PV which offering free energy resources constantly almost every day along the year, it is becomes more popular nowadays due to its less-cost solution.

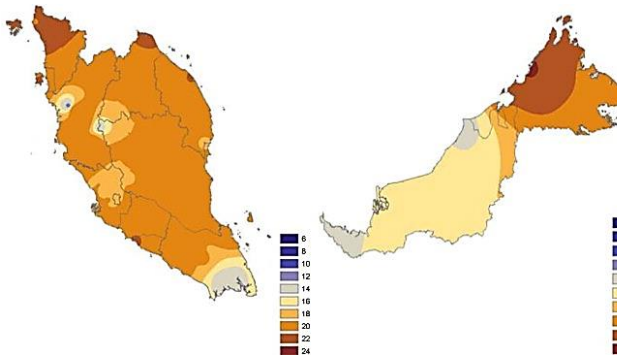

Fig. 1 Average Solar Radiation in Malaysia [1]

For the more productive yields and labours, most farmers prefer to plant their crops using fertigation approach. Fertigation system is one of a good alternative which could replace the traditional agriculture as it could reduce the wastage of water during the watering activity by monitoring the moisture of the soil. The word "fertigation" is actually comes from the combination words of 'fertilizer' and 'irrigation' [5]. This approach mixes the water and fertilizer in one container and then the liquid mixture will be watered to the crops in several periodic times and amount that has been set, appropriate to the type of the planted crops.

The objective of this paper is to propose a solar powered system for agriculture purpose. In this study, rock melon was used as the plant crop. In section I, an introduction and some works in this area has been presented. In section II, the proposed system will be demonstrated before the research method is explained in section III. The experimental results and research conclusion will be given in section IV and V, respectively.

II. SOLAR POWERED FERTIGATION SYSTEM

Typical solar powered system for fertigation plant is

shown in Fig. 2.

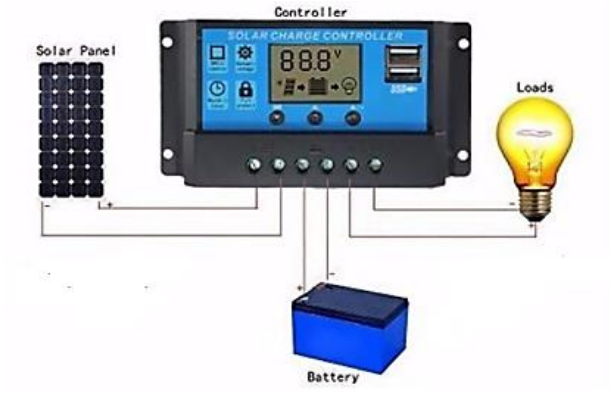

Fig. 2. Schematic diagram of typical solar powered system

Based on Fig.2., this project proposed the usage of battery-coupled system where the battery is connected to solar panel. Battery is used to store energy gained from solar panel. The presence of battery helps to avoid the wastage of energy. Solar charge controller is connected between solar panel and battery to avoid from overcharging or undercharging of battery.

III. METHODOLOGY

A. Proposed system

Fig. 3 demonstrates the diagram of the proposed solar powered system for rock melon fertigation plant in this study.

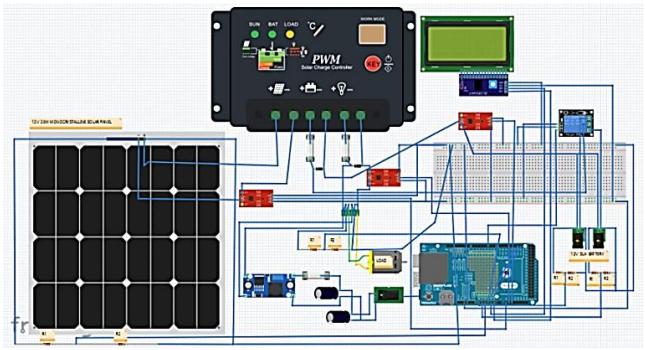

Fig. 3. Schematic diagram of proposed solar powered system

Based on Fig.3., the proposed system used an amount of two batteries as compared to typical system. Both batteries take turns to operate and connected via relay. The reason for the usage of two batteries is to improve the longevity of energy supplied to the load as low amount of solar radiation received by solar panel. One of the battery which connected to the system is operated as a backup battery when the operating battery is experiencing the loss of energy. This method is reliable to create a continuous supply to the load.

B. Main Components

There are four main components that must be identified and sized for the proposed solar powered fertigation plant system; solar PV panel, battery charger and its controller, and solar battery.

1. Solar PV panel

Electricity is produced by an extreme nuclear activity located at the center of the sun. This process generates an energetic particle called photons when a huge amount of solar radiation is produced [3][6]. Fig. 4 shows the process occurs on the surface of crystalline silicon solar cell before electricity is generated [3]. Electricity is generated in solar energy by using photovoltaic effect [6]. Solar panel (silicon) is made up of semiconductor material which able to conduct electricity and control current under certain conditions. Normally, the specification of semiconductor material is dependent on the amount of impurities added to it [4].

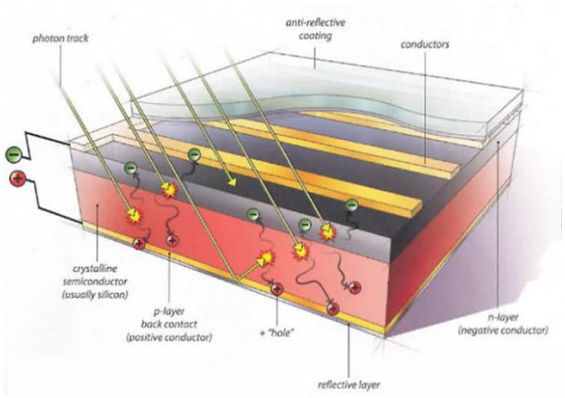

Fig. 4 Process occurs on the surface of crystalline silicon solar cell

To select an appropriate type of solar PV panel, it is necessary to consider these two items: calculation of average daily power consumption and capacity of battery. To estimate the average daily power consumption, the total energy consumption that absorbed by the loads must be calculated. List all the loads considered, list the power rating for each respective loads, and then, multiply the power rating for each load with the total hour used, before summed up all the energy consumed. To estimate the number of PV panel required, multiply the power rating of the PV panel with the number of hours of sunlight received by solar panel [7]. The size of PV panel however, should be larger than the average daily power consumption. For battery size, the system voltage must be identified first. Typically, system voltage is set to 12V or 24V. It also depends on how many slots/arrays that required by the loads. Battery is typically evaluated by Amp-hour (Ah) and its charging capability. Batteries have their own charging capacity. For instance, SLA or AGM batteries charging current are typically limited to 20% of the rated capacity. For instance, 12 Ah batteries cannot receive charge higher than 2.4A.

The solar PV used in this study is monocrystalline type (12V, 20W, with 1.14A rated current), while the battery used is from the SLA type (12V 7.2 Ah). The number of solar panel should be chosen based on the amount of charge can be

stored by the chosen battery in order to avoid a waste of energy [7].

2. Battery charger and its controller

Solar charger and its controller play an important role in monitoring and controlling the charging process of the solar battery. It helps to limit the amount of charge or current entering and leaving the battery. The function of charger controller is vital to block the reverse current and protect the battery from overcharged situations, besides avoiding the drainage problem. Battery is known as very sensitive and needs to be well maintained to retain its performance and life span. In battery charger, there is a regulator. Regulator has a function to stop the charging process when the battery voltage exceeded its maximum level. When battery supplies current to the loads, the regulator will be triggered when reached at a preset low-voltage and thus allows the charging process to be continued again [8][9][10].

In order to maintain the performance of battery, a suitable solar charger must be chosen. The consideration for choosing the suitable battery charger is calculating the controller array current and controller load current. Controller array current can be estimated using Eq (1) [10].

$$A\_SCC = M\_SCC \; x \; Mod\_parallel \; x \; SF \qquad \text{Eq (1)}$$

where A_SCC is the array short circuit current, M_SCC is the module short circuit current, Mod_parallel is modules in parallel and SF is safety factor, and assumed as 1.25 for this study. For this study, for a 20W solar panel, it has a short circuit current of 1.27A. Hence, the minimum value of the battery charger is 1.27 A x 1 x 1.25 = 1.6 A.

To calculate the controller load current, Eq (2) can be used [10].

$$Max\ Load\ Current = \frac{Total\ Connected\ Watts}{System\ Voltage} \qquad \text{Eq (2)}$$

For this study, the load connected to the PV panel is 20W and the system DC voltage is 12V. Hence, the controller load current is 20W/12V = 1.67A. Thus, 1.67 A is the minimum value of charge controller output current. This output current is pulled from the batteries through solar battery charger controller.

3. Battery

Two solar batteries used in this study are from the type of Sealed Lead Acid, 12V system voltage with battery capacity of 7.2Ah.

C. Logging parameter

For the data logging purpose, data logging shield with Real Time Clock (RTC) is used. Data logging is important to store the collected data and also to observe the functionality of the developed solar powered system. Some modification has been done in the logging shield before attaching the logging shield to the Arduino Mega by connecting pin A4 and pin A5, to pin 20 and pin 21, respectively. The attached SD Card also needs to be formatted to FAT32 into the SD card slot. The voltage sensing circuit was developed using a voltage divider where a resistor (R2) is connected to an analogue input and the Ground of Arduino Mega. The voltage divider concept is used to minimise the value of the voltage entering the Arduino pin to 5V. The circuit of this data logging is as depicted in Fig. 5.

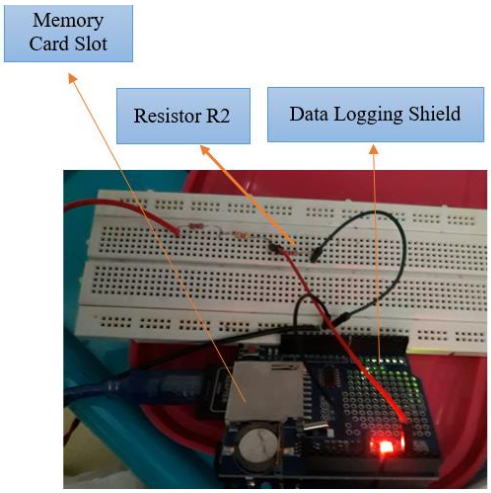

Fig. 5 Data Logging Circuit

The Arduino meter is created by using a voltage divider circuit, ACS 712 and LCD monitoring display. Arduino meter is developed to display the data parameters that read from the PV panel, batteries, and load. A current sensor (ACS712) is used to read the value of the current. Current sensor is also connected to the Analog pin of the Arduino. ACS712 has a limitation of high sensitivity to the magnetic field. Thus, it is quite difficult to achieve a stable and precise output reading of the current. For quality data collection and reading, the ACS712 needs to be calibrated by using Arduino. Then, the parameters gained from the Arduino meter (voltage sensing circuit and current sensors) can be projected on LCD display. In order to minimize the pin used on the Arduino circuit, an I2C LCD display module is used. The I2C LCD display is communicating through SCA (Arduino Mega pin 20) and SCL (Arduino Mega pin 21).

D. Circuit protection

In order to create a smooth changeover between two SLA batteries, a relay is used. The positive polarity of the battery is connected to the Normally Open (NO) point and another battery is connected to the Normally Closed (NC) points of the installed relay. Fig. 6 shows the circuit for the protection purpose. The circuit consists of a fuse that connected in series with the load. Meanwhile, a Zener diode is connected in parallel with the load to protect the circuit from overcurrent, overvoltage and reverse current problems.

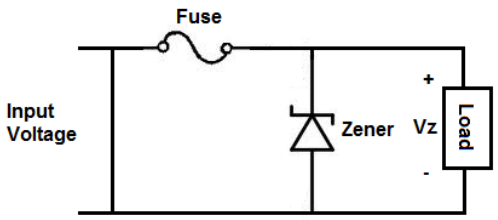

Fig. 6 Protection Circuit

E. Charging Algorithm

Since two batteries are used in this proposed system, there must be a specific rule to must be set to enabling an automatic charging and energy storing to be done systematically in such batteries. Fig. 7 shows the flow on how batteries are managed. To control the algorithm, Arduino IDE was used to program the Arduino Mega circuit. Arduino Mega is used for the purpose of controlling the voltage sensing circuit (voltage divider), the Hall Effect current sensor (ACS712), data logging shield (Adafruit), LCD display (20x4) and the process of changeover (relay).

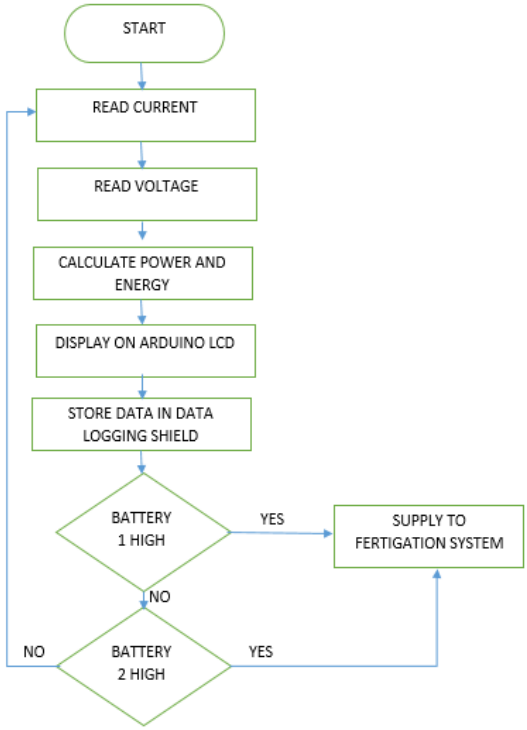

Fig. 7 Project Flow Chart

To make decision which battery should be firstly and secondly charged, program will read the current value first. Then, voltage value will be read, before calculating the power and energy used for every 10 minutes. These parameters then will be displayed on the Arduino LCD display. In the same time, data parameters will be stored in the data logging shield. Decision will be made then, by performing logic rules. If battery-1 is in HIGH state, energy will be supplied to the fertigation plant system. During this time, battery will operate as a source. Solar PV will charge the battery until reaches at least the minimum setting value before switching to the second SLA battery. This switching process is called as 'changeover'. The concept of changeover process is quite similar to the uninterruptable power supply (UPS) system, where the supply will be transferred to the backup supply when main power supply is interrupted. Next, flow will go to the next logic, where if battery-2 is in HIGH condition, energy will be supplied to the fertigation plant system. Otherwise, program will be repeated again, reading the current data and works continuously.

IV. RESULTS

In Fig. 8 and Fig. 9, the voltage signals of the PV panel that was recorded in two days are exhibited. The collected data was stored using the data logging shield that was connected to Arduino circuit and the voltage sensing circuit. The Arduino is programmed to log the voltage data that was setting to be stored for every 10 minutes in 48 hours, continuously.

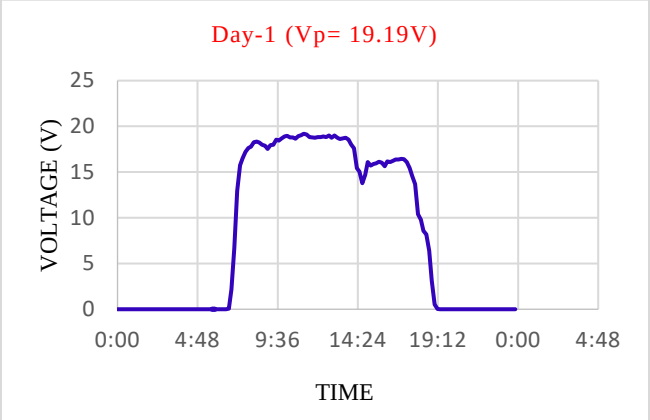

Fig. 8 PV voltage signal (Day-1)

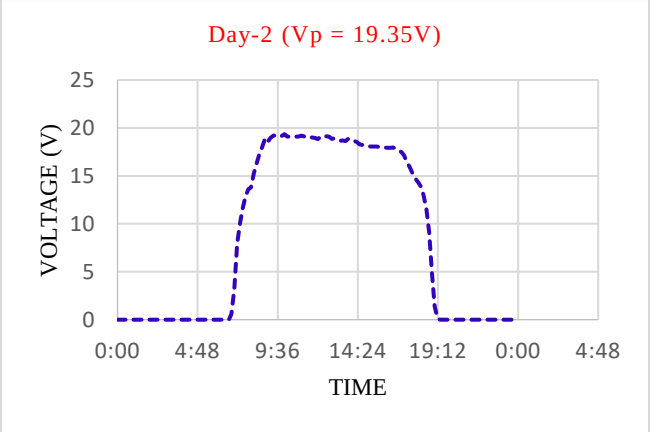

Fig. 9 PV voltage signal (Day-2)

As shown in these Fig. 8 and Fig. 9, it can be seen that the voltage signals show same pattern in both days. Also, it can be observed that the voltage produces zero voltage started around 7.10 pm to 6.40 am, daily. This is because sun starts to sink and rise again around 6.40 am on the next day. Besides that, from both figures, it is also depicted that the peak voltage could reach up to 19.19 V and 19.35 V in day-1 and day-2, at around 11:00 am to 1:00 pm daily, respectively. However, there are some differences in terms of voltage range during such period in which in day-2, voltage was generated smoother than day-1. This is because, in day-2, the weather is very good where the sun shines brightly where no clouds covered the sky. Meanwhile, in day-1, voltage signal fluctuates because the factor of sky was covered with clouds

after 2.00 pm and then the voltage keeps decreasing when influenced by the little rainfall.

Fig. 10 then shows the voltage signal of the solar battery charger during day-1. As shown in Fig. 10, the minimum battery is at 3.8V (32% from the rated value) when battery was started to be charged around 6:30 pm. Battery is charged rapidly at the beginning of several periods, and then, battery is charged constantly around 7V to 8V for 12 hours and 30 minutes from 7:00 pm to 7:30 am where the charge is temporarily stopped around 7:00 pm to 6:40 am. After charging for about 12 hours and 30 minutes, voltage seems increasing again from 8V to 13 V in 8 hours.

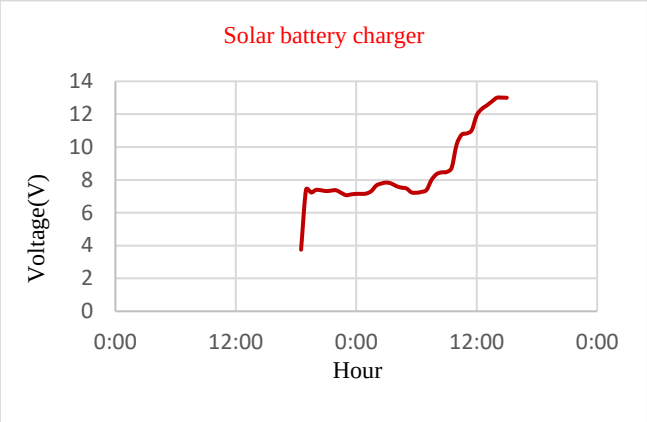

Fig. 10 Voltage signal of battery charger

V. CONCLUSION

In this paper, the concept on how a solar powered system for a rock melon fertigation plant was described and successfully developed for an experimental work in the real field. The control algorithm of the energy management of such system has been explained briefly in this paper. To improve the management of solar energy performance, two batteries were used where the latter battery was equipped with a relay. This then, improving the battery backup of the conventional solar powered with single battery system. The installed Arduino circuit in the solar powered fertigation system able to monitor the parameters of the voltage signal of the installed PV panel (12V, 20W) and the voltage signal of the installed solar battery charger. From the obtained results, it can be concluded that, the proposed solar powered system works well for the rock melon fertigation plant.

ACKNOWLEDGMENT

The authors express gratitude to the Malaysian Ministry of Education (MOE) and Universiti Teknologi Malaysia for Research University Grant 11H31 and facilities.

REFERENCES

[1] S. Mekhilef, A. Safari, W. E. S. Mustaffa, R. Saidur, R. Omar, and M. A. A. Younis, "Solar Energy in Malaysia: Current State and Prospects," Renewable and Sustainable Energy Reviews, vol. 16, pp. 386-396, 1// 2012.

[2] D. Green, "Advantages and Disadvantages of Solar Photovoltaic – Quick Pros and Cons of Solar PV," vol. 2016, ed. Nashua, NH: RenewableEnergyWorld.com, 2012.

[3] Seia. (n.d., 20 September). Photovoltaic (Solar Electric). 2017

[4] M. Rouse, "Semiconductor," in WhatIs.com, ed: TechTarget, 2015.

[5] KIDO, "Fertigation System," vol. 2016, ed. Malaysia: Blogspot, 2010.

[6] M. Boxwell, Solar Electricity Handbook 2012 Edition, 6th ed. United Kingdom: GreenStream Publishing, 2012.

[7] Photonic. (2012, 25 September). 12V Solar Panel.2012

[8] .J. Dunlop and B. Farhi, "Recommendations for Maximizing Battery Life in Photovoltaic Systems: A Review of Lessons Learned " Research Institute of the University of Central Florida, Washington, DC.2001

[9] G. B. Jenal, "Stand-Alone Photovoltaic (PV) System Design " Universiti Teknikal Malaysia Melaka, Melaka, Malaysia 2009

[10] L. BAS. (2010), How to Size a Charge Controller. 2010

[11] M. F. B. Vaz, M. S. S. Kambli, M. S. N. Bhat, and M. K. V. Bhat, "Cost Effective Irrigation and Fertigation System," IJSTE - International Journal of Science Technology & Engineering vol. 2 p. 4, March 2016.

[12] N. Stefan Matan, "Systems and Methods for Generating Renewable Energy," United State Patent, 2003.

[13] S. Ismail. “Rock Melon | Rock Melon Fertigation | Rock Melon” TKPM. 2013

[14] J. O'Connor. (2012), Choosing a Lead Acid Battery for Solar Charging.2012

[15] M. A. Maehlum. (2015), Which Solar Panel Type is Best? Mono- vs. Polycrystalline vs. Thin Film

[16] J. E. M. Salih, A. H. Adom, and A. Y. M. Shaakaf, "Solar Powered Automated Fertigation Control System for Cucumis Melo L. Cultivation in Green House," APCBEE Procedia, vol. 4, pp. 79-87, 2012/01/01 2012.

[17] J. A. O’Connor, "Simple Switchmode Lead-Acid Battery Charger," Unitrode Application Note 1999.

[18] Reference. (n.d.). What is the Function of a Voltage Regulator?

[19] T. L. Gibson and N. A. Kelly, "Solar Photovoltaic Charging of Lithium-ion Batteries," Journal of Power Sources, vol. 195, pp. 3928-3932, 6/15/ 2010

[20] W. Solar. (n.d)., 26 Oct). An Introduction to Charge Controllers. 2017

[21] Emily, "Home-grown Rock Melons," in Ipoh's Community Newspaper, ed. Ipoh, Malaysia: Ipoh Echo, 2013.

[22] P. H. C. E. Staff. (2003, Understanding Solenoid Valves. 2003

[20] M. Fuentes, M. Vivar, J. M. Burgos, J. Aguilera, and J. A. Vacas, "Design of an Accurate, Low-Cost Autonomous Data Logger for PV System Monitoring using Arduino™ that Complies with IEC Standards," Solar Energy Materials and Solar Cells, vol. 130, pp. 529-543, 11// 2014.

[21] S. Armstrong, M. E. Glavin, and W. G. Hurley, "Comparison of Battery Charging Algorithms for Stand-Alone Photovoltaic Systems," in 2008 IEEE Power Electronics Specialists Conference, 2008, pp. 1469-1475.

[22] M. E. Glavin, P. K. W. Chan, S. Armstrong, and W. G. Hurley, "A Stand-Alone Photovoltaic Supercapacitor Battery Hybrid Energy Storage System," in Power Electronics and Motion Control Conference, 2008. EPE-PEMC 2008. 13th, 2008, pp. 1688-1695.

[27] F. Ongaro, S. Saggini, and P. Mattavelli, "Li-Ion Battery-Supercapacitor Hybrid Storage System for a Long Lifetime, Photovoltaic-Based Wireless Sensor Network," IEEE Transactions on Power Electronics, vol. 27, pp. 3944-3952, 2012.

Car Park Assistance using Fuzzy Logic

Muhamad Imran Bin Mazlan
Faculty of Electrical Engineering
Universiti Teknologi Malaysia
Johor Bahru, Malaysia.
Imransenna12@gmail.com

Yahaya Bin Md Sam
Department of Control
Faculty of Electrical Engineering
Universiti Teknologi Malaysia
Johor Bahru, Malaysia.
yahaya@fke.utm.my

***Abstract* — This paper develops and experimentally demonstrates a parking mechanism for aiding drivers especially in bad weather conditions or when driving alone for better safety against intruders. In this project, 8 virtual sensors added to the Fuzzy Logic system, which deliver self-decision making mechanism for instructing the driver based on the car position for his/her action upon parking. These virtual sensors, are divided to 4 different sections of a vehicle to demonstrate each position of the car to the obstacle. This simulation results shows the output as the ideal instruction for the driver in form of text displays, with the inputs are directly from the virtual proximity sensors.**

Keywords—Fuzzy Logic Control; Parking Assistance; Virtual Proximity Sensor

I. INTRODUCTION

Fuzzy logic is the artificial intelligent algorithm that able to imitate human linguistic knowledge with numerical data. Human unable to think exactly specified in terms of numbers, but preferably in conceptual form. If we are encounter some situation with logic is required, it is almost impossible to confirm arguments whether it is true or not. With a decision we make, there is a little degree of membership of a thing in a concept [1]. Membership elements, which is a distinction key point between fuzzy signals and common digital signals, which provide range of values between true (1) and false (0). On the other hand, Fuzzy signals produce quite blur outputs like "merely true", "almost true" and "nearly wrong". In real world, there are lots of application with fuzzy logic control. Automatic Washing Machine is amongst the commercialized product powered by fuzzy logic control. For industrial application, fuzzy controllers and fuzzy reasoning have specific applications that are complicated and cannot be modeled correctly although the program undergo lots of assumptions and approximations. Therefore is not suitable to perform pixel perfect jobs [2]. Fuzzy logic works with a fuzzy set, which comprise one or more inputs to produce one output which the inputs are connected with logical operators such as AND, OR and NOT. These sequence of logical connectors connect each inputs to produce desired output.

As time flies, the world evolves to be even more globalized, hence quality life improves and a number of jobs are even more flexible, added to the reasons the car ownership grows exponentially these days. In fact, rate of vehicle ownership in Malaysia increases every year and the trend becomes a norm when Malaysia become the developed country status in 2020. According to Nielsen, Malaysia's rate of car ownership is 93% per citizen in 2014 [3], including 54% of them coincidence for multiple car owners that listed Malaysia was the third highest in car ownership by that particular year. However, the intention for Malaysians to acquire a car within next 2 years was 71%, slightly higher from the global average, 65%. If the rate keep increasing, parking are more demanding in the future especially in urban areas where people works [3]. Even though there are lots of public transportation in urban areas especially in Kuala Lumpur such public bus, monorails and Light Rail Transit (LRT) but essentially it doesn't enough to cope with the fast rate of car ownership over time and inadequate amount of parking will be an issue in the future. Even though city councils put their best effort to minimize car usage especially in hotspot areas where traffic jams are daily routines, but their common ways of increase the parking fees are not truly effective. Hence most road user opted to park somewhere at the roadsides as couldn't afford to park their car in the paid parking area.

II. PROBLEM BACKGROUND

From the situation described in introduction, this project is aimed at developing a fuzzy controlled parking for current road cars. The objective is to help drivers to park correctly in a tight parking spaces especially in urban areas. This is essential for road users especially for newly graduated drivers from driving schools as they did not receive proper parking practice during learning in driving school. Malaysia's driver licensing system require minimum 10 hours of practice before endure the driving test conducted by Road Transportation Officer to pass the test. There are lots of different parking positions in real life which is not covered in the curriculum itself, which more or less make drivers hesitant to do proper parking at tighter position, hence lead to double-parking.

Parking which is the most crucial part in driving, and every driver should master it. However drivers are facing a scenario when the driver face problems to see obstacles during parking on his seat. There are couple of blind spots, which is a region where a driver cannot see the area which are not covered by side mirrors and rear mirror. Even though advanced technologies such as rear parking beep sensors and parking cameras already come into road cars, but all of them have their own specialties and deficiencies.

In this project, the purpose of implementing fuzzy control is to reduce human elements to assist parking which helps the driver to park their vehicles. In real life, passenger sometimes help the driver a little bit when parking with scouting outside the car to see the right position of the car, and telling the driver in

which direction of steering wheel he need to spin. In case of the driver drives alone, it's hard for them to determine the car position alone as he/she has to estimate the car position without knowing the exact angle of the car pointed during parking especially for road rookies. In short, this project promotes an alternative for road users to park with assisted texts, which is derived from the current technology available in market.

A. *Related Technologies of Parking Assistance in Existing Cars*

Driving assist evolves these days, thanks to electronics development to improve driving which led to less driving distraction. From traction control to limit wheel spin during acceleration and wet surface drive to the active suspension which let the car maintains its height in all moments during the drive – including hard braking and massive acceleration to the parking assistance which evolves from rear parking sensor, to the parking cameras which currently available in the market.

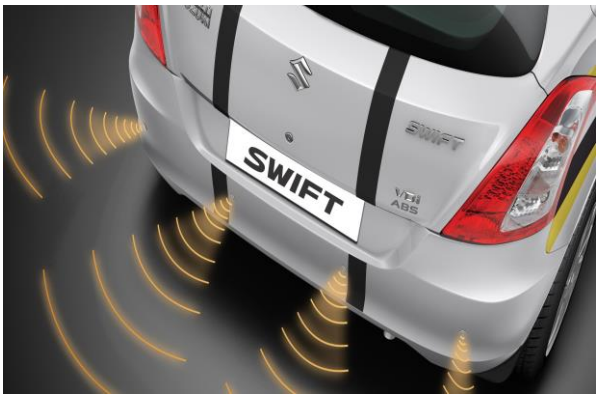

Fig. 1. *Reverse Parking Sensor System on Suzuki Swift*

First of all, Reverse parking sensor system, as shown in figure 1 normally uses proximity sensors such as ultrasonic sensors to detect obstacles during car reversing [4]. Literally these devices exists widely in cars with low-tier or mid-tier pricing. Malaysian carmakers, Proton and Perodua are still stick to this parking assist sensor for most of their models. There are two to four sensors attached at the back bumper of a vehicle varies with different carmaker and models. These sensors produce acoustic pulses, with a control obstacles behind. The system will notify the drivers with beep sound based on the distance between the vehicle and the obstacles. The rate of the beep sound getting faster when it is closer to obstacles. Since the system is amongst the cheapest in current market and available with OEM aftermarket accessories, therefore the system is still active and available in market. However, this system is only applicable to reverse parking style only, as it is not installed at the front with assumption it is the driver's view and driver him/herself may do a decision making when parking.

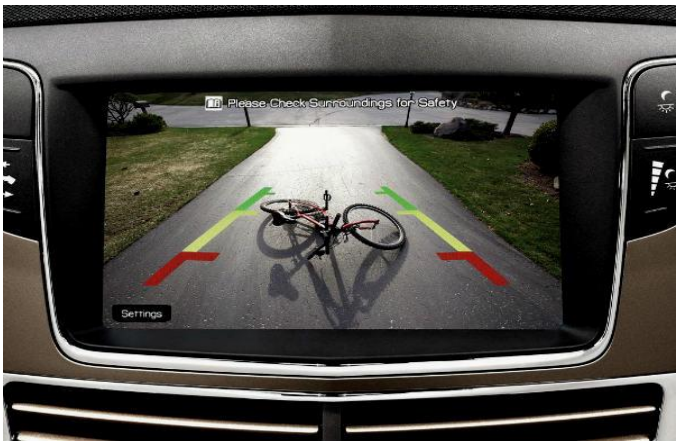

Fig. 2. *Rear Parking Camera*

Rear parking camera is the camera installed at the back of the car, and connected to the cockpit of the car or the screen of audio display to show the image of the rear view of the car to alleviate rear blind spot [4], so the driver can decide how to park their cars. Basically their design is different with other type of cameras as they display horizontally flipped image, so called mirror image. This is a must as the camera and driver may face opposite direction. The camera's right is the driver's left and the other way round. The camera positioned at the rear bumper with downward angles which display potential obstacle on the ground and approaching walls and typically uses wide lens or fish eye lens to aid larger view angle.

Even though the camera shows the rear image, their exact distance from the car cannot determined correctly as it spoils camera ability to see faraway objects which is a drawback of this technology. Even it works when parking in the cities, but improper lighting may hurt and led to misjudging.

III. METHODOLOGY

From the car model, 8 virtual proximity sensors are used and placed at selected side of the car. Theoretically, the space between the sensors is 45 degrees per sensor for better grasp of the car position. However, most obvious problem observed in real life parking situation is dealing with front and rear edges of the car. So the sensor position slightly adjusted to match with real life situation as shown in figure 1 and 2

A. *Fuzzy Logic Rules Set*

As mentioned above, the first step of building the system is creating fuzzy rules and table 1 shows the position where these sensors are located.

TABLE I. TABLE OF SENSORS ASSIGNMENT

Virtual Sensor number	Sensor Position
1	Front
2	Left_Front
3	Left
4	Left_Rear

Virtual Sensor number	Sensor Position
5	Rear
6	Right_Rear
7	Right
8	Right_Front

From these 8 sensors above, they are separated into 4 different sensor combination due to their position and detection, which require 4 different fuzzy rules to implement to produce desired output. As shown in figure 2, the car is divided into 4 parts which 3 sensors are used in each part to create a decision making which implemented using fuzzy logic. Table 2 shows the combination of the sensors for single fuzzy rules.

TABLE II. SENSOR COMBINATIONS AND ITS RESPECTIVE POSITIONS

Virtual Sensors Combination	Sensor Positions
1	Front - Left Front - Left
2	Left – Rear Left – Rear
3	Rear – Rear Right – Right
4	Right – Front Right - Front

From table 2, there are 4 positions of the sensors which overlap between each rules. Non-edge sensors are overlap within 2 rules which used to synchronize between 2 sets of rule. Initial test of using 2 positions of each combination gives simpler fuzzy rules but inaccurate car position during parking event occurs especially at a place which don't have proper parking lots.

Since there are 4 fuzzy rules to make the system. Table 3, 4, 5, and 6 are further explained the rules for each virtual sensor combinations.

TABLE III. FUZZY RULES FOR VIRTUAL SENSORS COMBINATION 1

No	Input Sensor Position			Output
	Left Front	*Front*	*Left*	
1	Far	Far	Far	Choose Your Direction
2	Far	Far	Close	Move slightly forward or left
3	Far	Far	Too Close	Forward only
4	Far	Close	Far	OK
5	Far	Close	Close	Move Slightly Forward
6	Far	Close	Too Close	Move slightly forward or left
7	Far	Too Close	Far	OK
8	Far	Too Close	Close	OK
9	Far	Too Close	Too Close	OK
10	Close	Far	Far	Move slightly forward or left
11	Close	Far	Close	Move Slightly Left
12	Close	Far	Too Close	Forward only
13	Close	Close	Far	Move Slightly Left
14	Close	Close	Close	Move slightly forward or left
15	Close	Close	Too Close	Move Slightly Forward
16	Close	Too Close	Far	OK
17	Close	Too Close	Close	OK
18	Close	Too Close	Too Close	OK
19	Too Close	Far	Far	Forward only
20	Too Close	Far	Close	Forward only
21	Too Close	Far	Too Close	Forward only
22	Too Close	Close	Far	Move Slightly Forward
23	Too Close	Close	Close	Forward only
24	Too Close	Close	Too Close	Move Slightly Forward
25	Too Close	Too Close	Far	OK
26	Too Close	Too Close	Close	OK
27	Too Close	Too Close	Too Close	OK

TABLE IV. FUZZY RULES FOR VIRTUAL SENSORS COMBINATION 2

No	Input Sensor Position			Output
	Left Rear	*Rear*	*Left*	
1	Far	Far	Far	Choose Your Direction
2	Far	Far	Close	Reverse Slightly or left
3	Far	Far	Too Close	Reverse only
4	Far	Close	Far	OK
5	Far	Close	Close	Reverse slightly
6	Far	Close	Too Close	Reverse Slightly or left
7	Far	Too Close	Far	OK
8	Far	Too Close	Close	OK
9	Far	Too Close	Too Close	OK
10	Close	Far	Far	Reverse Slightly or left
11	Close	Far	Close	Reverse Slightly Left
12	Close	Far	Too Close	Reverse only
13	Close	Close	Far	Reverse Slightly Left
14	Close	Close	Close	Reverse Slightly or left
15	Close	Close	Too Close	Reverse Slightly or right
16	Close	Too Close	Far	Reverse Slightly Left
17	Close	Too Close	Close	OK
18	Close	Too Close	Too Close	OK
19	Too Close	Far	Far	Reverse only
20	Too Close	Far	Close	Reverse Slightly or right
21	Too Close	Far	Too Close	Reverse only
22	Too Close	Close	Far	Reverse slightly
23	Too Close	Close	Close	Reverse slightly
24	Too Close	Close	Too Close	Reverse only
25	Too Close	Too Close	Far	OK
26	Too Close	Too Close	Close	OK
27	Too Close	Too Close	Too Close	OK

TABLE V. FUZZY RULES FOR VIRTUAL SENSORS COMBINATION 3

No	Input Sensor Position			Output
	Rear Right	*Rear*	*Right*	
1	Far	Far	Far	Choose Your Direction
2	Far	Far	Close	Reverse Slightly or right
3	Far	Far	Too Close	Reverse only
4	Far	Close	Far	Reverse slightly
5	Far	Close	Close	Reverse slightly
6	Far	Close	Too Close	Reverse Slightly or left
7	Far	Too Close	Far	OK
8	Far	Too Close	Close	OK
9	Far	Too Close	Too Close	OK
10	Close	Far	Far	Reverse Slightly or left
11	Close	Far	Close	Reverse only
12	Close	Far	Too Close	Reverse only
13	Close	Close	Far	OK
14	Close	Close	Close	Reverse Slightly or left
15	Close	Close	Too Close	Reverse Slightly or right
16	Close	Too Close	Far	Reverse Slightly Left
17	Close	Too Close	Close	Reverse slightly
18	Close	Too Close	Too Close	OK
19	Too Close	Far	Far	Reverse only
20	Too Close	Far	Close	Reverse Slightly or right
21	Too Close	Far	Too Close	Reverse only
22	Too Close	Close	Far	Reverse slightly
23	Too Close	Close	Close	Reverse slightly
24	Too Close	Close	Too Close	Reverse only
25	Too Close	Too Close	Far	OK
26	Too Close	Too Close	Close	OK
27	Too Close	Too Close	Too Close	OK

TABLE VI. FUZZY RULES FOR VIRTUAL SENSORS COMBINATION 4

No	Input Sensor Position			Output
	Right Front	*Front*	*Right*	
1	Far	Far	Far	Choose Your Direction
2	Far	Far	Close	Move slightly forward or Right
3	Far	Far	Too Close	Forward only
4	Far	Close	Far	OK
5	Far	Close	Close	Move Slightly Forward
6	Far	Close	Too Close	Move slightly forward or Right
7	Far	Too Close	Far	OK
8	Far	Too Close	Close	OK
9	Far	Too Close	Too Close	OK
10	Close	Far	Far	Move slightly forward or Right
11	Close	Far	Close	Move Slightly Right
12	Close	Far	Too Close	Forward only
13	Close	Close	Far	Move Slightly Right
14	Close	Close	Close	Move slightly forward or Right
15	Close	Close	Too Close	Move Slightly Forward
16	Close	Too Close	Far	OK
17	Close	Too Close	Close	OK
18	Close	Too Close	Too Close	OK
19	Too Close	Far	Far	Forward only
20	Too Close	Far	Close	Forward only
21	Too Close	Far	Too Close	Forward only
22	Too Close	Close	Far	Move Slightly Forward
23	Too Close	Close	Close	Forward only
24	Too Close	Close	Too Close	Move Slightly Forward
25	Too Close	Too Close	Far	OK
26	Too Close	Too Close	Close	OK
27	Too Close	Too Close	Too Close	OK

B. *Membership function*

Based on the rules and sensor combinations mentioned from previous part, 3 inputs are required to produce an output which is create using MATLAB Fuzzy Logic Designer as shown in figure 3.

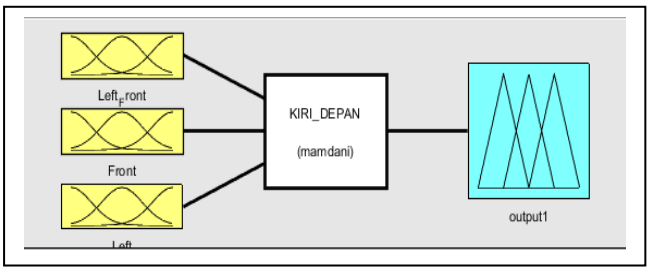

Fig. 3. *Fuzzy rules creator using Fuzzy Logic Designer for Virtual Sensors Combination 1*

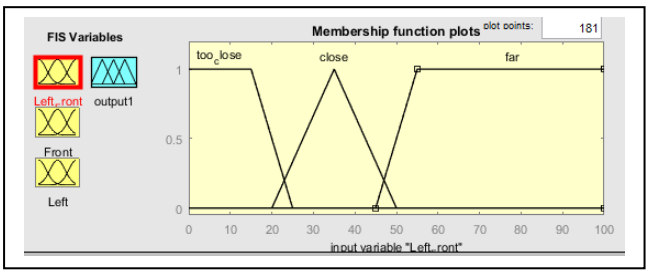

Fig. 4. *Membership Function Plots (input) for Fuzzy Logic Control*

Based on figure 4, X-axis of the display shows the input variable for left front and the axis values indicating the doubled distance between the car sensor with obstacle nearby in

centimeter unit. However for left and right sensors, the input variable is 4 times than the input range shown in figure 4 with consideration to open and close the door for passenger to go in and out of the car. Too_close membership lies between 0 cm to 50 cm in which the sensed point of a car is too close with the obstacle. Close membership lies from 40 cm to 100 cm and far membership lies from 90cm onwards. Assume the car symmetrical setup which all tyres possessed with same pressure and all the sensors are placed at the same height from the road in the car, then same membership functions for input sensors are identical for all 8 sensors used.

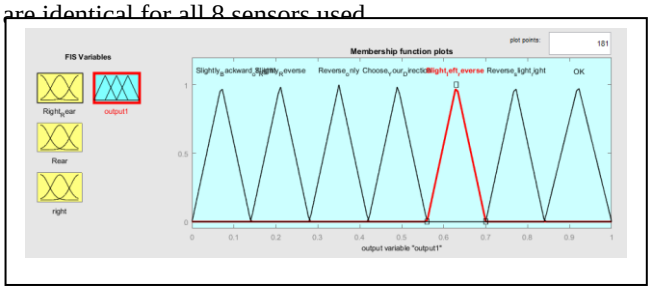

Fig. 5. *Membership Function Plots (output) for Fuzzy Logic Control*

Based on figure 5, the output members are not overlap between each other as it is for fulfill the inputs desired outcome for right rear parking situation. Overall, there are 7 desired outputs which its range is almost identically distributed in a range between 0 and 1 for output variable.

Membership function for the output is almost equally distributed and ranged 0.14 per output. In this part, the membership function is the test displayed instruction for the drivers during parking. Table VII shows the parameters of the membership function with all members are using triangular membership function.

TABLE VII. PARAMETERS OF MEMBERSHIP FUNCTIONS

Membership Function Parameters	Instructions (Output)
[0 0.07 0.14]	Slightly_Backward_or_Right
[0.14 0.21 0.28]	Slightly_Reverse
[0.28 0.35 0.42]	Reverse_only
[0.42 0.49 0.56]	Choose_Your_Direction
[0.56 0.63 0.7]	Slight_left_reverse
[0.7 0.77 0.84]	Reverse_slight_right
[0.84 0.92 1]	OK

C. *Operation*

Basically the operation starts when the car stop. Assuming the cars not driven over 20 km/h during parking event, the sensor starts working with display “choose your direction”. Once the driver seeking for right parking position, then the fuzzy logic interact between each other hence producing outputs as shown in table III, IV, V and VI.

D. *SIMULINK simulation*

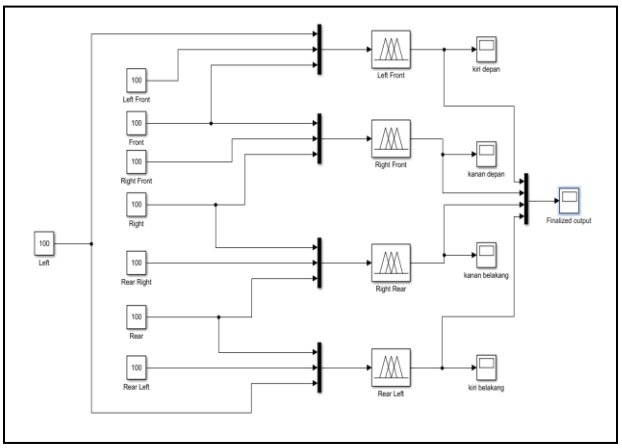

Fig. 6. *Simulink simulation for full model*

From figure 6, it is the initial simulation of the project where the sensor is replaced with constants, assuming the value of the constant is defined as the distance of the input sensors to the obstacle near to it. For the outputs, as of now, they are displayed using scopes in form of graph as ways to convert the output to word is still in progress.

IV. RESULTS

Since the desired output in form of text is still in progress, here are some initial results that displayed using oscilloscope. The results shown below is the result which using constant input where the car is static.

A. *Constant Input*

Based on figure 6, assuming a situation where car is currently placed between 2 cars in a parking lot as shown in figure 7.

Fig. 7. *Car Parking between 2 cars*

When the distance of a car to each front and rear is around 40 cm and facing obstacle 60 cm from the left side. Meanwhile the sensor edges are 54 cm from obstacle which is the front and rear car, subjected to 40° turn from front and rear sensor. When a simulation run with all the parameters filled as in figure 6, the output in form of graph pops out as shown in figure 8.

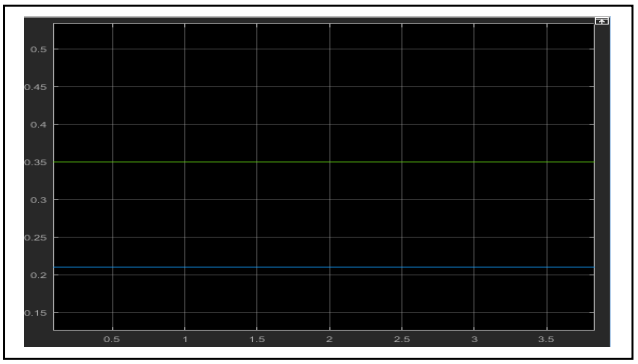

Fig. 8. *Simulation Output*

From Figure 8, the simulation shows the finalized output from each sensors combination. Blue line in the figure comes from 2 sensor combinations, which are from table 3 and 6. From table 3, that particular rule shows the instruction to move slightly forward for both output. The green line is the output from combination 2 which deliver a message for the driver to reverse only. In short, different situation generates different outputs based on proposed rules and currently still developing finalized text output and generate finalized simulation based on real time parking events.

V. CONCLUSION

This project is basically achieve its objective by implementing the rules but software limitation which disable to display real text makes it less fruitful so far. A proper way to display the output is still discovered and looking for a concrete solution. There are lots of room for development of this project in upcoming years in the future, and may realizing a proper, flexible device for hearing disability people to park or even tell them to identify the position as they are driving on the road. Even though there are more project are autonomous car control including parking, but this solution should be an alternatives in the future, as more people are looking for cheaper options to improve their driving experience and automobile makers can consider for different options for parking assistance in the future which aims for different people of the world.

REFERENCES

[1] L. A. Zadeh, Yager,R.R. '*An Introduction to Fuzzy Logic Applications in Intelligent Systems ". Klumer Academic Pub., 69-89.

[2] X.D. Fang, I.S. Jawahir, Predicting Total Machining Performance in Finish Turning Using Integrated Fuzzy-Set Models of the Machinability Parameters. Int. J. Prod. Res., 32 (4) (1994) 833–849.

[3] Nielsen, Rising Middle Class Will Drive Global Automotive Demand In The Coming Two Years. Available: http://www.nielsen.com/my/en/press-room/2014/rising-middle-class-will-drive-global-automotive-demand.html

[4] C-Class Sedan Brochure - Mercedes-Benz Available: https://www.mbusa.com/vcm/MB/DigitalAssets/pdfmb/brochures/MY15_C-Class_Sedan_093014.pdf

[5] M. Khoshnejad and K. Demirli, "Autonomous parallel parking of a car-like mobile robot by a neuro-fuzzy behavior-based controller," Fuzzy Information Processing Society, 2005. AFIPS 2005, pp. 814 - 819, 2005.

[6] Lim Thol Yong, "360 degree sensing car system," Universiti Teknologi Malaysia, 2014, pp. 1-81

Modelling and Simulation of Controller for Active Suspension System

Choo Yong Chien
Faculty of Electrical Engineering
Universiti Teknologi Malaysia
Johor Bahru, Malaysia.
yyyongchien@gmail.com

Yahaya Md Sam
Department of Control and Mechatronic Engineering
Faculty of Electrical Engineering
Universiti Teknologi Malaysia
Johor Bahru, Malaysia.
yahaya@utm.my

***Abstract*—The conventional suspension system on the car is known as passive suspension system and the behavior of the suspension system is fixed based on proper design. The response on the system is rigid no matter how the road profile is. Therefore, this work will focus on designing a suspension system that the behavior of the system will be adjusted based on the road profile that the car will pass through and the system is known as active suspension system. The controllers for the active suspension system proposed are state feedback controllers that designed based on Linear Quadratic Regulator (LQR) and Linear Quadratic Gaussian (LQG) concept. The state variables of the passive suspension system model should be measurable and feed to the controller in order to operate the force actuator installed on the passive suspension system. The active suspension systems designed should improve the ride comfort by a realistic and achievable way. This was achieved in this work by focusing on reducing the vertical displacement of car body without exceed the limit of the suspension travel that allow to be. The performance of LQR and LQG controller were verified by simulating the active suspension systems on the quarter car model in Simulink and the result shows that the controller work properly.**

***Keywords*—active suspension system, quarter car model, LQR, LQG**

I. INTRODUCTION

The suspension system of a car consists of tires, spring, shock absorber and the linkage which connecting the car body and the wheel to allow a relative motion between the wheel and the car body. It is an important component that must have in every vehicle as it absorbs the road shock experienced by the wheel and prevents the shock being transmitted to the car body and thus reduce the impact of the road shock on the car body. Therefore, the main function of the suspension system is support the vehicle body and increase ride comfort [1]. There are four parameters that are represent the performance of a suspension system significantly, the parameters are ride comfort, body motion, road handling and suspension deflection [2].

Ride comfort is defined as how comfortable the driving experience is. Ride comfort is affected by the body motion of the car. Body motion is the motion of the car body due to an external disturbance from the road surface. On the other hand, road handling ability of a vehicle is the ability of the vehicle wheel to stay contact with the road surface so that the vehicle will not out of control as the vehicle is uncontrollable if it does not contact with the road surface. Lastly, the suspension deflection refers to the deflection of the suspension system when a force exert on it. The deflection should be so low as possible so that the relative displacement between the wheel that connect to the suspension system and the road surface [3] will be lower and the wheel will keep grip with the road surface in order to have a smooth drive.

Currently, there are three types of suspension system, they are passive, semi-active and active suspension system. The passive suspension system consists of a spring and a damper to store the energy from the road surface in the spring and dissipate it by the damper [4]. In Semi-active suspension system, the damping force of the damper can be modulated based on the operating conditions that varies with the road surface. Active suspension system consists a force actuator to counter the force acting on the wheel due to the road surface.

The performance of a suspension system is determined by the road handling and ride comfort of the vehicle that the system installed in. The road handling and ride comfort are conflicting each other [5] due to the response of the suspension system. The behavior of the passive suspension is rigid and this will cause the performance of the system is depend on the road profile and caused an imbalance result in terms of comfort and road handling ability.

This project focuses on the active suspension to design a suitable controller for the force actuator to improve the performance of the suspension system by altering the behavior of the system in an acceptable range.

II. LITERATURE REVIEW

Quarter car model, as stated in name it is the model of a quarter of a full car. The quarter car model do not represent the geometric effects of a full car model such as the rolling effect due to the unsynchronized road input profile that acting on each of the wheel and the pitching effect due to a change in the center of mass of the car when a sudden brake. However, it contains the most basic features of the real problem and includes a proper representation of problem of controlling wheel and wheel-body load variation [6]. Fig. 1 shows the schematic diagram that represent the basic quarter car model that based on passive suspension system [6].

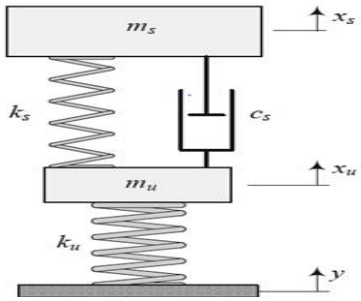

Fig. 1. Quarter car model with passive suspension system

The elastic and damping characteristics of the system is designed based on specific requirement and the parameter is fixed. Therefore, it shows a poor performance when the road profile is keep changing and deviate from the condition used during design the passive suspension system.

Active suspension system is another way to modify the passive suspension system by installing a force actuator parallel with the damper and the spring to counter the force acting on the wheel due to the road surface [7]. The force actuator in the system is controlled by a controller to give an output force to minimize the force due to the road input profile and the force generated is based on the feedback from the active suspension system. In order to get a great performance in terms of ride comfort and road handling, the controller require an effective control strategy in order to get a good performance in both terms. Fig. 2 shows the detailed structure of a basic active suspension system [8].

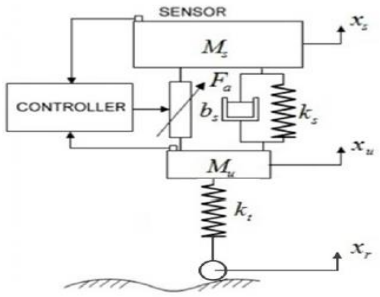

Fig. 2. Quarter car model with passive suspension system

The design strategy that will be focused on this thesis is state feedback controller. State-feedback control is a powerful tool for designing a controller for active suspension system [20]. The state variables are chosen based on the requirement and become the inputs for the state feedback controller. Hence, different state variable may be chosen and give a different result by same approach. To design a state feedback controller, the state variable must be measurable and must be available for feedback to the controller. It gives a clearer relationship between the controller parameters and controller behavior. This strategy was done and the result shows an improvement on the performance of the active suspension system [20].

The first type of state feedback controller is controller with pole placement control design. In this method, the closed loop poles of the system should be lied at the desired position depend on the requirement after the controller is installed in the system. This means that all the zeroes and poles should be manipulated and forced to be lied at specific desired location. Since the closed loop pole is at the desired location, the output of the system should be match with the design specification.

Linear Quadratic Regulator (LQR) is another approach to implement a state feedback controller. LQR is one of the solution to solve the LQG problems, one of the fundamental question in control design. The performance of the controller design is greatly depend on the weighting factor that determined and applied on a specific state vector. The active suspension system may not able to reduce the amplitude of the important parameters in the system if the controller was not designed properly [9].

In LQR controller, it is assumed that all the state variable is measurable and available for the controller all the time. This is unrealistic as all the state variable need to be measured accurately and this is hard to achieve due to the disturbance of noise. When the state variable is not fully observable and available, there is another technique to design a state feedback controller known as Linear Quadratic Gaussian (LQG) control. LQG is the optimal controller obtained as the combination of an optimal LQR state feedback gain with feedback from estimates from an optimal Linear Quadratic Estimator (LQE) without measuring the actual state variable. Hence, not all the state variable need to be measured and feed to the controller although the design of the controller involving all the state variables.

There are some advanced design strategies to implement a controller for active suspension system such as fuzzy self-tuning PID controller that is very effective and can be used in vehicles that will be manufactured in future[10]. But the design algorithm is complex and hard to design a suitable rule base for the controller. The other strategy to design the controller are variable structure control with sliding mode [11], adaptive controller [12], H∞ control [13], and by neural network [14] were developed by researchers.

III. METHODOLOGY

First, the quarter car model for passive and active suspension system is established so that the models can be represent in mathematical expression in terms of state space equation. After that, the controllers is designed based on pole placement control design, LQR and lastly LQG approach. Lastly, a suitable road input profile is modelled to verify the performance of the suspension systems.

A. Mathematical modelling for suspension systems

The mathematical expression is obtained start from identifying the motion of the wheel and the car body when there is a road input profile. Fig. 3 shows the schematic diagram for an active suspension system.

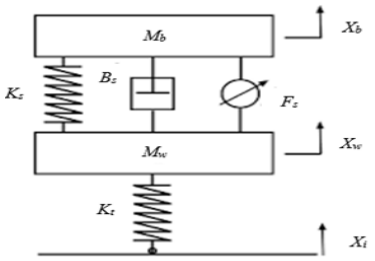

Fig. 3. Quarter car model with passive suspension system

Table I shows the related parameter in the active suspension system whereas Table II shows the related variables for the mathematical expression for the active suspension system.

TABLE I. PARAMETER IN ACTIVE SUSPENSION SYSTEM

Parameter	Symbol	Value
Mass of car body (sprung mass)	M_b	350 kg
Mass of wheel (unsprung mass)	M_w	40 kg
Dumper	B_s	1000 Ns/m
Suspension spring (spring stiffness)	K_s	15000 N/m
Tire spring (tire stiffness)	K_t	150000 N/m

TABLE II. VARIABLE IN ACTIVE SUSPENSION SYSTEM

Related variable	Symbol
Vertical displacement of car body	X_b
Vertical velocity of car body	$\dot{X}_b$
Vertical acceleration of car body	$\ddot{X}_b$
Vertical displacement of car wheel	X_w
Vertical velocity of car wheel	$\dot{X}_w$
Vertical acceleration of car wheel	$\ddot{X}_w$
Road input profile	X_i
Actuator force	F_s

The derivation of the mathematical expression start with identify the motion equation of M_b, the mass of car body and M_w, the mass of wheel based on Fig. 1.

For M_b:

$$M_b\ddot{X}_b = F_s - B_s(\dot{X}_b - \dot{X}_w) - K_s(X_b - X_w) \quad (1)$$

For M_w:

$$M_w\ddot{X}_w = -F_s - B_s(\dot{X}_w - \dot{X}_b) - K_s(X_w - X_b) - K_t(X_w - X_i) \quad (2)$$

Equation (1) and Equation (2) are then rewrite in state space equation form and the equation represent the mathematical model for the active suspension system:

$$\dot{x} = Ax + Bu + Ez$$

$$\dot{x} = \begin{bmatrix} \frac{-B_s}{M_b} & \frac{-K_s}{M_b} & \frac{B_s}{M_b} & \frac{K_s}{M_b} \\ 1 & 0 & 0 & 0 \\ \frac{B_s}{M_w} & \frac{K_s}{M_w} & \frac{-B_s}{M_w} & \frac{-(K_s+K_t)}{M_w} \\ 0 & 0 & 1 & 0 \end{bmatrix} x + \begin{bmatrix} \frac{1}{M_b} \\ 0 \\ \frac{-1}{M_w} \\ 0 \end{bmatrix} u + \begin{bmatrix} 0 \\ 0 \\ \frac{K_t}{M_w} \\ 0 \end{bmatrix} z \quad (3)$$

Where $\dot{x}$ is equal to $[\ddot{X}_b\ \dot{X}_b\ \ddot{X}w\ \dot{X}w]^T$, x is equal to $[\dot{X}_b\ X_b\ \dot{X}_w\ X_w]^T$, u is equal to $[F_s]$ and z is equal to $[X_i]$.

After substituting what value of parameters, Equation (3) become:

$$\dot{x} = \begin{bmatrix} \frac{-20}{7} & \frac{-300}{7} & \frac{20}{7} & \frac{300}{7} \\ 1 & 0 & 0 & 0 \\ 25 & 375 & -25 & -4125 \\ 0 & 0 & 1 & 0 \end{bmatrix} x + \begin{bmatrix} \frac{1}{350} \\ 0 \\ \frac{-1}{40} \\ 0 \end{bmatrix} u + \begin{bmatrix} 0 \\ 0 \\ 3750 \\ 0 \end{bmatrix} z \quad (4)$$

The difference between active and passive suspension system is only that the extra force actuator present in active suspension system. Therefore, the mathematical model for active suspension system can be convert into mathematical model for passive suspension system by remove the force actuator from the system by let the actuator force become zero at all time. The mathematical model for passive suspension system is represent by Equation (5) shown in below:

$$\dot{x} = \begin{bmatrix} \frac{-20}{7} & \frac{-300}{7} & \frac{20}{7} & \frac{300}{7} \\ 1 & 0 & 0 & 0 \\ 25 & 375 & -25 & 4125 \\ 0 & 0 & 1 & 0 \end{bmatrix} x + \begin{bmatrix} 0 \\ 0 \\ 3750 \\ 0 \end{bmatrix} z \quad (5)$$

B. Controller design by pole placement method

First, let the actuator force, u is based on the feedback signal of the state vector, x.

$$u = -kx \quad (6)$$

Where k is equal to $[k_1\ k_2\ k_3\ k_4]^T$.

Substituting Equation (6) into Equation (4):

$$\dot{x} = \begin{bmatrix} \frac{-20}{7} - \frac{k_1}{350} & \frac{-300}{7} - \frac{k_2}{350} & \frac{20}{7} - \frac{k_3}{350} & \frac{300}{7} - \frac{k_4}{350} \\ 1 & 0 & 0 & 0 \\ 25 + \frac{k_1}{40} & 375 + \frac{k_2}{40} & -25 + \frac{k_3}{40} & 4125 + \frac{k_4}{40} \\ 0 & 0 & 1 & 0 \end{bmatrix} x + \begin{bmatrix} 0 \\ 0 \\ 3750 \\ 0 \end{bmatrix} z \quad (7)$$

Since the aim of the controller is to reduce the vertical displacement of the car body, the only output of the compensated system that need to be obtain is the vertical displacement of the car body, X_b.

$$y = Hx$$

$$y = [0 \quad 1 \quad 0 \quad 0]x \quad (8)$$

Where y is equal to $[X_b]$.

The transfer function, *T(s)* that relating the input of the system, X_i(s) and the output of the system, $X_b(s)$ is shown in Equation (9):

$$T(s) = \frac{X_b(s)}{X_i(s)}$$

$$T(s) = \frac{10.714\left(s+\frac{15000-k_4}{1000-k_3}\right)(1000-k_3)}{s^4+\left(\frac{k_1}{350}-\frac{k_3}{40}+27.86\right)s^3+\left(\frac{k_2}{350}-\frac{k_4}{40}+4167.86\right)s^2 +(10.714k_1+10714.29)s+(10.714k_2+160714.29)} \quad (9)$$

In order to manipulate *T(s)*, all the zeroes and poles in *T(s)* must be under controlled. From Equation (9) we know that *T(s)* contains one zero and four poles and each of them need to be adjustable. Since *T(s)* is only consists of four adjustable parameter from *k*, therefore it is not possible to manipulate all the zero and poles in order to generate a desired output as there are five terms that need to be manipulated in *T(s)* .

In conclusion, the force actuator is not suitable to be controlled by the controller that designed based on pole placement method.

C. Controller design by LQR method

In LQR controller, the actuator force, u is still based on the feedback signal of the state variable, which means u is equal to the product of current value of the state vector and a constant gain vector, k as stated in Equation (6).

The control input, *u(t)* should minimize the performance index, *J* that represent the performance characteristic requirement related to *x(t)* as well as the controller input limitation related to *u(t)*. The expression of *J* is shown in Equation (10).

$$J = \int_0^\infty (x^T Q x + u^T R u)\, dt \quad (10)$$

The design start by considering Equation (3) as:

$$\dot{x} = Ax + Bu$$

Where:

$$A = \begin{bmatrix} \frac{-20}{7} & \frac{-300}{7} & \frac{20}{7} & \frac{300}{7} \\ 1 & 0 & 0 & 0 \\ 25 & 375 & -25 & -4125 \\ 0 & 0 & 1 & 0 \end{bmatrix}, B = \begin{bmatrix} 0 \\ 0 \\ 3750 \\ 0 \end{bmatrix} \quad (11)$$

Then the LQR controller has the following form:

$$u(t) = -R^{-1}B^T P x(t) = -kx(t) \quad (12)$$

And P can be calculated by algebraic Riccati equation:

$$PA + A^T P - PBR^{-1}B^T P + Q = 0 \quad (13)$$

Where *Q* and *R* are the controller design parameters with the condition of *Q* and *R* must be greater than zero. In this project, the value of *Q* and *R* are determined based on output weighting that *Q* and *R* are chosen based on the output that want to keep small, which is stated in Equation (8).

Let:

$$Q = \alpha * H^T H = \alpha * \begin{bmatrix} 0 & 0 & 0 & 0 \\ 0 & 1 & 0 & 0 \\ 0 & 0 & 0 & 0 \\ 0 & 0 & 0 & 0 \end{bmatrix} \quad (14)$$

And

$$R = \beta \quad (15)$$

Where α and β are the tuning parameters. The large value of *Q* indicates that the controller stabilize the system with least possible change in *x(t)* whereas a small value of *R* indicates that the controller is stabilizing the system with more energy.

By letting α = 5000 and β = 0.0001, *k* is equal to [524.7 1583.1 5.7 –1366.7] and *u(t)* is equal to [-524.7 -1583.1 -5.7 1366.7]**x(t)*.

The value of R is very small because the impact of the force from the actuator is very small as the mass of the car body is very big and lots of energy is required to move it. The value of *Q* is large as the magnitude of X_b is too small and is insignificant in order to design the controller.

D. Controller design by LQG method

LQG control is achieved by combining a LQR control law and a LQE as an observer to estimate the value of state variables. Based on separation principle, LQE and LQR in the LQG controller can be designed independently.

The aim of designing the LQE is to reduce the state variable that need to be measured from the actual active suspension system by designing an estimator to estimate all the state variable by only a single state variable from the real system. Kalman Filter is chosen as the LQE for the system.

The equation that represent the Kalman filter is:

$$\dot{\hat{x}} = A\hat{x} + Bu + L(y - C\hat{x}) \quad (16)$$

Where *L* is the optimal estimator gain which is calculated by the equation of:

$$L = PCR^{-1} \quad (17)$$

And P is calculated based on the algebraic Riccati equation stated in Equation (18).

$$AP + PA^T + PC^T R^{-1} CP + Q = 0 \quad (18)$$

Where *Q* and *R* are the tuning parameter. *R* is related to how noisy the output sensor is and *Q* is related to how rough the

system is. Since this project is not involving any hardware, the value of *Q* and *R* are set as 1.

The matrix *C* is depend on which state variable is chosen as the input for the estimator. In this project, the estimator is design based on the state variable, X_b and the matrix C is equal to matrix *H* stated in Equation (8).

The value of L calculated is [10.2268 4.5226 -207.5524 1.4165] ^{T}. The estimator is verified by matlab via Simulink and the estimated state variable is almost identical with the state variable of the simulated active suspension system.

For the LQR in the LQG controller, the LQR controller designed before is used to test the difference between the performance of the force actuator that drive based on the actual state variable and the estimated state variable.

E. Modelling of road input profile

One of the common road disturbance is due to the presence of bump that force the drive to speed down the speed of vehicle or else suffer from the vibration acting on the car body when the car across the bump. Since the main function of bump is to alert driver to slow down before but not when across the bump, the uncomfortable feeling should be reduced but not eliminated so that the bump is still will be alerted by the driver. The mathematical expression for a bump is as shown Equation (19) [15]:

$$r(t) = \frac{a}{2}(1 - 8cos\pi t) \tag{19}$$

Where *r(t)* road profile, *a* is the amplitude of the bump and *t* is the time that the car across the bump. In this project, X_i is defined as shown in Equation (20):

$$x_i = \begin{cases} \frac{a_1}{2}(1 - cos\,8\pi t)\,; & 0.5 \le t \le 0.75 \\ \frac{a_2}{2}(1 - cos\,8\pi t)\,; & 3 \le t \le 3.25 \\ 0\,; & elsewhere \end{cases} \tag{20}$$

IV. RESULT AND ANALYSIS

In order to analyze the performance of the suspension system, a suitable set of output need to be obtained from the system model. Table III shows the output variable and the formula to obtain the variable from the system model.

TABLE III. VARIABLE IN ACTIVE SUSPENSION SYSTEM

Output variable	Symbol
Vertical acceleration of car body	$\ddot{X}_b$
Vertical displacement of car body	X_b
Force acting on car body	$M_b \ddot{X}_b$
Displacement between road surface and the car wheel	X_i-X_w
Displacement of the suspension	X_b-X_w
Actuator force	u

The state space equation that represent the system output is shown in Equation (21):

$$y = \begin{bmatrix} \frac{-20}{7} & \frac{-300}{7} & \frac{20}{7} & \frac{300}{7} \\ 0 & 1 & 0 & 0 \\ -1000 & -15000 & 1000 & 15000 \\ 0 & 0 & 0 & -1 \\ 0 & 1 & 0 & -1 \\ 0 & 0 & 0 & 0 \end{bmatrix} x + \begin{bmatrix} \frac{1}{350} \\ 0 \\ 1 \\ 0 \\ 0 \\ 1 \end{bmatrix} u + \begin{bmatrix} 0 \\ 0 \\ 0 \\ 1 \\ 0 \\ 0 \end{bmatrix} z \tag{21}$$

Where y is equal to [$\ddot{X}_b$ X_b $M_b \ddot{X}_b$ X_i-X_w X_b-X_w u] ^{T}.

The most crucial output is the displacement of the suspension or the suspension travel as there is a limit for the extension and retraction for the suspension. The displacement of the suspension in active suspension system should not be larger than the maximum suspension travel in the passive suspension system.

Other than that, the force provided by the force actuator should within a reasonable limit. This means that the amplitude of the force used to improve the behavior of the passive suspension system should not be too high and is able to be generated by a force actuator.

The performance of the active suspension system is defined by the vertical displacement of the car body as the primary target of active suspension system is to reduce the vertical displacement of car body so that it is less noticeable and the driver will have a better riding experience in term of better ride comfort.

Fig. 4 shows the overall system that being simulated which consists of passive suspension system, active suspension system with LQR controller and active suspension with LQG controller.

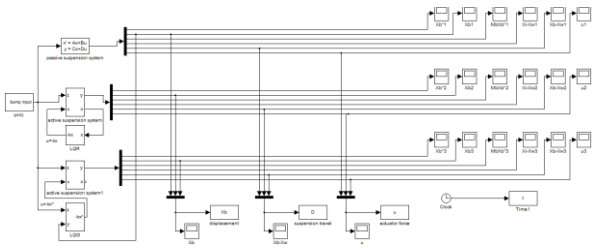

Fig. 4. Suspension systems simulated in Simulink

Fig. 5 shows the simulated result of the suspension travel in passive suspension system, active suspension system with LQR controller and active suspension system with LQG controller.

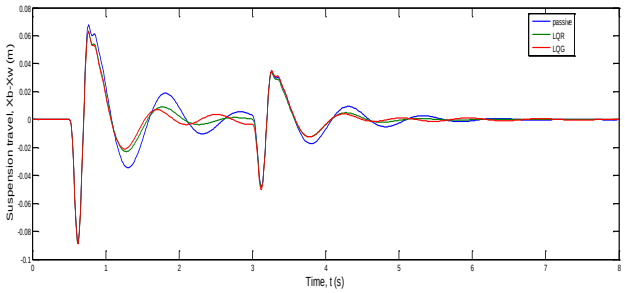

Fig. 5. Suspension travel of suspension systems

Fig. 6 shows the simulated result of the force of the force actuator in passive suspension system, active suspension system with LQR controller and active suspension system with LQG controller generated to improve the system's behavior.

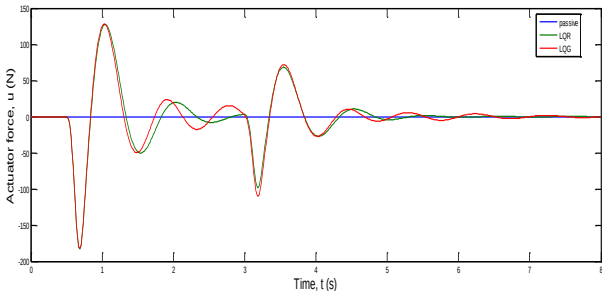

Fig. 6. Force generated by force actuator

Fig. 7 shows the simulated result of the vertical displacement in passive suspension system, active suspension system with LQR controller, and active suspension system with LQG controller.

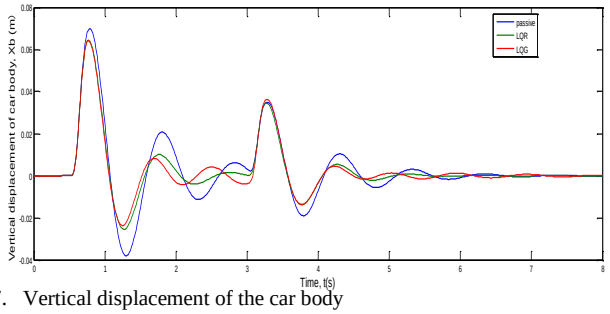

Fig. 7. Vertical displacement of the car body

V. CONCLUSION

The controllers that designed based on LQR and LQG approach are able to improve the behavior of the passive suspension system in order to improve the performance of the system by reducing the impact of the changes in the road profile to the car body. LQR controller requires the information of all the state variables to operate but with LQG controller, the controller only need to measure the road input profile and the vertical displacement of the car body in order to operate.

REFERENCES

[1] Aly, A. A., & Salem, F. A. (2013). Vehicle suspension systems control: a review. *International Journal of Control, Automation and Systems*, *2*(2), 46-54.

[2] Rosli, R., Mailah, M., & Priyandoko, G. (2014). Hardware-in-the-Loop Simulation for Active Force Control with Iterative Learning Applied to an Active Vehicle Suspension System. In *Applied Mechanics and Materials* (Vol. 465, pp. 801-805). Trans Tech Publications.

[3] Miller, L. R. (1988, December). Tuning passive, semi-active, and fully active suspension systems. In *Decision and Control, 1988., Proceedings of the 27th IEEE Conference on* (pp. 2047-2053). IEEE.

[4] Ahmed, A. E. N. S., Ali, A. S., Ghazaly, N. M., & El-Jaber, G. A. (2015). PID CONTROLLER OF ACTIVE SUSPENSION SYSTEM FOR A QUARTER CAR MODEL. *International Journal of Advances in Engineering & Technology*, *8*(6), 899.

[5] Van der Sande, T. P. J., Gysen, B. L. J., Besselink, I. J. M., Paulides, J. J. H., Lomonova, E. A., & Nijmeijer, H. (2013). Robust control of an electromagnetic active suspension system: Simulations and measurements. *Mechatronics*, *23*(2), 204-212.

[6] Jazar, R. N. (2013). *Vehicle dynamics: theory and application*. Springer Science & Business Media.

[7] Al-Mutar, W. H., & Abdalla, T. Y. (2015). Quarter Car Active Suspension System Control Using PID Controller tuned by PSO. *Iraqi Journal for Electrical & Electronic Engineering*, *11*(2).

[8] Emam, A. S. (2015). Fuzzy Self Tuning of PID Controller for Active Suspension System. *Advances in Powertrains and Automotives*, *1*(1), 34-41.

[9] DARUS, R. B. (2008). *Modeling and control of active suspension for a full car model* (Doctoral dissertation, University Teknologi Malaysia).

[10] Salem, M. M. M., & Aly, A. A. (2009). Fuzzy control of a quarter-car suspension system. *World Academy of Science, Engineering and Technology*, *53*(5), 258-263.

[11] Gao, W., & Hung, J. C. (1993). Variable structure control of nonlinear systems: a new approach. *IEEE transactions on Industrial Electronics*, *40*(1), 45-55.

[12] Agrawal, A. (2013). Performance Improvement of Automotive Suspension Systems using Inerters and an Adaptive Controller.

[13] Du, H., & Zhang, N. (2007). H∞ control of active vehicle suspensions with actuator time delay. *Journal of sound and vibration*, *301*(1), 236-252.

[14] Al-Holou, N., Lahdhiri, T., Joo, D. S., Weaver, J., & Al-Abbas, F. (2002). Sliding mode neural network inference fuzzy logic control for active suspension systems. *IEEE Transactions on Fuzzy Systems*, *10*(2), 234-246.

[15] Sam, Y. M., Osman, J. H. S., & Ghani, M. R. A. (2003, June). Active suspension control: Performance comparison using proportional integral sliding mode and linear quadratic regulator methods. In *Control Applications, 2003. CCA 2003. Proceedings of 2003 IEEE Conference on* (Vol. 1, pp. 274-278). IEEE.

Mobile Cranes' Safety System at Construction Sites

Nur Shafiqah Binti Abdullah
Faculty of Electrical Engineering
Universiti Teknologi Malaysia
Johor Bahru, Malaysia.
nurshafiqah.abdullah8@gmail.com

Zamani Mohd Zain
Department of / Centre of
Faculty of Electrical Engineering
Universiti Teknologi Malaysia
Johor Bahru, Malaysia.
zamani@fke.utm.my

***Abstract*— Safety issue involving mobile cranes at construction sites has become serious matter due to its working environment and the complexity of working practices. This project proposed a low cost automated monitoring system kit to help monitoring the hazard on the operation of mobile crane at construction site. The prototype system is an integrated electronic alert system for the crane operator when lifting a load using mobile crane. Sensor was used to obtained boom length and angle which then processed by the controller module installed in the driver's operating room using Arduino Mega as the processor. The data obtained will then being send to the Ground Monitoring Terminal (GMT) which is at ground worksite were done for supervision purposes. At the end of this project, an anti-accident algorithm was executed and the real-time data was recorded using MATLAB to ensure the safety of mobile crane during construction.**

Keywords— mobile cranes; Arduino Mega; monitoring system

I. INTRODUCTION

The field of construction today have become significant part of industrial culture, safety issue on construction site is highly concerns especially regarding mobile crane. Mobile crane is one of the heavy-duty equipment for moving heavy structure and materials on construction sites. The effectiveness and safety of the mobile crane is degrading due to the flexible nature of crane physical structures. Based on the figure from Department of Occupational Safety and Health, Ministry of Human Resources Malaysia, in 2014, the rate for an accident to happen in construction sites is 3.10 per 1000 workers while rate of fatality is 4.21 per 100000 workers. In 2015, the accident rate per 1000 workers in 2015 is 2.81 while fatality rate per 100000 workers is 4.84. Even though there is slightly decline of the accident rates between 2014 and 2015, the rates are still considered as big figures of numbers for construction field. Safety measure should be implemented by respective company in order to prevent the rate to increase from year to year. However, these studies only focusing on how to tackle armature crane operator handling crane which according to the load chart of a mobile crane and real-time data supervise problem. Fig.1 shows the mobiles crane parts.

II. LITERATURE REVIEW

1. Construction and Crane Security System Kit

This thesis that was published in 2016 focusing on an integrated electronic alert system for stress and strain movement on construction structure. The sensor module that was attached to the construction structure in order to detect any vibration or displacement events which will then send to Arduino Uno Board to compute the data and trigger the alert system for the user.

2. A Proactive System for Real-Time Safety Management in Construction Sites

This paper reports the development of a first prototype for the proactive safety management and real-time signaling of potential overhead hazards. It is expected to enhance standard safety policies and assist inspectors and coordinators in executing their tasks. The system performs real-time tracking using ultra wide band technology and implements proactive virtual fencing logics. The development of the system, its laboratory test results, the algorithm optimization, and the final field test results are reported herein. The results achieved demonstrate the capability of proactive logics to reinforce safety management policies and assist personnel in coping with unpredictable hazardous events.

3. Dynamic Responses of Hydraulic Mobile Crane with Consideration of The Drive System

This paper focusing on improvement of dynamic calculation of mobiles cranes. using the new method, the flexible multibody model of the structure will be couples with the model of the drive system. In that way the elastic deformation, the rigid body motion of structures and the dynamic behavior of the drive system can be determined in an integrated model. The calculation method has been realized for a hydraulic mobile crane. In addition to the structural elements, the mathematical modelling for hydraulic drive- and control system is described. The crane rotating simulation for arbitrary working conditions has been carried out. As a result, a more exact representation of dynamic behavior, not only for the crane structure, but also for the drive system is achieved.

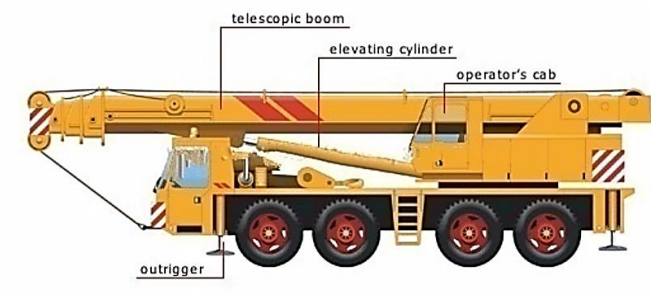

Fig. 1. Mobiles Cranes Parts

III. METHODOLOGY

The method conducted in this project was divided into software simulation and hardware development. In order, to compare the functionality of data logging concept in industrial mobile crane, simulation really important before transfer simulation circuit into hardware. Fig. 2 shows the block diagram of overall system. At the early stage of operation, the crane operator will insert the weight of the load and the crane working radius. Potentiometer that act as sensing module in the system was used to detect parameter when the crane is in operation. In the controller module, Arduino Mega board processed the data according to the load chart which give output to the Alert Kit and MATLAB.

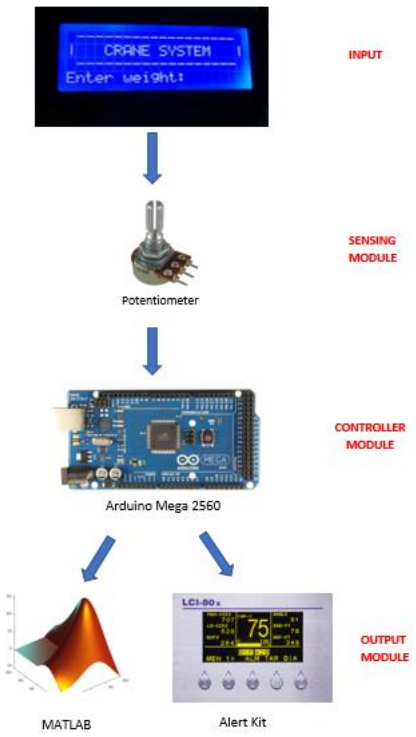

Fig.2 Flowchart of Overall System

A. *Hardware Developement*

1. *Sensing Module*

Various of sensor can be used in order to get the parameter needed to be measured. In this project, potentiometer was used to measure two values:

i) Angle of the telescopic boom.
ii) Length of the telescopic boom.

The variation of voltages 0-5V of potentiometer was map to the minimum and maximum value of boom length and boom angle so that it will produce the value needed. The implementation of the potentiometer is as shown in Fig.3 and Fig. 4.

Fig.3. Potentiometer to measure boom angle

Fig. 4 Potentiometer to measure boom lenght

2. *Alert Kit*

The alert kit function like data loggers, it consists of LCD 16x4, a keypad membrane, 4 LEDs and one buzzer. This kit will be stored in the operator's cab for the operator reference when lifting a load. In case, the operator exceeds the maximum length or angle fixed according to the load chart, red LED will be light up and buzzer will be triggered. If the potentiometer gives out the exact value according to the load chart, yellow LED will light up. The Alert Kit is as shown in Fig.5

Fig.5. Alert Kit

B. *Software Simulation and Designation*

1. *Arduino Mega 2560*

The Arduino Mega is the addition to the Arduino family. This board is physically larger than all the other boards and offers significantly more digital and analog pins. The MEGA uses a different processor allowing greater program size and more. The Mega2560 differs from all preceding boards in that it does not use the FTDI USB-to-serial driver chip. Instead, it features the ATmega16U2 programmed as a USB-to-serial converter. The Mega has

four hardware serial ports, which means maximum speed if you need a second or third (or fourth) port. The Arduino Mega works in the same way the Arduino Uno does but the difference is that it uses ATmega2560 microcontroller and has more number of digital pins, analog pins. In this project, Arduino Mega will process input from potentiometer, maps with the load chart and then gives output to the Alert Kit and MATLAB. Fig.6 shows the circuit diagram of the system.

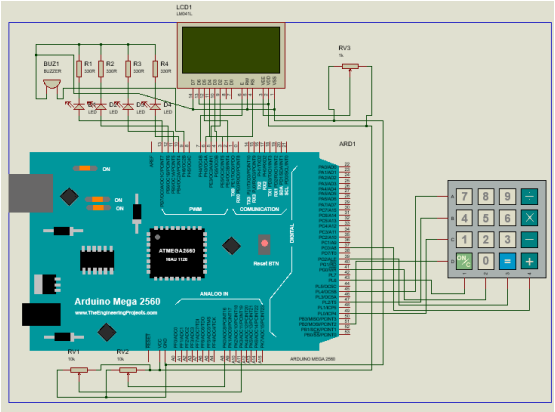

Fig.6. Circuit Diagram

2. *Mobile Crane's Load Chart*

Each crane has a load chart that, in short, specifies the crane's capabilities—detailing its features and how its lift capacity varies when considering distance and angle. Before a crane is rented, transported, employed or purchased, the crane chart must be consulted. Everyone, from the crane operator, to the job supervisors, to even the sales guys have to know how to read a load chart. Table 1 shows example of crane performance which will map to the load chart as shown in Fig.7

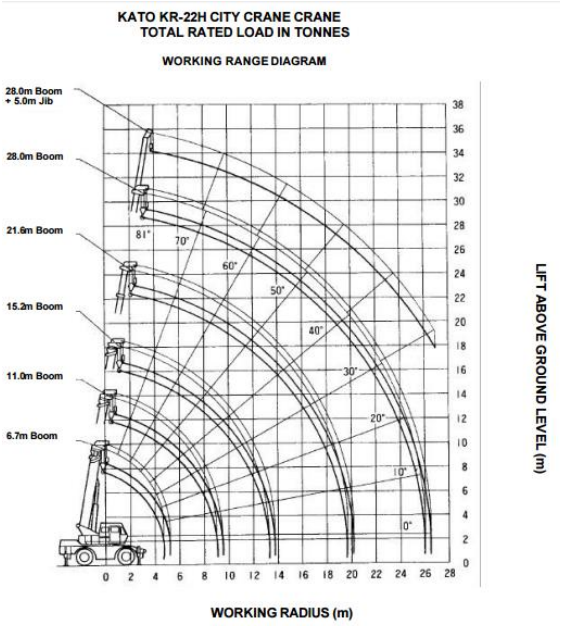

Fig. 7. Load chart of a mobile crane

Here, the chart illustrates the total weight able to be picked up at an 81-degree angle while outriggers is extended. The column to the left indicates the radius of the lift, the one to the far right, the maximum boom length each weight can be carried at. and on the x axis, indicates the working radius on how far the boom is extended from the initial position.

TABLE I. CRANE PERFORMANCE

Crane Performance		
	Boom Length	***Load Weight***
Maximum Total Rated load	6.70 m boom	22,000 kg
	11.00 m boom	12,000 kg
	21.60 m	8,000 kg
	28.00 m	6,000 kg

3. *MATLAB Graphical User Interface (GUI)*

In this project, GUI was used to communicate Arduino with MATLAB to show the output of potentiometer for supervision purposes. The GUI typically contains controls such as menus, toolbars, buttons, and sliders. Many MATLAB products, such as Curve Fitting Toolbox™, Signal Processing Toolbox™, and Control System Toolbox™ include apps with custom user interfaces. Fig.8 shows the GUI used to communicate Arduino Mega to MATLAB.

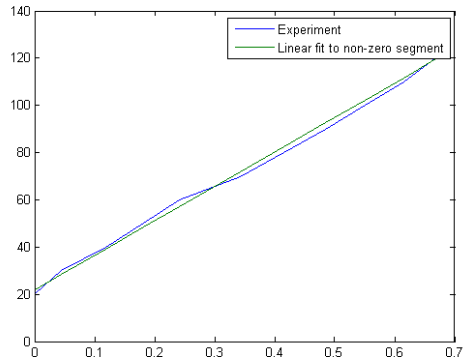

Fig. 8. Graphical User Interface (GUI)

IV. RESULTS AND DISCUSIONS

After entered value of load weight and working distance, Arduino calculate the potentiometer value and maps to the boom length and angle. In this example, 22000 is entered for the load weight and 2m for the working distance. From the load chart suppose the boom length is 6.7m and angle should be 60°, if the boom length is longer then red LED lights up. If not yellow LED lights to indicate it is safe.

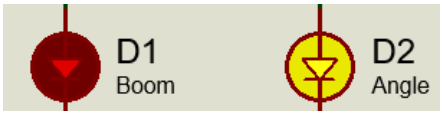

Fig. 9. Result 1

Fig.9 shows that LED from boom is still in red which indicate, it is still below rated length.

Fig. 10. Result 2

Fig. 10 shows that LED from angle is still in red which indicate, it is still below rated angle.

Fig. 11. Result 3

Fig. 11 shows that LED from angle and boom is still in red which indicate, both is still below rated length and angle.

Fig. 12. Result 4

Fig. 12 shows that LED from angle and boom is in yellow which indicate, both is at safe angle and length to operate. While in Fig. 13 shows the result of serial communication between MATLAB and Arduino. The GUI shows the weight load, working distance and graph on the potentiometer when it is operated.

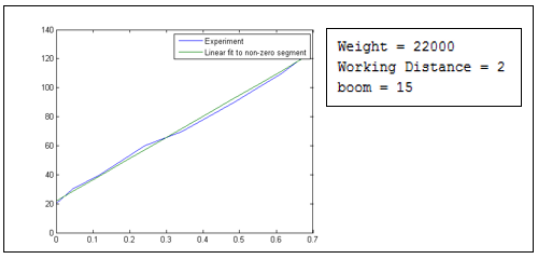

Fig. 13. Result 4

V. Conclusions and Recommendations

Construction sites are always prone to accidents especially when mobiles are involved. The proposed system, through the deployment of an alert kit and supervision system using MATLAB, aims at helping construction or safety personnel in making rapid decisions to avoid or minimize these accidents when in an operation. The results proof of concept– a demonstration that a relatively low-cost system kit can be used to mobile crane operator on harsh and dynamic construction sites.

In order to improve the performance of the system, a better sensor should be used to get the exact boom length and boom angle under any circumstance. Furthermore, the Internet of Thing (IoT) technologies should be implemented so that the supervision part will not limited to only at the construction site, in fact can be monitor by engineer from far.

References

[1] Muhammad Nasruddin Bin Mohd Shah. “Construction and Crane Security System Kit”, 2016, pp. 1-13.

[2] Daichi D. Fujioka, “Tip-Over Stability Analysis For Mobile Boom Cranes With Single- And Double-Pendulum Payloads,” Georgia Institute of Technology, 2010, pp. 23-24.

[3] Kevin Tantesevi, Burcu Akinci. “Automated generation of workspace requirements of mobile crane operations to support conflict detection” Carnegie Mellon University, 2010, pp. 1-4.

[4] Wolfgang Wilhelm, Ratmgen-Hosel,Kriiger GmbH & Co. KG, Essen, Fed. “Load-Monitoring System For Boom-Type Crane”, Germany, 1985, pp. 8-11.

[5] Alessandro Carbonari, Alberto Giretti, Berardo Naticchia, “A proactive system for real-time safety management in construction sites”, Università Politecnica delle Marche, 2011.

[6] Teach-ict. (n.d.). “Advantages and Disadvantages.” [Online]. Available:http://www.teach-ict.com/gcse_new/control/ data_logging/ miniweb/pg6.htm, [Accessed October 1, 2016].

[7] Mathworks. “Sonar distance graph on Matlab” [Online]. Available: https://www.hackster.io/Luis_R_A/sonar-distance-graph-on-matlab-6d3a1b, [Accessed November 4, 2016].

[8] Department of Occupational Safety And Health, Ministry Of Human Resource Malaysia. “National occupational Accident Fatality Rate” [Online]. Available: http://www.dosh.gov.my/index.php/en/national-occupational-accident-fatality-rate, [Accessed September 11, 2016]

[9] Ministry of Manpower Singapore, " New mobile cranes to be equipped with data loggers from 1st August 2015," [Online]. Available: http://www.mom.gov.sg/newsroom/press-releases/2015/new-mobile-cranes-to-beequipped-with-data-loggers-from-1-august-2015, [Accessed October 1st, 2016]

Indoor Security Surveilliance System with a Mobile Patrolling Robot

Muhammad Ishak Bin Mohamed Ibrahim
Faculty of Electrical Engineering
Universiti Teknologi Malaysia
Johor Bahru, Malaysia.
ishak.ibrahim94@gmail.com

Nasarudin Bin Ahmad
Department of Control and Mechatronic Engineering
Faculty of Electrical Engineering
Universiti Teknologi Malaysia
Johor Bahru, Malaysia.
e-nasar@utm.my

***Abstract*—Break in cases is one of major crime in our country. Current security system is not secure enough to alert the police or house owner went intruder enter the house. The objective of this project is to build a security system that can alert the house owner when it happens and allowed house owner to see the intruder indirectly. This system consists of two part which is motion detector and mini patrol robot. When motion detect by the motion detector it will alert the house owner through GSM module and the controller used in the motion detector is Arduino UNO. The user will use the patrol robot to confirm whether it is a false alarm or not and see what type of weapon the intruder bring indirectly. Controller used in this patrol robot is Raspberry PI 3B and it is integrated with raspberry PI camera module.**

Keywords—Security System; Motion Detector; Patrol Robot

I. INTRODUCTION

Malaysia is a nation which is outstanding with its wealth of culture and appealing tourism spots. However, the number of crime in Malaysia especially break-in cases which are increasing rapidly. An average of 419 break-in cases reported each day as of 2012 [1]. The occurrence of active crime in our nation add to a negative effect for tourism business, economic and increasing the fear among the people [2].

Based on a report by University of North Carolina at Charlotte's Department of Criminal Justice and Criminology, about 60% of convicted burglars stated the presence of a security system influenced their decision to target another home [3]. Basically, my project is to build a low-cost surveillance mobile robot to ensure the safety of home.

A. Problem statement

Present home based surveillance system enable users to record footage for later viewing, and to help nab criminals [4]. They cannot, however, stop a crime when it is in progress. They do not alert neighbours or the police like an alarm system would. Cameras by themselves can't prevent victims from having to fill out police reports, filing insurance claims and having to replace their stolen or destroyed belongings.

Besides, traditional surveillance camera is costly while dummy surveillance cameras may not be expensive, the real one's costs hundreds, even thousands of ringgits depending on the features and the number of cameras and monitoring systems user buy [5]. Getting them installed and their maintenance means added costs.

Lastly, traditional security system gives some protection via fixed cameras but still has some blind spot cannot be monitored [6]. Unfortunately, the fixed cameras system only captures those images within the coverage of fixed cameras. Therefore, there are some blind spot in the surveillance area. Thefts might secretly invade our home or working place by hiding themselves in those blind spots.

B. Objective

The main objective of this project is to design a system consist of mobile patrolling robot and motion detector. The sub-objective are stated below.

- To integrate warning system by notify owner of the house when any motion is detected through Short Message Service(SMS).
- To design a mobile robot where owner can control the robot using smartphone through internet.
- To build a webserver on the PI, so that real-time video stream can be watch from a Web browser.

C. Project Scope and Limitation

As to make the direction of this project clearer, there is some limitation that should be outlined. This project will comprise of three main parts which is the mobile robot, motion detector and the webserver and GUI part. All these parts comprise of its own hardware and sensor.

The mobile robot is to be design to have dimension of 20x20x15.5 centimetre. Hardware that install in the robot are Raspberry PI 3, Raspberry PI 5MP camera, MD10A motor driver and PG motor. The mobile robot only can function best in the single-story house with internet WIFI connection.

Second part is the motion detector which is the PIR sensor that will be connected to Arduino UNO and GSM module. It will be install in a fixed place on the edge above the window. GSM module is used to send alert message to the owner phone if motion is detected.

II. LITERATURE REVIEW

A. Sensor Control in Surveillance Vehicle

Tan Kok Hui built a Sensor Control in Surveillance Vehicle in 2002 for his final year project. This robot can identify intruder at certain place and then can alert user which are at home PIR sensor which is a motion sensor is utilized to identify for intruders. The PIR sensor is install on a remote controlled mobile robot. Thus, the robot can be controlled from home to identify for intruder.

Radio frequency module are used to send data to the owner if PIR sensor detect intruder. This will help the user to know whether there is any intruder. In any case, this robot had couple of downside. For instance, the robot has no "eye" thus; it is impractical to control the robot without seeing its way. Other than that, the passive infrared flag gives out false alert once in a while.

B. Previous Project and Existing Related Product

IRobot company has created a surveillance robot called iRobot 210 negotiator. iRobot 210 negotiator help in increasing awareness if there any dangerous activity for public safety. Besides, this robot can identify hazard material and bomb. iRobot 210 negotiator also used as surveillance purpose. It has camera which can capture image of its view and transmit to user. The robot can be control sing joystick which the camera be the eye to user that control the robot.

Subsequently, this robot can be utilized to check or overview territories where it can be a hazard for human to go. Besides, the iRobot 210 moderator is plan in such way that it could travel through unpleasant and uneven places. It can also climb stairs effectively. Subsequently, this makes it a more productive and a superior option contrast with human in managing a perilous circumstance [7].

III. METHODOLOGY

There are two part in this project which are the motion detector and patrol robot. After consideration about a lot of aspect regarding the robot features, the robot will have a simple mechanical design tank-like shape. The robot will be inserted with RPi camera module for surveillance. The robot will be communicated with the control panel through Wi-Fi. The robot will be using track wheel to navigate and will be using DC geared motor as the actuator. The power supply for the robot will be using Li-Po battery.

PIR sensor is used to detect motion of any intruder. In the motion detector Arduino uno is used as the controller and GSM module are installed in it to send message if it detect any motion. Below shows all the component used in this system.

A. Raspberry Pi

Main controller for the mobile robot is the processor to control the input and output of the robot [8]. For this mobile robot, the controller that will be use is Raspberry Pi 3B. Raspberry Pi has the capability to interrelate with the outside world, and has been utilized as a part of a wide exhibit of computerized creator ventures, from music machines and parent identifiers to climate stations and tweeting aviaries with infra-red cameras.

Raspberry Pi Camera Module which has 5 megapixels of resolution can be connected to the Camera-Serial-Interface (CSI) socket of the Raspberry Pi. Its clock speed is regularly 700 MHz while it gave the choices to permit user to overclock the processor keeping in mind the end goal to get higher processor speed, yet may bring about a shorter life expectancy for processor core. The Raspberry Pi board also built with WIFI module. Figure 1 shows Raspberry Pi 3B.

Fig. 1. Raspberry Pi 3B

B. Motor Driver

Looking that this project requires a DC motor with a high speed and torque so DC Planetary Gear motor was the most appropriate motor navigation. DC Planetary Gear Motor consist of a DC motor which was initially fixed with a gear box by the manufacturer to reduce the problem for mounting gear box onto the DC motor.

Only one motor driver is used on this robot which is Cytron MDD10A. The Cytron MDD10A drive higher current motor such as the motor navigation because need to move heavy load that might draw high current. The motor driver has 12V input voltage and 5V input signal. Besides, Cytron MDD10A can drive two motor by controlling the motor speed and direction. Figure 3.2 shows Cytron MDD10A motor driver.

Fig. 2. Cytron MDD10A motor driver

C. Arduino UNO

Arduino Uno is a microcontroller that has 14 digit input/output pins. It is open source electronics prototyping based on flexible, easy to use hardware and software. In addition, it is simply connect to the computer with a USB cable or use AC/DC source to power up the controller. Arduino can sense the environment by receiving input from a sensor and can affect its surroundings by controlling the motor, actuator and light.

In this project, arduino uno is used to control the flow of the project. It turn ON the buzzer when PIR sensor sense the motion and at the same time generate the message, send it to the user by GSM module.

Fig. 3. GSM SIM900A Module

D. GSM Module

GSM module allow programmer to make an arduino controlled calls and also send text messages. In this system GSM SIM900A was used to communicate with the user. This module supports communication in 900 MHz band. Most of the mobile network providers in Malaysia operate in the 900MHz band.

In this project, GSM required 5 volts input so it directly from Arduino's 5V out. Digi SIM card was inserted to the module. When arduino generate the message, GSM module will send it to the user.

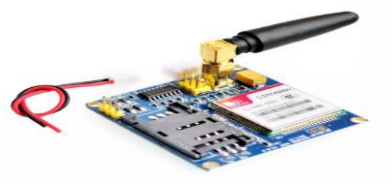

Fig. 4. GSM SIM900A Module

E. PIR Sensor

PIR sensor generally known as motion sensor or motion detector. It is consist of elements made of a crystalline material that generate an electric charge when exposed to infrared radiation. The changes in the amount of infrared striking the element change the voltages generated, which are measured by an on-board amplifier. The sensitivity range of PIR sensor approximately 20 feet and 110° x 70° detection range. It can be varied with the environment condition.

A PIR sensor has only 3 pins. One is Vcc which is +5 volts input, a ground pin and finally the digital output. Connect +5V from arduino to PIR sensor module, same goes to ground and digital output pin to any digital pin of arduino. In this system, digital output pin of PIR sensor have connected to pin 4.

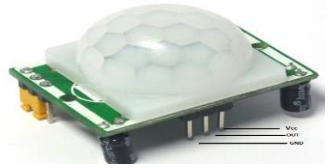

Fig. 5. PIR Sensor

F. Software Development

The software is developed on the Raspberry Pi itself by connecting mouse, keyboard, and monitor through HDMI and Wi-Fi adapter through USB port to the Raspberry Pi. The software development can be divided into two parts, the first one is the live streaming user interfaces and the second one is controller layout user interfaces. Above all, normal setup for Raspberry Pi needs to be done in for the Raspberry pi to work properly. The standard setup that needs to be done is communication setup so the computer can connect to the Raspberry Pi through the IP (Internet Protocol) address of the Raspberry Pi. The other setup is such as enabling camera, updating firmware and installing GPIO for the Raspberry Pi.

IV. RESULT AND ANALYSIS

The current result obtained so far after assembly of the robot is done. The result is indicated how the objective had been achieved. Basically, all the objectives is achieved.

A. Robot Assembly

The robot assembly is done successfully as what been designed on Solidwork CAD. The robot‟s part to be assembled is fabricated and 3D printed. All attachment for the actuator and circuit is done. The robot is fully design and assembled from nothing. Figure 6 shows the full robot assembly.

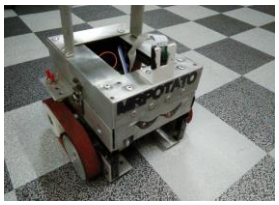

Fig. 6 Full Robot Assembly

B. Robot Movement

The robot is tested directly using the designed user interfaces. The robot movement speed tested. The robot total weight is less than 10 kilograms and to be exact 7 kilograms. The speed of the robots navigation is tested to 1 meter track. Figure 7 shows the robot navigated on the track and Table I tabulated the result for fastest speed.

Fig. 7 Robot Test Run on 1 meter track

Table I Result for speed test

Test Trials	Time Taken, t(s)
1st	4.15
2nd	4.14
3rd	4.15

Average time, tavg (s) = 4.14

Average velocity, V (m/s) = 0.24

C. PIR Sensore

PIR sensor was used to detect motion. The limitation of PIR sensor was obtained by using Arduino IDE serial monitor. Figure 8 shows the connection of PIR sensor on breadboard and Table II show the limitation of distance detected.

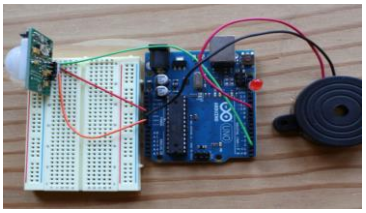

Fig. 8 Connection of PIR sensor

Table II limitation distance detected

Distance (m)	Motion detection
1	detected
2	detected
3	detected
4	detected
5	detected
6	Not detected

REFERENCES

[1] L. Hamid and N. Toyong, "Rural Area, Elderly People and the House Breaking Crime", Procedia - Social and Behavioral Sciences, vol. 153, pp. 443-451, 2014.

[2] A. Anuar, S. Bookhari and N. Aziz, "The Effectiveness of Safe City Programmed as Safety Basic in Tourism Industry: Case Study in Putrajaya", Procedia - Social and Behavioral Sciences, vol. 42, pp. 477-485, 2012.

[3] K.Blevins, J. Kuhn and Z. Lee, "Understanding Decisions to Burglarize from the Offenders Perspective", UNC CHARLOTTE, The University of North Carolina at Charlotte Department of Criminal Justice & Criminology, 2012.

[4] M. Govender, "THE PARADOX OF CRIME PERCEPTIONS: SAPS crime statistics, Victims of Crime Surveys and the media", South African Crime Quarterly, no. 46, 2016.

[5] G. Qiao, G. Song, Y. Wang, J. Zhang and W. Wang, "Autonomous network repairing of a home security system using modular self-reconfigurable robots", IEEE Transactions on Consumer Electronics, vol. 59, no. 3, pp. 562-570, 2013.

[6] M. Md Saad, "Room Searching Performance Evaluation for the JagaBotTM Indoor Surveillance Robot", KnE Engineering, vol. 1, no. 1, 2016.

[7] iRobot Corporation (2008). iRobot Negotiator Civil Response Robot [Brochure].

[8] Raspberry Pi Operating System and How Raspberry Pi works.Available: https://www.raspberrypi.org/

Car Front View Detection using AdaBoost

SHIRESH RAJENDRAN
Faculty of Electrical Engineering
Universiti Teknologi Malaysia
Skudai, Johor Bahru
shireshrajendran@gmail.com

AHMAD RIDHWAN WAHAP
Faculty of Electrical Engineering
Universiti Teknologi Malaysia
Skudai, Johor Bahru
aridhwanwahap@utm.my

***Abstract*— Viola and Jones have proposed an object detection algorithm using Adaboost. Adaboost is a boosting algorithm that selects and combines weak classifiers from an extremely large pool of weak classifiers. The Viola and Jones object detection algorithm has been proven to be very successful for detecting faces. We have followed their approach and applied it to detect front view of cars. The detector has been carefully examined and has been expanded in a way, such as varying the type and complexity of weak learners, using Real Adaboost. The outcome of this system shows a very high detection rate for front-view car detection.**

Keywords—detector; Adaboost; weak; classifiers; cars; system

I. INTRODUCTION

We have adopted the methods from face detection by Viola and Jones [1] and applied it for car front-view detection. We believe that face detection and car front-view detection are similar in nature and applying face detection methods for car detection is a natural choice. The success of face detection may be because face images have rich internal features. On the other hand, faces have very distinctive pattern, caused by eyes, nose, mouth, which can be well captured by simple filters encoding the intensity difference as in Viola and Jones [2]. Similarly, front views of cars also have distinctive patterns, such as the dark shadow region right below the car, and dark tire region, as shown in part III. Therefore, we have decided to apply the methods developed for face detection to car front-view detection using MATLAB R2015a software.

II. PREVIOUS WORK

A. Adaboost / Viola JonesFace Detector

Adaboost [4] is a meta-algorithm that is designed to boost the performance of any existing classifier. A popular choice of weak learner is decision tree of depth 1, which is simply a classifier that depends only on a single feature. When the number of features is very large, as in the case of rectangular features in [2], Adaboost can be viewed as a feature selection procedure. More than 45,000 features were tested in [2] and more than 170,000 features were tested in our work, but the discriminative features are only a very small fraction of it. Finding and computing only the discriminative ones is far more efficient than attempting to evaluate them all.

The biggest contribution of Viola and Jones [2] was in improving the speed of the detector to real time. This was possible due to some clever observations: evaluating only the necessary features chosen by Adaboost, using cascading structure to quickly reject negative samples, and using very simple features that are fast to evaluate using integral image.

Reducing the time spent on classifying negative samples is very important in reducing the time to evaluate an image, since a typical image has around 1~13 cars and 110,000 sub-windows of non-car. Viola and Jones [2] have used a cascade style detector that could quickly reject negative samples by evaluating only a few features. It is mentioned in their paper that cascading improves the running time by 10 times while slightly decreasing the accuracy. A less known benefit of cascading is that it effectively uses more training data (particularly more negative samples) than one would normally be limited by the time and computational resource needed for training. Each stage of cascade only trains on the samples that passed the previous stages, and since only a very small fraction of the negative samples pass through the previous stages, each stage can train on a small sample while having the effect of training on a much larger set. . Figure 1 (a) shows some of the images that were collected, Figure 1 (b) shows cropped region of front-view cars, and Figure 1 (c) shows cropped regions used for negative training images.

(a)

(b)

(c)

Figure. 1. (a) Images Collected from an Overhead Bridge (b) Cropped Regions of Cars (c) Cropped Regions of Non-Cars

B. *Extensions on Viola-Jones*

After the success of Viola and Jones [2], there have been a lot of extensions to their method, such as extension of the feature set by Lienhart and Maydt [5], extensions on the weak classifier and boosting method by Wu et al. [3], a tree structured cascade for multi view face detection by Huang et al. [6], and so on. In this paper, we have also examined the original work of Viola et al. [2]

III. OWN WORK

A. *Dataset*

The images were collected from an overhead bridge at Jalan Sri Putri using IPhone 6s with a camera quality of 12 megapixels. The images were taken at 5 in the afternoon as there would be many cars passing by and it would be a vital way to increase our positive training images. A total of 680 images of cars were collected and 80 images were set aside for the final testing. Of the remaining 600 images, 1040 cropped regions of front-view cars were extracted and sent for training.

Figure 2 shows the first 3 filters chosen by the boosting process. The shadow below the car is the most discriminative feature, and the left and right tire region are the second and third most discriminative feature. The quality of the detector is measured on the 80 images reserved for testing.

For the training images, we have managed to resize the images, using a software called, IrfanView [7], to a size of 100x100 to yield a better performance and it would be easier for us to execute the training process. Figure 3 shows how IrfanView graphical user interface looks like.

Figure. 2. First three filters selected by Adaboost

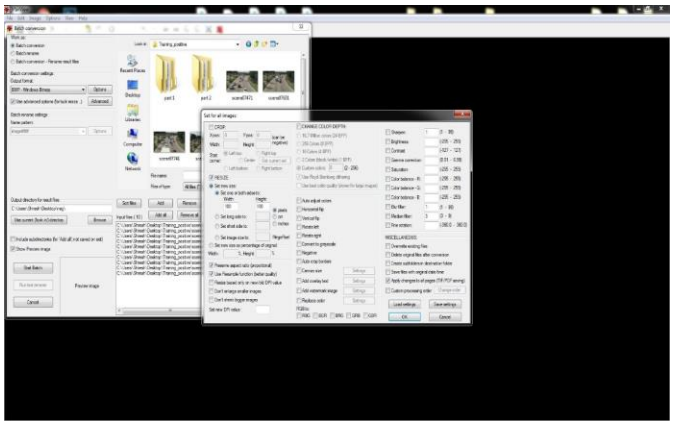

Figure. 3. IrfanView software for resizing and formatting image

B. *Real Adaboost*

Viola and Jones [2] have used discrete Adaboost and decision stump (single level decision tree) as the weak classifier. Upon comparisons, two versions of discrete Adaboost and Real Adaboost, the three settings were (1) a decision stump, (2) a slightly more complex binary classifier, and (3) Real Adaboost. The first two methods with binary classifier are trained with discrete Adaboost and the third method is trained with real Adaboost [8]. The algorithm for method (3) is given in Figure 4. Practically, method (3) gives the best performance and method (2) and (1) gives slightly lower performance. Even in the second and third case, no compromise in speed needs to be made if the weak classifier is stored as a look up table [3].

We have also noticed with weak classifier using 2 features to create a 2-dimensional histogram. This yielded in better performance in training set but gave slightly worse performance in testing set, which suggests the classifier have over fitted the training set given the power of a more complex classifier [8].

- Given example images $(x_1, y_1), \ldots, (x_n, y_n)$ where $y_i = -1, 1$ for negative and positive examples respectively.
- Initialize weights $w_i = \frac{1}{2m}, \frac{1}{2l}$ for $y_i = -1, 1$ respectively, where m and l are the number of negative and positives respectively
- for $t = 1, \ldots, T$
  - For each feature j
    - a real valued weak learner is defined as $h_j = \frac{1}{2}\log\left(\frac{p_{t,j}}{n_{t,j}}\right)$ where $p_{t,j}$ and $n_{t,j}$ is the weighted histogram of feature j for positive and negative respectively weighted with w_i
  - Choose the classifier h_t with the lowest error ε_t where error is computed by thresholding the real-valued confidence at zero and classifying as positive when greater than zero and classifying as negative when less than zero.
  - Update and normalize the weights

$$w_i \leftarrow w_i \exp(-y_i h_t(x_i))$$

$$w_i \leftarrow \frac{w_i}{\sum_{j=1}^{n} w_j}$$

- The final strong classifier is

$$h(x) = \sum_{t=1}^{T} h_t(x)$$

Figure. 4. Real Adaboost Algorithm

C. Dataset

We trained a cascade detector, which returns an XML file. We used that XML file to detect objects, cars (only from front-view) in this case, in an image. As we are going to use MATLAB R2015a, we have our MATLAB R2015a software installed on our PC along with image processing and computer vision toolboxes.

The process is of two steps:

- Train our cascade detector with all the data files.
- Use the output XML file to detect objects in a picture.

Figure 5 shows our line to train the data, which eventually gives an output xml file

```
'trainCascadeObjectDetector('shireshskudai.xml', mydata, negativeFolder);'
```

Figure. 5. MATLAB code line to train data

Figure 6 shows an overview on how the process works and how the XML is generated. Picture courtesy, MATLAB main web page.

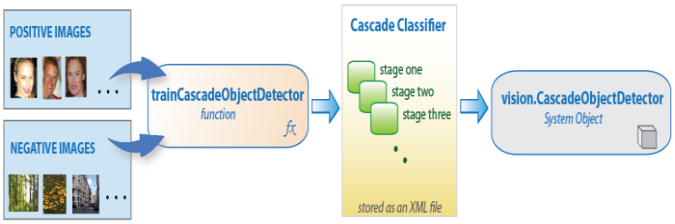

Figure 6 Overall process generating XML file

The first argument, an xml file is going to be saved in our current directory (MATLAB command window), so we used that to detect cars front-view. Next argument is a struct file in MATLAB, which is the data of all positive images. It contains two fields namely, 'imageFileName' and 'objectBoundingBoxes'. Size of this struct file would be 1x960 in this case as we have 960 positive images. Before doing so, Figure 8 is the graphical user interface of Training Image Labeler, we created a vector file containing all positive training images with the help of Training Image Labeler application which can be found in MATLAB. Figure 7 shows the lines needed to run to create the bounding box of 960 positive training images and Figure 9 shows the struct file containing positive training images.

```
mydata= struct('imageFilename', 'Just a random string', 'objectBoundingBoxes', 'Just a random string');

for i=0:549,
 mydata(i+1).imageFilename = strcat('trainImagesPos/pos-', num2str(i), '.pgm');
 mydata(i+1).objectBoundingBoxes = [1, 1, 100, 40]
end
```

Figure. 7. MATLAB code to create bounding box

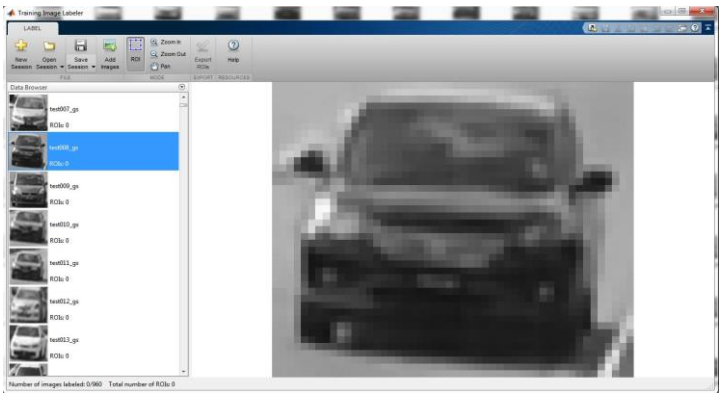

Figure. 8. Training Image Labeler Application

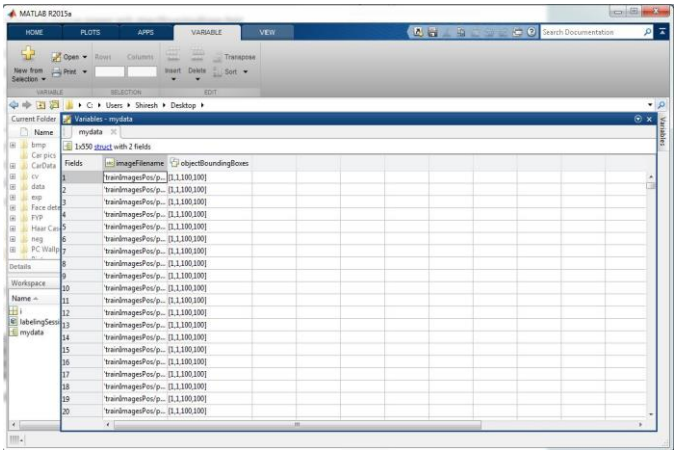

Figure. 9. MATLAB Struct file Positive Training Images

Furthermore, the third argument, 'negativeFolder' is just a folder containing negative images. We did not need of bounding boxes for negative images. So, no need of thing like struct. For a good training, there should be a large number of negative images. As the number of negative images in the dataSet are relatively low, we copied and pasted a lot of our personal images into that trainImagesNeg folder. Figure 10 shows the line to assign the folder path to this variable named negativeFolder,

```
negativeFolder=
fullfile('C:\Users\Shiresh\Documents\MATLAB\carD
etection\carData\trainImagesNeg');
```

Figure. 10. MATLAB code to assign Negative folder

IV. RESULTS

A. Training Images Process

Like we have discussed in part III, there were 960 images of cars front-view cropped and 1676 negative images which are non-front-view of cars sent for training. The number of stages training process went through was 15 and three selected features were chosen. The software used for training images was MATLAB R2015a as discussed in part III. This process took about 5 hours to complete 15 stages of training. Figure 11 and Figure 12 are the screenshots taken while training the images.

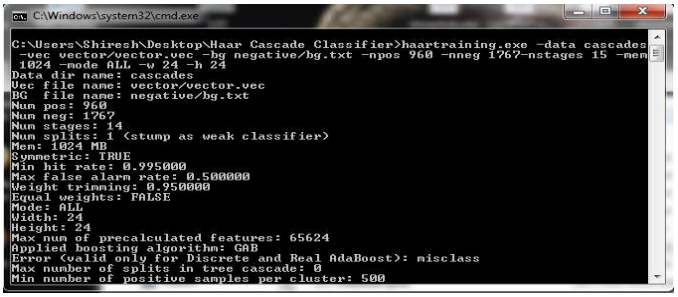

Figure. 11. Training Process

Figure. 12. Training Process Stage 14

As said earlier, we have allocated 90 images of cars moving on a highway snapped from an overhead bridge for testing purpose. The images were captured using Iphone 6 with a camera quality of 12 megapixels. Figure 13 is an example of images sent for testing.

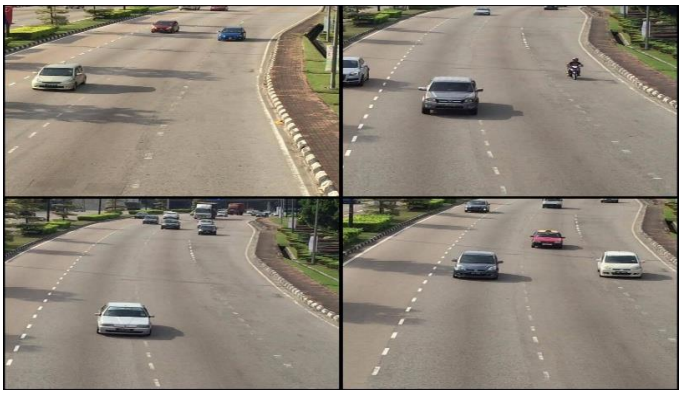

Figure. 13. Example of Images for Testing

Fortunately, the outcome of the testing pictures turned out to have a good performance overall. Figure 14 shows the MATLAB code to run our trained detector on an image file. Whereas, Figure 15 is an example of a few images collaged together after car front-view were detected.

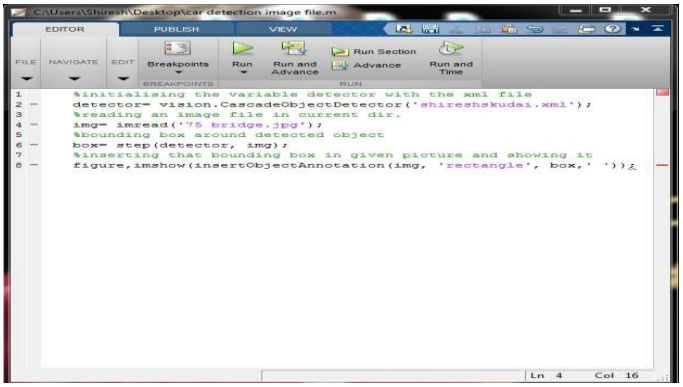

Figure. 14. MATLAB code to run trained detector on Image file

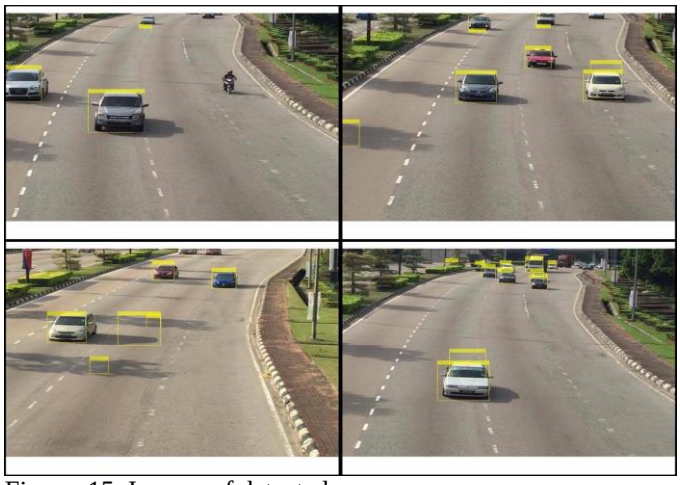

Figure. 15. Images of detected cars

From the results obtained, we have come up with Table I to analyse our performance result.

Table I. Performance Result for Car Detection

File Name	Hits	False	Miss
processed_images/0 bridge.jpeg	9	2	0
processed_images/1 bridge.jpeg	5	2	2
processed_images/2 bridge.jpeg	7	4	1
processed_images/3 bridge.jpeg	8	2	0
processed_images/4 bridge.jpeg	9	2	0
processed_images/5 bridge.jpeg	8	1	1
processed_images/6 bridge.jpeg	9	1	0
processed_images/7 bridge.jpeg	6	2	1
processed_images/8 bridge.jpeg	7	0	0
processed_images/9 bridge.jpeg	8	1	0
processed_images/10 bridge.jpeg	7	3	0
processed_images/11 bridge.jpeg	8	0	0
processed_images/12 bridge.jpeg	9	1	0
processed_images/13 bridge.jpeg	9	1	0
processed_images/14 bridge.jpeg	6	1	1
processed_images/15 bridge.jpeg	7	0	0
processed_images/16 bridge.jpeg	3	0	0
processed_images/17 bridge.jpeg	6	1	1
processed_images/18 bridge.jpeg	14	2	0
processed_images/19 bridge.jpeg	6	1	0
processed_images/20 bridge.jpeg	5	2	0
processed_images/21 bridge.jpeg	10	1	2
processed_images/22 bridge.jpeg	8	2	0
processed_images/23 bridge.jpeg	8	3	0
processed_images/24 bridge.jpeg	9	3	0
processed_images/25 bridge.jpeg	9	2	0
processed_images/26 bridge.jpeg	4	2	0
processed_images/27 bridge.jpeg	4	4	0
processed_images/28 bridge.jpeg	4	2	0
processed_images/29 bridge.jpeg	3	0	0
processed_images/30 bridge.jpeg	5	1	0
processed_images/31 bridge.jpeg	3	2	0
processed_images/32 bridge.jpeg	7	4	0
processed_images/33 bridge.jpeg	4	2	1
processed_images/34 bridge.jpeg	6	3	0
processed_images/35 bridge.jpeg	4	2	0
processed_images/36 bridge.jpeg	4	2	1
processed_images/37 bridge.jpeg	4	3	0
processed_images/38 bridge.jpeg	6	2	0
processed_images/39 bridge.jpeg	6	4	0
processed_images/40 bridge.jpeg	7	7	0
processed_images/41 bridge.jpeg	7	3	0
processed_images/42 bridge.jpeg	4	3	0
processed_images/43 bridge.jpeg	5	3	0
processed_images/44 bridge.jpeg	7	3	0
processed_images/45 bridge.jpeg	5	3	0
processed_images/46 bridge.jpeg	5	4	0
processed_images/47 bridge.jpeg	4	3	0
processed_images/48 bridge.jpeg	6	4	0
processed_images/49 bridge.jpeg	6	5	0
processed_images/50 bridge.jpeg	6	4	0
processed_images/51 bridge.jpeg	9	3	1
processed_images/52 bridge.jpeg	6	1	0
processed_images/53 bridge.jpeg	14	2	0
processed_images/54 bridge.jpeg	12	2	1
processed_images/55 bridge.jpeg	17	4	0
processed_images/56 bridge.jpeg	13	2	1
processed_images/57 bridge.jpeg	10	2	0
processed_images/58 bridge.jpeg	6	2	0
processed_images/59 bridge.jpeg	10	3	0
processed_images/60 bridge.jpeg	8	4	0
processed_images/61 bridge.jpeg	8	3	0
processed_images/62 bridge.jpeg	8	3	0
processed_images/63 bridge.jpeg	7	4	0
processed_images/64 bridge.jpeg	8	4	1
processed_images/65 bridge.jpeg	10	5	0
processed_images/66 bridge.jpeg	10	4	0
processed_images/67 bridge.jpeg	13	3	0
processed_images/68 bridge.jpeg	9	2	0
processed_images/69 bridge.jpeg	6	3	0
processed_images/70 bridge.jpeg	7	3	0
processed_images/71 bridge.jpeg	9	1	0
processed_images/72 bridge.jpeg	11	2	1
processed_images/73 bridge.jpeg	4	1	0
processed_images/74 bridge.jpeg	6	2	0
processed_images/75 bridge.jpeg	5	1	0
processed_images/76 bridge.jpeg	4	0	0
processed_images/77 bridge.jpeg	5	2	0
processed_images/78 bridge.jpeg	2	1	0
processed_images/79 bridge.jpeg	4	1	0
TOTAL	567	182	16

Hits = Car Detected
False = False Positive Detection
Miss = False Negative Detection

V. DISCUSSION

A. Calculations

Calculations:

Total number of cars = 583

Number of cars detected = 567

Numbers of cars not detected = 16

Positive rate = (567 / 583) x 100% = 97.26%

Negative rate = (16 / 583) x 100% = 2.74%

As we can see above, the positive rate is very high and in contrast, the negative rate is very low. This proves that the algorithm we used yielded a magnificent performance and almost every car in the 90 images were detected. Meanwhile, there were 16 cars not detected and that is due to other objects blocking the car, for instance light pose, other vehicle, advertising board, motorbikes and trees. The drawback of this system is that the number false positive detection is relatively high and it seems disturbing. This could probably be because of the resolution of our testing images. On another note, when the testing is done using an input file of video, the number of false positive detection decreases drastically. There is always a way to improve on that aspect. Figure 16 shows the MATLAB code to run our trained detector on a video file.

VI. CONCLUSION

In conclusion, we have carefully studied and observed the face detection method developed by Viola and Jones [2] and applied it to car front-view detection. The results with the best training process are shown in Table 1. Basically, on the 80 images set aside for the final testing, there were a total of 583 cars and 567 of them were correctly detected (97.26%) and there were 182 false positives.

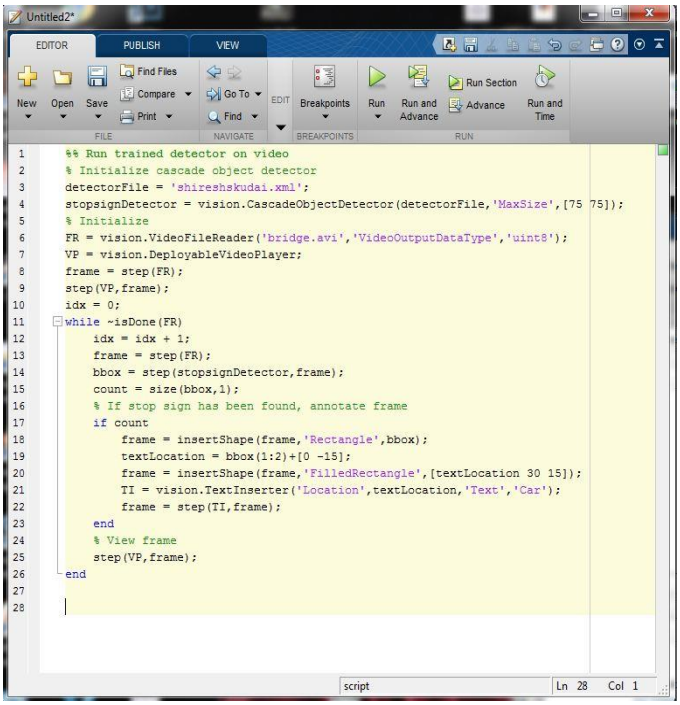

Figure. 16. MATLAB code to run trained detector on video file

REFERENCES

[1] Paul Viola and Micheal J. Jones, “Robust Real-Time Face Detection” *Inter-national Journal of Computer Vision* (IJCV), 2004.

[2] Paul Viola and Michael Jones, “Robust Real-time Object Detection” *Inter-national Journal of Computer Vision* (IJCV), 2004.

[3] Bo Wu, Haizhou Ai, Chang Huang, “Fast Rotation Invariant Multi-View Face Detection based on Real Adaboost”, *International Conference on Au-tomatic Face and Gesture Recognition*, 2004

[4] Y. Freund and R. E. Schapire, “A short introduction to boosting”, *Journal of Japanese Society for Artificial Intelligence*, 14(5):771-780, September, 1999

[5] Rainer Leinhart and Jochen Maydt, “An Extended Set of Haar-like Features for Rapid Object Detection,” *IEEE ICIP 2002*, Vol. 1, pp. 900-903, Sep. 2002.

[6] Chang Huang, Haizhou Ai, Yuan Li, and Shihong Lao, “Vector Boosting for Rotation Invariant Multi-view Face Detection,” *International Confe-rence on Computer Vision (ICCV)*, 2005.

[7] Boudreaux, Ryan (23 August 2011). "IrfanView: A robust (and free) image editor for your toolkit". TechRepublic.

[8] David C. Lee, and Takeo Kanade. "Boosted Classifier for Car Detection." 2007

Smart Advertising Robot with Image Recognition

Nik Ahmad Faisal Bin Mohd Kamarolzaman
Faculty of Electrical Engineering
Universiti Teknologi Malaysia
Johor Bahru, Malaysia.
nikfaisal05@gmail.com

Yeong Che Fai
Department of Mechatronics and Robotics
Faculty of Electrical Engineering
Universiti Teknologi Malaysia
Johor Bahru, Malaysia.
cfyeong@fke.utm.my

***Abstract*—This paper describes project to improve and interrupt digital advertising board market. The demand for the digital board keep on increasing and there is potential market to improve the system to make it more interesting. Instead of using current digital billboard approach, the project suggests to use moving robot carrying digital display and provide interaction with user either for advertisement, directory listing, and digital menu for restaurant. Most outdoor advertising has the issue to provide statistics of the ads performance. The analytics can be used to further improve ads shown at the boards. By using Microsoft Cognitive Services, the project can now analyze emotion, gender, and age group of people interacting with the advertising robot. Crowd profiling is useful to record user interaction preferences.**

Keywords— advertising analytics;face recognition; Autonomous navigation,

I. INTRODUCTION

This project sparks when our collaborator was approach by customers from shopping mall and retail restaurant that want to find other creative way to blast ads and attract people to their property. Recognizing the potential of the solutions, the team started to build prototype to validate the response for the solutions. Along the way, we noticed that the application can be varying from directory listing and menu listing for restaurant.

II. LITERATURE REVIEW

A. Bluebotics Geneva Airport Information Counter

Bluebotics has worked with Geneva Airport to develop information counter moving robot. The robot managed to move around in the airport environment around dynamic environment which involve people walking around[1]. The robot can gives guide to the users on where about of location inside building. Bluebotics claimed they use ANT navigation developed by Bluebotics themselves [2].

Fig. 1. Bluebotics Geneva Airport Information Counter.

B. Beam Telepresence Robot

The Beam Telepresence robot uses same differential drive system which is can apply to current project. The hardware design is simple and cost wise is better. The height of the screen need to be consider and adjustable height adjustment of the screen can be implemented. This robot is for users to interact with other people in remote location with the features of user can control the robot. Hence, telepresence robot name. This robot is a plain video conferencing system on a drive-able robot[3] .

Fig. 2. Beam Telepresence Robot.

III. METHODS

A. System Architecture

The project integrates different platform for different functions of the robot features. Among them is Microsoft Cognitive Services, Robot Operating System, Universal Windows Platform, Microsoft SQL Azure, and Microsoft Power BI. The navigation part of the project is using ROS [4]. The main software is running Universal Windows Platform.

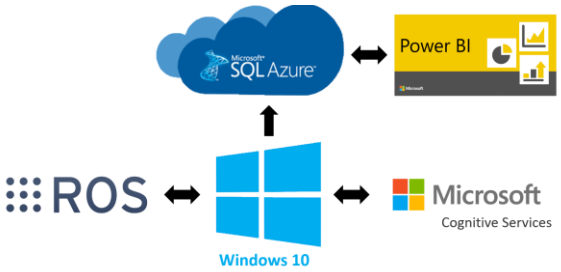

Fig. 3. System Overview.

B. Digital advertising

For our very first prototype, navigation part of the robot was to used standard ROS navigation stack in which it has path planning feature to

C. ROS-based Navigation

Robotic Operating System framework is used For our very first prototype, navigation part of the robot was to used standard ROS navigation stack in which it has path planning feature to let the robot moves around the obstacle by simply set the final point or target where the robot want to go. But different needs were found, instead of letting the robot plan and moves around, the planning part is removed to ensure the robot movement is within pre-plotted waypoints. One of the team members wrote part of navigation code for our collaborators and instead of reinvent the wheel, we will use the company navigation stack which is very easy to use.

D. ROS-based Navigation

For our very first prototype, navigation part of the robot was to used standard ROS navigation stack in which it has path planning feature to let the robot moves around the obstacle by simply set the final point or target where the robot want to go. But different needs were found, instead of letting the robot plan and moves around, the planning part is removed to ensure the robot movement is within pre-plotted waypoints. One of the team members wrote part of navigation code for our collaborators and instead of reinvent the wheel, we will use the company navigation stack which is very easy to use.

To localize itself, the robot use Adaptive Monte-Carlo Localization (AMCL) package [5]. Initial approximate coordinate in map must be set first to localize in the map correctly after any movement that are referencing to the laser data and encoder data.

We wrote navigation code to handle straight line movement and Bezier curve movement. In the map, path is pre-plotted based on these 2 types of path. For straight line, initial coordinate and final coordinate is needed.

Bezier Curve have 4 coordinates that determines the curvature of the line. We interpolate the curve to be use as reference by the robot [6]. Both of navigation type calculate linear error and angular error to be feedback to the robot base.

E. User Interface

In order to do targeted advertising, the project need to have vision analysis to process gender, age group and emotion. Instead of training new model using large datasets, we found out that Microsoft Cognitive Services has useful API to perform the analysis. The Face API, Emotion API, and Vision API is used in the project to make it more interesting to the people around. Adding value to the interactivity itself.

For Face API, person profiling can be integrated to offer ads or service based on the person preferences. The application can greet people by the name (if manual profiling was done) and show ads based on their interaction history with the robot. For targeted ads based on demographic alone can be used for initial interaction user with the robot.

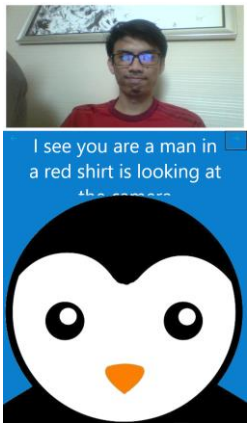

Fig. 4. User Interface.

F. Cloud based Database and Analytics

The project uses Microsoft SQL Azure to store data collected from the vision analysis. The data can be further visualized by using Microsoft PowerBI. From there, because of advertisement, advertiser can access the dashboard to improve their ads content based on data collected.

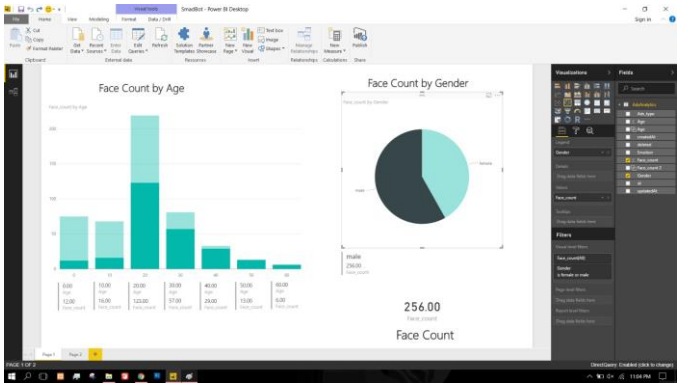

Fig. 5. Data analytics using Microsoft PowerBI.

G. Robot Mechanical

Fig. 6. CAD design of Smart Advertising Robot.

Fig. 7. Final Look Smart Advertising Robot.

The robot mechanical is using 2 brushless dc motor for non-holonomic movement[7]. The zero turning radius movement help the robot to rotate at one place.

IV. RESULT

The robot able to move autonomously based on pre plotted waypoints in a shopping malls and event. Double safety features which is R2100 Multi-Ray LED Scanner and bumper is working the way we expected. For now implementation of socket programming between UWP apps and Linux based ROS is lacking, yet it is still working on obstacle detection to stop and the function is redundant.

Since we wanted the robot to interact with the crowd, we added intelligent function for vision based on Microsoft Cognitive Services. As for now, the robot can speak means the speech synthesizer is working. But from user to the robot communication is based on touch screen monitor and vision control.

The front panel currently operates as event and malls approach and its operated in the following way:

- On face detect, the robot will greet and predict age and gender as to showcase the intelligent part.
- The robot notifies the user that it will show advertisement
- Advertisement shows based on demographic. After a while advertiser can choose whether to popup message to let the user to play game and claim coupon or discount based on QR code.
- Current game is based on emotion in which user need to show certain emotion to complete the game.

V. DISCUSSION

Current vision analysis system in need of reliable internet connectivity because of the trained model by Microsoft is on the Internet. Most of application in shopping malls, restaurant and event management must have internet connectivity to make sure this robot working. However, if there is no internet connectivity the panel will only show random advertisement to the user.

Smart Advertising Robot can be tailored to different needs of customer like restaurant, shopping malls, event management, museums and surveillance. However customized application need to be build to cater different application of the robot. As for this stage, the robot only caters for general event or malls advertisement display.

The cost of the hardware and sensor have been main concern, current development was overdesigned to ensure smooth research and development process. The hardware and sensor part of the robot can be further driven down to use cheaper sensor and motor.

VI. CONCLUSION

From our first prototype of the robot, we perform series of test in real scenario in which the robot interacts with people. A lot of feedback collected from the crowds has been used to improve functions of the robot. Using Microsoft Cognitive Services and Microsoft SQL Azure has cut development time of the project. Instead of train empty model with big dataset, the robot can just use the API to use well-trained model by Microsoft.

There is more to be done to achieve more functionality of the smart advertising robot. Using speech recognition and speech synthesizer altogether with Microsoft Bot Framework will further increase interactivity of the robot with the user. One more thing can be implemented is advertisement upload page which can be accessible to any advertiser to check their dashboard for ads performance and upload the advertisement itself.

REFERENCES

[1] BlueBotics: Mobile Robots at Your Service with ANT Navigation. (2016). Bluebotics.com [Online], Available: http://bluebotics.com, [Accessed May 10 2017]

[2] Tomatis, N. (2011). BlueBotics: Navigation for the Clever Robot [Entrepreneur]. *IEEE Robotics & Automation Magazine*, *18*(2), 14-16. http://dx.doi.org/10.1109/mra.2011.941629

[3] Herring, S. (2013). Telepresence robots for academics. Proceedings Of The American Society For Information Science And Technology, 50(1), 1-4. http://dx.doi.org/10.1002/meet.14505001156

[4] Open Source Robotics Foundation, "ROS: Robot Operating System" [Online] , Available: www.ros.org, [Accessed May 10, 2017].

[5] Gerkey, B. P., "AMCL ROS package" [Online], Available: http://wiki.ros.org/amcl, [Accessed May 10 2017].

[6] Jolly, K.G., Sreerama Kumar, R., Vijayakumar, R.: A Bezier curve based path planning in a multi-agent robot soccer system without violating the acceleration limits. Robotics and Automation Systems, vol. 57, pp. 23--33 (2009)

[7] Robert Holmberg, Oussama Khatib(2000, November). Development and Control of a Holonomic Mobile Robot for Mobile Manipulation Tasks.[Online]. Available: http://journals.sagepub.com/doi/abs/10.1177/02783640022067977

Automated Guided Vehicle(AGV) For High Mix Low Volume Manufacturing Industry

Poh Hung Yong
Faculty of Electrical Engineering
Universiti Teknologi Malaysia
Johor Bahru, Malaysia.
hungyongpoh@gmail.com

Rosbi bin Mamat
Department of Control and Mechatronic Engineering
Faculty of Electrical Engineering
Universiti Teknologi Malaysia
Johor Bahru, Malaysia.
rosbi@fke.utm.my

***Abstract*—Automated Guided Vehicles will become the necessity needs in the industrial world when automation takes over the world. There are different kind of AGV in the market and towing AGV have been used in this project because of the robust design and cost effective purposes. In a continuous changing industrial, a customize AGV is needed with high flexibility. Therefore, this work focus on developing a customize AGV with a normal AGV function and addition of a custom Graphic User Interface (GUI). Magnetic sensor is used to detect the magnetic line for AGV to navigate from one place to another. Magnetic approach is used because of the robustness compare to using colour sensor to detect colour where magnetic will not be affected by the surrounding light intensity. The configuration of sensor placement also stated in this project. Proportional Integral (PI) control is also used to control the output of the motor to be smoother. Graph is plotted when tuning the motor to acquire a more precise result and adjustment of the PI values. Arduino is used as the central processing unit (CPU) for the motor control and line following program. GUI is designed to let user to be more easily interact with the AGV and can manually to order the AGV to a specific location by clicking button. Qt creator is used as the platform for the GUI interface where the programming language is C++. This system provides a more flexible platform for company to directly access to AGV system. AGV able to correctly navigate to the specific location by following the schedule or task given. It can function normally as the other AGV.**

***Keywords*—AGV; GUI; Qt creator;hall effect sensor; colour sensor; arduino; PID; scheduling.**

I. INTRODUCTION

Automated Guided Vehicle (AGV) was built and introduced in 1953. It was built from tractor and used to moving raw materials or products from one place to another place. In the late 1950 and early 1960, AGV started to implement in many factories. In 1974, Volvo plant has largely deployed the use of AGV in Kalmar, Sweden. In 1984, more than 1500 AGVs is used in 3300 factories across the world [1]. AGV is widely used because it can increase the efficiency of production line, prevent aging workforce and protect the safety of workers. Moreover, Company used AGV to perform difficult reach task, highly repeatability task and also dangerous task. These enable humans to perform other tasks that required more challenges or thinking skills. AGV is implemented to focus on handling material from one place to another but now AGV has transformed into another type which AGV works with robots to perform welding or painting task [2]. AGV required a centralized control system to control its path and destination, although there can be on-board intelligence installed inside the AGV itself, making it able to communicate with other AGV when performing tasks.

AGVs have been transformed from the old type of towing into three main types of AGV which are Tractor type, Unit Load type and Forked type. Tractor type is to pull a trolley from behind the AGV. Unit Load type AGV floor plan is designed based on the factory's production line layout, which means AGV can share the workspace with other worker because AGV only occupy a specific space for a while to get the jobs done. The guide path is flexible, as high mix low volume company required changes from time to time, the guide path can be changed in a matter of minutes. AGV have different path to be guided which includes wired path, guide tape, natural and vision. Wired means wire must be embedded down the floor along the pathway of AGV need to follow. Guide tape means to put a tape whether is magnetic tape or colored tape along the guide path for AGV to track and follow. Natural guidance means AGV using range finder like laser range finder to detect the path to follow. Vision guidance is to use camera to know the path to follow.

II. LITERATURE REVIEW

A. wheel of AGV

In the manufacturing industry, the AGV developed mostly uses differential wheel. It is because differential wheel has the zero radius turning degree and is easier to control compared to other configuration of wheel [3] and [4]. Differential wheel is chosen because of the easy configuration and the simplicity in the design. Differential drive also has high precision where slip will not occur easily. Differential drive enables a more precise line follow with only controlling 2 motors. Figure 2.5 shows the differential drives.

B. guidance of AGV

Most of the industry used guided magnetic type to guide the AGV because the installation steps is easy [4]. By using magnetic as the guidance of AGV, AGV can determine its

position by scanning on the magnetic tape on the floor. Using line following method with magnetic provides the AGV with high accuracy and flexibility which will also increase the cost as well [4].

C. controller of AGV

Nowadays, RPi is starting to get more popular when it can function as a controller while having its own interface which is like a mini computer. RPi is already implemented in the industry to make car for a factory when Peugeot Citroen car engineer uses RPi to make robot [5]. RPi have many function but only sold at low cost. RPi is also used to create a management system in a sports stadium by using multiple sensor [6]. It controls the audio, video output, lighting and fragrance of the stadium.

While considered RPi is also stable and able to create a User interface for the user. RPi is selected as the controller for GUI while microcontroller is used as a low level control system to control motor and sensor data.

D. tuning method of AGV

Proportional Integral Derivative (PID) controller is widely used in the industry to control the speed of motor. The simplicity to apply the control method to a system and able to get the desired output make many users to implement it in their system. PID controller can be divided into 4 parts, P controller, PI controller, PD controller and PID controller. Different type of controller fits for different system. P in PID control the proportional gain or transient time while I in PID enables to eliminate the offset and D in PID is to eliminate the overshoot from the define value [7].

E. Type of AGV

Towing AGV is commonly seen in factories where AGV towed trolley from one end of the factory to the other end. A single tractor AGV is used to compare to multiple tractor AGV. Simulation is carried out and indicates that multiple tractor reduce the effectiveness of AGV [8].

III. PROJECT METHODOLOGY

In product design, there are 2 main controller is going to be used in this project, which is raspberry pi 3 and Arduino Mega. Raspberry Pi 3 is mainly in charge of the high level design which is creating a GUI for user to operate the AGV, communicating with the server through Wi-Fi and communicating with Arduino to send data. Moreover, Arduino Mega is used for the low level design which is motor control, data acquisition and process of sensor data, communicating with Raspberry pi and user input.

Fig. 1 .AGV

Fig. 2. Floor plan

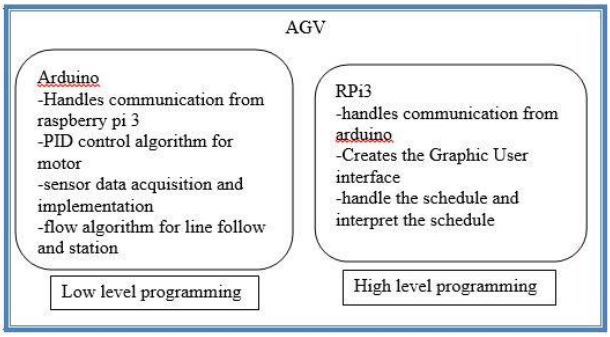

Fig. 3. Overview of AGV system

A. Raspberry pi 3 and GUI

Raspberry Pi 3 is used as the controller for Graphic User Interface in AGV. It also acts as the intermediate point to connect the server (computer) to the AGV. Raspberry Pi 3 provides a Raspbian operating system which is similar to the Linux interface then many programmers are familiar. RPi3 also preloaded with many different programming languages which allow user to program using python and communicate with the other devices. RPi3 also have a WI-FI integrated onto the board and does not need an external shield for it to connect to the router to communicate with the server. Overall, RPi 3 is a low cost microcomputer which can integrate with different electronic device while have its own user interface [9].

The purpose of creating GUI is to enhance user experience when using AGV and let them operate the AGV by ordering the AGV to move to the desired destination in the program. The GUI is programmed to create a text file that loaded with information when a button in the GUI is clicked. The text file is then used to communicate with the server or Arduino.

The GUI can perform four tasks. The first task is by security which call the user to key in log in user and password before using. Secondly, User can view the status of AGV on where the AGV is moving to. Thirdly, the interface able to upload the table from server. Lastly, the interface also let the user to key in manually by setting the AGV current and next destination.

B. Arduino Mega

Arduino Mega 2560 is a microcontroller which based on ATmega2560. It has 54 Digital Input Output pin where 15 of it provides Pulse Width Modulation (PWM), 16 analog pins and 4 Universal Asynchronous Receiver Transmitter (UART) which is enough to use to combine sensor reading and motor reading. Arduino is used to get sensor reading because sensor needed an analog output from Arduino which Raspberry Pi did not have. Arduino Mega is a microcontroller which is used to control the motor speed and movement. Sensor data acquisition, filter and processing also included in Arduino.

C. Ultrasonic Sensor

Fig. 4. Ultrasonic sensor

Hc-Sr04 is one of the ultrasonic sensor which will transmit ultrasonic wave to measure the distance from the object to the HR-Sr04 sensor. The ultrasonic sensor is used for obstacle sensing whether to detect a human passing by or even object blocking the way of the path AGV is directed to. Ultrasonic sensor act as the safety feature so that collision between AGV and other object will not occur.

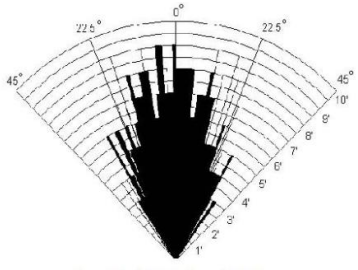

Fig. 5. Ultrasonic sensor coverage

This type of ultrasonic sensor is low cost and it is most suitable used for this project because its coverage is not too big where the effectual angle is <15°. The ranging distance is between 2cm-400cm and the resolution is only 0.3cm. Due to the ultrasonic sensor only detects for obstacle in front of AGV to avoid collision with people or object, resolution 0.3cm is enough to detect obstacle because we do not need the detected location to be too specific. The range of detection required to detect people is around 50cm so this ultrasonic sensor is used. Fig 5 shows the ultrasonic sensor coverage.

D. Vexta driver

Fig. 6. Vexta drive

The motor driver give out speed output in the form of waveform and have a fixed interval of time for each section in the waveform. To calculate the speed from the speed output pin give out from the driver, external interrupt is used to detect the rising or falling edge of the signal in order for use to calculate the speed output of the motor.

In the datasheet, the driver speed output pin will give out a constant length (in millisecond) of a full pulse. The full pulse will have different pulse width of bit 1 and bit 0 which depends on the speed given to the motor. If the PWM given is at full speed, the pulse width will be equal to the full pulse length.

$$frequency = 1/(current\ time - previous\ time) \quad (1)$$

By calculating the speed of the motor, frequency is needed to calculate first. Since external interrupt only executed the function calculatepos() when it detected the rising edge of the signal sent out from the speed output pin, we can calculate the interval between the one full pulse with another. Frequency is calculated using equation 1 and function calculatepos is in fig 7.

$$Velocity(rpm) = frequency*60/30 \quad (2)$$

$$Velocity(m/s) = velocity(rpm)*2\pi r/60 \quad (3)$$

$$Distance(m) = velocity(m/s)*(1/frequency) \quad (4)$$

After we know the frequency, velocity(rpm) is calculated by using equation 2. Equation 3 is used to convert from velocity(rpm) to velocity(m/s) to SI unit for easier calculation. Distance can also be disclose by using equation 4 to know the AGV can be travel for how long. The velocity afterwards is being used in PID to tune the vexta motor for better output.

```
void calculatepos() {   //left motor
    currentMicros = micros();
    frequency= (double)1/((currentMicros-PreviousMicros)*0.000001);
    velocityrpm=(frequency*60.0/30.0); //speed in rpm
    velocitycms=velocityrpm*100.0*3.1419*0.12/60.0/10.0;//speed in m/s
    distance= velocitycms*(1/frequency);    //convert rpm to m/s  diameter motor shaft=0.01meter ((rpm* 2pi r/60s))
    totaldistance+=distance;
    PreviousMicros = micros();   //motorspeed(rpm)=(frequency/30*60)
}
```

Fig. 7 external interrupt function (calculatepos())

E. Hall effect sensor

Fig. 8. Analog hall effect sensor

In this project, analog hall effect sensor is used because it able to detect magnetic field of -10G to 10G. Since the magnetic tape only give out 5G magnetic field, the analog can detect the magnetic field with no problem while unipolar magnetic sensor will only give out a HIGH output when it detect a magnetic field at 35G, therefore analog magnetic sensor is used. Second reasons is that analog magnetic sensor able to differentiate between both polarity and able to justify whether the route path or station path. The AGV route is made with two polarity of magnet where the normal route is North Pole while the station path is South Pole. This is to make the route to be more robust and AGV will not detect the wrong path or miscalculate station.

IV. RESULT AND ANALYSIS

This project involves both software parts which are high level part and lower level part. High level part refers to GUI while low level part refers to the motor control and sensor data acquisition, filter and processing.

A. GUI

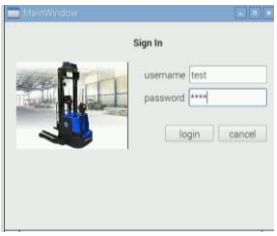

Fig. 9. Login page

AGV application is developed to perform navigation functions and status of AGV. The GUI have 3 pages which are login page, status page and path page (manual mode).

On the login page in fig 9, the user required to login in with the correct username and password in order to go into the status page. The application will pop up message to notify the user when the user has successfully login. The password and username is set in the program and read as a string when user key in the username and password.

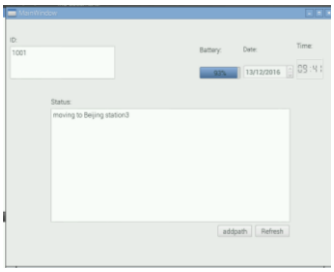

Fig. 10. Status window

After login, the user interface will show the current AGV status. The interface will show the AGV ID, Battery Level, Date and Time. There is also a status window to indicate where the AGV currently going. Fig 10 shows the interface of the status window. There is a “refresh” and “add path button” on the bottom of the status window. “Add path button” is clicked to change the interface to another interface while “refresh button” just refreshing the status display.

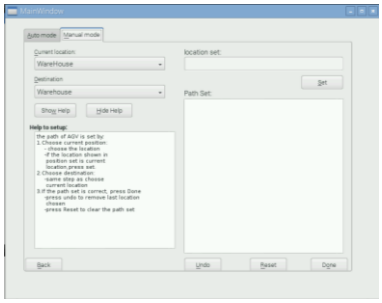

Fig. 11. Manual mode

Manual mode lets the user to select the destination of the AGV that the users want the AGV to proceed. When the user click the “Set Button”, the path set window will show the path set by the user. When done is click, the AGV will go to the destination set by the user.

B. PID control

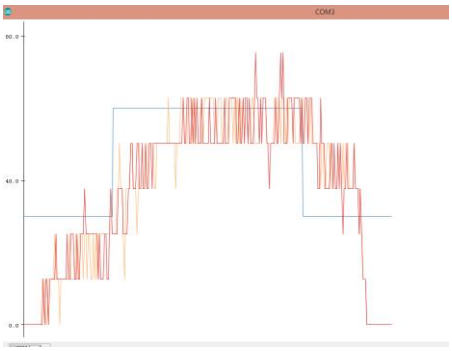

Fig. 12. PID output

PID controller is the most frequent controller used in the industry nowadays. The feedback mechanism is reliable and easy to be implemented. PID contains of 3 term which is proportional, Integral and derivative. By calculating the error which the output vary from the setpoint, PID controller is able to apply correction based on the given P,I and D values.

When tuning the PID, 3 distance and 3 speed is set and it divided into 3 section to see the response of motor. The first section is 2meter is set to speed 0.3m/s then in the next section is 6meter and is set to speed 0.6m/s and lastly is also 3meter and is set to speed 0.3m/s.

As we can see the motor react accordingly to what setpoint is given although there are some oscillation in the graph but response output is very good given that the motor can run in a straight line. Using different speed in tuning able to let us see the motor reacts from low to high speed and vice versa.

V. CONCLUSION

The floor plan is customize and the AGV is program to suit the floor. The program can be change easily to suit different floor plan according to the factory design. The GUI enable people to access and identify the problem occurred in the AGV easily. First time user also able to easily understand the interface and able to quickly operate the AGV.

The result shows that the AGV perform as expected where it can transport material from the warehouse to the station appointed. Even with different lighting condition, the AGV able to perform task as appointed. Magnetic line follow is prove to be same as detecting colour of line. GUI also prove t be useful as the operator does not need to go to the control centre to control the AGV but just access to the AGV on the spot. AGV also can be troubleshoot easily as a monitor is place on the AGV. By applying these into the AGV, AGV can have less breakdown time while more operating time.

REFERENCES

[1] J. Zygmont, "Guided vehicles set manufacturing in motion," *High Technology*, p. 16, December 1986.

[2] S. Yaghoubi, S. Khalili, R. M. Nezhad, M. R. Kazemi and M. Sakhaiifar, "DESIGNING AND METHODOLOGY OF AUTOMATED GUIDED VEHICLE ROBOTS/ SELF GUIDED VEHICLES SYSTEMS, FUTURE TRENDS," *International Journal of Research and Reviews in Applied Sciences*, vol. 13, no. 1, 2012.

[3] S. Yu, C. Ye, H. Liu and J. Chen, "Development of an omnidirectional Automated Guided Vehicle with MY3 wheels," *Perspectives in Science*, vol. 7, p. 364—368, 2016.

[4] G. J. Cawood and I. A. Gorlach, "Navigation and locomotion of a low-cost Automated Guided Cart," *2015 Pattern Recognition Association of South Africa and Robotics and Mechatronics International Conference (PRASA-RobMech), Port Elizabeth*, pp. 83-88, 2015.

[5] "PEUGEOT CITROEN: RASPBERRY PI FACTORY ROBOT," The MagPi Magazine, [Online]. Available: https://www.raspberrypi.org/magpi/peugeot-citroen-robots/. [Accessed 29 November 2016].

[6] Designerz, "Raspberry PI and Arduino in industrial environments," DESIGNSPARK, 29 April 2016. [Online]. Available: https://www.rs-online.com/designspark/raspberry-pi-and-Arduino-in-industrial-environments. [Accessed 29 November 2016].

[7] X. Li, C. Luo, Y. Xu and P. Li, "A Fuzzy PID controller applied in AGV control system," *2016 International Conference on Advanced Robotics and Mechatronics (ICARM)*, pp. 555-560, 2016.

[8] U. Bilge, Tanchoco and J.M.A, "AGV Systems with Multi-Load Carriers: Basic Issues and Potential Benefits," *Journal of Manufacturing Systems*, vol. 16, no. 3, 1997.

[9] H. Guerra, A. Cardoso, V. Sousa, J. Leitão, V. Graveto and L. M. Gomes, "Demonstration of programming in Python using a remote lab with Raspberry Pi," *2015 3rd Experiment International Conference (exp.at'15), Ponta Delgada*, pp. 101-102, 2015 .

Balloon Networked Control System

Nurul Amirah Binti Azman
Faculty of Electrical Engineering
Universiti Teknologi Malaysia
Johor Bahru, Malaysia.
nurulamirahazman@outlook.com

Nurul Adilla Binti Mohd Subha
Department of Control and Mechatronic Engineering
Faculty of Electrical Engineering
Universiti Teknologi Malaysia
Johor Bahru, Malaysia.
nuruladilla@utm.my

***Abstract*— The paper is concerned with the design of multiple balloon-networked control system with direction angle control. It presents a low cost networked multi-agent system consisting of multiple balloons, where each of them comprises a wireless fidelity (Wi-fi) for signal communication. One balloon is called master agent who able to receive signal from the user at ground-based station and able to transmit signal to other agents. Other agents are called slave agent will receive the transmitted signal from the master agent and execute the order immediately corresponding to the received signal. Consequently, all agents will reach the consensus for direction angle of the balloon.**

Keywords— network control system, multi-agent, Wi-Fi, balloons

I. INTRODUCTION

Networked Control System (NCS) is a control system where the control loops are closed through a communication network. The basic elements for NCS are sensors, controller, and actuators of a digital controller reside on different computer nodes linked by a communication network. The application of NCS is aim to overcome the disadvantages of conventional digital control system, such as difficulty of modification, vulnerability to electrical noise, difficulty in maintenance and upgrades, at the application level. The research of the NCS is categorized into two: (1) *Control over network*; and (2) *Control of network*. Control over network deals more with control strategies and control system design over the network to minimize the effect of adverse network parameters on NCS performance [8]. Control of network is more on study and research on communications and networks to make them suitable for real time NCS, such as routing control, congestion reduction, networking protocol, etc. The project that is being discussed in this paper is the application of the control over network of NCS.

The application of NCS can be seen in various industries for example, unmanned aerial vehicles (UAV), remote diagnostic and troubleshooting, space and terrestrial exploration, access in hazardous environments, manufacturing plant monitoring and also tele-operations

The application of helium balloons to access dangerous and hazardous environment is proven in several case studies [14]. It is also frequently use for other scientific research purposes, for example, in weather or atmosphere research which is used to gather information on the temperature, wind speed, humidity, atmospheric pressure and also use for mapping geographical area. A balloon networked control system can fly ceaselessly for undetermined periods (provided enough energy supply using battery or solar energy), achieve steady buoyancy, and also suitable for high altitude [4]. Balloon is chosen as an agent to minimize cost of monitoring and maintenance. Besides that, during launching, it does not require high technical skills. Therefore, with these advantages, this research proposes the use of helium balloons for balloon-networked control system with direction angle control.

II. METHODOLOGY

A. General Construction

Figure 1 shows the general construction of an agent of the balloon networked control system, which made up of balloon, string, box, servo motor, as well as fan. For this project, a 36 inch latex balloon with helium as lifting gas is chosen as an agent. There will be no potential hazard and no ecological damage resulting from the use of the helium as it is natural, non-flammable and non-toxic gas. The box is made up by 3D printing material.

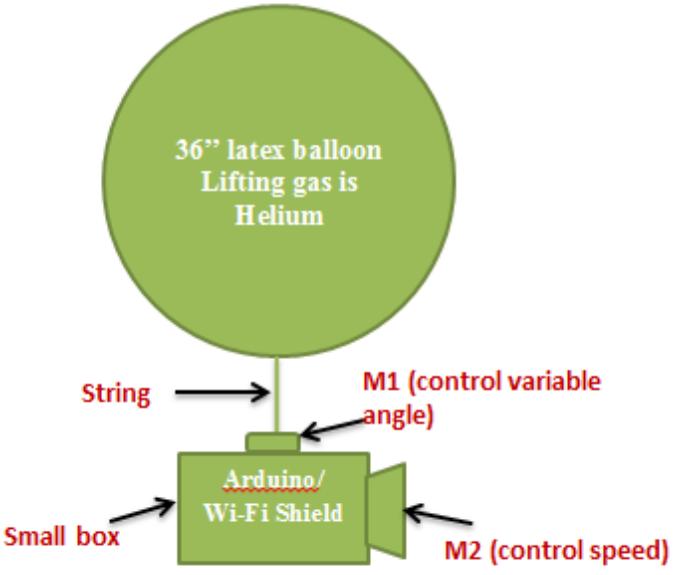

Figure 1: Hardware setup for each agent

B. Project Overview

There are two major parts that need to be fulfilled the design specification of the project which involves the hardware and software part. In the hardware, there are four components that are used, which are arduino UNO, ESP8266 Wi-Fi shield and two servo motor. The arduino UNO is used as microcontroller for the overall system such as processing the input, execute the instruction and also real time monitoring. In order to use the Wi-Fi as the communication network, ESP8266 Wi-Fi Shield is choosing as the communication platform as it is completed with transmitter and receiver. A fan is attached to a servo motor to drive the agent forward, while another motor is attach to the top of box to change the direction angle of the balloon. In software part, it involved the coding and programming of arduino UNO for processing input, execute the instruction as well as real time monitoring. BLYNK application is used as the user interface as a platform to control the arduino UNO by sending the input to the microcontroller to be executed.

The proposed system was divided into two parts; the development of the single agent and the communication between the agents.

a. The development of the single agent (balloon)

In this part, the structure for the single agent (balloon) was built. The main objective is to change the direction of the balloon using BLYNK application. The BLYNK application was installed in the smartphone. The main components used to build the single balloon are helium balloon, stacked up arduino UNO with ESP8266 Wi-Fi shield, the attached servo motor on the top of the box and the widget button used in the BLYNK application. These components are shown in Figure 3.

Figure 2: Helium balloon for a single agent

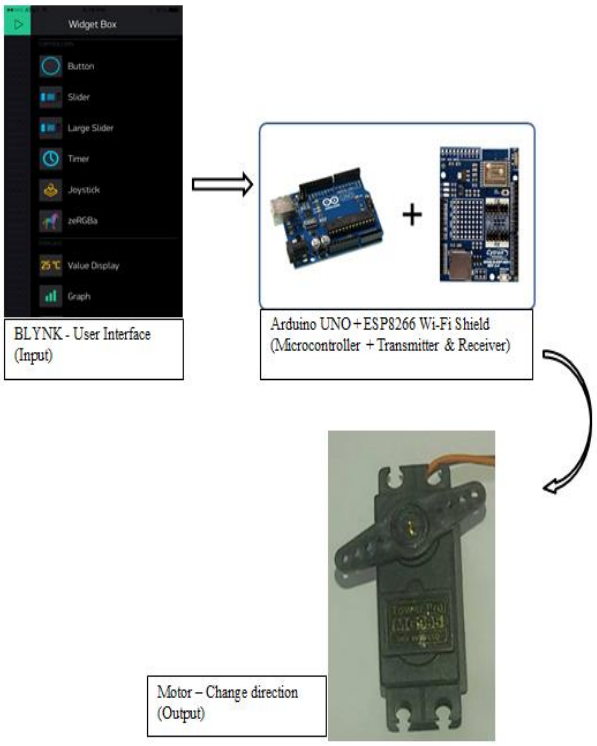

Figure 3: The electronic components for a single agent

b. The communication between the agents

For this part, the communication between two agents over Wi-Fi was established. The components involved are two set of arduino UNO, which act as the microcontroller and two set of Wi-Fi shield as communication platform. The master agent (Agent 1) will received the input from the user at the ground – based station simultaneously sends the signal to another agent (Agent 2). This involved a client-to-server communication model. Figure 4 shows the concept of the communication between the agents.

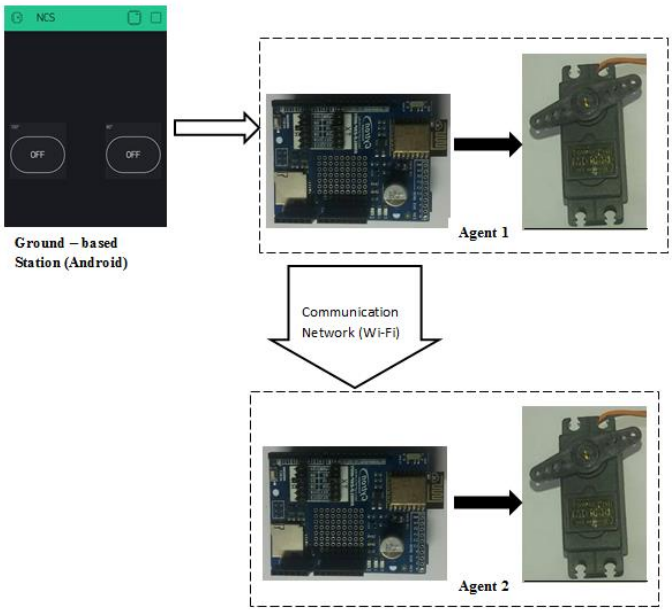

Figure 4: General concept of the communication setup between the agents

III. Result and Discussion

A. *The System of A Single Agent*

Firstly, the connection between the laptop and transmitter/receiver need to be established. The ESP Wi-Fi Shield which, act as the transmitter/receiver, a specific IP address is used to ensure the connectivity of the internet. The IP address can be obtained from the Serial Monitor after the sketch is uploaded. The IP address is entered to any search bar of web browser. As the webpage shown the display that has been set in the sketch, the connection is successfully established.

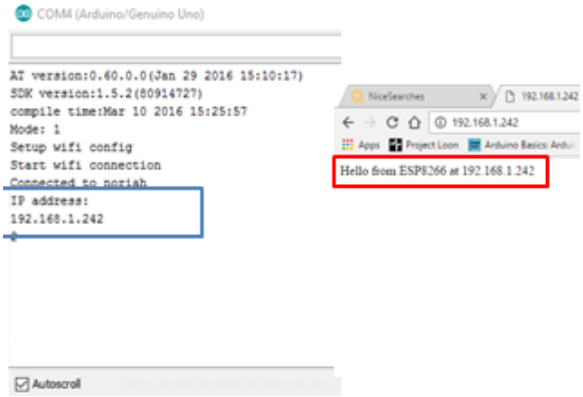

Figure 5: Serial monitor and display from IP address

Next, a simple test is done in order to develop the communication between arduino UNO board and BLYNK. The test involves a LED and a button widget in the BLYNK application. When the button in the BLYNK is on, the LED is supposed to light up. In order to do that, a simple sketch that involving the communication between the board and BLYNK is uploaded. The functions in the figure 6 not only involve the communication between arduino UNO and BLYNK application, but also ESP Wi-Fi Shield as well. This shows that the communication between the microcontroller and the android application is possible and sending instruction also possible.

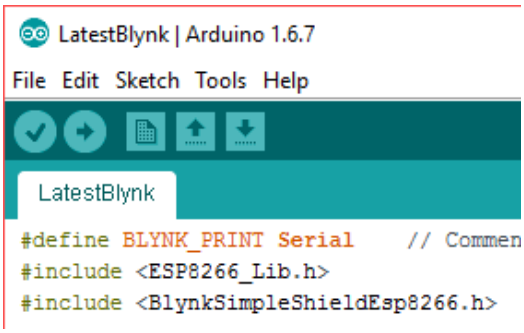

Figure 6: Functions of ESP library and BLYNK

Since the communication between the stacked up UNO, Wi-Fi shield and the BLYNK application is established, the previous sketch is combined with the sketch for servo motor. In this coding, the virtual pin is used to send any data from the arduino to the BLYNK and vice versa. The widgets used for this part are two buttons, where the first button is defined with 145 degree and the second button is define with 35 degree. When the first button is pressed, the motor moved its angle to 145 degree from the original position. Hence, the direction of the balloon is also changed as the motor is attached to the box containing the electronic components.

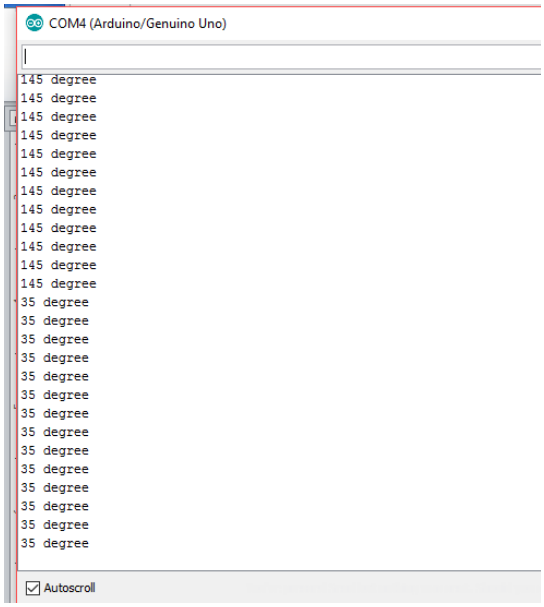

Figure 7: Results when button pressed

B. *The Communication Between The Agents*

Once the components are assembled, the connection between the microcontrollers is set up. A simple programming was done to test the communication of the agents, where a master device sends an input to another

device which assigned as slave. The communication between the microcontrollers is successfully established once the same pipe of data is connected between the master agent and the slave agent.

To ensure that the second agent received the input that has been sent to the main agent, the signal received need to be executed simultaneously by both agents. However, a delay of execution is expected from the second agent due to the network stabilization.

IV. Conclusion

The main objective of this project is to develop the consensus of direction angle for multiple balloons-networked control system, which can be control over Wi-Fi as communication network. Using arduino UNO and ESP8266 Wi-Fi shield, the objectives of the project are successfully achieved. The two motors (agents) can be controlled through Wi-Fi by using BLYNK application as platform by pressing the widget buttons. Next, all agents achieved the consensus in direction angle even though the user's input only connected directly to the master balloon. The communication between the microcontrollers was successfully established even though with stability problem. This system has potential to be applied in wide range of application such as access to dangerous environments and hazardous activities.

References

[1] E. N. Mambou, G.M. Yamga, J. Meyer & H. C. Ferreira (2016). Development of a helium gas balloon flying system for aerial photographing and observation. Communication Software and Network (ICCSN), 2016 8th IEEE International Conference on. 681 – 685

[2] I. Vandermeulen, M. Guay, & P. J. Mclellan (2016). Formation control of high-altitude balloons by distributed extremum seeking control. American Control Conference (ACC). 2524 – 2529

[3] Y. Shibata, Y. Sato, N. Ogasawara, G. Chiba, & K. Takahata (2009). A New Ballooned Wireless Mesh Network System for Disaster Use. Advanced Information Networking and Applications, 2009. AINA '09. International Conference on. 816 – 821

[4] S. Kubo, A. Sakaguch, & T. Takimoto (2014). Development of flying observation system with helium gas balloon and tilt rotors. Proc. Int. Conf. on Control Automation and Systems. 1627 – 1630

[5] B. Silva et al. (2014). Mapping Two Competing Grassland Species from a Low-Altitude Helium Balloon. IEEE Journal of Selected Topics in Applied Earth Observations and Remote Sensing, vol. 7. 3038 – 3049

[6] T. G. Guzik (2015). The High Altitude Student Platform (HASP) as a Model Multi-Payload Balloon Platform. IEEE Aerospace Conference. 1 – 10

[7] N. Inagawa, I. Yamamoto, & T. Nakamura (2009). Research on network system of unmanned flying observation robot. Proc. ICCAS-SICE. 2644 – 2647

[8] R. A. Gupta & M. Chow (2010). Networked Control System: Overview and Research Trends. IEEE Transactions On Industrial Electronics, vol. 57, 2527 – 2535

[9] A. C. Sniderman, M. E. Broucke, & G. M. T. D'Eleuterio (2015). Formation control of balloons: A block circulant approach. American Control Conference (ACC) 2015. 1463 – 1468

[10] M. Guay, I. Vandermeulen, S. Dougherty, & P. Mclellan (2015). Distributed extremum-seeking control over networks of dynamic agents. American Control Conference (ACC) 2015. 159 – 164

[11] D. Kim (2013). A Survey of Balloon Networking Applications and Technologies. CSE570S: Recent Advances in Networking – Data Center Virtualization, SDN, Big Data, Cloud Computing, Internet of Things. 1 – 13

[12] A. G. Andurkar & PrachiZodpe (2016). A Review Paper on Project "LOONS". International Journal of Advanced Research in Computer and Communication Engineering, vol. 5. 132 – 138

[13] K. Matsuo & K. Tajima (2014). A Study of Network Emulation for IP Network – Based Control System of a Small Motor. Electrical Machines and Systems (ICEMS), 2014 17th International Conference on. 2216 – 2220

[14] B. Lonneville, C. Stal, B. De Roo, B. De Wit, A. De Wit, & P. De Maeyer (2014). Helium Balloons For 3D Modeling: Off To A Flying Start? Low Cost 3D Workshop Conference.

[15] A. Fallis (2013). Arduino UNO. J. Chem. Inf. Model, vol. 53, no. 9. 1689–1699

[16] "Introducing project loon: Balloon-powered internet access", Official Google Blog, 2013, [online] Available: http://googleblog.blogspot.ca/2013/06/introducing-project-loon.html.

[17] "Loon for all - project loon", Google, 2015, [online] Available: http://www.google.com/loon/.

Water Flow Meter and Monitoring System

Muhammad Zulhilmi Bin Halim
Faculty of Electrical Engineering
Universiti Teknologi Malaysia
Johor Bahru, Malaysia.
mzulhalim43@gmail.com

Norhaliza Binti Abdul Wahab
Department of Control & Mechatronics Engineering
Faculty of Electrical Engineering
Universiti Teknologi Malaysia
Johor Bahru, Malaysia.
aliza@fke.utm.my

***Abstract*—This study about extending the flow meter reading from site to the control room using internet, simple Internet of Thing (IoT). The existing flow meter in industries need workers to go to site to take reading of flowing liquid or gas. This is sometime having their own risk to the workers if the site classified as hazardous area**

I. INTRODUCTION

Flow meters widely used in many industries around the world. Some of the industries that usually use the flow meters are the food and beverage industry, oil and gas plants and chemical or pharmaceutical factories. Flow meters used to measure the flow rate of fluid (liquid or gases) through a pipe. The factors for choice the right flow meters are fluid flow profile (laminar, turbulent, or transitional), fluid characteristics (viscosity, turbidity, single or double phase etc.). Some of other considerations are output-connectivity options and mechanical restrictions. There are many types of flow meters available that usually used in industries. Some of flow meters are, differential-pressure, electromagnetic or magmeter, Coriolis, ultrasonic (Doppler-shift and transit-time) flow meter. Each of these flow meters has their own application but its function still the same, to measure flow rate. In industry, these flow meters fixed install between two pipes and the meter's display attached together to the flow meters. In other hand, the workers need to take the reading for inspection at field. This is one of the risk that can cause accident at workplace.

II. OBJECTIVE

A. Investigate the effect of water flow before and after 90° pipe fitting

For this objective, this research would like to investigate the flow of water inside pipe before and after 90° pipe fitting. This related to investigate either the water flow in laminar flow or turbulent flow.

B. Viewing flow measurement from field to control room

The existing flow meter in industries, if the workers want to inspect the flow of liquid, they need to go to field to record the reading, but for this paper study, all the reading regarding to the flow will show directly to control room via internet or Bluetooth. But this paper focusing on internet only.

III. METHODOLOGY

This paper study used some method in lab experiment to fulfill all the objectives.

Some of the method of experiment are:

A. Designing the flow of experiment

For this study, the concept of design thinking is used to achieve the objective. In design thinking, there are several parts that can be implement as research guidelines. Design thinking involve conceive, design, implement and operate (CDIO).

Conceive is a part that where all the ideas are develop from the problems. From this part, problem statement developed. From conceive and half of design part, some of the process happen here such as sense and sensibility, empathy, ideation and prototype. Both of this part let the idea to grow more to get the better design that meet end user requirements.

In implement part, all the decision, plan and agreement made. These is involving tool, utensil or other apparatus or equipment for the purpose. Implement also involve design realization. This part needed to test the designing ideas if it is reliable or not.

The operate part is a part where all the data from testing design is collected and analyze. If there are problems occur, some modification needed to overcome the problems. Hence, fulfill the end user requirements. This part is a part that designer can implement all the engineering aspects that can be consider.

B. Flow Simulation

Flow simulation conducted by using SolidWorks software using uncomplicated design. The simulation divided by two parts, part 1 is for study the flow before the 90° pipe fitting and part 2 is for after the 90° pipe fitting. These to study the flow behavior before the 90° pipe fitting and after it.

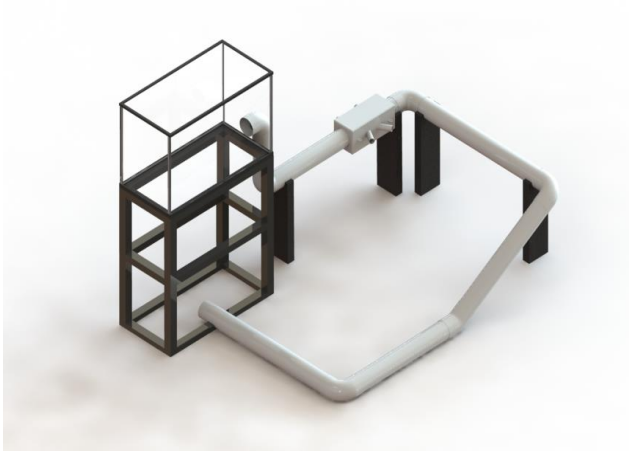

Fig. 1. The flow simulation design using SolidWorks

Fig. 1, shows the simulation design using SolidWorks. This is purposely for experiment in lab only. These also indicate the water flow from reservoir tank to the end users such as resident water supply.

C. *The System Flow*

The system flow starting from the sensor detect the water flow inside the pipe. Then, the signal from ultrasonic sensor beam from upstream transmitter to downstream receiver. When the signal reach the downstream receiver, the time of flight from the upstream transmitter to the downstream receiver recorded in microcontroller. Immediately, the downstream transmitter emits the signal to the upstream receiver and once the upstream receiver receives the signal, the time of flight from downstream to upstream recorded in microcontroller. Then different between two time of flight calculated in microcontroller as programmed. The flow measurement from microcontroller will sent to the computer and computer will process and visualize in LabVIEW.

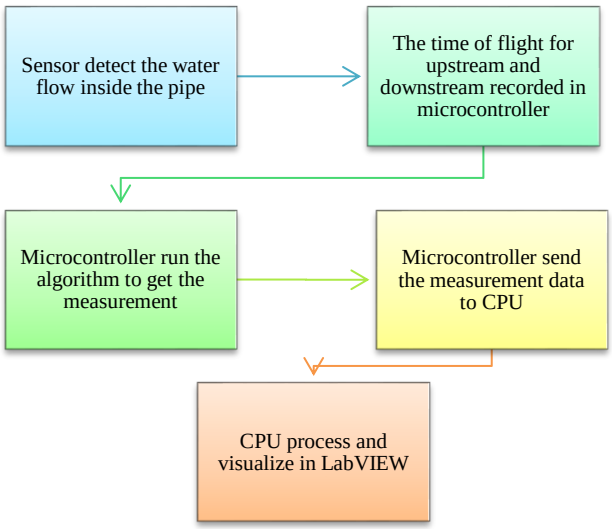

Fig. 2. The process flow of the system

IV. Result and Discussion

It covered the effect of flow before and after 90° pipe fitting and the ultrasonic sensor data based on time of flight concept. This part also included data from flow simulation done using SolidWorks.

A. *Flow Simulation*

Flow simulation done using SolidWorks software. In this experiment, the design of piping fixed in size, diameter 100 mm, as shown in Fig. 1. This flow simulation is to study the effect of the water flow in pipe before and after the 90° pipe fitting. In this simulation, three type of flow selected to study the effect of the flow before and after 90 pipe fitting such as (Laminar-Turbulent flow, Laminar flow, and Turbulent flow).

1) *Laminar-Turbulent Flow Simulation*

In this simulation, the water inlet velocity set to 10 ms^{-1}. This to make the easy way to detect any changes in velocity. Fig. 3 show the overall flow simulation for the system.

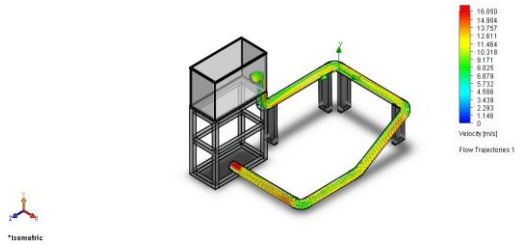

Fig. 3. Laminar-Turbulent Flow Simulation

Fig. 4 shows the flow simulation at 90° pipe fitting. As result, before the 90° pipe fitting, the flow in uniform flow of yellow and green. Yellow show the flow rate around 11 ms^{-1} while green show the flow rate around 8 ms-1. After the 90° pipe fitting, the flow slightly change and vary. The flow rate seems slightly increase (the yellow more than green).

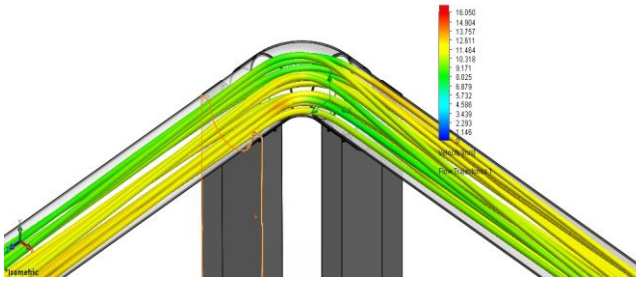

Fig. 4. Flow simulation at 90° pipe fitting

Fig. 5 shows the top view of the flow simulation at 90° pipe fitting. As result, the flow rate slightly increase after 90° pipe fitting around 11 ms-1. Besides, some orange spot shown in this

figure. This means, the flow rate at the orange spot around 13 ms^{-1}.

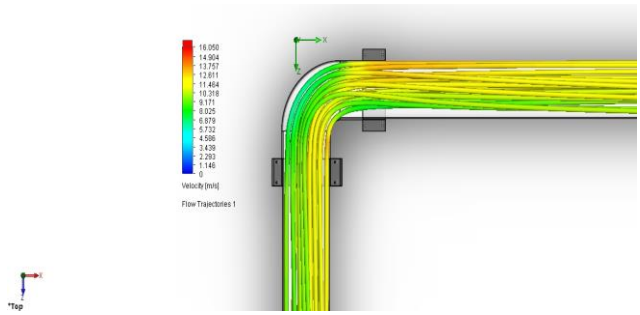

Fig. 5. Top view of flow simulation at 90° pipe fitting

2) Laminar Flow Simulation.

Fig. 6 shows the full simulation result for Laminar flow. For this simulation, the velocity of the water inlet set to 10 ms^{-1}.

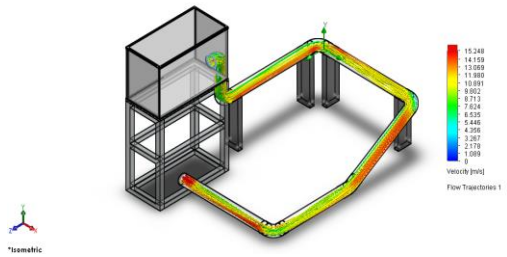

Fig. 6. Flow simulation for Laminar Flow

As result in Fig. 7, there is slightly different flow pattern before and after the 90° pipe fitting. Before the 90° pipe fitting, the flow pattern seems to be organize with variation of flow rate. At the below of pipe, the flow rate is about 13 ms^{-1}. In the middle pipe, the flow rate is about 10 ms^{-1} to 11 ms^{-1} while at top of pipe, the flow rate is about 8 ms^{-1}.

After the 90° pipe fitting, the flow pattern slightly seems to rotate. Its means, the water inside the pipe is flowing in a rotation pattern. In Fig. 8, the result shows that after the 90° pipe fitting, there is red spot at outside the pipe. This means, the velocity at the red spot is about 15 ms^{-1}.

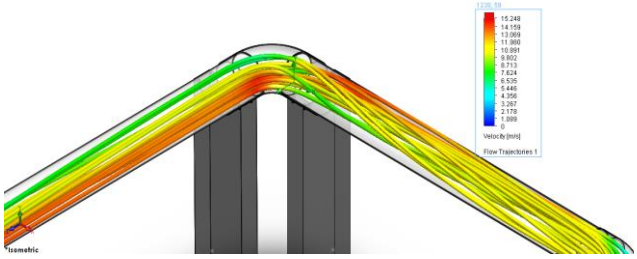

Fig. 7. Flow simulation at 90° pipe fitting

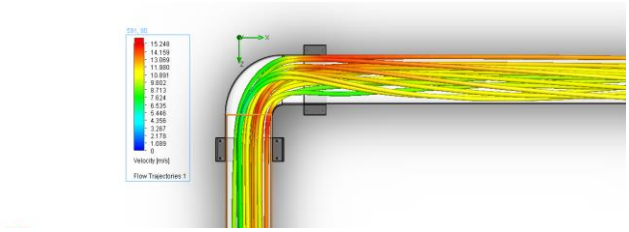

Fig. 8. Top view of flow simulation at 90° pipe fitting

3) Turbulent Flow Simulation

Fig. 9 shows the flow simulation at 90° pipe fitting. As the result, the flow pattern flow smoothly with variation of flow rate. At the bottom of pipe, the flow rate is higher than flow rate at top of pipe with about 13 ms^{-1} and 9 ms^{-1} respectively. At the middle of pipe, the flow rate is about 10 ms^{-1}.

Besides, after 90° pipe fitting, the flow pattern keeps the flow as the flow pattern before the 90° pipe fitting. But the flow rate varies from the original flow rate.

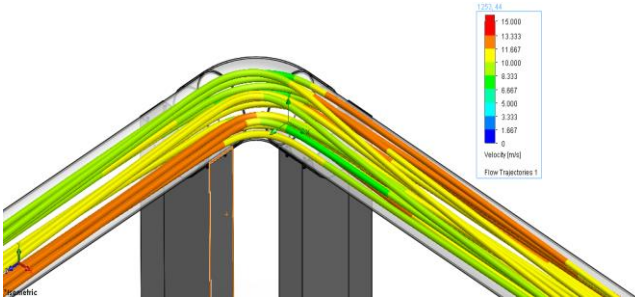

Fig. 9. Flow simulation at 90° pipe fitting

Fig. 10 show the top view of flow simulation. As result, after 90° pipe fitting, the flow rate maximum at the outside of pipe with 13 ms^{-1}, while the other side of pipe is about 10 ms^{-1}.

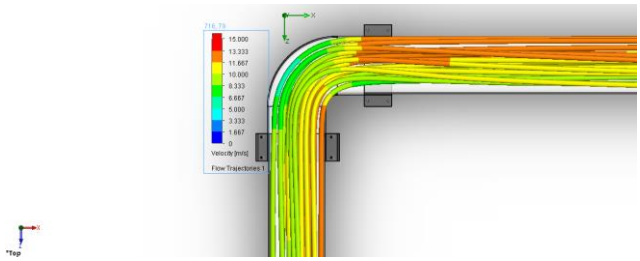

Fig. 10. Top view of flow simulation at 90° pipe fitting

V. CONCLUSION

The conclusion part made based on the overall result obtained from the simulation or experiment. From the result of simulation that has been presented in the previous chapter, it can be seen that:

1. For the laminar-turbulent flow and turbulent flow, the flow pattern of water particles seems not much different compared to the laminar flow simulation.
2. For laminar flow simulation, there is unique transformation of flow rate after the 90° pipe fitting.
3. The pressure before the 90° pipe fitting is higher than the pressure after the 90° pipe fitting for the three simulation.
4. For the laminar-turbulent flow and turbulent flow, the pressure at 90° pipe fitting's wall is at high pressure. While the laminar flow has uniform pressure at the 90° pipe fitting.

REFERENCES

[1] Yuto Inouea, H.K., Hideki Murakawa, Masanori Aritomi, Michitsugu Mori, "A study of ultrasonic propagation for ultrasonic flow rate measurement," 21 June 2007.

[2] Yong Chen, Y.H., Xiaoqian Chen, "Acoustic propagation in viscous fluid with uniform flow and a novel design methodology for ultrasonic flow meter," 22 October 2012.

[3] V.E. Sakharov, S.A.K., B.D. Zaitsev, I.E. Kuznetsova, S.G. Joshi, "Liquid level sensor using ultrasonic Lamb waves," 2003.

[4] Tao Huang, L.Q., "Chaos Theory Based Ultrasonic Doppler for Velocity Measurement of Fluid in the Petroleum Channel," Fifth International Conference on Natural Computation, 2009.

[5] Slavik Lubomir, R.J., Novak Miroslav, "Optimization of magnetic circuit in electromagnetic flow meter," 17th International Carpathian Control Conference, 2016.

[6] Santhosh KV, B.R., "An Intelligent Flow Measurement Technique using Ultrasonic Flow Meter with Optimized Neural Network," International Journal of Control and Automation 4 December 2012, 5(4).

[7] Sanehiro Wada, K.T., Noriyuki Furuichi, "Effect of low-frequency ultrasound on flow rate measurements using the ultrasonic velocity profile method," Journal of Nuclear Science and Technology, 10 May 2013.

[8] Noriyuki Furuichi, H.S., Yoshiya Terao, Masaki Takamoto, "A new calibration facility for water flowrate at high Reynolds number," 4 November 2008.:

Mobile Robot for Outdoor Monitoring

MOHAMAD FIRDAUS BIN MOHD NOR
Faculty of Electrical Engineering
Universiti Teknologi Malaysia
Johor Bahru, Malaysia.
apihfirdaus207@gmail.com

Nasarudin Ahmad
Department of Control and Mechatronic Engineering
Faculty of Electrical Engineering
Universiti Teknologi Malaysia
Johor Bahru, Malaysia.
e-nasar@utm.my

Abstract- The proposed automated unit is utilized for video surveillance of remote place and also remotely control of the unit utilizing Wi-Fi as medium. Raspberry pi fill the need of server and also the microchip for the framework. An implanted web server makes a simple route for observing and controlling any gadget which is at remote place. Video is caught through the webcam set on the automated unit and vivacious transmitted to the remote end. Controls are given on the comfort page where one can see the live spilling and additionally can control the development of mechanical unit. This paper gives an approach towards video surveillance and control utilizing propelled processor like raspberry pi. The proposed framework can be utilized as a part of military applications just by including couple of sensors like infrared sensors so as we can distinguish the developments. In medicinal services applications the proposed framework can be utilized just by changing the plan the automated unit.

I. INTRODUCTION

An installed web server makes a simple path for observing and controlling any gadget which is at remote place. For planning the framework we require remote pc alongside the internet facility at the remote areas. On the off chance that we don't have web network still we can utilize the unit utilizing Wi-Fi. We actualize a framework which is versatile, minimal effort and having less upkeep. The detailing of this ongoing information relating to the procedure plants is along these lines be of extraordinary use for future investigation.

As the internet of things is the concept, newly introduced in the field of electronics. The concept is about handling the things with the use of internet and the best model for these applications is raspberry pi. When the surveillance is considered, raspberry pi serve his purpose as it is good at connectivity because it is ready embedded with Wi-Fi features.[5].

Robots are being utilized as a part of assortment of modern applications for different exercises like pick and place, painting, gathering of subsystems and in perilous spots for material taking care of and so on. Robots are ending up plainly more progressed as innovation addition in the regions of CPU speed, sensors, recollections and so forth. Also, there is perpetually requesting applications even in protection. With the quick development of the Internet, an ever increasing number of cutting edge gadgets or sensors have been implanted into it for playing out the coveted work, conveyed PC frameworks, reconnaissance cameras, telescopes and controllers. In spite of the fact that the usage of Internet mechanical autonomy or online apply autonomy is moderately new and still in its initial stage, it has accumulated the enormous enthusiasm of numerous scientists on the planet.

The proposed system consist of two units mainly a robotic unit and remotely control unit. The robotic unit is consisting of the webcam the heart of the project, raspberry pi along with the MDD10A containing motor driven IC and step-down dc-dc converter.

II. SYSTEM OVERVIEW

A. Manual mode

Here in this project, one can control the robot from remote end say mobile or laptop with the use of Wi-Fi as well as Internet and also we can get the live streaming of video from the robot for the purpose of surveillance, this video is obtained on web browser of the remote device from where we are operating the device also we are able to control the robotic movement. DC motors are being used for the movement of robotic wheels and servo motor is used for camera movement. Raspberry Pi B+ is used for video processing and sending the processed video to user PC with the help of Wi-Fi as well as internet.

The wheels of robot are controlled by DC motor and the development of camera by the servo motor. With the assistance of web program, one can without much of a stretch controls the automated unit and can screens video gushing of the encompassing condition of that robotic unit. At the robotic unit, Raspberry pi is utilized for the control of DC engines and servo motor. Raspberry Pi requires 5 volt supply with least of 1500-2000mA current. This raspberry pi is controlled through small scale USB link. 5 volt is required for the USB ports. It works at 700 MHz. We can utilize python to compose the code into the raspberry pi.

B. Autonomous mode

Secondly, Autonomous mobile robot for this application will use Neo-6M GPS module. Many considerations have been made for this application. The main factor for the consideration is the 4 channel GPS receiver designed to operate with L1 frequency and GPS receiver continuously tracks and uses the signal to compute and update position. Small sizes make it light and easy to handle and also can be use in rugged terrain because of water proofing. Due to minimum power requirement which is 3v it is suitable for autonomous mobile robot that needs longer power for localization and navigation. With proper calibration the accuracy will be ±2 with ±5 degrees extreme northern and southern latitudes and 1 degree resolution.

Along the navigation from the first waypoint to final waypoint sonar sensor will detect the obstacle within range.

Basic principle of movement of mobile robot is avoid the obstacle and after successfully avoid the particular obstacle mobile robot will correct the waypoint from the current position. This paper focused on the sonar sensor for obstacle avoidance system. The selection of sonar sensor is base on the specification of the sonar sensor.

On the mobile robot three sonar sensors implemented in front of mobile robot for obstacle avoidance system. For each left and right the position of the sensor are 20 cm in between with 45 angle and one sonar sensor in the middle of left and right sonar sensor.

The left and right sensor will detect the obstacle on each side and the centre sensor will detect the opposite obstacle of mobile robot. The system did not include back sensor because mobile robot only avoid obstacle by moving left and right only. From this experiment output data from the sonar sensor using pulse width output. Pulse data can be converted to centimetre or inches from equation (1) and (2).

$$Distance(inches) = \frac{\#microsecond}{58} \quad (1)$$

$$Distance(inches) = \frac{\#microsecond}{148} \quad (2)$$

III. HARDWARE REQUIREMENT

For the manual mode, raspberry pi is used to control and monitor the robotic unit. A webcam is connected to one of its USB ports. A Wi-Fi dongle is already provided so that raspberry can communicate over Wi-Fi. Internet can be provided to the raspberry through this. Secondly, a GPS module and sonar sensor is required for the navigation of the mobile robot and the obstacle avoidance system.

A. Raspberry Pi

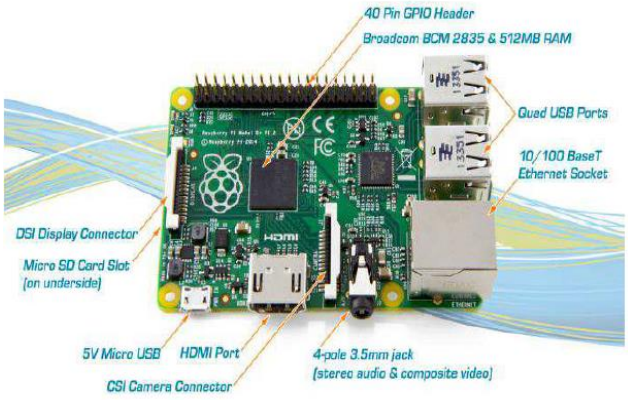

Fig 1. Raspberry Pi development Board

The Raspberry Pi is a minicomputer PC which can be utilized as a part of electronic applications or ventures, and for a hefty portion of the things that your desktop PC likes, browsing, word processing and amusements. It additionally plays top quality video and it has an inherent Ethernet Connection so one get simple network, at any rate for the most widely recognized sheets. What's more, we can without much of a stretch include Wi-Fi availability by module a Wi-Fi dongle on one of the USB port. Raspberry Pi B+ has a solid preparing limit in light of utilizing the Linux-based framework. there are basic and simple utilized open source peropheral driver libraries [3].

B. MDD10A

MDD10A is the dual channel version of MD10C which is designed to drive 2 brushed DC motors with high current up to 10A continuously. Just like MD10C, the MDD10A also supports locked antiphase and sign-magnitude PWM signal. It is also using full solid state components which result in faster response time and eliminate the wear and tear of the mechanical relay. This motor controller has been designed with the capabilities and features of:

- Bi-directional control for 2 brushed DC motors.
- Support motor voltage ranges from 5V to 25V.
- Maximum current up to 10A continuously and 30A peak (10 second) for each channel.
- Solid state components provide faster response time and eliminate the wear and the tear of mechanical relay.
- Fully NMOS H-Bridge for better efficiency and no heat sink is required.
- Speed control PWM frequency up to 20 KHz.
- Support both locked-antiphase and sign-magnitude PWM operation
- Onboard push button to control the motor manually.

C. DC Motor

Generally speaking, motors serve the function of (rotationally) accelerating some components, and torque is what provides this acceleration. Most systems at some point have to accelerate from an angular velocity of 0, in one direction or the other, which is another way of describing the condition where the "starting torque" value is applicable. In many cases, the magnitude of that acceleration, and the quickness the device reaches its operating speed (angular velocity), the better the performance is considered. So for this mobile robot, IG-42 dc motor is used due to the high torques..

IV BLOCK DIAGRAM

A. Manual Navigation

The robotic unit comprises of, a raspberry pi camera, an motor driver and venture down dc-dc converter hardware. The User unit comprises of a PC inside the Wi-Fi extend. HTML page is composed having alternatives of controlling the dc engines and stepper engines. It demonstrates the live video

streaming of the environment..

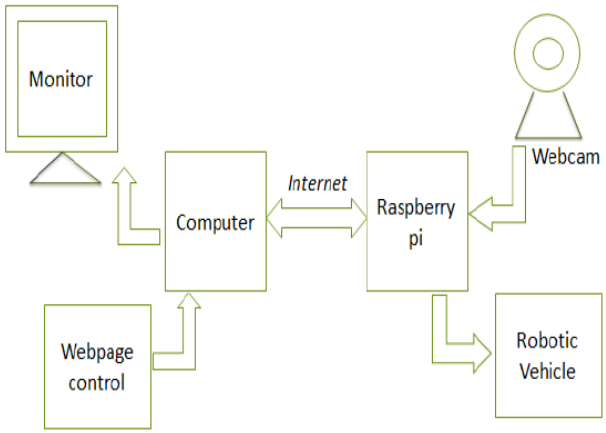

Figure 2: Manual navigation diagram for input and output

The raspberry unit is powered via the micro USB connector, only the power pins are connected, so it will not transfer data over this connection. A standard modern phone charger with a micro USB connector or a portable power bank will do, providing it can supply at least 700mA at +5Vdc [6].

B. Auto navigation

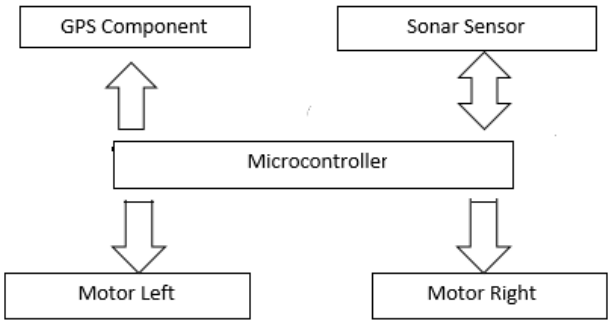

Figure 3: Block diagram for microcontroller input and outputs

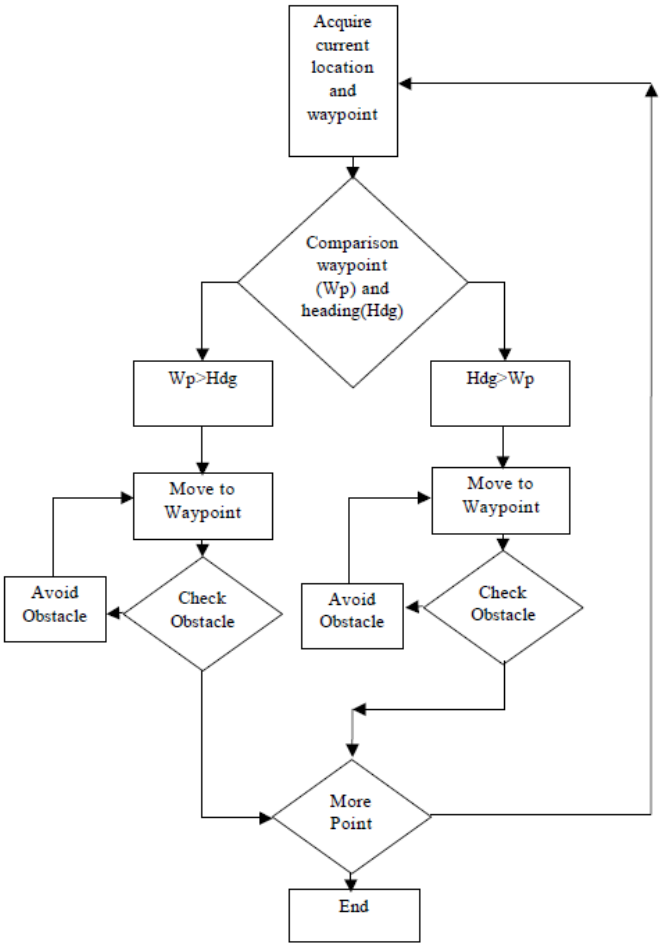

Figure 4: Flow chart for GPS navigation and obstacle avoidance

Global Positioning System (GPS) is widely use in navigation and localization. Nowadays many vehicles are equipped with GPS for navigation from desire route. From the GPS user can determine which direction they should follow with time and other data such as bearing etc. This project will benefit the use of data transmit from satellite to GPS module.

V. IMPLEMENTATION METHOD

A. Manual navigation

Model comprises of a web camera, voltage controller hardware with MDD10A motor driver and raspberry pi. The ongoing video and control are shown in the website page which can be seen from anyplace on the planet utilizing web or inside the Wi-Fi range and one can control it utilizing those control gave.

a) Setting up the raspberry pi and installation of operating system from raspberrypi.org. Here we used raspbian OS.Selection

b) Install the required packages in the pi using suitable commands in terminal window and connect the webcam to the pi, after this you will get MJPG streamer folder.

c) Now design the control page that provides a way to control our robot this page is designed with HTML and PHP and write the controlling of the robot code based on the MDD10A we have used.

d) To setup wifi configuration,we can use ifconfig command. Once we got the IP address we can use it for controlling purpose.

e) Now build the robotic unit, we can use DC motor based simple robot. To control the motor, we need the MDD10A for controlling teo motors.

f) Connection of power supply. Here we used 12v rechargeable battery for driving the motor.

g) Pi gets turn on as soon as you connect 5v supply; you can see green LED blinking while start-up process. After some time open browser in the Laptop or mobile and write down following link: IPaddress/filename

B. Auto navigation

The setting is only different on the implementation of the sonar sensor and the GPS module.

VI EXPECTED RESULT

a) Manual navigation

Utilizing this automated framework a remote region can be checked effortlessly from remote end. One can without much of a stretch screen and also control the action of the mechanical unit. This framework can be utilized any conditions and territories where it is troublesome for the security powers to achieve it can screen the zones. As the correspondence is finished with the assistance of web so restriction of scope of operation does not emerge and along these lines we can screen any remote regions. In the event that this robot is inside the Wi-Fi go there is no need of web as well. We control the robot utilizing the Wi-Fi as a medium.

b) Auto navigation

The mobile robot can move as indicated by preset waypoint with hindrance evasion executed in the framework. The precision of the route profoundly rely on upon the flag from satellite with change from 4 to 12 enter satellites. The exactness of hitting the stamp can float from 10 feet to 20 feet. In the event that the waypoints are preset starting with one point then onto the next between 12 feet and the precision is 20 feet the waypoint 1 and 2 will be perceive as one point. To make framework more compelling because of the less exactness of the framework the preset waypoint should be a long way from every more than 20 feet.

The obstacle avoidance can detect rock and small tree on it path. The main issue of the obstacle avoidance system are the detection of the grass as an obstacle can make the system unreliable. The position of the sonar sensor needs to move higher than the grass.

VII CONCLUSION

We can utilize this framework for military applications introducing appropriate sensors. Just by changing the automated unit plan we can utilize it in doctor's facilities for patient checking. Utilizing some substance sensors we can recognize destructive gas spillage in the chamber the time postpone which happens in the execution of orders can be diminished and in this manner we can have all the more ongoing access to the robot. With lessened time postpone we can have speedier operation and fast reaction to any unlawful exercises in the observed zone. Additionally it can be utilized as a spy robot. The robot is exceptionally practical.

REFERENCES

[1] [1] Wi-Fi Robot for Video Monitoring &Surveillance System By Pavan C & Dr. B.Sivakumar, International Journal of Scientific & Engineering Research Volume 3, Issue 8, August- 2012 J. Clerk Maxwell, A Treatise on Electricity and Magnetism, 3rd ed., vol. 2. Oxford: Clarendon, 1892, pp.68-73.

[2] robot using Zigbee Communication By Krishnaswamy Kannan and Gowtham S, International Journal of Engineering Science and Technology (IJEST), ISSN : 0975-5462 Vol. 4 No.10 October 2012. K. Elissa, “Title of paper if known,” unpublished.

[3] Secured Spy IP Control Robot Using Raspberry Pi By V. Meenakshi, Ch. Lakshmi Saketh, K. KalyanKumar, International Journal of Emerging Technology and Advanced Engineering, Volume 5, Issue 2, February 2015.

[4] Y. Yorozu, M. Hirano, K. Oka, and Y. Tagawa, “Electron spectroscopy studies on magneto-optical media and plastic substrate interface,” IEEE Transl. J. Magn. Japan, vol. 2, pp. 740-741, August 1987 [Digests 9th Annual Conf. Magnetics Japan, p. 301, 1982].

[5] Wi-Fi Robot for Video Monitoring & Surveillance System by Pavan C & Dr. B. Sivakumar, International Journal of Scientific & Engineering Research Volume 3, Issue 8, August- 2012

[6] Md Athiq UR Raza Ahamed M., Wajid Ahamed, A Domestic Robot for Security Systems by Video Surveillance Using Zigbee Technology, International Journal of Scientific Engineering and Technology (ISSN : 2277-1581) Volume 2 Issue 5, pp : 448-453 1 May 2013.

[7] P. Saucy and F. Mondana, KhepOnTheWeb: Open access to a mobile robot on the Internet, IEEE

Energy Harvesting from Rooftop Ventilator

Nurul Nadiah Binti Zulkifli
Faculty of Electrical Engineering
Universiti Teknologi Malaysia
Johor Bahru, Malaysia.
nadiahzulkifli.utm@gmail.com

Dr. Leow Pei Ling
Faculty of Electrical Engineering
Universiti Teknologi Malaysia
Johor Bahru, Malaysia.
leowpl@fke.utm.my

***Abstract*—Malaysian energy sector is still highly dependent on non-renewable source of energy such as fossil fuel and natural gas. In the long term, the burning fossil fuel and natural gas will deplete and become more expensive. To overcome this problem, the researchers have been widely interested in Renewable Energy field which is more abundant and environmental friendly. Development of the renewable energy using wind can be used to replace fossil energy and natural gas. This study is focusing on the modification of the rooftop ventilator system equipped with a small DC motor to generate electricity by applying the concept of Vertical Axis Wind Turbine. A small DC motor is installed in 16-inch rooftop ventilator. 1:2 gear ratios is installed to the turbine shaft to allow the rotation of rotor inside the DC generator while the ventilator is spinning. The results are showed that the DC generator would begin to generate voltage of 4.63 volt at fan speed of 1 which is the lowest fan speed and produce 21.44mW power which is sufficient to supply small DC loads such as LED light.**

Keywords—rooftop ventilator, dc generator, vertical axis wind turbine

I. INTRODUCTION

Broiler industry has been giving great impact to the country. The common risk and challenges for Malaysian broiler farmers are the high indoor temperature inside the broiler house can lead to heat stroke of broilers and cause loses to the farmers. Generally, exhaust fans are installed to ensure good ventilation and keep the indoor temperature low. However, not many farmers afford to install fans as there will be additional cost for the energy consumption. To overcome this problem, the researchers have been widely interested in Renewable Energy field to ensure the energy security and global environment. Renewable energy from the roof top ventilator helps to provide clean electricity and at the same time provides a sustainable energy solution for the broiler house. Therefore, it can be used to replace fossil energy such as oil and coal, that causing the environmental pollution.

II. LITERATURE REVIEW

The concept of natural ventilation by using non-electrical energy is lead to be the roof top ventilator [1]. Roof top ventilator is common for factories and even residential houses to keep the temperature indoor low by encouraging ventilation within the house. There are several advantages using roof top ventilators which include that they do not need electrical supply to work. Roof top ventilator is cost saving because there is no operating cost and no maintenance needed [2]. Fig. 1 shows how the working principle of the rooftop ventilator in controlling the temperature inside a building.

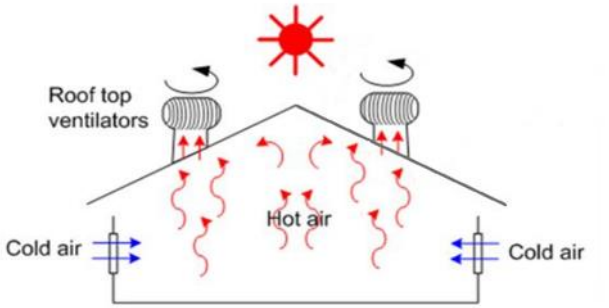

Fig.1. How the rooftop ventilator control the temperature inside a building

Roof ventilator consists of stationary part that composed of base and fixed shaft and rotational part that composed of blades and disc bearing that connect the fixed shaft on stationary part [3]. Fig. 2 shows the construction of rooftop ventilator.

Fig.2. Construction of rooftop ventilator

By using the concept of wind energy, from past to present there are a lot of study on the probability to adapt the wind energy to generate electricity. One of the applications is by using vertical wind turbine to generate energy by converting the kinetic energy from the rotating windmill into mechanical energy that will move the rotor to generate energy [4].

The wind turbines produce electricity by converting the kinetic energy in wind into mechanical power and the

mechanical power is used to turn the rotor of generator [5]. The rotor spinning produces the electromagnetic induction, thus generate the electrical energy. In modern times, the wind turbines design falls into two configurations, the Horizontal Axis Wind Turbines (HAWT) configuration and the Vertical Axis Wind Turbines (VAWT) configuration [4]. The roof top ventilator has the same basic concept as VAWT [6] as it turns whenever there is movement of hot air rises inside the building. Fig. 3 shows the configurations of the vertical axis wind turbines.

Fig.3. Vertical Axis Wind Turbine

The advantages of using the HAWT are the maximum amount of energy that can be collected by the turbine due to the optimum angle of wind flow. HAWT configuration also has more stability since the propellers are in a direction away from the turbine's center of gravity. The disadvantages of using the HAWT are difficulties in transportation and installation because of the tall towers and long blades

The advantages of VAWT are easy for maintenance since the generator and other equipment can be placed on the ground. The transportation and installation of VAWT is also easy compared to HAWT. The disadvantage of VAWT is less efficient due to additional drag that exists when the blades turns. They also create noise due to high vibration produced by the air flow near the ground [6].

There are numerous studies in the integration of electrical generator driven by roof top ventilators in the recent years [1, 3, 7]. The modified roof top ventilator has the same basic concept as VAWT [6] as it turns vertically whenever there are movement of hot up rises in the building, therefore by developing coupling mechanism system the rotation motion of the ventilators can be used for generating energy.

There are several techniques of roof top modification for electricity generation. The first technique is by using Axial Flux Permanent Magnet (AFPM). The coreless stator AFPM generator is the main component of this system. The kinetic energy captured from the low wind speed is converted into electrical energy [1]. This method is more efficient as the design have higher power density.

The torque generator must be low to allow the generator start at the low speed. From the experimental result, large number of pole-pairs are needed to increase the output power [1]. This type of prototype requires high skill and precision for winding the coil, therefore there is another method which is direct harvesting method by modifying the shaft of the ventilator and get the rotation of the rotating shaft to connect to generator.

The main component of the system is the DC generator that is connected directly to the shaft of the ventilator. The specification of the DC generator is important as it requires the torque to be low so that it can rotate at low wind speed. The generated voltage from the generator is connected to the DC Step-Up Converter to boost the voltage. This method is less effective [4] than AFPM machine since the voltage generated is small compared to AFPM. However, this method is more direct and straight forward and it seems to be like a plug and play device rather than modifying the whole of the roof top ventilator.

In this paper, the main objective of the study is to develop energy harvester for roof top ventilators using wind turbine technologies. The scope of the project is to modify roof top ventilators for energy harvesting and to convert rotation movement to electrical energy.

III. RESEARCH METHODOLOGY

The aim of this project is to harvest the electrical energy from the roof top ventilator. Fig. 4 shows the block diagram of electrical generation from roof top ventilator.

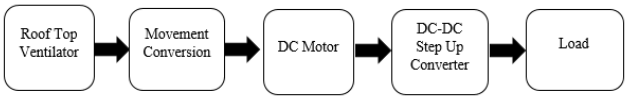

Fig.4. Block diagram of electrical generation from roof top ventilator

The roof ventilator is modified by install the DC generator to generate the electricity. To attach the turbine shaft to the generator, a gear system (1:2 ratios) is installed to the turbine shaft inside the ventilator. Fig. 5 shows the installation of the gear to the rooftop ventilator.

Fig.5. The installation of the gear

This modification allows the rotation of rotor inside the DC generator while the ventilator is spinning and to increase the speed of rotation of the rotor inside the generator. Fig. 4 shows the DC-DC Step-Up Module used to boost up voltage.

Fig.6. DC-DC Step Up Module

The output from the DC generator is fed to the DC-DC Step-Up Module before connecting to the load.

IV. Result and Discussion

The ventilation is tested by using the wind source from a table fan. Fig. 7 shows that the ventilator is being tested with a table fan at a fix distance.

Fig.7. DC Motor Testing Experimental Setup

The study on the ventilator RPM and generated voltage from DC motor is crucial for this project to determine the characteristic behaviour of the motor. Tachometer is used to measure the RPM of the ventilator. Table I is the tabulated result from the experiment.

TABLE I. Generated Voltage From DC Generator At Different RPM of Ventilator

Ventilator RPM	*Generated Voltage from DC Motor (V)*
52.8	4.85
61.6	5.85
72.0	6.48
96.8	9.34
105.9	10.26
175.2	14.95

From the Table I, it shows the range of ventilator rpm is from 52.8 rpm to 175.2 rpm. From the result, it shows that the lowest rpm which is 52.8 rpm can generate an average voltage of 4.85V and at 175.2 rpm generates an average voltage of 14.95v.

An LED with 1k ohm resistor is connected to the output. The output voltage (V) is measured through the resistor (R). The current (I) can be measured by dividing the voltage with the value of the resistor. The power can be determined by multiplying the current and voltage. Table II shows the result from the experiment.

TABLE II. Generated Voltage From Ventilator

Fan Speed	*Rooftop Ventilator Revolution Per Minute (RPM)*	*DC Voltage (V)*	*DC current (mA)*	*Power (mW)*
1	50.2	4.63	4.63	21.44
2	58.3	5.00	5.00	25.00
3	64.2	5.37	5.37	28.84

From the Table II, it shows the lowest fan speed can generate voltage at 4.63V and 21.44 mW power. The high fan speed can generate voltage at 5.37V and 28.84 mW power. The current increased when the speed of fan increased but in small value. The rotation of the ventilator depends on the amount of the air flow from the wind source. The higher the wind speed, the higher the power generated from the DC generator. From the experiment, the generated power can be used to light up LED.

V. Conclusion

This project is to adapt the roof top ventilator for electricity generation. By applying the vertical axis wind turbine concept, the rooftop ventilator can be modified by adding gear to harvest the electrical energy from the rotation of the ventilator. The performance result from the modification of the rooftop ventilator shows that the developed system able to produce power. The voltage generated from the system is directly proportional to the speed of the rooftop ventilator. The system able to supply

small DC loads such as LED light for lighting. Future recommendations such as adding extra fins to the ventilator to allow more wind passing to the ventilator can be suggested to improve the system in future.

REFERENCES

[1] C.H Ming, D.K Jair, M.C. Huann, "The Development of a New Type Rooftop Ventilator Turbine Engineering," 2013. vol.5, pp. 16-20.

[2] S.V Rode, G. Damdhar, C. Gadhikar, V. Dhumale, M. Deshpane, T. Ratnaparkhi, "Electricity Generation Using Rooftop Ventilator," International Journal of Advanced Research in Electronics and Communication Engineering 2016. vol. 5(4), pp. 1009-1012.

[3] S. Dangeama, "An Electric Generator Driven by a Roof Ventilator," Energy Procedia, 2011. vol.9, pp. 147-158.

[4] C. Torasa, and N. Sermsri, "The Application of Roof Ventilator for Electricity Generation," Procedia - Social and Behavioral Sciences, 2015. vol.197, pp. 1690-1696.

[5] M.R. Patel, "Wind and Solar Power Systems," 2nd ed,. 1999, USA, Taylor & Francis.

[6] I.Daut, C.S., M.Irwanto, A.N. Syafawati, S.S Shema, "Power Generation Roof Ventilator," International Conference on Environment and Industrial Innovation, 2011. vol.12, pp. 183-187.

[7] Y. Ting, H.Gunawan, S. Amelia, K. Lin Hsu, J. Tong Teng, "Analysis and Design of Roof Turbine Ventilator for Wind Energy Harvest," 2010 2nd International Conference on Mechanical and Electronics Engineering, 2010. vol.2, pp. 265-269.

Autotuned Electrical Muscle Stimulator With Electromyogram Biofeedback

Muhammad Naqiuddin bin Nazali, Leow Pei Ling
Faculty of Electrical Engineering
Universiti Teknologi Malaysia
Johor Bahru, Malaysia
naqiuddin.nazali@gmail.com

***Abstract*—This paper discusses on the implementation of electromyogram sensor as the biofeedback of the improvised electrical muscle stimulation technology to improve the muscle strength. Some understandings on muscle behavior are explained followed by the issues regarding muscle weaknesses. The techniques of muscle stimulation are discussed together with the solutions to overcome the problems encountered by the current muscle stimulation techniques. The project methodology is explained with proper circuit configurations and programming technique. Some preliminary works and validation process upon the wrist extensor muscle done are clearly stated with appropriate results presented in technical representations. Finally, the project functionality is described based on simulation results showing the system behavior with respect to the muscle contraction reading. The limitations of project is included for the improvement in any related future works.**

Keywords—electrical muscle stimulator; muscle contraction; muscle strengthening; electromyogram; automatic tuning; digital potentiometer; block diagram; user interface; biofeedback application.

I. INTRODUCTION

A survey conducted by National Health and Morbidity Survey (NHMS) in 2011 shows that the level of poor self-rated health among Malaysians were significantly greater compare to Japans, Canadians, and Americans with 20.1% prevalence [1]. As reported, the number of musculoskeletal disorder was increased rapidly in Malaysia, especially among workers. A study conducted in Selangor to investigate the prevalence of work-related musculoskeletal disorder showed 77.3% of non-healthcare working population suffered this problem [2]. This proved that the number of people having muscle weaknesses was high. The most crucial issue regarding the musculoskeletal disorder is the chronic injuries that led to paralyze. These paralysis patients are unable to do the daily activities due to the weaknesses of their muscles. As to improve their muscle strength, the physiotherapists would advise them to do a lot of exercises. However, the active treatments like weight lifting, running, light sports activities and the other exercises cannot be done by the person with weaker muscle strength, especially for those patients with muscle grade less than 2. These patients cannot even move their limbs against gravitational force. Therefore, the experts had introduced the muscle stimulation technique as a passive treatment for the paralysis.

The Electrical Muscle Stimulation (EMS) is the new method to improve the muscle weakness suffered by most of the chronic disease patients like stroke, spinal cord injury, accidents and so on. This technology applies certain current intensity upon the weak muscle depends on the muscle power itself. The muscle contracts once the current is applied at the origin point and the insertion point of the muscle; just like how the brain signal works to initiate movements. However, the EMS technology nowadays is an open loop system without any feedback. Therefore, the user needs to manually adjust the current intensity that need to be applied across the weak muscle. This may cause an inaccurate tuning and results in less effective treatment.

The main goal of this project is to control the intensity of the current EMS device automatically by analyzing the biofeedback of muscle. This project implements an electromyogram sensor as the biofeedback of the system. This sensor is used to measure the muscle strength. Then, the EMS will stimulate the muscle with suitable current intensity controlled by Arduino through MATLAB Simulink according to the biofeedback of the electromyogram measurements. To prove the functionality, the project is tested onto the wrist extensor muscle as the scope of project. The reason of choosing this muscle activity is due to its body mechanics criteria and the wrist itself is one of the lighter body parts.

II. LITERATURE REVIEW

A. Physiology of Muscle

In every human body, there are three different muscles tissues with their respective functions; namely as skeletal muscles, cardiac muscles and smooth muscles. All these muscle tissues have the ability to contract and relax, initiate a motion, provide stabilization and also generate heat. The project is focusing on the skeletal muscles only because the human limbs can move when these muscles are contracted. The contractions of skeletal muscles support the movement of skeleton as the muscles are attached to the bone [3]. All the skeletal muscles are placed opposing with the other skeletal muscles. In order to move a limb, the respected skeletal muscle must be contracted while the opposite muscle relaxed or sometimes stretched [4].

The contractions of a muscle are depending on the impulses of motor neurons that transmitted to the muscle fibers. This transmission produces an electric field due to the depolarizes of the muscle fibers. With sufficient electric current propagates

across the muscles, it is then able to contract to initiate the movements [3]. The muscle strength can be improved by alternately contract and retract the muscle during the active exercises. Nevertheless, the sustained activities of muscles can cause fatigue once it reaches the limits. Muscle fatigue are known as the gradual decreases in muscle force due to the repeated contractions. The definition of muscle fatigue has been focused as an exercise-induced reduction in the production of muscle force during the sustained activities [5, 6]. The muscle fatigue must be avoided in any muscle treatment, otherwise, the task cannot be done due to the decreases of force. It will take some times for the muscle to develop back gradually. With this condition, the muscle fatigue is justified as not the reason of any task failure [7]. Instead, the muscle getting weaker due to the other reasons.

In Malaysia, most reported cases involving musculoskeletal disorder are related with work activities in an awkward posture [8]. This are resulted in the weakening of the muscle among these populations. Without appropriate exercises, the muscles are getting much weaker. The worst cases may lead to paralyze. Clinically, the muscle can be strengthening by appropriate stimulation technique. One has proved that the electrical stimulation can improve the muscle strength, increase the motion range, reduce pain and heal the muscle tissue. [9] One of the modern stimulation technique is by applying the electrical current across the muscle. This technique is known as the Electrical Muscle Stimulation.

B. Electrical Muscle Stimulation

The primary study of electrical stimulations has done by Michael Faraday in 1831 after he observed the active movement once the current is applied across a nerve [10]. The electrical stimulation earlier application was to relieve muscle pain [11], but it has now been commonly used to treat the weak muscle became stronger [12]. The concept is by applying a transcutaneous electrical current across the muscle to produce the muscle contractions [13]. The repetitions in muscle contractions helped to strengthening the muscle as a passive treatment.

However, the disadvantages of EMS have shown that it may lead to muscle fatigue when overstimulated because the delivery of the treatment are not well-customized [9]. Barbara M. Doucet, A.L., and Lisa Griffinb (2012) had discussed the important parameters that must be considered during the stimulation. The most important parameter is the current intensity and the pulses frequency of the EMS device. The higher intensity are essential to improve the muscle strength [14]. Meanwhile the pulses frequency are said to be at constant lower level so that the muscle contracted smoothly at low force [15], Unfortunately, there are no parameters that indicates whether the muscle are getting fatigue or not when applying the current intensity and the pulse frequency across the muscle. Therefore, the system needs a suitable sensor to monitor the muscle capability.

C. Biofeedback Instruments

Sinkjaer, T., et al. (2003) had proposed the implementations of electromyogram (EMG) sensor, electroneurogram (ENG) sensor and electroencephalogram (EEG) sensor in the development of EMS technology [16]. The EMG sensor is used to obtain the biopotential reading of the skeletal muscle. Meanwhile, the ENG sensor and EEG sensor are used to record the nerve signal and brain signal respectively [17]. There are also several instruments that can measure the electric potentials and magnetic fields through the surface of human body including electrooculogram, electroretinogram, electrocochleogram, electrocardiogram and so on. All these instruments are measuring the electric fields produced from the depolarization of muscle membranes and also the conduction of nerve impulses that can be obtained through body skin [18]. In this project, only the EMG sensor are used since the projects dealt with skeletal muscle behavior only.

Electromyography is a study on the measurement of skeletal muscle biopotentials. It measures the electric potential on the skin through the electrode. Every skeletal muscles are contracted under the voluntary control once instigated by the neurons impulse. These motor neurons are producing the electrical potentials known as motor unit action potentials (MUAPs) [4]. As the muscle tissue conduct these MUAPs, the electrical potential can be obtained by placing the electrode onto the respective muscle tissue. In short, the electromyography measures the presence MUAPs in the superficial muscle tissue that can be easily obtained on the body surfaces.

The EMG readings are having a lot of noises because the electrode is contacted on a single motor unit with many muscle fibers. Therefore, the EMG will measures a combination of MUAPs when muscle is contracted [19]. Since the raw EMG signal are disturbed with a lot of noises, a proper signal conditioning technique is implement in the development of EMG sensor. The earlier research has introduced the technique to obtain the enveloped EMG signal for better measurement with the implementation of the rectifier, the amplifications and the filters [20, 21]. This project implements a smart EMG sensor as the biofeedback sensor with integrated signal conditioning circuits and Arduino compatible instead of building the new EMG sensor.

III. METHODOLOGY

The project is made to control the current intensity of the EMS device automatically by sensing the muscle strength. The Arduino UNO R3 is used as the microcontroller of the system programmed using MATLAB Simulink. This tools also used to be the user interface with the dashboards libraries. Therefore, the user can observe the treatment behavior through this application.

A. Project Design

In order to ensure the reliability of the system, the current EMS device, BioMed 2000 XL, was hacked instead of developing the new device. Basically, the current EMS devices are using potentiometer to tune the current intensity. In this project, the potentiometer is replaced by the digital potentiometer, MCP4161 from Microchip Technology Inc. the microcontroller are programmed to control this digital potentiometer through Serial Peripheral Interface(SPI) communication to achieve desired current intensity of EMS.

The controlled current intensity of the EMS device depends on the muscle strength. Therefore, the electromyogram sensor, MyoWare, is implemented as the input of the system. This

sensor also used to measure the biofeedback of the system to make the closed-loop system.

The MATLAB Simulink toolboxes is used to control the output of the system. A few dashboard components in this applications also used as the user interface. The user can control the system through this Simulink application as shown in Fig. 1.

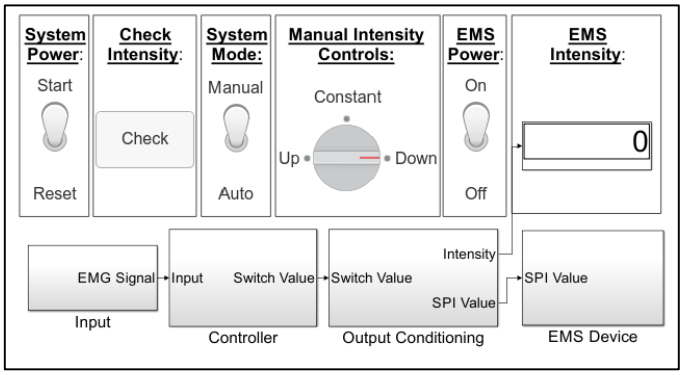

Fig. 1. Simulink block diagram of the system with dashboard components as user interface

B. Research Procedure

The project is carried out within two semester of studies. After going through the planning, preliminary studies and preparations, the project begins with the preliminary experiments as follows:

1) Measuring Muscle Strength: The objective of this experiment is to analyze the method to retrieve the muscle strength by using the MyoWare sensor. It is important to find out the best signal conditioning technique with optimum sampling time to be used in MATLAB Simulink program.

2) Investigating EMS Parameter: Before hacking the EMS device, each of the tunable components were analyzed. Since the optimum setting of the frequency and pulse width parameter are known, these two potentiometers are fixes with suitable resistance value. The only parameter that need to be controlled is the current intensity of the EMS device.

Then, the project continues with the development of electronic circuits. The Arduino is connected to the MyoWare sensor as the analog input and the digital potentiometer as the output via SPI communication. This digital potentiometer are then replacing the actual potentiometer for the current intensity controller. Another connection between the Arduino and the EMS device is to switch on and off the device via direct digital write of the Arduino. Hence, the project came out with the Simulink programming. The details of the Simulink block diagram is in Fig. 2. There are several important component used in the block diagram:

- *Arduino Input:* This block retrieves the analog input from the Arduino pin A5. The signal is converted into double format and map it to the range of 0 to 5.
- *Maximum:* This block finds the maximum of the input signal to check if the EMS device has reach its suitable intensity. This block can be reset by the constant block 'Reset' that controlled by the 'Check Intensity' dashboard button.
- *Controller Switch:* This block is used to switch intensity either increase the SPI value by 5 or 0.
- *Saturation:* This block saturates the SPI value from 0 to 255 as to control the EMS intensity.
- *Output Conditioning Switch:* This block checks the constant block 'Mode' value controlled by the dashboard toggle button 'System Mode' to set the mode of the system between manual and automatic.
- *Arduino Digital Output:* This block is connected to Arduino pin D8 as the switch of EMS device. The dashboard toggle button 'EMS Switch' controls this block.
- Arduino SPI WriteRead: This block reads the input array and write into the Arduino SPI slave select pin 10 to control the EMS intensity.

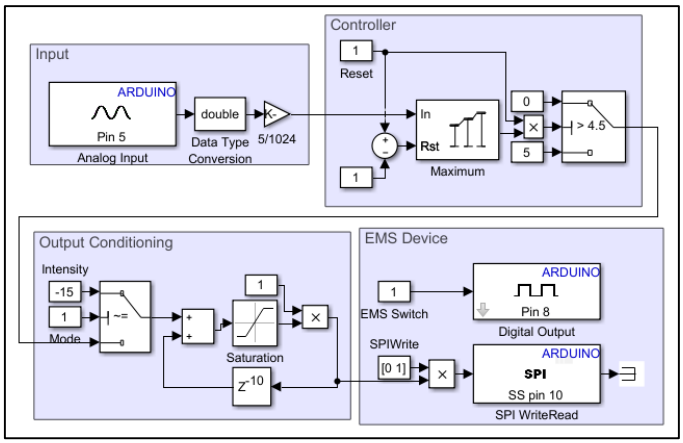

Fig. 2. Details of the Simulink block diagram of the system.

C. Functionality Test

Once the project is done with the circuits connections with proper programming, it is then being test for the functionality validation. This experiment is conducted towards the human wrist extensor muscle as the subject. Two electrode pads of the electromyogram is placed onto the mid muscle while the reference electrode pad of the electromyogram is placed on the other muscle that not contracts when the wrist is extend. This will ensure the MyoWare sensor read the input of the system accurately. In the other hand, the output of the system in terms of current intensity is delivered across the muscle by placing both electrodes at the origin and the insertion point of the muscle respectively.

To test the system, toggle button 'System Power' must be turned once the muscle is completely relaxed. Select the system mode to automatic to see the EMS device tune automatically to the suitable intensity. The user can simply press the 'Check' button if the intensity is not achieve their desired value.

IV. Results and Discussions

A. Preliminary Findings

As in the preliminary works, an experiment has been conducted to see ability of MyoWare sensor to measure the muscle strength. It is connected to the Arduino and observed the

muscle reaction once the EMS treatment is applied across the muscle by using the current EMS device. The results of this experiment recorded from the Simulink Scope are shown in Fig. 3. The signal indicates the desired muscle contraction during the EMS treatment. After several investigation, the repeatability of the results prove that the sensor can record the muscle contraction with the implementation of Simulink block diagram as in the subsystem Input as shown in Fig. 2.

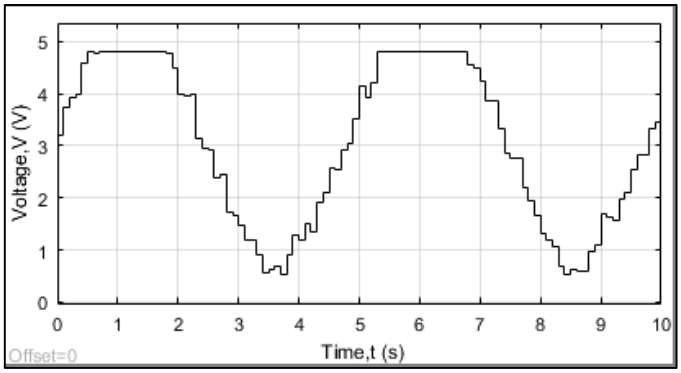

Fig. 3. Output signal representing the desired muscle contraction during the EMS treatment.

At the same time, the resistance of potentiometer for each parameters used in producing the desired signal are investigated. It is proven that the potentiometers of pulse width tuning and frequency tuning can be fixed at 5kΩ to obtain the desired signal. However, the resistance of potentiometer used to determine the amplitude of the signal must be tunable in the range of 0Ω to 5kΩ. It needs to be adjusted according to the muscle strength.

B. Simulations Results

The finished project is tested onto the subject muscle to shown the functionality of the system. The simulation is carried out in about 100 seconds. Fig. 4 shows the results when the system is tested towards the actual wrist extensor muscle. All the dashboard components are simulated and the output is recorded in Table I. These results proves that the system can be used safely without overstimulation that may cause muscle fatigue. At $t = 27s$, the controller of the system stop increasing the current intensity when the muscle contraction reading is more than 4.5V, which is much lower than the maximum capability of muscle contractions. However, if the user did not satisfy with the lower intensity, the system can find another higher suitable intensity by pressing the 'Check' button as shown at $t = 45s$, $t = 60s$, $t = 75s$ and $t = 95s$ Nevertheless, if the user feels that the current intensity is high, by toggling button 'System Power' to 'Reset' will help in turning down the intensity to zero as what happen at $t = 90s$. Besides, the system enable user to choose between manual tuning stimulation and automatic tuning stimulation mode. It takes less than 51 seconds to achieve the desired signal.

TABLE I. DASHBOARD COMPONENT OUTPUTS

Component	State	Output
System Power (Toggle Button)	Start	Enable the intensity to increase from zero.
	Reset	Turn down intensity to zero.
Check Intensity (Push Button)	Released	Do nothing.
	Pressed	Reset the maximum of input signal to find the new suitable intensity.
System Mode (Toggle Button)	Manual	Enable the manual tuning of EMS device.
	Auto	Enable the automatic tuning of EMS device.
[a]Manual Intensity Control (Knob)	Up	Increase the intensity by 15 of 255.
	Constant	Maintain the intensity at current value.
	Down	Decrease the intensity by 15 of 255.
EMS Power (Toggle Button)	On	Switch on the EMS device.
	Off	Switch off the EMS device.

[a.] Used in Manual mode.

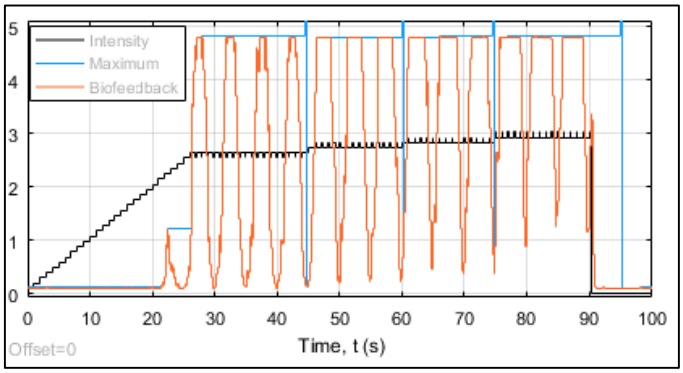

Fig. 4. Stimulation output of the improvised EMS device

C. Project Limitations

After several modifications during the development of projects, it is founded that the memory of the microcontroller is in important thing to consider especially when using the MATLAB Simulink with a lot of toolbox. Some of the essential toolboxes like filters, adaptive controllers, statistics functions and so on cannot be used due to the insufficient memory. As a result, there might be inaccuracy in the system due to noise and unstable signal.

Moreover, the controller can stop finding the suitable intensity if the muscle is not relax. Some body movement might effects the contraction of wrist extensor muscle. These small contractions are amplified in the MyoWare sensor and cause the fluctuations in the input signal of the system. The fluctuation of signal above 4.5V will immediately stop the controller to keep increasing until the suitable value. Therefore, the desired signal of EMS treatment cannot be obtained unless by pressing the 'Check' button to reset the maximum value.

Since the system runs in MATLAB Simulink application, it needs the user to install the MATLAB Simulink in their computer to use the system. It will be much easier if the system can be package as a standalone application that can be used in any computers without installing MATLAB Simulink.

V. CONCLUSION

It is concluded that the project can be safely used to treat weak muscle as the passive treatment to strengthening the

muscle. The automatic tuning function of the project is verified as it produces slightly the same output signal as the current technologies. The main advantage of this automatic tuning system is that it can avoid overstimulation of the muscle due to the error in the setting of current intensity of the EMS device. In addition, the progress of the treatment also can be observed through the simple user interface.

REFERENCES

[1] Chan, Y.Y., et al. (2015), Lifestyle, chronic diseases and self-rated health among Malaysian adults: results from the 2011 National Health and Morbidity Survey (NHMS). BMC Public Health.

[2] Balakrishnan, R., M.E. Chellappan, and E. Changalai (2016), Prevalence of work-related musculoskeletal disorders among non-healthcare working population in different gender at Selangor. International journal of physical education, sports and health.

[3] Mohsen S, Kim K. J., Mehrad M. (2007), Anatomy and Physiology of Human Muscle, in Artificial Muscles, Taylor & Francis Group, LLC.

[4] Reaz, M., M. Hussain, and F. Mohd-Yasin (2006), Techniques of EMG signal analysis: detection, processing, classification and applications. Biological procedures online.

[5] Bigland-Ritchie B & Woods JJ (1984). Changes in muscle contractile properties and neural control during human muscular fatigue, Muscle Nerve.

[6] Søgaard K, Gandevia SC, Todd G, Petersen NT & Taylor JL (2006). The effect of sustained low-intensity contractions on supraspinal fatigue in human elbow flexormuscles. J Physiol

[7] Enoka, R.M. and J. Duchateau (2008), Muscle fatigue: what, why and how it influences muscle function. The Journal of Physiology.

[8] Md. Mainul Islam (2012). The exposure workers at risk is necessary to prevent injury Common, Musculoskeletal Disorders Among Physiotherapist, CRP.

[9] Barbara M. Doucet, A.L., and Lisa Griffinb (2012), Neuromuscular Electrical Stimulation for Skeletal Muscle Function. YALE JOURNAL OF BIOLOGY AND MEDICINE.

[10] Cambridge NA (1997). Electrical apparatus used in medicine before 1900. Proc R Soc Med.

[11] Deyo RA, Walsh NE, et al. (1990). A controlled trial of transcutaneous electrical nerve stimulation (TENS) and exercise for chronic low back pain. New Engl J Med.

[12] Sluka KA, Walsh D (2003). Transcutaneous electrical nerve stimulation: basic science mechanisms and clinical effectiveness. J Pain

[13] K. W. Eric Cheng, Y.L., et al. (2004), Senior Member, IEEE, Development of a Circuit for Functional Electrical Stimulation IEEE TRANSACTIONS ON NEURAL SYSTEMS AND REHABILITATION ENGINEERING.

[14] Gondin J, Cozzone PJ, Bendahan D (2011). Is high-frequency neuromuscular electrical stimulation a suitable tool for muscle performance improvement in both healthy humans and athletes? Eur J Appl Physiol.

[15] Bhadra N, Peckham PH (1997). Peripheral nerve stimulation for restoration of motor function. J Clin Neurophysiology.

[16] Sinkjaer, T., et al. (2003), Biopotentials as command and feedback signals in functional electrical stimulation systems. Medical Engineering & Physics.

[17] Webster, J.G. (1998), Medical Instrumentation Application and Design. John Wiley & Sons, Inc.

[18] Robert B. Northrop (2002), Measurement of Electrical Potentials and Magnetic Fields from the Body Surface in Noninvasive Instrumentation and Measurement in Medical Diagnosis, CRC Press LLC.

[19] Kleissen RFM, Buurke JH, et al. (1998). Electromyography in the biomechanical analysis of human movement and its clinical application. Gait Posture

[20] Masshor (2010), M.A.b., Design of An Electromyogram System, in Faculty of Electrical Engineering, Universiti Teknologi Malaysia.

[21] Meyer-Waarden (2005), W.W.v.M.a.K., Bioinstrumentation, CRC Press LLC.

Vision Aided Automated Guided Vehicle

Mohamad Danial Bin Yazid
Faculty of Electrical Engineering
Universiti Teknologi Malaysia
Johor Bahru, Malaysia.
daniyalyazid94@gmail.com

Leow Pei Ling
Department of Control and Mechatronics Engineering
Faculty of Electrical Engineering
Universiti Teknologi Malaysia
Johor Bahru, Malaysia.
leowpl@fke.utm.my

***Abstract*—This paper presents an automated guided vehicle that are use two navigation method that is track and trackless navigation method. This project use image processing approach in order to develop the trackless navigation method. There are some experiments have been conduct to test the vehicle in order to achieve the objective and scope of this project. The objective of this project is to design a track and trackless AGV by using image processing method for human following feature. The scope of the study is to design a prototype that can lift the weight up to 20 kilograms and develop an AGV system with track and trackless mechanism for indoor navigations. The experiment result shows that the first scope of this project have been achieved.**

INTRODUCTION

Automated Guided Vehicle (AGV) has been introduced to the world for the first time in 1953[1]. At that time, the AGV is a modified towing tractor that are follow imbedding wire in a grocery warehouse floor. This AGV detect the magnetic field that are produce by the imbedding wire [2]. Through 60 years of continuous research and development, AGV has integrated with modern technologies for better performance. The growth of AGV usage in China has been reported to be roughly about 16,000 units in 2015 and the demand is expected to increase up to 22,000 in 2020. This technology is very demanding in advance country in order for them to evolve their factory sector and increase the productivity of the factory. This growth has been followed by Malaysia in order to be at par with the other advance country such as China, Japan, America and others.

Besides that, there are many cases of injuries that happened in workplace such as back pain, joint problem and many more. The cause of this problem were caused by heavy lifting goods that is too heavy such as boxes of assembled goods, raw materials, office materials and more. By having this technology, it will help human in order to moving the heavy from one place to another. This technology also can do the transport and deliver job continuously. Like example, when we reading a book in the library, we have to put it back to a trolley at the certain place. Imagine that the trolley is moving to collect the books and returned to the collection counter. That will save your time in order to return the book.

LITERATURE REVIEW

Automated Guided Vehicle

The first reported AGV in the 1953 is made up from a towing truck that have been modified to pull a trailer and follow an overhead wire [3]. After that, this technology was going through his first development process in middle of 1970. At this time, this technology has been developing by adding up their ability and design from the first model. The development process has changed the pulling system to the platform for moving the desired item. Later, the navigation system of this technology has been develop by adding the control and information unit rather than just follow the overhead wire.

As the electronic and microprocessor become more advance, the new navigation system was developing and it is called “Dead Reckoning Algorithm” [4]. This system is used to increase the capabilities of AGV in traverse the steel expansion joints on the factory floor or to cross the steel gate. In other words, the AGV could leave the track, turn at a programmed radius and then continue its course by follow the track after the turn was done by using this navigation system. In 1980, the non - wire navigation system was introduced. There are four types of navigation system that are currently used in AGV system and this paper focuses on trackless navigations. These navigations will be explaining on the other subtopic.

There are six types of AGV in the world. The first type is a towing vehicle AGVs. This is the first model of AGV that are introduced in 1953. This type can tow the load that are more than 1000 lb. and it can move the load more than 1000 feet of distance. This AGV can be modified from a flatbed trailers, pallet trucks and custom trailers.

After that, the unit load type AGV was introduced. This AGV is used to transport individual unit load onboard the vehicle. It is equipped with powered or non – powered roller, chain or belt deck, or custom deck. The load that can be moved by this AGV can also be moved by a pallet truck, automatic load/unload equipment and many more. Next type is a pallet trucks AGVs. This AGV is widely used in distribution work because of the mechanism design. As you can see, it’s base are fixed for palletized load and the base cannot move up and down. The maximum load that this AGV can lift is about 1000 – 2000

lb. and the speed of this AGV are less than 200ft/min depends on the weight of the load that it is carries.

The fourth type is a forklift trucks AGV. The abilities of this truck are the same with the pallet trucks but the different is the palletized load can be pickup and drop at floor level and on stands compare to the pallet trucks AGV that can only pickup and drop the palletized load at floor level. Both type of AGVs are widely used in distribution function. Next type is the light load transporter AGV. This AGV are used to lift light and small load that are less than 500 lb. and it is usually used to distribute between storage and number of workstations. The speed of this AGV is 100ft/min and it has a fixed turning radius that is 2 feet. This type of AGV is almost the same with the unit load AGV but different in size as this AGV cannot lift the loads that are more than 500 lb.

Lastly, the assembly – line vehicle AGV is one of a type in the AGV family. The function of this AGV is actually the same as the conveyer belt that is to move the product from one workstation to another. This AGV is commonly used in serial assembly process. This AGV provides flexibility for the manufacturing processes but it's required complex computer control and extensive planning in order to integrate the system.

Trackless AGV Navigation

This trackless guidance method is more flexible than track guidance system. This guidance system is mostly like "host follow" type. The first one is using Radio Frequency Identification (RFID) guidance system as shown in Figure 1

Figure 1 : Radio Frequency guidance system concept

This system used radio frequency as the guidance in order for AGV to follow the host command. The system works where the host transmit the radio frequency signal that are fills with the command and then the receiver will attach at the AGV to receive the radio frequency and process the signal [5]. This guidance method also can help the AGV to visualize the environment of the indoor area using RFID tags as landmarks [6]. The position of the AGV also can be obtained by used Partial Pulse Positioning technique that used Radio Frequency transmitter as AGV position tracking [7].

Next is Image Processing Guidance System. This guidance system uses image as guide for AGV to move. The image processing method usually use camera as their sensor. With image processing techniques, the AGV will have the new way of navigations system. Image processing is a method that processes the image into a form of information for navigation. There are many stages that occur in image processing that is preprocessing, information processing and postprocessing. These stages output are depending on how this technology is used in a sensor network and the objective of the network [8].

There are many reported research work regarding the image processing with AGV system. Let us take a look in example project using image processing to follow the track. In other project used image processing to assist the AGV in tracking the line when the line is missing. A CCD camera was used as the image processing sensor in order to detect the red line that have been construct on the floor [9].

Next, the image processing is combined with the Fuzzy Control Algorithm to improve the navigation system in order to follow the marking line [10]. This system is actually will increase the efficiency of AGV in tracking the guided line. In image processing, the track color are very important and it must be in opposite color from floor color like example the white line on the dark green floor [11].

A Mobile Robot Code (MR code) has been introduced in order to provide position and navigation information. This MR code is a regular pentagon shape and it has binary code on its surface [12]. This MR code was place on the floor surface with guided line.

The image processing that are used two – dimension(2D) and three – dimension image(3D). In other project, the Kinect Camera are used to scan three - dimension image[13]. This is because the camera is capable of acquiring depth and color data in real – time. The Kinect Camera also comes with infrared projector and infrared camera in order to detect the depth of the image.

The two–dimension and three–dimension image also provide the AGV an accurate position and attitude determination in any indoor environment [14]. This image also is the alternative way for the AGV to know their accurate position because Global Positioning System (GPS) sometimes not capable in indoor area due to shadowing, significant signal attenuation and deception.

Furthermore, there are some project that used stereoscopic vision as their image processing method. First, the stereo image processing and three-dimension mapping are used for navigation and obstacle detection of AGV [15]. This stereo image also can be used as recognition system that helps the AGV to classify the object into one specific category [16]. Next, this stereo image processing can be used as real time

image feed in order for the AGV to track and follow an object [17].

By using Kalman Filter, the image processing can be used to follow an object based on a certain color. The color that are commonly used in image processing are red, green and blue. This color algorithm can be obtained using RGB frames [18].

In conclusion, there are many ways to use image processing as the guiding method for an AGV. From the example above, we can see that the development of the image processing itself in order to fit in AGV system. For my project, I used Hue – Saturation –Value (HSV) frame in order to follow human by detect the color of shirt and IR sensor module for line following navigation system.

In this paper, the main objective of this project is to design and develop a track and trackless AGV by using image processing technique. This paper will describe about development of an AGV system with track and trackless mechanism for indoor area navigation with human following feature.

RESEARCH METHODODLOGY

the overall operation of this project are shown in Figure 2

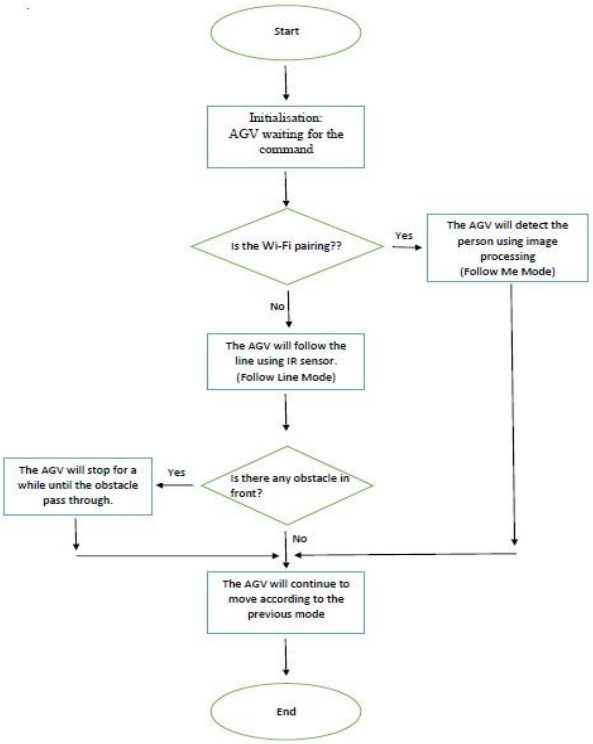

Figure 2 : Flowchart of the AGV operation

When the AGV turned on, the AGV is on standby mode waiting for the command from the user through WiFi connection. There are 2 modes for user to choose that is Follow Line Mode or Follow Me mode.

In "Follow Me Mode", the AGV will scan the color of the user shirt. The user must be standing in front of the AGV in order to detect the color of the user shirt.

When the user selects "Follow Line Mode", the AGV will used IR sensor module that are placed at the bottom of the AGV to detect the line. The Ultrasonic Sensor is placed in front of the AGV in order to detect the obstacle in front of the AGV. When the ultrasonic sensor detects the obstacle, the AGV will stop until the obstacle pass through the AGV track and then continue follow the track.

The electronic component and circuit that are used in this project are very important in order to control the movement of the AGV. The overall electronic component used are shown in Figure 3

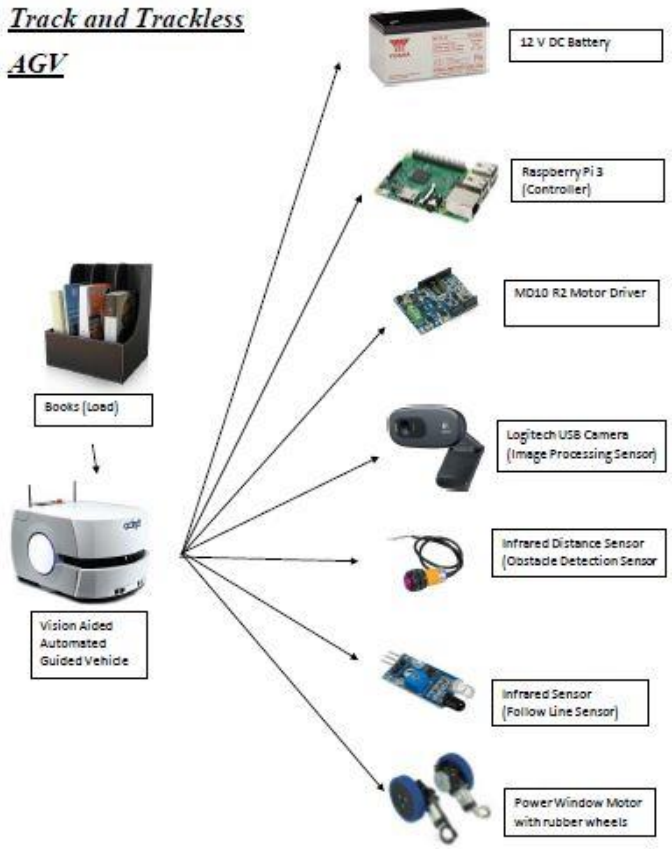

Figure 3 : Block diagram of the AGV

There are seven main components that are used in building the prototype of this project. The components that are used in this prototype are a 12 V Lead Acid Battery with Charger, Raspberry Pi 3, MD10C motor driver, Logitech USB Camera, Infrared Distance Sensor, Infrared Sensor and lastly Power Window DC Motor.

Design of the AGV

The design of this AGV must have a mechanism that can carry and lift the item in order for the AGV to move the item from one place to another.

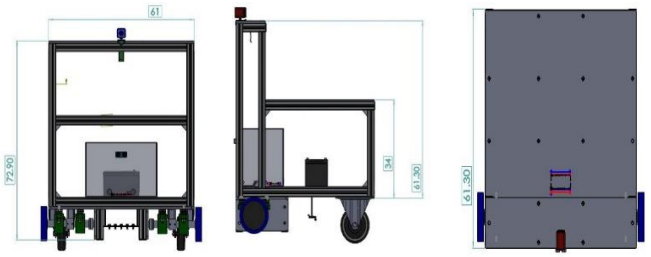

(a) (b) (c)

Figure 4 : The Conceptual Design of the AGV (a)Front View (b) Side View (c) Top View

Figure 4 shows the conceptual design of this project. From the figure, the frame is made of aluminum profile. The aluminum profile was chosen because it is easy to assemble, strong and lightweight. The C connector and L Connector are used in this frame in order to connect between two aluminum profile. The fastener nuts are used to fastened the connection between the aluminum profile and the connector. At the motor shaft, there are two pillow blocks at each side. These pillow blocks are used to distribute the overall weight of the AGV so that the motor shaft is not overloaded and able to support the total weight of the AGV and prevent the shaft from misaligned and break.

There is a box at the lower level of the AGV and it is called “electronic box”. The box contains a pair of motor driver, a breadboard and a Raspberry Pi 3. The Infrared sensor is placed at the bottom of the AGV. The black box that is placed behind the electronic box is a 12 V battery that are used to power up this AGV. The upper part of this AGV contains a Logitech USB Camera and a separated place to put the carried item.

Experiment Setup

An experiment was conduct to test the maximum load that the AGV can carry. The experiment setup as shown in Figure 5.

Figure 5 : Load test experiment

The AGV is tested by varying the weight loads that are placed on the top of the AGV. The time taken for the AGV to reach a specific location that is 2 meter from the starting point was recorded. Four bottle of 10L bottle and two bottle of 1.5L are used as loads in this experiment. The weight of the loads is measured by using luggage scale before it was placed on top of the AGV.

Next, the lifetime of the battery was tested by let the AGV running on the specific track until the battery is finished. Figure 6 shows the setup of the experiment.

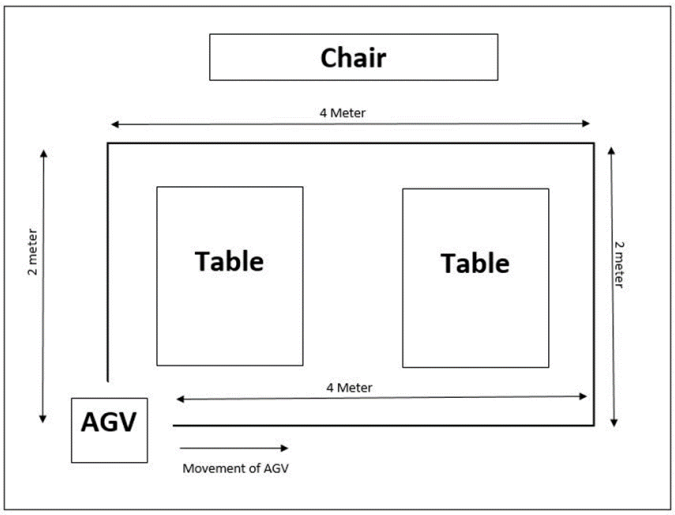

Figure 6 : The lifetime Battery experiment setup

After that, the obstacle avoidance test was carried out to test the efficiency of the AGV in avoiding the moving obstacle. The experiment setup was shown in Figure 7.

Figure 7 : Obstacle Avoidance Testing work setup

Lastly, the Color Following experiment was carried out in order to know the range of detection for the camera to detect the light blue color. Figure 8 shows the setup of the experiment.

Figure 8 : Color Following experiment setup

These four experiment will be discussed on the next chapter.

RESULT AND DISCUSSION

The result of the load test experiment are shown in Table 1

Table 1 : Load test result

Weight (Kg)	Time Taken to travel 2 m (sec)					
	T1	T2	T3	T4	T5	Average
5	9.51	9.97	9.72	9.63	9.77	9.72
10	9.93	9.70	9.78	9.84	9.95	9.84
15	9.89	9.76	9.82	9.97	9.87	9.86
20	10.03	9.92	9.89	9.86	9.97	9.93
25	10.81	10.51	9.79	9.81	9.76	10.13
30	10.15	10.24	9.93	9.89	10.51	10.14
35	10.35	10.27	10.48	10.36	10.19	10.33
40	-	-	-	-	-	-

From Table 1, the time taken for the AGV to reach the desired location increases due to the increases in weight of the load. The weight of the AGV that is 22.5kg will add up with the specific load as shown in Table 1 are being carry by the motor at a distance of 2 meter. At weight of load equals to 40 kg, the AGV does not move because the motor cannot carry the load. The increase in time taken is because when the load is increase, the torque of the motor will increase in order to pull the weight of the load. Then, the speed of the motor will decrease as the torque increase. This experiment was success because it clarifies the relationship between speed and torque that is the speed in inversely proportional to the torque.

Next is the battery lifetime experiment. The experiment was conducted in a room as shown in Figure 6. The track is a 12 m loop track. The AGV was programmed to follow the track that has been setup in the room. The AGV was allowed to follow the track until the battery is totally drained. The average worktime for one full cycle battery is 13 hours. This long hour performance of the AGV is because there are 2 batteries used in this AGV and those batteries are connected separately to each motors. Therefore, the uses of the charge in the battery are at minimum.

For the obstacle avoidance experiment that has shown in Figure 7. This experiment uses human as the obstacle. The AGV was programmed to use “Line Following” mode as navigation system. The obstacle can be detecting by the AGV is from 5 cm to 25 cm and the height of the obstacle must exceed 25 cm. This is because the infrared was located at the high placed in order to detect the human. The infrared is able to sense anything in front of it regardless the type of material of the obstacle.

Lastly, the Color Following experiment as shown in Figure 8. The object that was holding by the user is a blue pen and the blue pen is used as the target for the AGV. The AGV are able to sense the blue pen below 35cm from the camera. Then, the sticky note is used as the target and the size of the sticky note is 10cm × 10cm. The camera is able to detect the sticky note below 55cm. This is because the pen is too small for camera to detect at the longer distance and the area of the detected object is less than 500. Meanwhile, the sticky note that are in square shape have the bigger size than the pen is able to detect by the camera more farer than the pen. This shows that the size of the target influences the camera ranges of detection.

CONCLUSION

As a conclusion, the AGV has been tested and it is able to work without depending only one navigation system only. From the conducted experiment, this project is able to achieve the objective of this project that is navigation system by using infrared sensor and image processing method.

The implementation of image processing in this project has increased the flexibility of the AGV by not depending on one navigation system only. By using image processing also, user can monitor the target of the AGV whether it is following the right target or not and knows the current location of the AGV in a workspace.

The mechanism of the AGV is important in order to achieve the objective of this project. The usage of the pillow block has increased the ability of the motor to carry the load by converting the weight force of the load into the rotational force. The existence of the rotational force was because the ball bearing that is placed in the pillow block. The usage of pillow block also increases the durability of the AGV motor shaft by distributed the weight force equally without harming to the motor shaft.

The usage of infrared sensor as obstacle avoidance also increased the safety feature of the AGV. This is because the used infrared sensor can detect anything in front of it within 20cm. Therefore, this AGV are safe to use in indoor application area such as supermarket, warehouse, library and any environment that involving moving and sorting work.

REFERENCES

[1] L. Han, H. Qian, W. K. Chung, K. W. Hou, K. H. Lee, X. Chen, G. Zhang, and Y. Xu, "System and design of a compact and heavy-payload AGV system for flexible production line." pp. 2482-2488.

[2] T. Muller, *Automated Guided Vehicle*, Kempston, England: IFS Ltd., 1983.

[3] H. Martínez-Barberá, and D. Herrero-Pérez, "Autonomous navigation of an automated guided vehicle in industrial environments," *Robotics and Computer-Integrated Manufacturing*, vol. 26, no. 4, pp. 296-311, 8//, 2010.

[4] D. Yaling, G. Xiaoying, L. Zhun, and S. Mei, "The new navigation system for automatic guided vehicle." pp. 4653-4658.

[5] J.-L. Hou, and T.-G. Chen, "An RFID-based Shopping Service System for retailers," *Advanced Engineering Informatics*, vol. 25, no. 1, pp. 103-115, 1//, 2011.

[6] T. Tsukiyama, "RFID Based Navigation System for Indoor Mobile Robots," *IFAC Proceedings Volumes*, vol. 44, no. 1, pp. 1084-1089, 1//, 2011.

[7] E. Hammerle, P. Winton, and S. Fett, "A multipath-mitigating indoor carrier-phase position tracking system." pp. 671-673.

[8] L. Grewe, and B. Shahshahani, "Image Processing Background," *Distributed Sensor Networks, Second Edition*, Chapman & Hall/CRC Computer & Information Science Series, pp. 59-92: Chapman and Hall/CRC, 2012.

[9] S. Butdee, and A. Suebsomran, "Automatic guided vehicle control by vision system." pp. 694-697.

[10] C. Wang, L. Wang, J. Qin, Z. Wu, L. Duan, M. Cao, Z. Li, Weiguangli, Z. Lu, Y. Ling, M. Li, Y. Wang, J. Long, M. Huang, Y. Li, and Q. Wang, "Development of a vision navigation system with Fuzzy Control Algorithm for Automated Guided Vehicle." pp. 2077-2082.

[11] A. H. Ismail, H. R. Ramli, M. H. Ahmad, and M. H. Marhaban, "Vision-based system for line following mobile robot." pp. 642-645.

[12] A. Ye, H. Zhu, Z. Xu, C. Sun, and K. Yuan, "A vision-based guidance method for autonomous guided vehicles." pp. 2025-2030.

[13] E. Hitomi, J. da Silva, and G. Ruppert, "3D scanning using RGBD imaging devices," *Computational Vision and Medical Image Processing IV*, pp. 197-202: CRC Press, 2013.

[14] E. Dill, and M. U. d. Haag, "Integration of 3D and 2D imaging data for assured navigation in unknown environments." pp. 285-294.

[15] G. Spampinato, J. Lidholm, C. Ahlberg, F. Ekstrand, M. Ekstr, x00F, and L. Asplund, "An embedded stereo vision module for industrial vehicles automation." pp. 52-57.

[16] N. K. Verma, G. Kumar, A. Siddhant, P. Nama, A. Raj, A. Mustafa, N. K. Dhar, and A. Salour, "Vision based obstacle avoidance and recognition system." pp. 1-7.

[17] N. K. Verma, P. Nama, G. Kumar, A. Siddhant, Ocean, A. Raj, N. K. Dhar, and A. Salour, "Vision based object follower automated guided vehicle using compressive tracking and stereo-vision." pp. 1-6.

[18] A. V. Gulalkari, D. Sheng, P. S. Pratama, H. K. Kim, G. S. Byun, and S. B. Kim, "Kinect camera sensor-based object tracking and following of four wheel independent steering automatic guided vehicle using Kalman filter." pp. 1650-1655.

Application of Sensors in Quality Evaluation of Mangoes

Journal Low Sze Kit
Faculty of Electrical Engineering
Universiti Teknologi Malaysia
Johor Bahru, Malaysia.
Lskjournal2@live.utm.my

Khairul Hamimah Abas
Control and Mechatronics Engineering Department (CMED)
Faculty of Electrical Engineering
Universiti Teknologi Malaysia
Johor Bahru, Malaysia.
khairulhamimah@utm.my

***Abstract*— This paper describes about the final year project on the application of 200kHz ultrasonic sensor in the quality evaluation of mangoes. In this project, a quality evaluation device was built to assess the ripeness of mangoes: unripe, ripe and over ripe. Two units of 19mm metal 200kHz ultrasonic transceiver were interfaced with an Arduino Uno microcontroller, whereby the output was shown on an 16x2 Liquid Crystal Display (LCD). The usage of ultrasonic sensor in evaluating the quality of mangoes is non-invasive as compared to the conventional method where samples of mangoes were sacrificed to determine the quality of the batch harvested. Besides, the usage of ultrasonic sensor promotes repeatability in measuring the ripeness of mangoes, whereby the ripeness of all the mangoes harvested can be assessed, rather than judgement based on samples tested. From the results, it was found that for an unripe mango, the voltage reading is 1.15V. For an over ripe mango, the voltage reading is 1.24V, whereas for a ripe mango, the voltage reading is 1.01V. In this project, the type of mango evaluated is MA165, a common cultivar found in Malaysia.**

Keywords—ultrasonic; quality evaluation; mangoes; ripeness;

I. INTRODUCTION

Mango (Mangifera Indica) is one of the most popular tropical fruit in the World. [1] It is also known as the "king of fruits." [2] Due to its popularity throughout the world, mangoes are being cultivated, harvested and exported rapidly. Traditionally, a mango is harvested based on judgements by the growers by observing the appearance of the fruit. [3] Naked eye observation is used to assess the quality of mango. [4] Traditional approaches are either subjective or time-consuming, so it should be a surprise that how to measure fruits' internal and external attributes nondestructively and rapidly has become a research hotspot. [5] With the drawbacks of the traditional invasive techniques in postharvest procedure, in which the quality of the mangoes are being evaluated. Numerous works are being carried out to explore some non-destructive methods such as Near Infrared (NIR), Nuclear Magnetic Resonance (NMR), X-ray and Computed Tomography (CT), electronic nose, machine vision and ultrasound for quality determination of fruits. [6] The problem statement of the project is the replacement of invasive techniques with non-invasive techniques with implementation of sensor instrumentation in quality evaluation of mangoes. Two objectives were identified for this project: (1) to develop a mango quality evaluation device for non-invasive assessment in quality of mangoes, (2) to fulfill the requirement as a part of assessment for the degree of Bachelors of Engineering (Electrical-Mechatronics). Six scopes were identified upon commencing with this project: (1) two units of 19mm metal 200kHz ultrasonic transceiver are used, with one acting as the transmitter and the other as receiver, (2) a quality evaluation device is built to ease the assess the ripeness of mangoes, (3) the configuration of ultrasonic transducer in this project is reflection mode, in which the acoustic wave transmitted from the transmitter reflects upon contact with the seed of the mango and detected by the receiver, (4) the quality evaluated is the voltage reading of the ultrasonic receiver, where the readings are further being classified according to the ripeness of the mangoes, (5) the type of mangoes cultivar being assessed is Maha 65 (MA 165), a common cultivar available in the country, (6) the target user of this device will be daily consumers, which consists of adult members of different age, gender and background in the society.

II. LITERATURE REVIEW

A. Ultrasonic Transducer

Ultrasonic transducer applies the working principle of ultrasound. When a disturbance occurs at a portion in an elastic medium, it propagates through the medium in a finite time as a mechanical sound wave by the vibrations of molecules, atoms or any particles present. [7] There are a few characteristics of ultrasonic waves: reflection, refraction, diffraction, and absorption. When a wave is traveling through one material and impinges on a boundary between it and a second medium, part of the energy travels forward as one wave through the second medium while a part is reflected back into the first medium, usually with a phase change. [8] This is known as Reflection. Time-of-flight (TOF) is used to measure the time for the ultrasound waves to travel from the transmitter to the receiver, with possible reflections involved upon contact with another medium. It is also used in absorption, also known as transmission mode. One of the condition for the medium in TOF measurement is that the medium must be clean, with no impurities involved. Or else, Doppler's effect of measurement should be taken into account. Doppler effect is the change in frequency or wavelength of a wave (or other periodic event) for an observer moving relative to its source. [9] Refraction is a phenomenon, whereby a wave traveling from one material into

another material can experience a change in its course. [10] a wave passing near the edge of an object has a tendency to become bent toward and around it. [10] The bending is known as diffraction. [10] In wave absorption, Ultrasonic waves may lose energy and get absorbed depending on the type of material and distance it traveled. [10] These days, most practical ultrasound sources are based on the piezoelectric principle of transconduction. [11] Piezoelectric has an advantage of simple construction and operation, which makes them suitable for a variety of applications. Ultrasonic transducer has been applied widely in nondestructive evaluation: high temperature monitoring in harsh environments and also imaging (also known as tomography). Process tomography is the general name given to a range of techniques in which data are recorded using remote sensors and then manipulated to provide measurements of concentration distribution and flow phenomena within process equipment such as pipes and reactors. [12]

The exponential increment in the relationship between receiving and transmitting making ultrasonic sensor a good sensor in evaluating the ripening of mangoes. The attenuation in the transmitting and receiving signals of ultrasonic sensors matches the graph of maturity level and total sugar across a certain period. **Error! Reference source not found.** Studies have proven that ultrasonic sensor is a suitable sensor in evaluating the maturity level of a mango.

B. Near Infrared Spectroscopy (NIS)

Near infrared spectroscopy shows the best results among the other ranges of the magnetic spectrum. [14] Voltage is applied across the system to launch the infrared optical power generated by the light source NIR emitter diode. [14] When fruit is in contact with the infrared optical transmitter, infrared optical power light is transmitted through the fruit texture to the receiver circuit which based on photo-detector to detect the infrared optical power light and to convert it into an electrical signal. [14] The obtained result was in the range of 3.5 V to 4.2 V for unripe mango fruit and the ripest one. [14] This method developed has proven that the quality of fruit can be determined non-destructively.

The visible and near infrared (Vis/NIR) spectroscopy, multispectral imaging and hyperspectral imaging techniques can also be applied in the quality evaluation of mangoes. [5] Imaging and spectroscopy are two important directions of conventional optical technology. [5] Imaging techniques obtain the images of fruits and spatial information. [5] Spectroscopy provides information about the chemical components and physical properties of fruits by obtaining optical information. [5] Imaging spectral techniques enable the acquisition of fruit images and spectral information simultaneously, with high spectral resolution and multiple wavebands. [5] According to the spectral resolution, imaging spectroscopy can be divided into multispectral imaging, hyperspectral imaging and ultra-spectral imaging. [5] Multispectral imaging and hyperspectral imaging are proved to be feasible for the measurement of fruit quality parameters. [5] Visible and near infrared (Vis/NIR) radiation covers the range from 380–2500 nm in the electromagnetic spectrum. [5] As the signals of almost all major structures and functional groups of organic compounds can be detected with a considerably stable spectrogram, therefore these spectra are commonly used for analysis. [5] Wavebands which are used in multispectral and hyperspectral imaging technologies can also be used. [5] When incident radiation hits on a surface, it can be reflected, transmitted or absorbed. [5] This reflects the physical attribute and chemical constitution inside the samples. [5] With the obtained spectrum, chemometric methods are applied to obtain the information on the quality of mangoes and eliminate the interference factors of the samples. [5] The reflectance spectroscopy to measure the soluble solid contents (SSC) and pH values of mangoes. [6] Schmilovitch et al. later applied the near infrared (NIR) reflectance spectroscopy to measure the firmness, SSC, acidity and storage period of mangoes. [15]

III. METHODOLOGY

A. Block Diagram

The push button and 200kHz ultrasonic transceiver serve as analog input components to the system. The 200kHz of the transmitter pulse was generated by Arduino Uno with the pulse width modulation (PWM) script as in timer2 programming of microprocessor. At all times, the transmitter is generating pulses at 200kHz. Only when the push button is hit, the transceiver unit reads the sensor input. The sensor reading is converted from analog to digital (ADC) to fit in the maximum of 5V input of Arduino Uno. Fig. 1 shows the block diagram of the quality evaluation system.

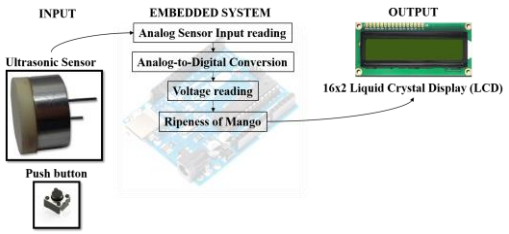

Fig. 1. Block diagram of the quality evaluation system

The voltage reading is then sent to the 16x2 liquid crystal display to enable the users to access the sensor input.

B. Flow Chart

As microcontroller is implemented in the quality evaluation system, therefore a flow chart is constructed to provide an overall flow for programming. Fig. 2 shows the flow chart of the quality evaluation system.

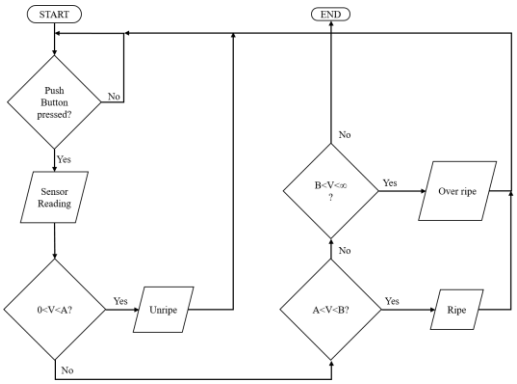

Fig. 2. Flow chart of quality evaluation system

As there are three classification of ripeness of mangoes, therefore in the flow chart there are three conditions to be checked. However, the evaluation of mangoes cannot be done if the push button is not hit. Therefore, the condition of the push button must be first checked and placed on the top priority of the flow chart. The voltage values of A and B are determined during the experiment upon completion of the hardware.

C. Circuit System Design

The circuit was first connected as shown in Fig 3. The transceiver unit which acted as the transmitter was connected to pin 3 of Arduino Uno, whereas the receiver was connected to pin A0. Pin 4 to pin 9 were to connected to the 16x2 liquid crystal display (LCD) in an orderly manner: RS, E, D4, D5, D6, D7. On the LCD, pin VSS, RW and pin K were connected to the Ground terminal, pin VDD was connected from the 5V power supply terminal. Pin V0 was connected from the output of 10kΩ potentiometer, whereas pin A was connected to a 330Ω resistor and the other terminal of the resistor was connected to 5V power supply terminal. The three units of normally open push button (NOPB) were connected to pin 10, 11 and 12 of the Arduino Uno. A 10kΩ resistor was connected to each of the NOPB from Ground to act as a pull up resistor for the NOPB. From the 9V battery, the positive terminal was connected to the common terminal of slide switch, the output of the slide switch was connected to the DC power plug positive terminal. The negative terminal of the 9V battery was connected to the negative terminal of the DC power plug. The DC power plug was plugged into the Arduino Uno to power up the circuit. The LCD, NOPB, and slide switch was connected on a separate board. Jumper wires were used to provide power supply to the components and feed the inputs and outputs (I/O) to and from the microcontroller.

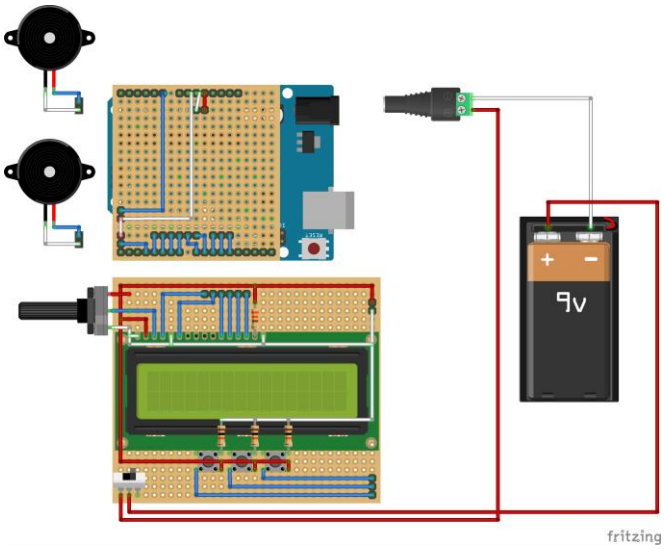

Fig. 3 Circuit System Design

After the circuit was connected, testing was done on the functionality of each component, especially on the LCD and push button. In order to do this, a series of Arduino source code was compiled and ran.

D. Procedures

The profiles of the subject tested, which are the Maha 65 (MA165) mangoes, were created. Nine mangoes, with three of each ripeness classification were purchased from the Taman Universiti Market. The mango samples were tested on the voltage characteristics according to the classification of ripeness of mangoes. Both the transmitter and receiver were placed on the surface of the fruit. In order to obtain the most effective placement of transmitter and receiver unit on the fruit, the experiment was conducted at three separate distance: the minimum distance whereby both the transmitter and receiver were placed next to each other, the maximum distance which is the farthest separation of the transmitter and receiver on the fruit, as well as the distance in between the maximum and minimum. The button was pressed and the reading at the receiver was detected. The analog sensor input value was then processed, went through analog-to-digital conversion (ADC) to be read as voltage value. The process of ADC was done by Arduino Uno. The voltage value was then sent to the LCD for observation. All observations were recorded and tabulated. The procedures were repeated for the other eight samples, and the experiment was repeated for seven continuous days.

IV. Results and Discussion

An experiment was conducted in identifying the voltage reading on the 200kHz ultrasonic transceiver for each classification of ripeness of mangoes. The voltage reading for each sample was taken for seven straight days. The results and analysis were further discussed in this section.

A. Results and discussions

Table I shows the minimum, maximum, median, mean and mode distance recorded from the experiment.

TABLE I. MINIMUM, MAXIMUM, MEDIAN, MEAN AND MODE DISTANCE RECORDED

Ripeness	Distance (cm)				
	Minimum	Maximum	Median	Mean	Mode
Unripe	0.0	10.0	4.0	3.8	4.5
Over ripe	0.0	9.5	4.2	3.9	4.5
Ripe	0.0	10.0	3.7	3.8	4.5

The maximum distance between transmitter and receiver was much limited by the length of the mango samples. However, upon analysis it was found that for all classification of ripeness, an effected distance between transmitter and receiver recorded was 4.5cm. This was shown from the mode distance, 4.5cm separation between transmitter and receiver was recorded as effective distance eight times in seven days. Therefore, it can be said that the ripeness of mangoes can be measured by placing the transmitter and receiver of 200kHz ultrasonic transceiver 4.5cm apart from each other for the most effective measurement.

Table II. shows the voltage reading of unripe samples of mangoes at minimum, maximum and effective separation distance between transmitter and receiver.

TABLE II. VOLTAGE READING OF UNRIPE SAMPLES OF MANGOES AT MINIMUM, MAXIMUM AND EFFECTIVE SEPARATION DISTANCE BETWEEN TRANSMITTER AND RECEIVER

Day	Minimum	Maximum	Effective Distance
1	3.20	0.91	2.58
2	0.22	1.60	1.53
3	0.92	1.32	1.48
4	1.54	1.83	1.48
5	1.32	1.04	1.15
6	1.41	1.35	1.08
7	0.92	0.64	0.64

From Table II., it can be seen that as the unripe mangoes ripen across seven days, the voltage reading decreases. This is due to the fact that as an unripe mango ripens, the concentration of sugar increases, and the total soluble solid (TSS) reduces. [16][17] This results in the wall of the fruit softens, less energy was needed to transmit ultrasonic wave into the fruit and reflect to the receiver.

Table III. shows the voltage reading of unripe samples of mangoes at minimum, maximum and effective separation distance between transmitter and receiver.

TABLE III. VOLTAGE READING OF OVER RIPE SAMPLES OF MANGOES AT MINIMUM, MAXIMUM AND EFFECTIVE SEPARATION DISTANCE BETWEEN TRANSMITTER AND RECEIVER

Day	Minimum	Maximum	Effective Distance
1	1.97	2.89	2.15
2	0.66	0.51	0.59
3	0.34	0.19	3.50
4	1.14	0.97	1.19
5	1.51	1.08	1.01
6	1.40	1.24	1.00
7	1.51	0.84	1.27

From Table III., it was found that as the over ripe mango further ripened, the voltage reading decrease drastically in two days, and increase gradually in the following five days. The wall of the fruit softened resulting in less energy needed to transmit ultrasonic wave into the fruit and reflected back to the receiver. Further softening in the wall of the fruit resulting in the ultrasonic wave transmitted came in contact directly with the seed of the fruit. The hard surface of the seed reflected the transmitted ultrasonic wave to the receiver. However, in Day 3, there was a sudden spike of voltage reading in effective measurement distance. This reading was considered as extreme values and discarded in analysis.

Table IV. shows the voltage reading of unripe samples of mangoes at minimum, maximum and effective separation distance between transmitter and receiver.

TABLE IV. VOLTAGE READING OF RIPE SAMPLES OF MANGOES AT MINIMUM, MAXIMUM AND EFFECTIVE SEPARATION DISTANCE BETWEEN TRANSMITTER AND RECEIVER

Day	Minimum	Maximum	Effective Distance
1	3.11	3.24	3.47
2	0.19	0.15	0.20
3	1.09	1.05	0.91
4	0.87	1.11	0.78
5	1.34	0.76	0.79
6	1.01	1.14	0.82
7	1.52	1.12	0.83

According to Table IV., the voltage reading for the ripe mango samples decreased in the first two days. However, the voltage reading increased and was maintained at a quite similar value for the remaining five days. From the effective separation

distance between the transmitter and receiver, it can be said that the voltage reading for ripe mangoes is about 0.50V. The earlier drastic decrease could possibly due to the fact that the ultrasonic transceivers were unstable and the duration between reading once the button was hit was 400 milliseconds. Another possible reason was due to the presence of air gap between the ultrasonic transceiver and the surface of the fruit. Therefore, to overcome this problem, couplant was suggested to prevent air gaps between the transceiver and the surface of the fruit.

V. CONCLUSION

As a conclusion, a quality evaluation device was built with two units of 19mm metal 200kHz ultrasonic transceiver, Arduino Uno and 16x2 liquid crystal display. Quality evaluation of mangoes were done with the ultrasonic transceiver configured into reflection mode, whereby one unit acted as the transmitter while the other as receiver. The separation distance between the transmitter and receiver obtained was 4.5cm Non-invasive techniques was implemented successfully. The type of quality parameter being assessed is the ripeness of the mangoes. As mango ripens, the total soluble solids (TSS) contents and sugar content increases. The wall of mangoes softens. The type of mangoes being used in this project is Maha 65 (MA165). The target users for the quality evaluation device is daily consumers.

For an unripe mango, the voltage reading is 1.15V, whereas for an over ripe mango is 1.21V and 1.01V for a ripe mango.

REFERENCES

[1] Mango Facts. (n.d.). Retrieved from http://www.mango.org/en/About-Mangos/Mango-Facts

[2] Purseglove, J.W., 1972. Mangoes west of India. Acta Horticulturae, 24: 107–74.

[3] Sivakumar, D., Jiang, Y., & Yahia, E. M. (2011). Maintaining mango (Mangifera indica L.) fruit quality during the export chain. Food Research International, 44(5), 1254-1263. doi:10.1016/j.foodres.2010.11.022.

[4] Rashmi Pandey, Prof. Nikunj Gamit, & Prof. Sapan Naik. (2014). A novel non-destructive grading method for Mango (Mangifera Indica L.) using fuzzy expert system. Paper presented at 2014 International Conference on Advances in Computing, Communications and Informatics (ICACCI): Advances in Computing, Communications and Informatics, New Delhi, India. doi: 10.1109/ICACCI.2014.6968366.

[5] Wang, H., Peng, J., Xie, C., Bao, Y., & He, Y. (2015). Fruit Quality Evaluation Using Spectroscopy Technology: A Review. Sensors, 15(5), 11889-11927. doi:10.3390/s150511889.

[6] Jha, S. N., Narsaiah, K., Sharma, A. D., Singh, M., Bansal, S., & Kumar, R. (2010). Quality parameters of mango and potential of non-destructive techniques for their measurement — a review. Journal of Food Science and Technology, 47(1), 1-14. doi:10.1007/s13197-010-0004-6.

[7] Mukhopadhyay, S. C., & Huang, R. H. (2008). Sensors: advancements in modeling, design issues, fabrication and practical applications (Vol. 21). Berlin: Springer. ISBN: 978-3-540-69030-6.

[8] Carlin B (1960) Ultrasonics, 2nd edn. McGraw-Hill, New York.

[9] Doppler, C. (1842). Über das farbige Licht der Doppelsterne und einiger anderer Gestirne des Himmels (About the coloured light of the binary stars and some other stars of the heavens). Publisher: Abhandlungen der Königl. Böhm. Gesellschaft der Wissenschaften (V. Folge, Bd. 2, S. 465-482)

[10] Terzic, J., Terzic, E., Nagarajah, R., & Alamgir, M. (2013). Ultrasonic Fluid Quantity Measurement in Dynamic Vehicular Applications. Cham: Springer International Publishing. ISBN: 978-3-319-00632-1

[11] Kuttruff H (1991) Ultrasonics—fundamentals and applications. London, Elsevier Applied Science

[12] Williams, R. A., & Beck, M. S. (1995). Process tomography: principles, techniques and applications (1st ed.). Oxford: Butterworth-Heinemann. ISBN: 9780750607445

[13] Ibrahim, S., Ramli, A., & Yunus, M. A. (2015). An ultrasonic system for determining papaya physiological properties. doi:10.1063/1.4915734

[14] Izneid, B. A., Fadhel, M. I., Al-Kharazi, T., Ali, M., & Miloud, S. (2012). Design and develop a nondestructive infrared spectroscopy instrument for assessment of mango (Mangifera indica) quality. Journal of Food Science and Technology, 51(11), 3244-3252. doi:10.1007/s13197-012-0880-z

[15] Schmilovitch, Z.; Mizrach, A.; Hoffman, A.; Egozi, H.; Fuchs, Y. Determination of mango physiological indices by near-infrared spectrometry. Postharvest Biol. Technol. 2000, 19, 245–252.

[16] Islam, M. K., Khan, M. Z., Sarkar, M. A., Absar, N., & Sarkar, S. K. (2013). Changes in Acidity, TSS, and Sugar Content at Different Storage Periods of the Postharvest Mango (Mangifera indica L.) Influenced by Bavistin DF. International Journal of Food Science, 2013, 1-8. doi:10.1155/2013/939385

[17] Valente, M., LAUX, D., & PRADES, A. (n.d.). Changes of ultrasound characteristics of mango juice during fruit ripening. Retrieved November 5, 2016, from https://agritrop.cirad.fr/567096/1/document_567096.pdf.

Automatic Sluice Gate Control at Paddy Field

Muhammad Fauzan Bin Saafi
Faculty of Electrical Engineering
Universiti Teknologi Malaysia
Johor Bahru, Malaysia.
fauzansaafi@gmail.com

Herlina Bt. Abdul Rahim
Department of Mechatronic and Control
Faculty of Electrical Engineering
Universiti Teknologi Malaysia
Johor Bahru, Malaysia.
herlina@fke.utm.my

***Abstract*—This paper introduce the solution of the problem at paddy field canal. The design utilize GSM technology, microcontroller, and non-contact sensor to measure the water level. The GSM monitoring was being used because of the people and the location of the project problem. This system result have been shown the sluice gate can be automated and monitored by GSM. So, this system are really suitable to be apply at the project location.**

Keywords—automatic;gsm monitoring;paddy field;sluice gate;

I. INTRODUCTION

As we know rice is the most importance food in Asian. So that to make Malaysia as a main rice producer, Malaysian government has set its rice independence level at 65% and is fit for producing this sum at present to satisfy Asian rice request [1]. Therefore to make the rice production in Malaysia fulfill the level that the Malaysia government have set, the technology of rice cultivation must be improve to increase the rice production while reduce the work force of the farmer. The automation technology must be introduce to the farmer so that they can use it in their rice cultivation.

Automation technology have been always applied in agriculture to reduce work force and increase the crop yield. In rice production or cultivation, an automation system for the water control will really help in reducing the work force of the farmer and increase the rice production. It also helps to reduce wastage, effective usage of fertilizer and thereby increase the crop yield [2]. If the automated irrigation take place, the farmer will be easy to monitor their crop [3]. The paddy cultivation are not same as other crop which is need the sprinkle to watering them.

Paddy growth are really influence by the water supply. Water should be keep standing in the field throughout the growth period of paddy. The paddy need flooded soil to grow them so the water are really needed to irrigate well in their growth period. Flooded soils helped improve stand establishment by compensating for reduced germination and mortality of seedling when flooded at early stages [4]. It also have greater availability in nutrient and can suppress weed competition. The flooded soil also a micro-climate which favorable to the paddy production.

Even though flooded soil have many advantages to the crop, excess water can lead to reduction of the crop production. Excess water may harmful to the crop which is crop may be affected to the pest and diseases. It also may cause the moisture stress and effect to the root growth. Fertilizer loss also might occur if the crop have excess water. It will lead to poor germination of the crop. The irrigation layout also may affected if the field have excess water. The soil wall that have been built by the farmer to separate their field may collapse because of the excess water.

So that, to overcome the excess water problem of the excess water, the sluice gate at the drainage must be apply automated system. Therefore the farmer not need usually to go check the water level whether he need to open the sluice gate or not.

II. LITERATURE REVIEW

A. Introduction

This chapter covers the literature review for this project. It will be the backbone that support the proposed idea for this project system. The literature review of this project have been separate into 3 part which is water level measurement, alert and monitoring system, and the sluice gate and its actuator. At first, the information and theories about water level measurement will be explain. Next, about monitoring system and lastly about sluice gate and it actuator.

B. Water level measurement

Water level can be measure by using many sensor and technique. It became important to measure the distance in many application such as water level in drainage. The water level monitoring could give early cautioning flood and the loss could be diminished [5]. There are many method of measuring the water level. Some method to measure water level are using mechanical sensors such as resistive, capacitive, or magnetic sensor. Although there are many method, the method can be separate in two main group. The first one is continuous level measurement for process monitoring while another one is point level measurement to activate alarm [5]. The method that might been used in this project is point level measurement.

A perfect water level sensing system must be capable to feature stability, high resolution and low cost [6]. Thus, to select the most suitable sensor in an application, there are many aspect must be consider before selecting it. Level sensors are categorized into two type which are invasive and non-invasive.

This criteria are need to consider whether the liquid which want to measure whether it can rust the sensor or not. It is because usually the rod that connected to the liquid measured is iron or steel. The environment factor are need consider too. As example, infrared sensor, the light intensity will be affect in the performance of sensor. Usually for river and agriculture, the commonly used sensor for water level measurement is ultrasonic sensor [7-11]. The river and paddy field drainage are almost same size even though the drainage size is a bit smaller. The environment of drainage is also same like the river so, theoretically the properties of paddy field drainage and the river is about same.

a. Ultrasonic Sensor For Water Level Measurement

Ultrasonic sensor are commonly used in automation system to measure the distance, position change and level measurement. It used principle of measuring the time of flight of ultrasonic wave [12]. Its mean this principle is free from colour rendering of the object and its surface. That why ultrasonic sensor can detect materials such as liquids, bulk materials, transparent objects, glass and so on.

According to koval et. al (2016), they said the characteristic of ultrasound same as audible sound in the environment. Ultrasound can be propagate in gaseous, liquid and solid and it usually considered as a sound frequency which is higher than 20 kHz [12]. In their paper, they classified ultrasound into two group which is active ultrasound and passive ultrasound. Active ultrasound generate the output in higher value. It usually used for cleaning, wielding and drilling. Meanwhile, passive ultrasound generate much lower output than active ultrasound and it usually used for measuring distance, detecting defects in materials and thickness of the materials, measuring the flow of liquids and gases and also diagnostics in healthcare [12].

Type of environment it moves and the current temperature of the environment will affect the speed of sound. It varies depend on condition.

Table 1: Velocity of sound in materials

Gases		Solids		Liquids	
(m/s)		(m/s)		(m/s)	
Air (0°C)	331	Al	5100	Water (20°C)	1481
Air (20°)	343	Steel	5000	Water (25°C)	1497
He (25°C)	965	Concrete	1700	Gasoline (20°C)	1170
H (25°C)	1284	Cu	3500	Hg (25°C)	1450
He – Helium H – Hydrogen Al – Aluminium		Cu – Cuprum Hg - Quicksilver			

Ultrasonic sensors operate on the principle of measuring the time of flight between sending and receiving the reflection of the transmitted signal. First, high level signal is sent for 10us using transmitter. Next, it sends eight 40 KHz signals automatically to detects whether the pulse is received or not. If the signal is received, then it is through high level. The high signal duration is the time of flight between sending and receiving the signal.

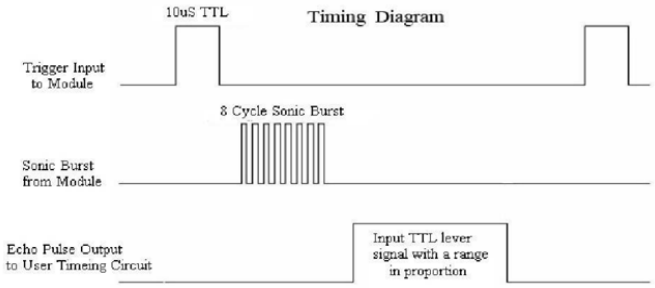

Fig. 1: Timing diagram of ultrasonic pulse

The ultrasonic sensor is operate by using two block which are transmitter and receiver. Transmitter block may be compose of two type of transducer which are magnetostrictive transducer and piezoelectric transducer. Magnetostrictive transducer operate at low frequencies and their principle is based on a mechanical change in the length of magnetic material while piezoelectric transducers operate at high frequencies and the principle is based on the inverse piezoelectric effect [12]. Meanwhile, ultrasonic receiver is based on the principle of the transfer of mechanical waves reflected back to an electrical signal [12].

C. Alert and monitoring system

Water level measurement data are really crucial in some water-related field such as water level in the drainage at paddy field [13]. Usually, water level measurements are manually done but it can led to an error cause of measurement site, human error, etc. So to overcome this problem, the monitoring system was introduced. By using monitoring system, the measurement will be done automatically by using the water level measurement device such as ultrasonic sensor. Then, the alert system will take places to alert the user about the current condition of the site.

Usually the monitoring and alert system that have been used to monitor the water level in agriculture and environment which river is GSM monitoring system [13-18]. It will help to improve the awareness of the user about the current condition on their field. So, it mean it is possible to send the data of the sensor to the user via GSM technology.

According to Arpana et. al (2015), they design their system to monitor the water in the dam using various sensor by integrate all of the sensor with microcontroller. Then, from microcontroller it send it to GUI at personal computer by using Xbee module. After that, it send alert SMS via GSM module when the measured data exceed the maximum or minimum threshold.

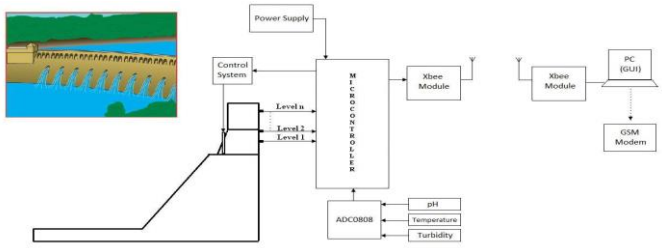

Fig. 2: System block diagram [19]

Meanwhile, according to Saraswati et. al (2012), it is possible to send SMS data measured by connecting the GSM module directly to the microcontroller. They used ultrasonic sensor to measure the water level then send it data to the cell phone by using GSM module [16]. The GSM module that they have been used is SIM300C which is compatible with their country communication band [16]. The user can request the data from microcontroller then microcontroller will calculate the water level then it send the data to the cell phone.

D. Sluice Gate and Actuator

Sluice gate is a moveable gate that control the quantity of water flow through it by rising it or lowering it. To increase the flow of the water, the gate needed to rise and to decrease it the gate is needed to lower. There are several style of sluice gate that presently used such as vertical rising sluice gate, flap gate, and radial sluice gate. The style of the gate are depending on the condition of the water flow and the size of the drainage. Usually the traditional sluice gate is manually operate sluice gate but nowadays people use actuator to open the gate.

By referring Ibrahim et. al (2015), in their paper they propose to build gate automation and control module (GACM) to automatically open and closed the gate. The present system that they want to apply their system is hydraulic vertical rising sluice gate operate manually. So, they want to improve the current system to automatic. The actuator they used to open the gate is 3.75HP Permanent Magnet DC Motor. The decision of using DC motor rather than AC motor can be justified with regards to creating world as far as cost-adequacy and adaptability [20]. For the most part, AC motor are 3 stage phase motor requiring a 3 stage supply not really accessible in a large portion of the channel system of Indus Basin.

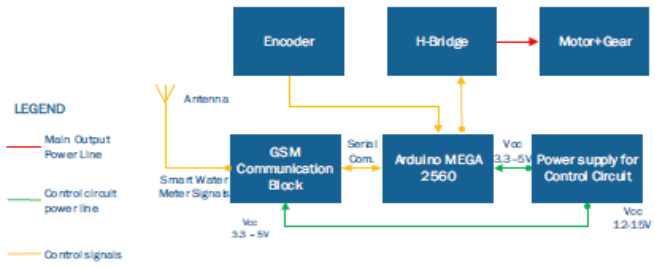

Fig.3: Gate Automation & Control Module Architecture [20]

III. METHODOLOGY

The control system of this project use arduino UNO as controller as well as its processing unit for the data. The coding for the arduino are done by using arduino IDE. Since the ultrasonic sensor input and output are digital input, therefore it can use digital port at arduino. After the arduino receive the input from the sensor the distance are needed to calculate by calculating the time of flight of it signal.

Distance = (Time x Speed of Sound in Air (340 m/s))/2

After some calculation, the arduino will decide whether the actuator need to ON or OFF to open and close the sluice gate. Then, the arduino will send the message via GSM module to the authorities.

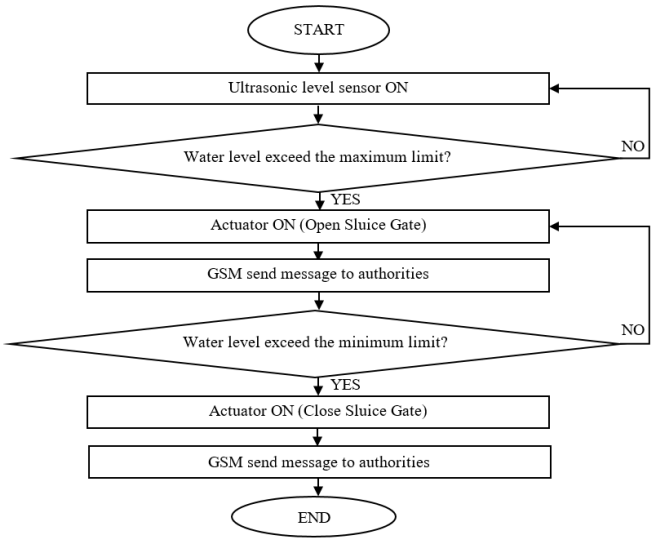

Figure 4: Flowchart of the system

A. Main Component

The main component in this project is Arduino UNO, HC-SR04 ultrasonic sensor, SIM900A GSM module and GA12-N20 Geared Mini DC Motor.

1) Arduino UNO and Arduino IDE

Arduino UNO is selected as a controller for this project due to it advance technology capability. It used ATmega328P as it microcontroller which is high performance but low power microcontroller and use 16 MHz crystal oscillator. Arduino UNO use 5V as its operating voltage and it recommended input voltage is 7-12 volt. It also have 14 digital input and output pin whereas 6 of it provide PWM output. The software will be used to program the arduino is Arduino IDE which use C and C++ as it programming language. Furthermore, arduino has a vast open resources and community which really help the understanding. Figure 3.3 shows the arduino UNO.

Fig 5: Arduino UNO and USB cable

2) HC-SR04 Ultrasonic Sensor

To measure the water level, HC-SR04 ultrasonic sensor is selected. This sensor is selected because it is economical sensor that gives 2cm to 400cm of non-contact measurement capability and its accuracy is up to 3mm. It operate at 5V DC and 15mA current. Furthermore, its measuring angle is only 15º which make it possible to put in the designated sensor holder. Figure 3.4 shows HC-SR04 ultrasonic sensor.

Figure 6: HC-SR04 Ultrasonic Sensor

3) SIM900A GSM module

To allow arduino send text message, SIM900A GSM module is selected. It is very low cost and simple arduino GSM module. The reason this module is selected because this module support 900 MHz communication which is most of mobile network provider in Malaysia is using 900 MHz communication band. It also use AT command control which make it easy to program. The AT command resource is really vast and have large community which really help. The figure 3.5 shows SIM900A GSM module.

Fig 7: SIM900A GSM Module

4) GA12-N20 Geared Mini DC Motor

The actuator used to open and close the sluice is GA12-N20 Geared Mini DC Motor. The reason for choosing this motor because it have 2 kg.cm torque at 3~12 V which make it possible to open the miniature sluice gate for this project. It load speed is 80 RPM, which is suitable to rotate the shaft attached at the gate to open it. It stall current only 1A which is compatible to use relay to switch on the motor. Figure 3.6 shows GA12-N20 Geared Mini DC Motor.

Fig 8: GA12-N20 Geared Mini DC Motor.

5) 5V Two 2 Channel Relay Module with Optocoupler

To control the switching and rotation of the motor to open the gate, 5V Two 2 Channel Relay Module with Optocoupler was used. The connection of the motor and power supply which were connected to the relay module was built to make the motor can rotate clockwise and anti-clockwise direction. This connection is recognize as H-bridge connection.

Fig 9: 5V Two 2 Channel Relay Module with Optocoupler

IV. RESULT AND DISCUSSION

As been told in methodology, this system focus on automation and monitoring. The experiment on miniature model of the project location have been conducted and running desired.

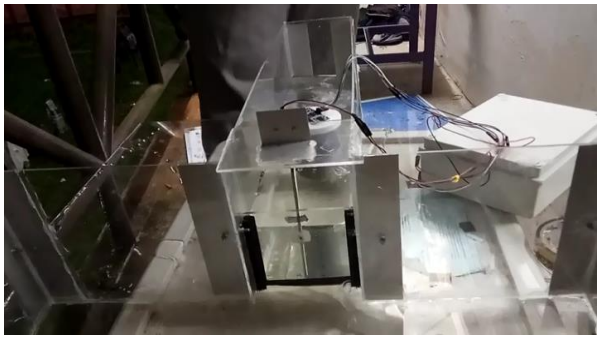

Fig. 10: Photo taken before the gate open

The photo shown the water level at the maximum point which is the gate must be open so that the water can flow out.

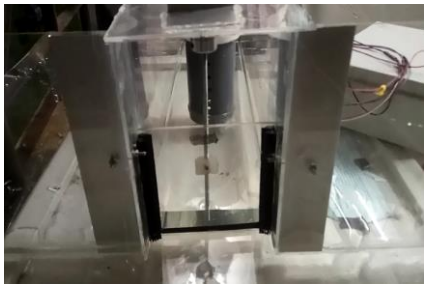

Fig. 11: Photo taken after the gate open

The photo shown the water level at the minimum point which is the water must be reserved for the emergency condition such as the next day or the next week there are no rain occur.

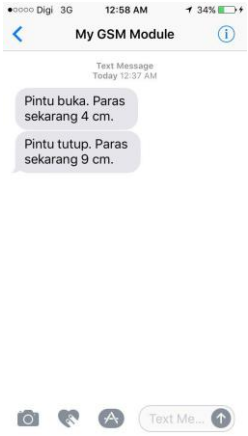

Fig. 12: The message receive from GSM module

After the gate was open it will send the message to the authority to inform him and it will notify again after the door closed.

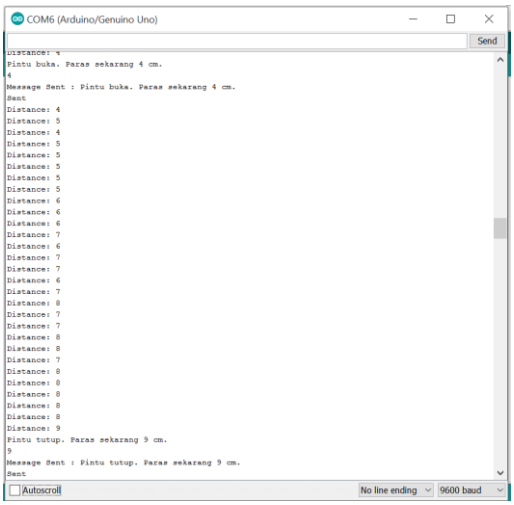

Fig. 13: Serial monitor of the microcontroller

While running the system the microcontroller have been monitored through the serial monitor to see the sequence of the program code.

V. CONCLUSION

After completing the project, the sluice gate should be able to running automatically by deciding whether to open or close the gate according to the water level in drainage. After it open or close the gate, the system should send text message to the authorities which is user whether it open or close the gate. Hope that, this project can be implement in the real sluice gate so that the excess water problem at paddy field can be solved. Lastly, after this problem have been solve, the rice production can be increase. So that, Malaysia food security can be secure.

[1] Najim, M. M. M. et al. "Sustainability of Rice Production: A Malaysian Perspective“, The Journal of Agricultural Sciences, 2007, vol. 3, no. 1

[2] P. Rajalakshmi and S. Devi Mahalakshmi, "IOT based crop-field monitoring and irrigation automation," 2016 10th International Conference on Intelligent Systems and Control (ISCO), Coimbatore, 2016, pp. 1-6.

[3] S. Saseendran and V. Nithya, "Automated water usage monitoring system," 2016 International Conference on Communication and Signal Processing (ICCSP), Melmaruvathur, 2016, pp. 0099-0103.

[4] Lal, B. et al. "Agronomic Manipulations Can Enhance The Productivity Of Anaerobic Tolerant Rice Sown In Flooded Soils In Rainfed Areas". Field Crops Research (2016): n. pag.

[5] Chetpattananondh, K. et al. "A Self-Calibration Water Level Measurement Using An Interdigital Capacitive Sensor". Sensors and Actuators A: Physical 209 (2014): 175-182.

[6] Loizou, Konstantinos and Eftichios Koutroulis. "Water Level Sensing: State Of The Art Review And Performance Evaluation Of A Low-Cost Measurement System". Measurement 89 (2016): 204-214.

[7] A. Kruger; W. F. Krajewski; J. J. Niemeier; D. L. Ceynar; R. Goska, "Bridge-Mounted River Stage Sensors (BMRSS)," in IEEE Access , vol.PP, no.99, pp.1-1

[8] M. Mousa, X. Zhang and C. Claudel, "Flash Flood Detection in Urban Cities Using Ultrasonic and Infrared Sensors," in IEEE Sensors Journal, vol. 16, no. 19, pp. 7204-7216, Oct.1, 2016.

[9] N. Ahmed, A. K. Azad, M. R. Khan, A. Habib, S. Ghosh and S. Shahid, "ShonaBondhu: a cloud based system to handle flash flood," 2016 International Conference on Networking Systems and Security (NSysS), Dhaka, 2016, pp. 1-6.

[10] L. L. Pfitscher et al., "An automated irrigation system for rice cropping with remote supervision," 2011 International Conference on Power Engineering, Energy and Electrical Drives, Malaga, 2011, pp. 1-6.

[11] S. P. Bhat and S. R. Hirekhan, "Automation of water discharge process at canals," 2015 International Conference on Applied and Theoretical Computing and Communication Technology (iCATccT), Davangere, 2015, pp. 609-613.

[12] Koval, L., J. Vaňuš, and P. Bilík. "Distance Measuring By Ultrasonic Sensor". IFAC-PapersOnLine 49.25 (2016): 153-158.

[13] M. Saraswati, E. Kuantama and P. Mardjoko, "Design and Construction of Water Level Measurement System Accessible through SMS," 2012 Sixth UKSim/AMSS European Symposium on Computer Modeling and Simulation, Valetta, 2012, pp. 48-53.

[14] Sagar Sudhakar Mane and M. K. Mokashi, "Real-Time Flash-Flood Monitoring, Alerting and Forecasting System using Data Mining and wireless sensor Network," 2015 International Conference on Communications and Signal Processing (ICCSP), Melmaruvathur, 2015, pp. 1881-1886.

[15] A. M. Telgote, V. Narayanan and N. A. N. Dave, "Design and implementation of water environment monitoring system using GSM

technology," 2015 International Conference on Technologies for Sustainable Development (ICTSD), Mumbai, 2015, pp. 1-4.

[16] M. Saraswati, E. Kuantama and P. Mardjoko, "Design and Construction of Water Level Measurement System Accessible through SMS," 2012 Sixth UKSim/AMSS European Symposium on Computer Modeling and Simulation, Valetta, 2012, pp. 48-53.

[17] Kuchekar, Nilesh D. "GSM Based Advanced Water Deployment System For Irrigation Using A Wireless Sensor Network & Android Mobile". International Journal of Electrical Electronics and Data Communication 3.8 (2015): n. pag.

[18] Suhasini, Chimata and Diwakar R. Marur. "Gsm And Wireless Sensor Network BASED Smart Automated Irrigation System". IJIREEICE 3.4 (2015): 50-53.

[19] A. M. Telgote, V. Narayanan and N. A. N. Dave, "Design and implementation of water environment monitoring system using GSM technology," 2015 International Conference on Technologies for Sustainable Development (ICTSD), Mumbai, 2015, pp. 1-4.

[20] S. Ibrahim, M. Soban, F. Akhtar and A. Muhammad, "Gate Automation for Closed Loop Control of Distributary Irrigation Canals in the Indus Basin," 2015 13th International Conference on Frontiers of Information Technology (FIT), Islamabad, 2015, pp. 341-346.

Vision Based Text Recognition Reading Assistive System

Tan Siu Fong
Faculty of Electrical Engineering
Universiti Teknologi Malaysia
Johor Bahru, Malaysia.
s.f.tan94@gmail.com

Sham Ismail
Control and Mechatronics Eng, Department
Faculty of Electrical Engineering
Universiti Teknologi Malaysia
Johor Bahru, Malaysia.
fatimahs@utm.my

***Abstract*— Reading has always been a problem for the population who suffered from visual impairment including total blindness. They have restricted access to the content of printed material and usually need assistance from care takers to aid them in reading. A reading assistive system which captured the reading content in term of images, extract and translate the information to the user through speech output is proposed. The designed system is targeted to be wearable, portable and able to read full A4 sized document which made up of Tesseract Optical Character Recognition (OCR) Engine and Flite Speech Synthesizer. However, the system itself has to have high output accuracy to provide a reliable reading. Hardware and software approaches to enhance focusing, flashing external light on reading material to provide constant illumination and image pre-processing techniques such as hand detection, image sharpening, thresholding, skew angle correction, Stroke Width Transformation (SWT), panoramic image stitching and morphological transformation in image text region localization and extraction are proposed. From the result, the lens gives zooming effect on text images and external light source ensure uniform illumination meanwhile the applied text image pre-processing has further enhanced the text recognition accuracy better than raw original image, from F1 scores of 0.68 to 0.87 with reading board and 0.48 to 0.79 without reading board. In short, the reading assistive system is successfully implemented associated with some basic button interface, providing instruction using speech synthesizer and read out image text to user with fair accuracy.**

Keywords—Oprical character recognition; visual impairment; reading assistive system; Text to speech

I. INTRODUCTION

World Health Organization estimated that 285 million people to be visually impaired worldwide where 90% of them live in low-income condition and 82% of people living with blindness aged 50 and above. The statistic of visual impairment population is further supported by the study conducted by WHO in six regions, namely African, America, Eastern Mediterranean, European, Southeast Asian and western pacific region as shown in Fig. 1 [1]. Meanwhile, in 2009, there are approximate 23,738 people from Malaysia who suffer from blindness and visual impairment, according to a study of Melisa Ng Lee *et al*. [2]. They, who suffered from visual impairment, are usually having difficulties in developing their personal skills and thus affecting their ability to work, which has caused a significant effect to their living quality. Mobile assistive technologies have been an active research topic to make handheld devices more accessible through various sensory channels [3]. This is to provide better quality of life and independence for them to be able to participate in social activities or contributing to the community.

People who are visually impaired have difficulties in accessing content from books or document. This has slowed down their learning process as their knowledges are limited only to materials, which have been converted to braille text or have been translated for them in term of audio format. Although there is available assistive smart reader device such as OrCam [4] has been developed to help them in reading, however, these devices are not affordable by them who are low in income. This device only practicable to low vision individual, but is not applicable to those who suffered from total blindness as they do not know the location of text to be read. Therefore the objective of this project is to come out with an alternative reading assistive system that have enhanced accuracy of text recognition rate through the mean of hardware and software design. Besides that, the system must able to provide an alternative way in solving aiming problems such as through a speech feedback to aid users in A4 sized document alignment and apply text localization in the captured document image.

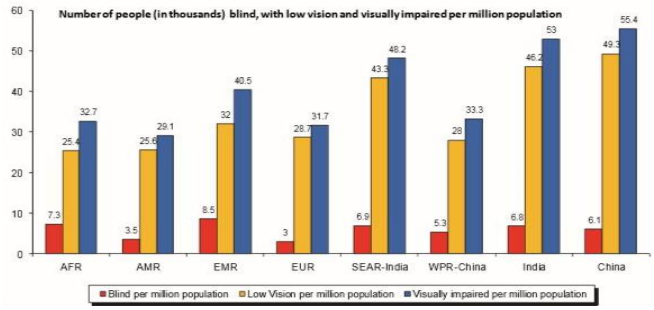

Fig. 1. Number of people (in thousands) blind, with low vision and visually impaired per million population in the year 2010

II. LITERATURE REVIEW ON PREVIOUS WORK

In terms of ongoing research regarding the reading assistive devices, [5] has designed a glass with a Logitech webcam

capable of auto focusing to read text and product labelling from handheld objects. It solves the aiming problem through a motion based approach where user has to shake the handheld object to isolate interest object from background. It involves the uses of laptop as its data processing unit and for generating audio output. Meanwhile, [6] uses a scanner to scan physical A4 sized document into text images before performing the text extraction. The designed system included a scanner which is large in size and not to be wearable by the user. This has restricted the portability of the system. A Linux based operating system, namely the VimpyOS is used as the control unit in producing output on any VimpyOS compatible hardware. Finger Reader proposed by [7] introduced the use of wearable ring like devices on finger to read papers with printed text. Coupled with haptic feedback and real time auditory, it guides user to scan through text via vibration pulses generated by the vibration of the motor on the device. As the software is a standalone PC application, it is presumed that it involves a personal computer in processing. A high resolution mini video is in use during the finding. On the other hand, [8] allows skew text images detection up to $\pm 15^{o}$ and perform orientation correction by performing simple image rotation. It uses a web camera to capture the text images with Raspberry pi as the main processing unit.

A. Building Block of Reading Assistive System

From the review of finding by [5-12], it can be concluded that all of the related work which work on a reading assistive system consist 5 stages. Firstly, an image of text is captured through a text capturing devices such as a camera or scanner. After that, it undergoes pre-processing to detect and enhance the region of text before it is fed into an OCR Engine for text extraction. The extracted text is written as a file with an extension such as ".txt" where this file is then being read out by a speech synthesizer to the user.

B. OCR Engine

It is the engine that in charge of extracting text in capturing images and write the extracted content into a file to be used by a speech synthesizer. [8] uses Template matching with the ASCII value of recognized character as a method of character recognizing rather than using third party developed packages as the OCR Engine. Meanwhile [5] has tested OmniPage and ABBYReader closed source solutions and Tesseract as the open source solution in performing the text recognition and extraction. [7] also proposed the use of Tesseract as an image to text engine. Lastly, Cuneiform software packages is used by [6] to read printed text from images.

C. Speech synthesizer or Text To Speech

Speech synthesizer is used to read the text extracted output file from the OCR Engine and convert it into audio format by saving it into MP3 files or is directly read to the user. eSpeak software package is used as the Speech synthesizer in generating output audio by [8] & [6]. With laptop used as the data processing unit, [5] used Microsoft Speech Software Development kit to load files and play the text information to the user. The translation of text to speech is accomplished in [7] with the used of the Flite package as the Speech synthesizer.

D. Pre-Processing involved in text recognition

Text detection has been an important process, which depends muchly on content-based image analysis task [13] in a reading assistive system. The importance of pre-processing in enhancing text region by ensuring efficient foreground extraction has been stressed by [12]. An improved algorithm for background subtraction can reduce the effect of complex background must be implemented. As a reading assistive system emphasized the accuracy of speech translated text content, poor image quality such as uneven lighting, degradation and blurring can cause noise, therefore text in an image or video must be robustly detected before feeding to OCR Engine. Besides that, the performance of OCR drops drastically when applied to scene images. First, this is mostly due to OCR is designed for scanned text images and greatly depends on page segmentation to isolate text from background pixels. Second, natural scene images are captured under various imaging conditions which imposed noise, blur, occlusions. Therefore, text segmentation played an important role in providing great text recognition performance [14]. Sophisticated text reading system usually will employed page segmentation scheme to identify text regions in images, as this will help to reduce the time spent by OCR Engine in interpreting nontext item [15].

Text segmentation, text images enhancement and background subtraction can be categorized as the pre-processing of text images or scenes text. These pre-processing involves learning gradient features of stroke orientations and distributions using Adaboost model [5], using Matched Wavelets and MRF Model in locating text [16] and OTSU thresholding, morphological transformation in generating drawing contour which used to draw the bounding boxes for each character [15] before the extracted character is applied in the OCR Engine.

Stroke Width Transform (SWT) [14] transforms the image data from containing color values per pixel to containing the most likely stroke width of image pixel which likely to be a character in a natural scene. SWT proposed by this paper is robust where it's able to detect text regardless of its scale, direction, font or even language compared to traditional, dependable text detection such as different language character training model or matching in searching text region. With a local image operator combined with geometric reasoning can be used to recover text reliably. All the previous work proved that pre-processing and post processing is significant in implementing a reliable reading assistive system.

III. METHODOLOGY

Image of document must be taken before it can be read out, therefore fitting a full A4 size reading material in a camera view is difficult as there is a tradeoff between pixel containing character information and distance between the reading materials. Moreover, a low vision user might have problem to know the exact position of the document and the reading assistive device to fit in the full sized document. It is important that the output extracted text has to be accurate enough to provide reliable reading as the TTS engine read according to what has been extracted in the form of text. Therefore, the proposed method is used to address the text alignment, localization, and enhance the accuracy of text recognition rate through the mean of hardware and software design. To illustrate

the design, Raspberry pi 3 model B single board computer is used as the center processing unit which in charge of decision making meanwhile Raspberry pi camera will be used as text images capturing device. The overall system will consist of a wearable glass attached to the pi camera meanwhile a single board computer, earpiece, and some input switches for basic interaction with the device on a wearable arm wristed band. The chosen OCR Engine and speech synthesizer are Tesseract package and Festival package respectively. These packages are chosen due to their open sourced availability and they are still under active development by the developer community.

A. Hardware Design

As the pi camera is a low cost embedded camera which lack of auto focusing capability, certain degree reading glasses lens (diopter strength +1.00, +1.50, +2.00) is proposed to add in front of the camera to give a clearer focus in a shorter shooting distance. As the normal reading distance is usually within arm reachable range, lens with a fixed focal length can be calculated to give best focus and magnification to the document. 1 diopter is said to be lens with 1 meter focal length. For reading glasses, magnification increased as the focal length gets shorter whereby the magnification on reading lens is called diopter strength. Given a formula as in (1), it is known that diopter is the reciprocal of the focal length. However, this doesn't necessarily mean small focal length is suitable for this application as focal length decreased, the document has to be within the focal length to give better focus, or else it will blur the image. Therefore, by assuming maximum reach of human arm to be 60 cm (0.6 meter), it gives +1.66 diopter approximate to +1.5 diopter to give focus plus magnification, which provide clear image within reading distance of 60 cm. With the diopter strength increased, the reading distance has to be decreased or place document closer to the camera. However, this calculation does not include the focal length of pi camera itself, so it is just a rough approximation.

$$\text{Diopter} = 1 / (\text{Focal Length (meter)}) \quad (1)$$

Besides that, to provide consistent lighting during day and night, flashing of external light on reading material is proposed. The images of text are to be taken under the external light source to eliminate noise on text extraction due to nonuniform illumination on the captured documents. It also used to enhance the contrast between black colored text and printed paper's background.

B. Software Design

Firstly, in order to fit the document into camera view, video streaming is started and user is requested by the system through speech instruction by Flite to center their document in front of them. This is done by ensuring both hand of user which are holding the document is inside the camera view. Therefore hand contour detection is used to extract user's hand in YRCB color space as stated in [17]. This paper finding proposed different range of color code for different skin color where for normal skin color, hand is represented by [(0, 133, 77) to (255, 173, 127)] in a YRCB image. However, object which shares the same color code as our hand tends to make the image noisy. Therefore, each contour is filtered by its area and solidity whereby contours that fulfilled certain properties as hand is differentiated from nonhand object. By taking both sides and bottom of camera view as reference as shown in Fig. 2, user is given instruction to align the document in a left to right motion until both hands is fit into both sides view, then the user is prompted again to align the document in a top to bottom manner until the hand contour is fit in the bottom reference zone. After alignment is done, video streaming is stopped and an image is captured as shown in Fig. 2. In order to further provide uniform light illumination, external light source is flashed during the document capturing interval.

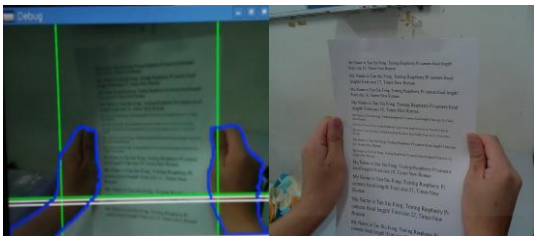

Fig. 2. Line drawn in green is the system reference for document alignment through hand contour detection (left) and image taken after video streaming is stopped (right)

The operation of capturing images is applied with a pre-set parameter named sharpness in pi camera setting. Sharpness is defined as the boundaries between zone of different tones in images where their boundaries are usually crisp step and clearly seen (not blur). From the available scale of -100 to 100, sharpness of 100 is applied to provide clearer text character boundaries throughout the capturing of images. However, from Fig. 2 it is obvious that only part of the document is being captured. Problem arises when it comes to take full view of document while maintaining the high amount pixels content of a character. To issue this problem, two images are to be taken; one on the top edge of the document, and another taken on bottom edge of the document as shown in Fig. 3. The two images are then stitched together to produce a panoramic image of a full sized document. Prior to the stitching, both original images will undergo grayscale conversion, thresholding, Laplacian edge operator, edge enhancement and morphological filtering to produce two binary images. This is to prevent stitching two original images that might have different light exposure on background due to movement while aligning the document. Edge enhancement, dilation and erosion are used to maintain and preserve the text or character edge generate by Laplacian operator in the binary image. However, it is recommended to hold the document around the center edge of the document.

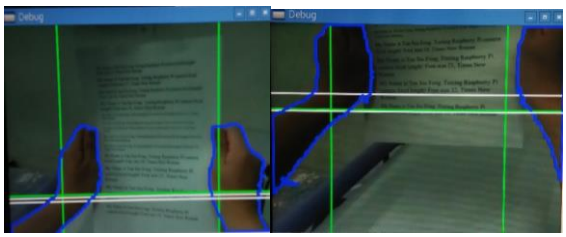

Fig. 3. Two reference (top and bottom) for system to captured two images that will be stitched into full document view

The effort in improving the output recognition rate is to emphasize on the pre-processing on text images before feeding the image to Tesseract OCR engine. Sequence of proposed method involved in the pre-processing is discussed. After getting the stitched binary image, foreground document has to

be isolated from noisy background. Canny edge detection and dilation is first applied to search for connecting contour that represent the document's edge.

Text localization is to enable the system to automatically detect text region in the binary image and perform text segmentation for easy character recognition by the OCR Engine. SWT operator from [14] is used to perform this job through detecting character stroke width. This is to get Region of Interest (ROI) on character or text in the binary image. The ROIs obtained allow a mask to be created to mask out noncharacter region such as picture or nontext component. The pre-processing process ends with the use of parent rectangles to enclose segment of child rectangles or ROIs to produce a few bounding rectangle that eventually being used to crop text regions from the background.

Pre-processed image is then feed into the Tesseract OCR engine to extract text from an image. The recognized text in image is split into sentences by using an appropriate delimiter to indicate the end of sentences such as the full stop, exclamation mark, question mark and etc. The text is splited into sentences, this made the speech playback, fast forwarding and pausing possible with button interfaces to adjust according to the individual preference. The system also incorporated volume control button and some logic to initiate the system again after the process ended.

IV. Result and Discussion

The prototype is being worn as shown in Fig. 4. The samples are being categorized as document placed on reading board and document without reading board where accuracy rate is being compared and discussed. As part of document edge will be occluded by user's hand, the purpose of reading board is to enhance the document edge; if the edge is nicely detected, hence allow perspective transformation to take place else the document undergoes skew detection and correction. This is to compare the method being used and how they affect the document on a noisy background. The sample as shown in Fig. 4 to identify the effect of addition of reading lenses, flashing of external light source and application of pre-processing on the accuracy of text recognition. The reading glasses lens of +1.5 diopter strength is identified physically to give the best zooming effect under the raspberry pi Camera.

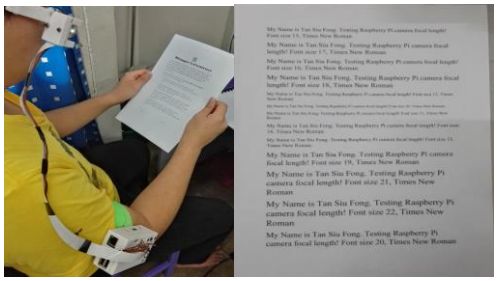

Fig. 4. Reading assistive system prototype being worn by user (left) and created sample text (right)

The proposed method through hand contour detection is shown in Fig. 5, which then speech instruction given by system to aid users in aiding document alignment in left-right motion, the document is fitted inside both sides of camera view. Meanwhile, the stitching of two images taken at bottom and top of document has successfully captured the full A4 sized document. To provide consistent comparison, stitched binary image are chosen as the original image to be compared in this section. The representation for the image labelling is described as follows:

- vBorder represent image taken with reading board while noBorder represent image taken with absent of reading board
- original represent image taken without any presence of flash light, added reading lens and pre-processing
- vProcessing represent image taken without any presence of flash light, added reading lens but with pre-processing
- vLightLens represent image captured under the presence of flash light and added reading lens with pre-processing

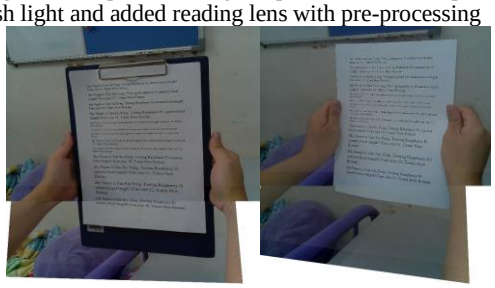

Fig. 5. Aligned document and stitched image showing full sized document

A. Qualitative analysis

This section covers observational analysis of the proposed method on hardware design and software design based on the captured image and OCR extracted text file respectively. The effect of flashing light and added +1.5 diopter reading lens when capturing document is compared as in Table I based on Fig. 6.

TABLE I. Observational Result Comparison Between Original Image and Image Captured With Light Plus Reading Lens

	Remarks on captured sample text image
Original image capture under normal condition	The image looked blur and not clear. The character edges are less striking and loses focus.
Image captured under presence of light and added reading lens	The captured image looks brighter and the contrast between black and white color tones is more obvious. The added reading lens is more obvious to be seen on sentences.

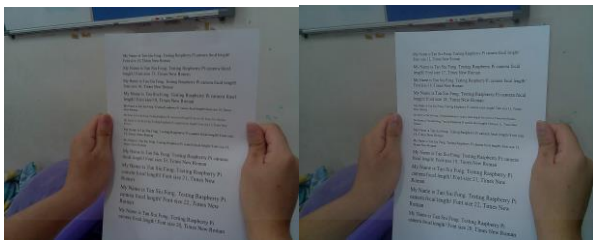

Fig. 6. Original image (left) and image captured under presence of light and added reading lens (right)

B. Quantitative analysis

From the extracted text file, the qualitative analysis is illustrated directly by comparing the output of extracted text from each of the proposed methods. As some of the proposed method produce almost similar recognition text output, in order to provide a more descriptive analysis, quantitative analysis is

carried out in term of F1 score or F-measure. Precision is defined as total correctly extracted word counts over the total extracted word counts or alternatively as how many extracted words are relevant in the extracted text as given in (2). Meanwhile, Recall is defined as total correctly extracted word counts over total word counts of original document or alternatively as how many relevant words are extracted compared to the original document as given in (3). A tool named wdiff is used to compare extracted text file with the original document, which is typed in a text file. This tools compares the two files on a word per word basis and produce statistical output regarding total number of words in each files and number of common words between two files as tabulated in Table II.

Precision = (total correctly extracted word counts)/(total extracted word counts) (2)

Recall = (total correctly extracted word counts)/(total word counts of original document) (3)

From the obtained precision and recall, F1 score is then formulated as in (4).

F_1 score = 2×(precision×recall)/(precision+recall) (4)

Table II shows the F1 score or also known as the measure of accuracy increased with the proposed hardware and software design applied.

TABLE II. WORD COUNTS OF CREATED SAMPLE UNDER DIFFERENT APPLIED METHOD AND F1 SCORE FOR TEXT EXTRACTION

Image Label	original		vProcessing		vLightLens	
	vBorde-r	noBor-der	vBorde-r	noBorde-r	vBorde-r	noBorde-r
Total Extract-ed words	213	191	201	155	228	188
Total words in Original typed text	234	234	234	234	234	234
Words in common	152	101	155	155	201	166
Precision	0.71	0.53	0.77	1.00	0.88	0.88
Recall	0.65	0.43	0.66	0.66	0.86	0.71
F1 score	0.68	0.48	0.71	0.80	0.87	0.79

Raw original images extracted text output has lowest F1 score recorded as 0.68 and 0.48 for with reading board and without reading board among the result. With the pre-processing applied to the original image, the accuracy increased to 0.71 and 0.80 respectively. With reading lens added and flashing of light plus the pre-processing, the F1 score further improved to 0.87 for vBorder and dropped 0.01 to 0.79 for noBorder. The drop might due to the noise during pre-processing under lighting and without lighting. But in overall, the accuracy still increased when compared to original raw image without the proposed method.

Beside the sample created for analysis purposes, random samples as shown Fig. 7 are also tested with the system. This is to show that system works not only on created sample but also for document which are in A4 sized and the characters are horizontally printed on white paper.

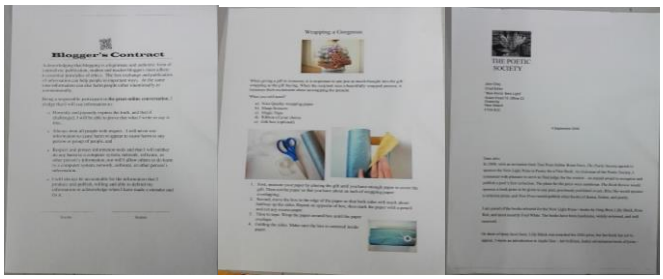

Fig. 7. Sample of randomly picked document

TABLE III. WORD COUNTS OF RANDOMLY PICKED SAMPLE AND F1 SCORE FOR CORRESPONDING TEXT EXTRACTION

Image Label	Blogger's Contract		The Poetic Society		Wrapping Gorgeous	
	vBor-der	noBord-er	vBorde-r	noBorde-r	vBorde-r	noBorde-r
Total Extracted words	196	198	215	167	153	167
Total words in Original typed text	197	197	197	197	163	163
Words in common	186	182	165	128	118	120
Precision	0.95	0.92	0.77	0.77	0.77	0.72
Recall	0.94	0.92	0.84	0.65	0.72	0.74
F1 score	0.95	0.92	0.80	0.70	0.75	0.73

V. CONCLUSION AND FUTURE WORK

A prototype of reading assistive system has successfully been implemented and able read out image text with fair accuracy. Through the hardware design, a lens with +1.5 diopter is added to provide better focus and external light source has reduced the effect of non-uniform illumination on captured documents. The proposed method has shown improved accuracy better than raw text image's extracted text, from F1 scores of 0.68 to 0.87 with reading board and 0.48 to 0.79 without reading board. In conclusion, the objectives of the project to enhance the accuracy of text recognition rate and proposal of alternative ways in solving document aiming problems are achieved.

Future work on post post-processing on the extracted text can be carried out to make the recognition better. For instance, by performing automatic spelling correction or spelling corrector such as dictionary to correct the wrongly recognized characters. This is to prevent the speech synthesizer from reading wrongly extracts words or text output by the Tesseract OCR engine. Besides that, the power consumption of the system has to be taken into consideration to extend the operation time.

REFERENCES

[1] Mariotti, S. P. (2012). Global data on visual impairments 2010. *World Health Organization*, *20*.

[2] Lee, M. N., Abdullah, Y., & Mey, S. C. (2011). Employment of People with Disabilities in Malaysia: Drivers and Inhibitors. *International Journal of Special Education*, *26*(1), 112-124.

[3] Hakobyan, L., Lumsden, J., O'Sullivan, D., & Bartlett, H. (2013). Mobile assistive technologies for the visually impaired. *Survey of ophthalmology*, *58*(6), 513-528.

[4] Wexler, Y., Shashua, A., Tadmor, O., & Ehrlich, I. (2013). *U.S. Patent Application No. 13/914,792*.

[5] Yi, C., Tian, Y., & Arditi, A. (2014). Portable camera-based assistive text and product label reading from hand-held objects for blind persons. *IEEE/ASME Transactions On Mechatronics*, *19*(3), 808-817.

[6] Tripathy, A., Pathak, A., Rodrigues, A., & Chaudhari, C. (2012, October). VIMPY—A Yapper for the visually impaired. In *Information and Communication Technologies (WICT), 2012 World Congress on* (pp. 167-172). IEEE.

[7] Shilkrot, R., Huber, J., Liu, C., Maes, P., & Nanayakkara, S. C. (2014, April). FingerReader: a wearable device to support text reading on the go. In *CHI'14 Extended Abstracts on Human Factors in Computing Systems* (pp. 2359-2364). ACM.

[8] Velmurugan, D., Sonam, M.S., Umamaheswari, S., Parthasarathy, S & Arun, K.R. (2016, March). A Smart Reader for Visually Impaired People Using Raspberry PI. *International Journal of Engineering Science & Computing*, *6*(3), 2997-3001. doi:10.4010/2016.699

[9] Hassan, E. A., & Tang, T. B. (2016, July). Smart Glasses for the Visually Impaired People. In *International Conference on Computers Helping People with Special Needs* (pp. 579-582). Springer International Publishing.

[10] Pégeot, F., & Goto, H. (2012, November). Scene text detection and tracking for a camera-equipped wearable reading assistant for the blind. In *Asian Conference on Computer Vision* (pp. 454-463). Springer Berlin Heidelberg.

[11] Yi, C., & Tian, Y. (2015). Assistive Text Reading from Natural Scene for Blind Persons. In *Mobile Cloud Visual Media Computing* (pp. 219-241). Springer International Publishing.

[12] Nagaraja, L., Nithin, D., Nagarjun, R. S., Murthy, V. S., & Anand, N. M. Vision based text recognition using raspberry PI. In *National Conference on Power Systems & Industrial Automation (NCPSIA 2015)*.

[13] Liu, J., Su, H., Yi, Y., & Hu, W. (2016). Robust text detection via multi-degree of sharpening and blurring. *Signal Processing*, *124*, 259-265.

[14] Epshtein, B., Ofek, E., & Wexler, Y. (2010, June). Detecting text in natural scenes with stroke width transform. In *Computer Vision and Pattern Recognition (CVPR), 2010 IEEE Conference on* (pp. 2963-2970). IEEE.

[15] Wu, V., Manmatha, R., & Riseman, E. M. (1999). Textfinder: An automatic system to detect and recognize text in images. *IEEE Transactions on pattern analysis and machine intelligence*, *21*(11), 1224-1229.

[16] Kumar, S., Gupta, R., Khanna, N., Chaudhury, S., & Joshi, S. D. (2007). Text extraction and document image segmentation using matched wavelets and MRF model. *IEEE Transactions on Image Processing*, *16*(8), 2117-2128.

[17] Chai, D., & Ngan, K. N. (1999). Face segmentation using skin-color map in videophone applications. *IEEE Transactions on circuits and systems for video technology*, *9*(4), 551-564.

Convolutional Neural Network For Optimal Pineapple Harvesting

Ahmad Aizuddin bin Azman
Faculty of Electrical Engineering
Universiti Teknologi Malaysia
Johor Bahru, Malaysia.
aizuddinmuo94@yahoo.com

Fatimah Sham Ismail
Control & Mechatronic Engineering Department (CMED),
Faculty of Electrical Engineering
Universiti Teknologi Malaysia
Johor Bahru, Malaysia.
fatimahs@fke.utm.my

***Abstract*— Pineapple ripeness can be divided into seven stages of maturity indices. Upon ripening, pineapple's peel gradually changes colour from green to yellowish, which spreading from bottom to the top. Conventional method of inspection is prone to human errors as it is done manually by farmers with different knowledge and experience. This project proposes new intelligent method using convolutional neural network (CNN) that has the ability to learn unique features from the given task automatically through supervised learning. The simulation results show that the method achieved 100% classification's accuracy for determining unripe and fully ripe level and 82% accuracy for partially ripe level.**

Keywords—convolutional neural network(CNN); pineapple ripeness classification; python programming language; keras

I. INTRODUCTION

First Convolutional Neural Network has been introduced to public in early 1990 by LeCun [1] for handwritten zip code recognition trained using backpropagation. To this date, CNN has been widely implemented for multiple task recognition task, such as action recognition [2], object recognition [3], detection of pedestrian [4], classification of traffic sign [5], face detection [6] and digit recognition [7] which have successfully show competitive result.

In Malaysia, Federal Agricultural Marketing Authority has been entrusted the duty to control and monitors the fruit production. The fruits will undergo a controlled standard process before being marketed to the public. The process of fruit quality inspection can be done either by FAMA or the farm owner who have a license called Self-Regulated by Regulated Entities (SRBRE) granted by FAMA [8]. However, the inspection is prone to human error due to different knowledge and experience.

Machine vision system has been widely practice for quality evaluation for automated sorting and grading system in agricultural sector. Hence, with the assist of vision system, assessment of pineapple maturity will be more accurate. Moreover, the labor cost can be reduced and the production rate will be maximized. Therefore, the main objective of this project is to develop a CNN for pineapple system's classification for having automated pineapple sorting and grading system using python language with 'Keras' library.

II. PINEAPPLE RIPENESS

A. *Pineapple's Maturity*

Pineapple ripeness can be distinguished based on the external view skin's color. The maturity is divided into seven stages based on the exhibited color of pineapple's peel. Fig. 1, shows the different type of pineapple maturity based on FAMA's guideline [8]. Table I shows the ripeness level based on the index maturity.

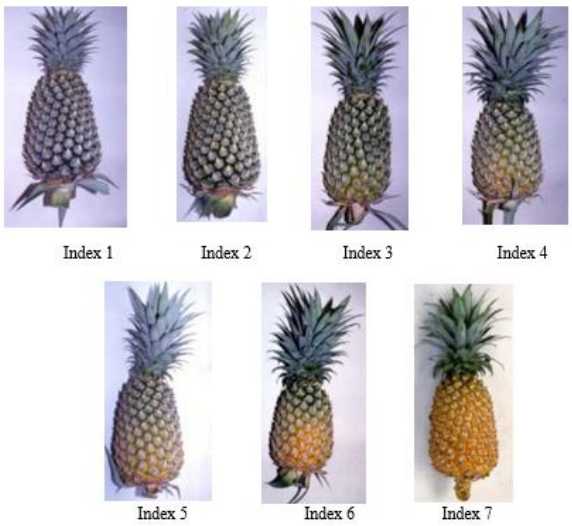

Fig. 1. Different index of pineapple maturity.

TABLE I. Ripeness level with corresponding index of maturity.

Level of ripeness	Index of maturity
Unripe	1,2
Partially Ripe	3,4,5
Fully ripe	6,7

B. *Previous Works*

Pineapple maturity classification system has been developed using simple neural network based on RGB colour space [9]. All the sample images are having same size dimensions or pixels. The features extracted from the sample images are based on the total of green pixels and red pixels from the selected region, which are region A and region B. The coordinate of region A is between 91 to 270 in both x and y direction, and region B is from 271 to 450 in both x and y direction. The range of RGB for red pixels is within (1,1,1) to (250,250, 150) and green pixels is from (1,1,1) to (150,250,150). When the desired pixels lie in the range within the interest region, the counter will count the number of both red and green pixels. This system only able to distinguish Index 4 with 75% classification's accuracy, 25% for Index 5, 65% for Index 6 and 60% for Index 7.

Apart from that, RGB and HSI colour space has been used for determining ripeness of pineapple using Fuzzy Logic [10]. The features extracted are based on red, green and saturation channel. Here, Index 1,2 are categorized under unripe level, Index 3,4,5 are grouped under partially ripe level and Index 6,7 are under fully ripe category. The range of required red channel and green channel are from 150 to 200 and for saturation channel is between 0.3 to 0.5. Counter will count the number of pixels that lies between the range over the sample image. This method has yielded 85% classification's accuracy for unripe and partially ripeness level and 100% classification's accuracy for fully ripe level.

III. SAMPLES PREPARATION

A. *Collecting Samples and Labelling*

Flowchart in Fig. 2, describes the process to carry out this project. Initially, the experiment begins with preparing the sample of different maturity based on the FAMA's guideline. The samples are then cropped, only considering the region of pineapple skin without the crown and to remove the background. The samples are then resized to 200*200 pixels in size and allocated to respective ripeness level.

The samples are then given associated target label based on the respective ripeness level as in Table 1. Each sample of unripe pineapple is given label [1 0 0], partially ripe pineapple is given label [0 1 0] and the last category, fully ripe pineapple is labelled with [0 0 1]. Labelling is necessary for training purpose.

B. *Colour Image Representation and Normalization*

In this project, we will consider only RGB colour space for image representation. The raw pixel values of the image will be the input data into the network. The number of image channels are 3 for colour image. Scaling the input pixels is necessary to ease the computation and for faster convergence of the network. For each pixel value in the channel is scaled down in range of [0,1] using equation (1), given x denotes as the input pixel:

$$x = {}^{x}/_{255} \qquad (1)$$

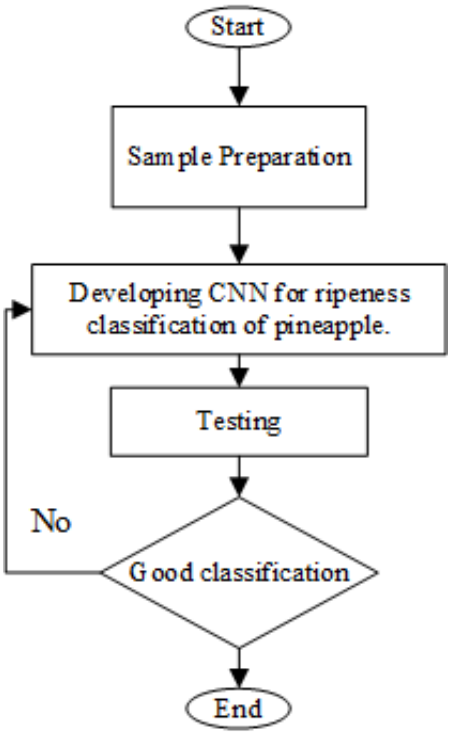

Fig. 2. Experimental Process Flow

IV. CNN DEVELOPMENT PROCESS

A. *Architecture Details*

The CNN architecture includes both feature extraction and classification into a single framework. By using CNN, the design for classifier system does not need to rely on difficult hand-crafted feature extraction as the local receptive detector learns by itself through supervised learning.

The proposed architecture is inspired by LeCun [7] as in Fig. 3, comprises of input layer, two convolutional layers, C1 and C3, two non-overlapping pooling layers, P2 and P4, one fully connected layer and one output layer. The input image's size is $(200 * 200)$. C1 is composed of 8 feature maps of size $(196 * 196)$ that is obtained through convolution operation using filter of size $(5 * 5)$ with input image. Each non-overlap $(2 * 2)$ local receptive field in each feature map in C1 layer is applied with max-pooling operation, resulting in total of 8 feature map of size $(98 * 98)$ of P2 layer.

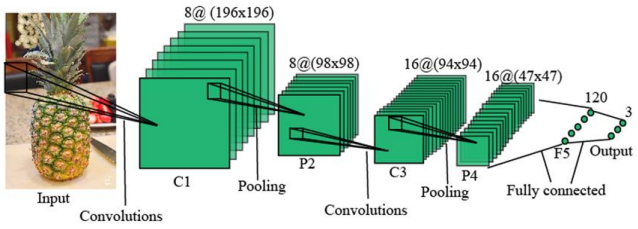

Fig. 3. Le-Net4 Architecture

C3 layer is composed of 16 feature maps of size $(94 * 94)$ resulting in convolution operation using $(5 * 5)$ filter with previous feature maps. Layer P4 has 16 feature maps of size $(47 * 47)$, which each unit in feature map of layer P4 is connected to non-overlap local receptive field of size $(2 * 2)$ in the corresponding feature map of C3.

All the multi stage feature maps are then fully connected to 120 neurons in F5 layer. Here, a dropout function with a rate value of 0.25 is introduced in F5 layer. Both convolutional layers and the fully connected layer will be passed to ReLu activation function, in order to introduce non-linearity in the network.

Neurons of F5 layer are then fully connected to output layer. Output layer will consist of 3 neurons corresponding to the number of classification. Softmax activation function is applied to each unit in output layer by squashing the highest output value amongst the units in output layer to '1' and suppressing the rest to '0'. Highest probability value gives the predicted class.

Basically, the CNN tries to find the correct weight value that gives the minimal error between the targeted/labelled output and predicted output for every iteration in an epoch.

B. *Learning Process*

The dataset is divided into two, which are training sample and validation sample. 90% of samples corresponding to 243 samples are used for training the network and 27 samples as validation samples. The batch size chosen is 27 for each iteration, specifically, an iteration process consist of forward propagation and backward propagation.

Throughout the training process, the weight and bias are updated frequently during back-propagation by calculating the gradient of loss function with respect to the weights in all layers (gradient descent) using normalizer algorithm. A loss function measures the discrepancy between desired output of the image and probability output of the system.

The trainable parameters (weights and biases) are trained using back-propagation algorithm which is 'adadelta' function with learning rate 1.0 on training samples in randomized order. Hence, the gradient will update the trainable parameter 9 times for every epoch with 'categorical-cross entropy' used as the loss function.

The network will be trained for 100 epochs. For every epoch, the classifier system is tested on validation sample to observe the accuracy and loss. Early stopping during training is applied whenever the network stops learning any new features.

C. *System's Performance on Classification*

Initially, validation samples are used to obtain the confusion matrix of the chosen network in order to visualize precision of individual ripeness level. Next, the network is tested on the random images which are not from either training dataset and validation set to determine the reliability of the network.

V. Result And Discussion

A. *Learning Process*

In this project, the early stopping criterion is based on the validation loss. Fig. 4, shows the graph of 'training loss versus validation loss'.

From observation, after 30th epoch, both training loss and validation loss has slight converging. The reason to this problem is the network has stopped learning any new features. At such state the training and validation performance should both become stationary distributions and the optimal value should occur with uniform probability anywhere between the epochs in which local optimum is reached and infinity. Hence, the training is stopped at 40th epoch to avoid overfitting.

The proposed network has yielded an accuracy of 92.6% in classification of pineapple ripeness and 0.09 categorical cross entropy error. Specifically, lower categorical cross entropy error tells the difference between targeted label and predicted output is small.

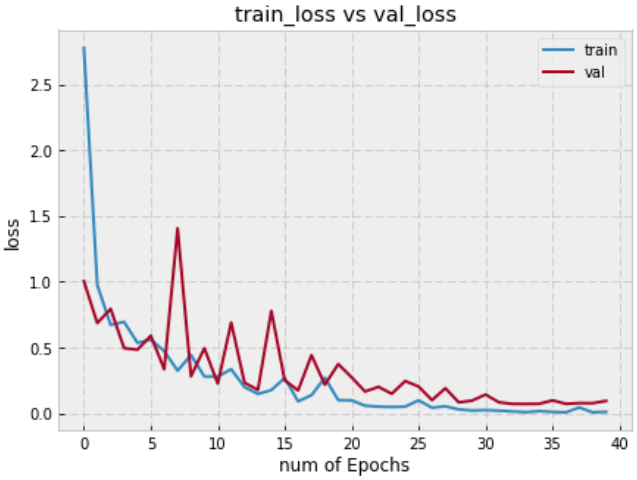

Fig. 4. Training loss versus validation for 40 epochs of training.

B. *System's Performance on Classification*

The yielded accuracy of the network is based on the classification of the validation sample. A total of 27 samples consists of 8 samples of unripe category, 9 samples of partially ripe category and 10 samples of fully ripe category are used on the performance of system's classification evaluation of the proposed network.

The summary of prediction results on validation sample for RGB color space are shown in confusion matrix as in Table II. Confusion matrix is used to visualize the precision of each individual ripeness category. Here, precision intuitively describes the ability of the classifier not to label negative sample as positive.

TABLE II. Confusion Matrix

Ripeness Level	Unripe	Partially ripe	Fully ripe	Precision
Unripe	8	0	0	1.00
Partially ripe	0	9	0	0.82
Fully ripe	0	2	8	1.00
Average Precision				0.94

Based on Table II, the proposed network has lowest precision, 0.82 for determining the partially ripe category, compared to unripe category and fully ripe category. Out of 10 fully ripe samples, 2 of them is classified wrongly under partially ripe category. All the samples from unripe category and partially ripe category are categorized correctly, yielding 1.00 accuracy.

From the confusion matrix, we may say that the proposed system has outperformed [10] in classification's accuracy for unripe ripeness level with 7.5% improvement. On contrary, classification for partially ripe level has shown 1.5% increase in error. Both systems have 100% classification's accuracy of fully ripe level. Using CNN approach still produces competitive result even without the use of hand-engineered feature extraction and selection.

The CNN predicts the ripeness of pineapple by yielding the percentage of probability as shown in Table III. Based on Table III, both unripe category and fully ripe category, each category yielded 99% and 98% accuracy in average. On other hand, partially ripe category yielded 93% accuracy in average. This is due to the proposed network has lowest precision when determining the partially ripe category.

TABLE III. Output probability of random sample.

Category	Sample Image	Output Probability
Unripe		Predicted Output: Unripe:[99.95396423]% Partial:[0.04603098]% Fully:[8.23526807e-06]%
		Predicted Output: Unripe:[99.46776581]% Partial:[0.5322184]% Fully:[1.44846299e-05]%
Partially ripe		Predicted Output: Unripe:[3.99420786]% Partial:[87.64442444]% Fully:[8.36136341]%
		Predicted Output: Unripe:[0.46672243]% Partial:[99.53290558]% Fully:[0.00037365]%
Fully ripe		Predicted Output: Unripe:[2.47598146e-05]% Partial:[2.97924185]% Fully:[97.02073669]%
		Predicted Output: Unripe:[1.18656814e-07]% Partial:[0.95786518]% Fully:[99.04213715]%

CONCLUSION

In conclusion, FAMA's guideline for distinguishing different maturity of pineapple has been used as the benchmark for preparing the sample images in this project. Besides that, the use of Convolutional Neural Network by Keras for classifying the pineapple into 3 main categories which are unripe, partially ripe, fully ripe has been demonstrated in this project. The analysis on the classification's performance of the proposed system has showed competitive result even without difficult hand-engineered feature extraction and selection.

In the future work, the designed classifier has to be make more flexible and robust. The sample images used for training have to be at good resolution and at varying environment's condition, for example - light intensity such as morning, evening, afternoon, night at different position. Moreover, comparative performance using different colour space has to be addressed too. Lastly, choosing appropriate optimizer and learning rate are also necessary for smoothing the learning process.

REFERENCES

[1] Y. LeCun, B. Boser, J. S. Denker, D. Henderson, R. E. Howard, W. Hubbard, and L. D. Jackel, "Backpropagation applied to handwritten zip code recognition," Neural Computation, vol. 1, no. 4, pp. 541–551, 1989.

[2] S. Ji, W. Xu, M. Yang, and K. Yu, "3D convolutional neural networks for human action recognition," IEEE Transactions on Pattern Analysis and Machine Intelligence, vol. 35, no. 1, pp. 221–231, 2013.

[3] A. Krizhevsky, I. Sutskever, and G. Hinton, "ImageNet classification with deep convolutional neural networks," in Advances in Neural Information Processing Systems, vol. 25, pp. 1106–1114, 2012,

[4] P. Sermanet and K. Kavukcuoglu, "Pedestrian detection with unsupervised multi-stage feature learning," in International Conference on Computer Vision and Pattern Recognition, in press, 2013.

[5] D. Ciresan, U. Meier, J. Masci, and J. Schmidhuber, "A committee of neural networks for traffic sign classification," in International Joint Conference on Neural Networks, pp. 1918–1921, 2011.

[6] M. Osadchy, Y. Cun, and M. Miller, "Synergistic face detection and pose estimation with energy-based models," The Journal of Machine Learning Research, vol. 8, pp. 1197–1215, 2007.

[7] Y. LeCun, L. Bottou, Y. Bengio, and P. Haffner, "Gradient based learning applied to document recognition," Proceedings of the IEEE, vol. 86, no. 11, pp. 2278–2324, 1998.

[8] FAMA, "Menuju kearah Kualiti Malaysia's Best Siri Panduan Kualiti Nenas", 2006.

[9] R. Shamsudin, W.R. Wan Daud, M.S Takrif, O. Hassan, S.M. Mustapha Kamal, and A.G.L. Abdullah, "Influence of Temperature and Soluble Solid Contents on Rheological Properties of the Josapine Variety of Pineapple Fruit (Ananas Comosus L.)", International Journal of Engineering and Technology, vol. 4, pp. 213-220, 2007.

[10] J. I. Asnor, S. Rosnah, Z. W. H. Wan, and H. A. B. Badrul," Pineapple Maturity Recognition Using RGB Extraction",World Academy of Science,Engineering and Technology,vol.78 ,pp. 147-150 ,2013.

Motorized Turning Seat

Vinod a/l Vijayan
Faculty of Electrical Engineering
Universiti Teknologi Malaysia
Johor Bahru, Malaysia.
vijayanvinod47@gmail.com

Anita binti Ahmad
Department of Control and Mechatronics
Faculty of Electrical Engineering
Universiti Teknologi Malaysia
Johor Bahru, Malaysia.
anita@fke.utm.my

***Abstract*—An improved portable motorized turning seat comprising a small wheeled base having a vertically disposed telescoping lifting column extending upwardly therefrom. A patient support means extends from the column to support the patient. A crank, accessible to both patient and attendant, is used to raise and lower the lifting column for transfer between surfaces with different heights, such as beds, wheelchairs, and car seats. The lift will be closed and temporarily attached to a wheelchair for convenient transport with a patient. The lift is small and lightweight and may be easily transported and stored. The lift is further economical to manufacture.**

I. INTRODUCTION

Nowadays, wheelchair users are increasing every year. According to the Malaysian National News Agency (2009) [7], there are 1.3 million people with various type of disabilities and most of them are wheelchair bound patients. Conveying a patient from a wheelchair into a conveyance can be a time consuming and arduous process. The quandary is magnified when the patient is moved into a conveyance with an elevated seat height, such as an SUV car. While some technologies subsist to avail with this quandary, they are often sumptuous and too cumbersomely hefty to be peregrinate to different locations. A portable wheelchair hoist would greatly increase accessibility for wheelchair-bound patients and increment their options to move one location to another easily. Therefore, we have run some research regarding to the project to improvise and to apply the consumer's need. From the research we came out with a design a portable handicap chair to avail people in transferring from their wheelchair into a high conveyance seat, such as in a Sedan car and increase their options for transportation.

II. LITERATURE REVIEW

Based on the findings that we have studied related to my project, from reading the articles to the journals, there was a presence of related work in the past times. But the ideas of the applications are different among the findings. The idea of the motorized turning seat could be applied to solve a problem regarding to the wheelchair bound patient [1]. Some even use the idea of control the compact portable patient lift by manually and it works as by rotating the gears which it will move up and down [1]. Last but not least, there are even some prototype or idea of this innovation created to lifting lifting the wheelchair into the vehicle and it can raised and lower at specific platform [4]. There are also some of prototype which the chair can separated from the wheeled chasis and supported on an automobile seat .

Although all the projects are different from the aspect of the methodology, using different kinds on controller to control the prototype and different kind of approach towards the innovation,there are also some of prototype which the patient can independently enter a vehicle and drive from wheelchair without transferring or leaving. An ameliorated portable patient transfer contrivance comprising a minute wheeled base having a vertically disposed telescoping hoisting column elongating upwardly therefrom. A patient support designates elongates from the column to fortify the patient. A crank, accessible to both patient and attendant, is utilized to raise and lower the hoisting column for transfer between surface with different heights, such as beds, wheelchairs, and car seats. The lift may be closed and ephemerally annexed to a wheelchair for convenient convey with a patient. The hoist is diminutive and lightweight and may be facilely conveyed and stored. The hoist is further economical to manufacture. [1,3,4].

The concept of the prototype plays an important role to ensure the problem solving of the idea and also to achieve the objective of the idea so it could contribute and beneficial towards the users [5]. As for the most studies that we have studied, there are some concepts that attract my interest to have a deeper review regarding the conceptual and also the integration of system that enables the prototype works according to the plan[6]. Therefore, this is some of the projects which we would elaborate regarding their conceptual design and how the prototype works[7].

III. PROJECT METHODOLOGY

A. Hardware Design

In hardware design, the Arduino ATmega328 is used as central processing unit for controlling the movement of the chair. All hardware used including a dc motor, push button, motor driver and limit switch. Then, the microcontroller to control the dc motor via servomotor by sending the signal to lift up and down of the seat.

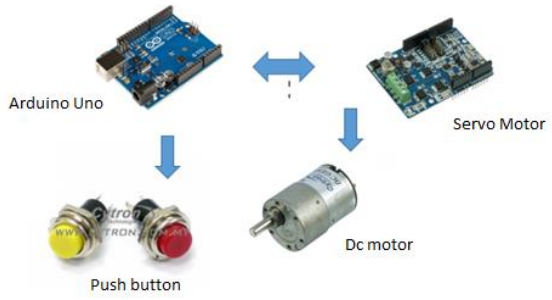

Fig 1: The overall development of hardware

B. Assemble Process

After all the hardware and components are prepared, it is the time for the process of assembling the components to take place. In this process of creating the prototype, there are 6 steps that must be followed in order to ensure the best quality of the product and an illustration is shown below. Also the elaboration of the process of each step will be provided for a clearer picture regarding the topic.

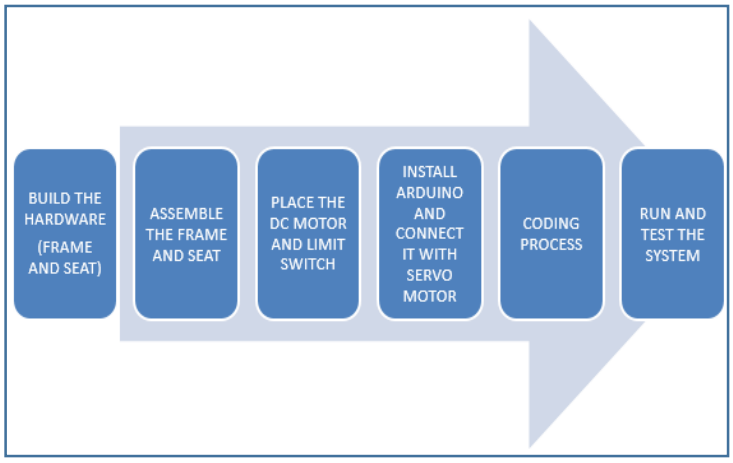

Fig 2: Flowchart in assembly process of the prototype

C. Software Implementation

In software development, Arduino software version 1.5.7 had been use to write a programming order to control the dc motor movement by connect it at servomotor. It can move up and down and also forward and backward by a limit. Besides that, limit switch are used to limit the movement of the motor. The push button are installed to allow the mechanism to start and stop according to the height of the seat and bed. Finally, the TeamViewer software had been used to make the network communication between a server computer and a client computer.This software is a free license for personal or non-commercial use only where the communication can be done.

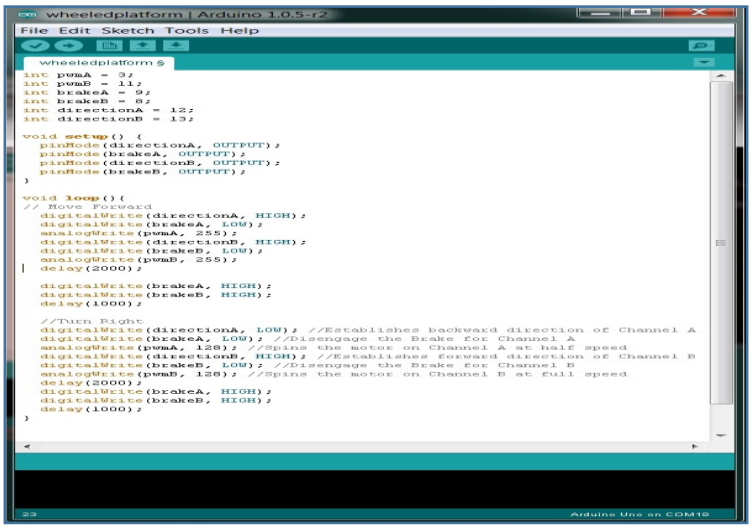

Fig 3: Arduino software had been used to write the programme and upload to the Arduino board in order to control the dc motor functionality.

IV. RESULTS

A. Mechanical Design

First and foremost, we design the mechanism of the prototype using 3D CAD design Solidwork. Then I build it using some materials based on my design. Figure 4 shows the design of the motorized turning seat prototype. The prototype also can be fold and portable to move one location to another. Besides that, the prototype can be placed into the car trunk without disassembly. Figure 5 shows the design of the prototype which can be fold.

Fig 4 : The design of motorized turning seat

Fig 5 : The design can be fold and portable

DD

Based on the studies and research done in the literature review, the designed mechanism should perform the desired output. There is a need for a compact, lightweight and easily portable patient transfer device to assist caregivers in transferring patients between beds, wheelchairs, cars, etc.; for use in the home, in institutional settings, and in the outside world. Transferring of disabled patients is a leading cause of injury in the health-care industry, with the nursing occupation having among the highest incidence of back injury, despite the prior art and the availability of commercial patient lifts. These lifts are under-utilized for a number of reasons, such as restricted space in many hospital wards and bathrooms, cumbersome operating requirements, the indignity involved in the mode of transport, the additional time required for performing the transfer, and the unavailability of the lift at both the patient's starting and destination locations. A device is required that can work in confined spaces, is simple to set up and use, feels safe, secure and is not intimidating for the patient, and can be transported with the patient.

The problem is pervasive in the home health care industry as well, where spaces are not designed for safe patient transfers, and the caregiver is often alone and has no help during lifts. Since lifts are available in less than 10 percent of the homes visited by home health care professionals, a device that can be easily brought from home to home is also required. Many patients are essentially home-bound due to the unavailability of a conveniently portable lift, reducing their quality of life unnecessarily. A device is required that would allow a single, and often elderly, spouse to bring their disabled spouse out of the house, on car trips, cruises, etc. The device must be versatile and be able to move in the confined spaces found in many homes and public accommodations. It must also be easily transported, and must transfer patients in a dignified manner if it is to be used outside the home

V. CONCLUSIONS

As for the expected results, based on my findings from the related work previously, We have done this project, the prototype would be working smoothly as planned, with also showing the criteria that we expected. Firstly the criteria that we are expecting that it can be easy to use and able to transfer wheelchair bound patient to the car safely. By this it would help me to solve the problem statement. Next, the prototype would be able to transportable between locations and able to transfer disable people between different heights surfaces to the car seat. In addition, to provide a prototype which is compact and lightweight. In a nutshell, by all of these, We believe that it is not only could solve the problems from the problem statement, but also achieving the objective of the project.

VI. ACKNOWLEDGEMENT

Foremost, I would like to express my sincere gratitude to my advisor Dr Anita binti Ahmad for the continuous support of my my study and research, for her patience, motivation, enthusiasm, and immense knowledge. Her guidance helped me in all the time of research and building this project. I could not have imagined having a better advisor and mentor for my project. Besides my advisor, I would like to thank the rest of my friends and parents for their encouragement, insightful comments, and hard questions.

REFERENCES

[1] Alexander Brandorff.,(2012 August 13).Compact Portable Patient Lift,US 6,430,761 B1

[2] Rodvinon I,Zamotin.,(1987 January 2).Wheelchair for transferring occupant to motor vehicle, US 4,669,943

[3] Clifford I,Wolfe.,(1991 October 1).Wheelchair lift and transfer system,US 5,052,879

[4] William B, Plewright.,(1989 June 20).Patient transfer and conveying vehicle, US 4839933 A

[5] J Fowler.,(1973 January 13).Lift device, US 3710962 A

[6] http://www.ameriglide.com/item/ameriglide-325-fp.html

[7] http://www.braunability.com/millennium.cfm

Low Cost Webcam based Color Sorting System

Mohamad Faezzudin Bin Ahmad Jaafar
Faculty of Electrical Engineering
Universiti Teknologi Malaysia
Johor Bahru, Malaysia.
paedz02@gmail.com

Mohamad Noh Bin Ahmad, Mohamad Amir Bin Shamsudin
Department of Control and Mechatronics
Faculty of Electrical Engineering
Universiti Teknologi Malaysia
Johor Bahru, Malaysia.
noh@fke.utm.com, amir@fke.utm.my

***Abstract*—This paper describes an automatic color sorting by using webcam and be controlled by Programmable Logic Controller (PLC). Manual system for color inspection for product's sorting requires a lot of cost including the vision system and manpower. Using an automated system by using low cost webcam can produce more consistence result with a minimal cost. PLC is currently used widely by the industry to control the process or machine in factory or manufacturing system. The existing industrial camera was especially design so that it can be integrate with PLC to produce an output. For example is the final product inspection. But the costs were mostly can be categorized as expensive. In this project, the use of a low cost webcam is used to detect the product's color to be read by PLC as the controller. In other word, to design a low cost PLC based system that capable of sorting the product according to their colors as well as establish the communication between the webcam and PLC. This model is using MATLAB software to classify the product's color and Arduino Uno as the medium for the output signal. Pneumatic system applied as the actuator to sort the product according to their color which in this model is between red and green. As the result, the product will be sorted into red, green or neither both. This may be a significant key especially for small industries to use an automated system for their manufacturing processes.**

I. INTRODUCTION

It is an important step to determine the quality and validity of a product. For example, quality inspection of fruit is mostly using their colors to distinguish between a good and bad fruits. Until 1990s, the inspection of fruit products was performed manually and its result were not consistence due to human error cause by fatigue and boredom.[5] Machine or robot was used to replace human for more consistence, low cost, and effective result. As for the vision system, machine vision early application was in the sixties for various purposes and nowadays being applied widely in many fields such as agriculture, inspecting product label, inspecting colors, robot handling, analyzing terrestrial image and in manufacturing process.[4] Now, the industrial automation had at the level which Programmable Logic Control (PLC) is a common in controlling the process in the industries. PLC is an industrial solid-state computer that monitors inputs and outputs, and make a logic-based decisions for actuation or automation. PLC read input from input devices such as sensors, push button, digital or analog input.[7] For image processing integrated with PLC, there are a lot of product that can provide the camera for industrial purpose. But for a low cost machine vision system, webcam was used in this project to distinguish between colors for inspection and sorting purposes. By using a medium for data transfer from PLC and webcam such as Arduino, the input color from the webcam can be send to PLC for the output response. But this system also has its limit as it cannot cover the whole product image for processing which it may need the usage of more than one camera such as Intelligent Fruit Sorting System project.[5] There is several literature review were made based on the system.

A. Manual and Automatic Inspection

There are two methods that being used to inspect a product for quality or sorting that is manual and automatic inspection. Manual inspection is totally using the worker's vision and automatic inspection is using the machine vision to capture and processing the image to produce a signal for the output responses. The disadvantage of human eyesight compared to the machine vision is that different people have their own perception in color classification and uniformity that might yield to uncertain output. For example is the inspection on hardwood panel product which they need to determine the uniformity for the product.[1]

B. Color Classification Techniques

First is RGB representation (red, blue and green). This method was using these three colors as the reference. It can be used to differentiate between colors for color inspection. For example in MATLAB, LabVIEW and Vision Assistant software, the color was verified based on the number of pixels and the measurement between the difference of reference RGB value with the product's color.[2]

Another technique is by using HSI image (hue, saturation and intensity). This technique is more advance compared to RGB method as it simplify algorithm for color classification and save more memory space and time.[4]

For fast processing, Ohta color space technique was fast as it can complete the algorithm within 50 milliseconds. It also has a better accuracy and stability. In short, this method is better than HSI image technique.[5]

II. System Description

This project was divided into three parts which is vision, data processing and control. The hardware used is a webcam, an Arduino Uno, Omron CPM2 PLC, push buttons, relay module, conveyor and pneumatic elements. The software used is MATLAB version 2014a, Arduino IDE and CX-Programmer. The whole configuration can be seen from fig.3.

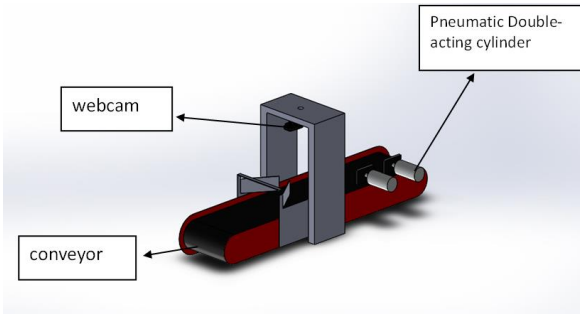

Fig.1 shows the sketch of webcam based color sorting system

A. *Vision and image acquisition*

For vision part, a webcam will be placed on the top to capture the top view of the product. The color classification were using MATLAB version 2014a by using RGB color representation. The program will classify two colors that is red or green.

B. *Data Processing*

- For red or green color, signal will be trigger in MATLAB and serial communication was set up with Arduino so that the signal will be transfer into output from the Arduino's I/O pins.
- To transfer the signal as the input to the PLC, relay module was configured to act as switches to supply the signal to the input of PLC. I/O pins from Arduino cannot be connected directly to the PLC as the voltage from Arduino was not sufficient to activate the signal input for PLC.

C. *Control and Actuation*

The goal for the project is to sort the product according to their color which in this case is either red, green or others (rejected). CX-Programmer is used to create an Omron's PLC programming sequences for the application. The actuator was using electro-pneumatic system whereas electrical control was use to the pneumatic system. In this case, pneumatic cylinder is controlled by two 5/2 pneumatic directional control valve. These valves were triggered by the signal from PLC and power supply to sort between red and green color. The pneumatic circuit diagram is shown as in fig.2.

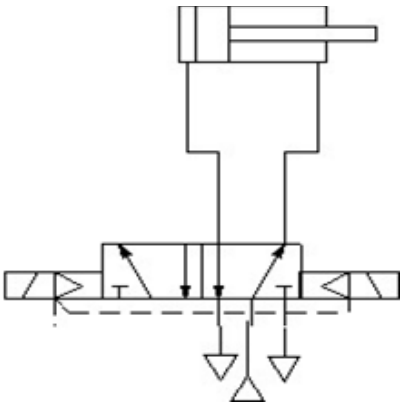

Fig.2 shows the pneumatic circuit for the actuator

Omron CPM2 can be considered have less features compared to the other model such as CP1H which have the analog feature. But for this project, it was acceptable to use even a basic PLC as it only required basic features to perform it application.

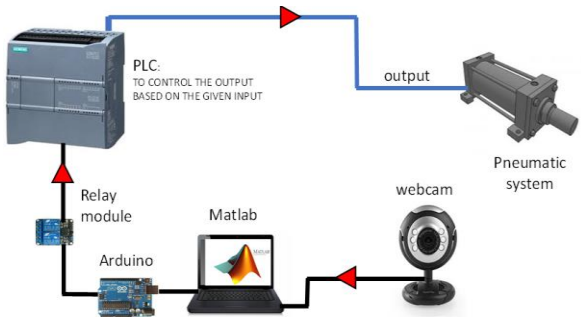

Fig.3 shows the setup of the project.

III. Experiments

To create communication between webcam and PLC, there must be a medium for data processing and signal transfer. In this project, Matlab software is used to create a color classification from the webcam and Arduino Uno as the transit for the signal transfer to the PLC. The programming in Matlab yield to color classification and integration with Arduino. First, video capturing object must be initializing to create a communication between the video inputs from desired webcam to the Matlab. '*videoinput*' function was use to initialize the input data from the webcam. There are several ways to communicate between Matlab and Arduino such as serial communication, using RS232 communication and Matlab Arduino Support Package.

A. *Serial Communication between Matlab and Arduino*

To communicate with Arduino, serial communication must be initialized by setting up the port number and the baud rate. The port number is refer to port number was set for the Arduino and the baud rate must be the same as set in Arduino serial communication which in this case, the baud rate was set to 9600

To track red and green color in real time, the red and green component is subtracted in the grayscale image to extract the red or green color from the image. As this project is using RGB color representation, the color of product either red or green must be according to the red or green color references or it will not detect the color as required. The results then transfer to the Arduino Uno by 'fprintf' function to send the signals which indicate there is red or green color in the image. From the data received from Matlab, the programming in Arduino IDE is to give an output signal which will be connected to the input of PLC via 5v relay.

By using serial communication, the data sent to the Arduino are limited to only one color which is either red or green. The data is transfer to PLC through the function '*fprintf*" that will be print data to the Arduino and to be convert to an output signal.

B. *RS232 serial communication*

By using 5V RS232 converter, we can connect the Arduino with PLC without any external wiring from Arduino pins. It also is using serial communication with Matlab. However, this method need some protocol for the setup. It takes time and more coding on the system.

C. *Arduino Support Package for Matlab*

Starting from 2014 version, Matlab have a support package installer whereas the user must install the packages according to their needs such as image acquisition, Arduino and USB webcam. The Arduino support package allows the user to directly control the Arduino with only use the USB cable to PC. The control of the Arduino I/O pins can be set on the Matlab itself. With this method, the project was able to send the red and green color tracking to be sent as the output of the Arduino. The red and green color was successfully been written as the output to be supply to the PLC.

To integrate input pins of PLC with Arduino's I/O pins, connection to relay must be configured. The function of relay is to trigger the signal from Arduino to the PLC. As we know, Arduino Uno need 5v signal to activate the input. But for Omron CPM2A, it needs a 24v signal to activate the input connected to its I/O pins. The relay switching method allow the signal from Arduino to be read by PLC by using 24v power source as the common connection as shown in fig.4.

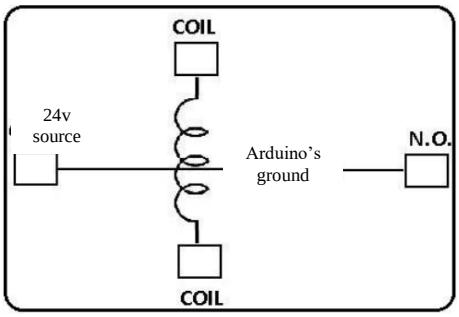

Fig.4 shows connection of relay

The ladder diagram programming in CX-Programmer is construct with timer for delay purpose. For the input, two push buttons is used to indicate ON/OFF of the system and signals from the Arduino to indicate the detection of red or green color. 4 timers were also applied to the programming to control the actuation of cylinders. The programs start with an ON push button to activate the system. When a 'red' input was detected, the first timer is activated to create a delay for the product to arrive at the actuation part. As the product arrived at the sorting part, the solenoid is activated to trigger the extension of the pneumatic cylinder. Then, the second timer will be initialized to make a delay as the product flow by the conveyor movement toward the first sorting box. Lastly, the solenoid will be deactivated and forced the cylinder to retract.

The same program was applied to the green signal. When a 'green' input was detected, the third timer is activated to create a delay for the product to arrive at the actuation part. As the product arrived at the sorting part, the solenoid is activated to trigger the extension of the pneumatic cylinder. Then, the fourth timer will be initialized to make a delay as the product flow by the conveyor movement toward the second sorting box. Lastly, the solenoid will be deactivated and forced the cylinder to retract.

Other than red or green color will be assume as rejected product and will directly moving by the movement of the conveyor toward the end. The flow of the program is shown in fig.5 and the ladder diagram can be seen at in fig.6.

To achieve a perfect timing for the product to be sorted into the sorting box provided for each color, the delay time must be adjusted for all the timers used in the programming.

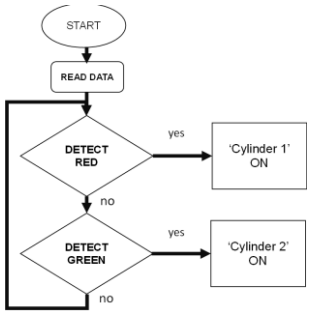

Fig.5 show the flow chart of the PLC programming

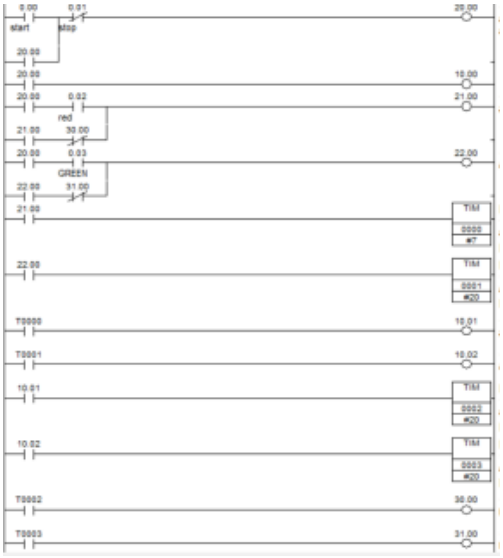

Fig.6 show the ladder diagram of the PLC program.

IV. Result and Discussion

As coded in Matlab Simulink version 2014a, the red object detected by the webcam will be labeled its pixel values and the centroid. The object will be also surrounded by a red rectangular box. The result of the red color detection is shown in fig.7. The red phone was tested into the webcam video to verify the red color tracking in real time. The test was also conduct with other objects. Although all items has different kind of red color but the program still recognize them as red component.

Fig.7 shows the real time red color tracking

Same goes for green object. But he object will be also surrounded by a green rectangular box. The result of the green color detection is shown in fig.8. The green phone was tested into the webcam video to verify the green color tracking in real time.

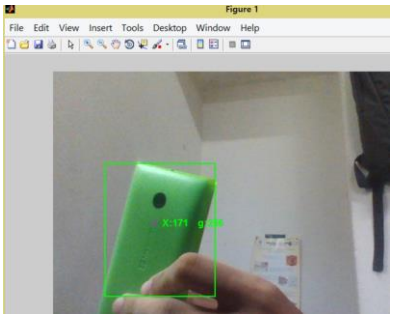

Fig.8 shows the real time green color tracking

In the project, the vision station was covered so that it only can detect the object move on the conveyor. But the color was not clearly seen as the dark surroundings. So, LED light was used together with the webcam to provide a good lighting for a better image for processing. Plus, the time taken for an object to arrive at red color sorting station and at green color sorting station was taken to measure the time for actuation and sorting purpose. Time taken to arrive at red and green sorting station after the object detection is 24 second and 35 second at first, whereas the conveyor having some technical problem that make its movement slower. But after the issue was solved, there is approximately 1 seconds delay for the object to move to the red color sorting station and 2 seconds to arrive at green color sorting station.

Conclusion

As the consequence of the test conducted, the application turned out to be successfully run in the preliminary stage which is the color classification and sorting system.

The RGB color representation method was convenient to be set as it was widely use in color classification. The serial communication between Arduino and Matlab Simulink was successfully established to transfer the color data signal. But we cannot avoid internal error cause by the system itself.

Webcam application on PLC to give out the input signal was done via Arduino connection. It function can be also applied to other inputs such as sensors, LCD display and other application as for the further improvement.

References

[1] Lu, Q., et al. (1997). Machine vision system for color sorting wood edge-glued panel parts. Industrial Electronics, Control and Instrumentation, 1997. IECON 97. 23rd International Conference

[2] Huang, C. T., et al. (2007). Construction of an automatic inspection system with capability of identifying color characteristics of product.

2007 IEEE International Conference on Industrial Engineering and Engineering Management.

[3] Liwei, Z., et al. (2005). "Development of a mechatronic sorting system for removing contaminants from wool." IEEE/ASME Transactions on Mechatronics **10**(3): 297-304.

[4] Buzera, M., et al. (2008). Techniques of Analysing the Colour of Produces for Automatic Classification. 2008 International Conference on Intelligent Engineering Systems, February 25-29,2008 Miami, Florida

[5] Guo, F. and Q. Cao (2004). Study on color image processing based intelligent fruit sorting system. Fifth World Congress on Intelligent Control and Automation, 2004. WCICA, June 15-19, 2004, Hangzhou, P.R. China

[6] Wang, L., et al. (2013). Machine Vision Applications in Agricultural Food Logistics. 2013 Sixth International Conference on Business Intelligence and Financial Engineering.

[7] Carlos Gonzales (2015). Engineering Essential: What is a Programmable Logic Controller.2015 http://www.machinedesign.com/engineering-essentials/engineering-essentials-what-programmable-logic-control

Development of the Internet of Things (IoT) for an Industrial Automated Guided Vehicle (AGV) System

Muhammad Nadzmi Abd Rahman
Faculty of Electrical Engineering
University Technology of Malaysia
Johor, Malaysia
mnadzmi23@gmail.com

Herman Wahid
Faculty of Electrical Engineering
University Technology of Malaysia
Johor, Malaysia
herman@utm.my

***Abstract*—This paper describes the implementation of the Internet of Things for an industrial Automated Guided Vehicle (AGV). Wireless communication is used as a platform to make the connection between AGV and server. The server would control the activity of the AGV such as traffic, motor speed, sensor reading and others. Therefore, many interfaces were designed by using the software like login and register form, connection and AGV control form. Error would be shown if the user wrongly put the data. Besides that, the data also would be sent to the cloud for monitoring the AGV.**

Keywords—Wireless communication, server, data, interfaces

I. INTRODUCTION

Nowadays, technology has come to its peak where every country in this world is advancing their technology day by day. But somehow perhaps what people all over the world needs from advancing technology is conducive medium for them to enhance their day by having most of their time connected to the internet either they can access through mobile's application or website. Soon in the future, maybe everything in this world would be connected to the internet so that all people around can access it anytime and anywhere.

The Internet of Things (IoT) is the name given to computerization of everything in our lives. It allows public and objects to be connected anytime and anyone are allow to use it. Soon everything will be on the Internet: the things we own, the things we interact with in public, autonomous thing that interact with each other.

Mostly the technology used especially in the heavy industry because they need such a large amount of production within a specific time to supply their products to the customer. One of the technology used is Automated Guided Vehicle (AGV). This AGV is a mobile robot that follows markers or wires in the floor, or some uses vision, magnets or lasers for navigation. They are most often used in industrial applications to move the materials around the manufacturing facility or warehouse.

The main problem that usually occurs to the AGV's user is if there is multiple AGVs operate around the workplace. It seems very hard to monitor and control the traffic especially at the junction or one way road. Somehow, if there is no safety and uncontrolled traffic, probably the AGV would be collided each other and crash. Therefore to overcome this problem, tracking sensor is used to monitor and track the current location of the AGV and design the algorithm to avoid them from collide.

There are three main objective in this project which is to investigate the remote control of high dense low volume of Automated Guided Vehicle, develop wireless communication based on Internet of Things (IoT) and test the data transmission between client and server.

This paper is organized as follows: in Section 2, explanation about the list of material and software use. Section 3 describes the methodology to develop the software on AGV. In the last two sections, the result of the motor speed and sensor reading from the cloud using ThinkSpeak followed by the conclusion section

II. PROJECT METHODOLOGY

The definition of the methodology is a system of methods used in a particular area of study or activity, to achieve a certain goal or objective. In this chapter, the methodology regarding the idea of the innovation would be explain deeply from the hardware, software to the parts of project assembly and the development.

A. List of Material

To ensure the project will be working according as planned, the right choice of hardware used in the project is crucial in order to ensure the project is develop and working as planned. Therefore, the list of materials will be provided and elaboration will be made for the understanding of reason why the following materials is chosen in order to develop the project.

i. RASPBERRY-PI 3

The hardware that used as client in this project is Raspberry-Pi 3. This device would be connected to the server through internet (*IP Address)* and also connected to the cloud services. From the research, this Raspberry-Pi 3 as shown in the figure 1 play a role as a client for the AGV compared to other controller because this controller mostly used in industrial application and user friendly. It also have some features which is wireless built-in, Bluetooth connection, and many IO pin. It has been tested to operate in 1 month before, and still working and stable.

Fig. 1 Raspberry Pi 3

B. *List of Software*

Overall of this project mostly are programming part. Therefore, the licensed software are needed to make sure this project is stable and run smoothly. Therefore, the list of software will be provided and elaboration will be made for the understanding of reason why the following software is chosen in order to develop the project

i. *Microsoft Visual Studio Community 2015*

This software have many style of programming and interfaces. Therefore, in this project, visual basic was used to design the graphic user interface (GUI) on the server for the AGV and also used for test the multiple clients. Besides that, it also used to track the movement of the AGV and receive/send data from/to the AGV.

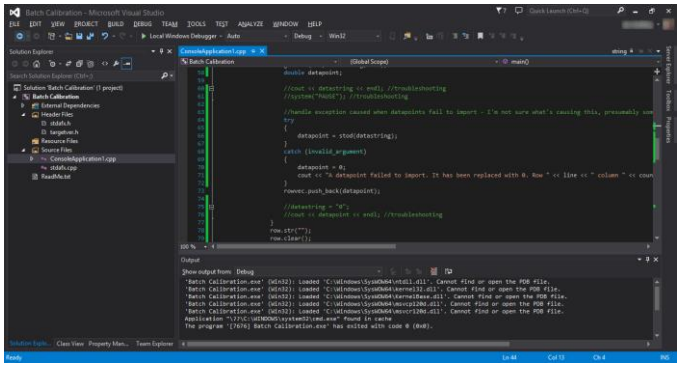

Fig. 2 Microsoft Visual Studio Community 2015

C. *Method*

Firstly, from this project, Raspberry-Pi 3 was used as a client and also the microcontroller of the AGV and the server is from the personal computer (PC). This means that the client is fully controlled by the server. The client would be connected to server and cloud through wireless communication. Figure 3 below shows the overall connection of this project.

Fig. 3 Overall connection

Server

The server of this project is PC. The flow of program would be explained based on each figure that shown below. All this interface was designed by using Microsoft Visual Studio with windows form application in visual basic programming.

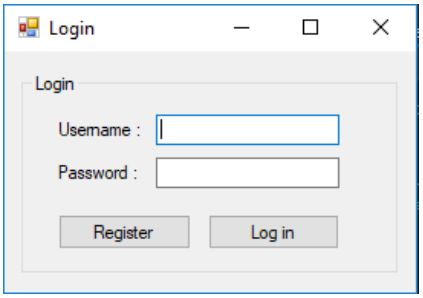

Fig. 4 Login Form

The interface that is shown in Fig. 4 is the first form that will be displayed once you have opened this software. It is login form which the user must insert their username and password that have registered before. If not, the register form will pop-up as shown in figure 5.

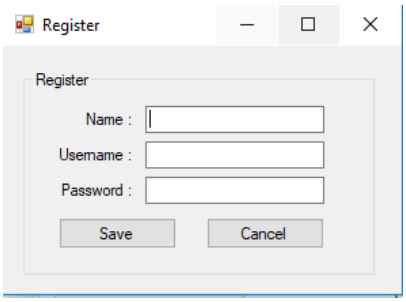

Fig. 5 Register Form

If the login is successful, it will direct to the server connection form in figure 6. This form will make the connection from the server to the client. The server start listening and waiting the request from the client with the same port and IP address. If the connection is successful, the client and server can send or receive the data each other.

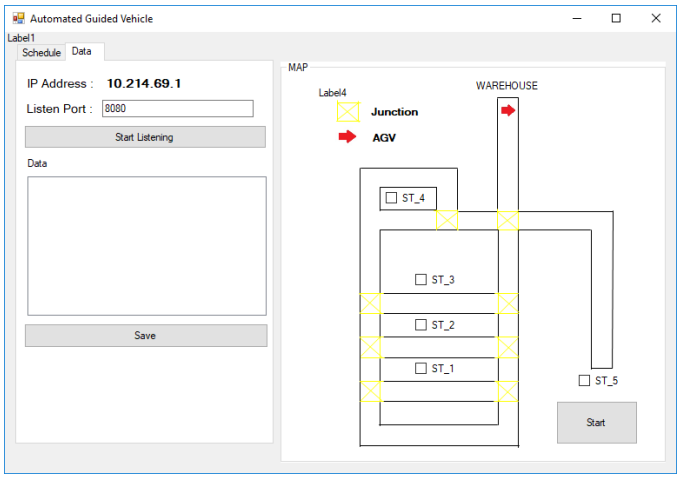

Fig. 6 Connection Form

Besides that, in this form also have the map of the AGV and several checkpoint for the AGV to stop to desire location. From the figure 7, there is 5 checkpoints and 8 junctions. This form will track the location of the AGV either is moving or stop.

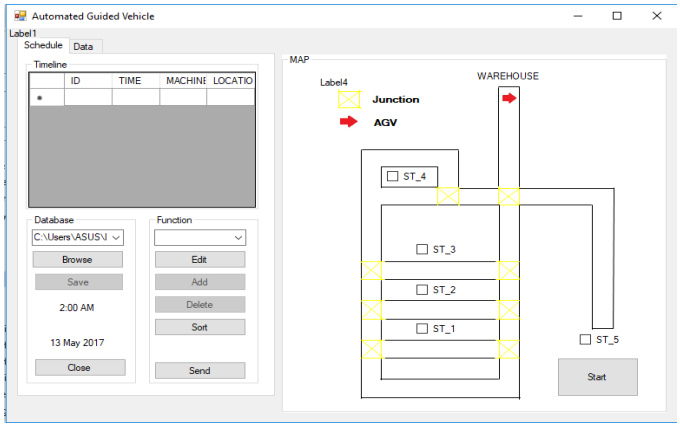

Fig. 7 Database Form

In addition, there is another additional function in this form which is database. The user can upload the schedule of the AGV from the database and send it to the Raspberry Pi to make sure the AGV can reach the checkpoint on time.

III. RESULT AND ANALYSIS

From this project, there are some results that would be displayed which are the motor speed and internal temperature of Raspberry-Pi that uploaded from the ThinkSpeak. In Fig. 8 as shown below describes about the speed of the AGV while running on the track. Because of the short distance of track, the maximum speed of the AGV is limited. From the graph, the maximum speed that can be achieved is 110 rpm. The AGV had already stopped at the checkpoint for 5 seconds at zero speed. Based on the graph, it take 1 minute 35 seconds to reach four checkpoints in the track.

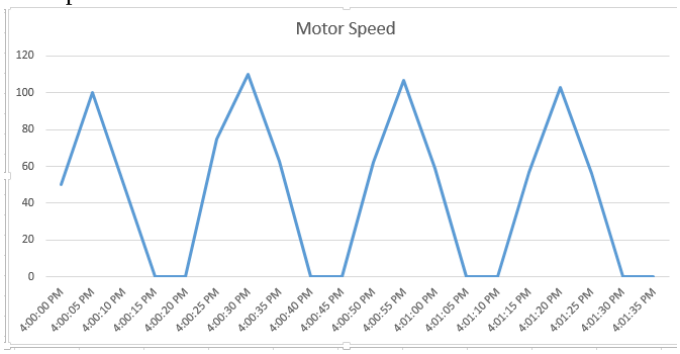

Fig. 8 Motor Speed vs Time Graph

Besides that, another result for the AGV is about the internal temperature of Raspberry-Pi. This is important to make sure that the controller can operate smoothly because the AGV would be running in 24 hours per day. If the temperature is so high, the server will stop the operation of the AGV to avoid any damage and other consequences. From the graph as shown in Fig. 9, it describes about the internal temperature with time in 40 sec. The maximum temperature is 59 Fahrenheit and minimum temperature is 58 Fahrenheit.

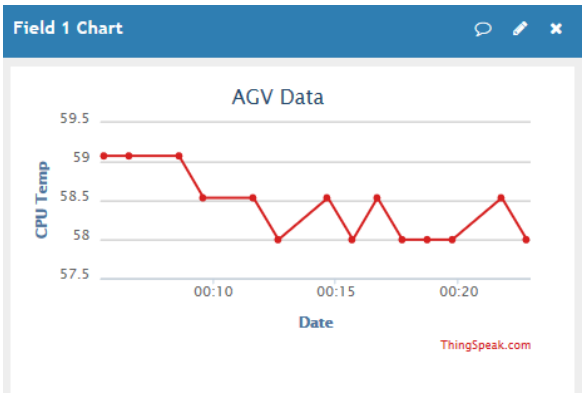

Fig. 9 CPU Temperature (F)

IV. CONCLUSION

In conclusion, the connection between AGV and server can be achieved through wireless communication using socket connection. Therefore, the server and client can communicate each other and send or receive the data. Besides that, AGV also can send the data like motor speed and sensor reading to the cloud services using ThinkSpeak platform. In addition, the server also able to track the current location of the AGV either it is moving or stop at the checkpoint. So, the AGV can communicate in two ways either server on PC or Internet of Things.

ACKNOWLEDGMENT

The completion of this project could not have been possible without participation and assistance of so many people. Their

contribution are sincerely appreciated and gratefully acknowledged. However the group would like to express their deep appreciation and indebtedness particularly to the following. Dr. Herman b. Wahid as supervisor for this project and guide me through all the pain to make sure this project successful. To all relative, friends and others who in one way or another shared their knowledge and support, either morally, financially and physically. Above all, greatly thank you for all the cooperation and helping hand through this project.

REFERENCES

[1] R. Shete and S. Agrawal, "IoT based urban climate monitoring using Raspberry Pi," *2016 International Conference on Communication and Signal Processing (ICCSP)*, Melmaruvathur, 2016, pp. 2008-2012.

[2] F. Corman *et al*., "Optimizing hybrid operations at large-scale automated container terminals," *2015 International Conference on Models and Technologies for Intelligent Transportation Systems (MT-ITS)*, Budapest, 2015, pp. 514-521.

[3] D. Pavithra and R. Balakrishnan, "IoT based monitoring and control system for home automation," *2015 Global Conference on Communication Technologies (GCCT)*, Thuckalay, 2015, pp. 169-173.

[4] M. Vanitha, M. Selvalakshmi and R. Selvarasu, "Monitoring and controlling of mobile robot via internet through raspberry Pi board," *2016 Second International Conference on Science Technology Engineering and Management (ICONSTEM)*, Chennai, 2016, pp. 462-466.

[5] T. N. Gia, M. Jiang, A. M. Rahmani, T. Westerlund, P. Liljeberg and H. Tenhunen, "Fog Computing in Healthcare Internet of Things: A Case Study on ECG Feature Extraction," *2015 IEEE International Conference on Computer and Information Technology; Ubiquitous Computing and Communications; Dependable, Autonomic and Secure Computing; Pervasive Intelligence and Computing*, Liverpool, 2015, pp. 356-363.

[6] N. A. Zaini, N. Zaini, M. F. A. Latip and N. Hamzah, "Remote monitoring system based on a Wi-Fi controlled car using Raspberry Pi," *2016 IEEE Conference on Systems, Process and Control (ICSPC)*, Melaka, Malaysia, 2016, pp. 224-229

[7] P. H. Kulkarni, P. D. Kute and V. N. More, "IoT based data processing for automated industrial meter reader using Raspberry Pi," *2016 International Conference on Internet of Things and Applications (IOTA)*, Pune, 2016, pp. 107-111.

[8] C. A. Cosmas and N. Y. Dahlan, "Development of visual basic GUI for Option C energy saving of IPMVP," *3rd IET International Conference on Clean Energy and Technology (CEAT) 2014*, Kuching, 2014, pp. 1-6.

[9] K. Osman, J. Ghommam and M. Saad, "Combined road following control and automatic lane keeping for automated guided vehicles," *2016 14th International Conference on Control, Automation, Robotics and Vision (ICARCV)*, Phuket, 2016, pp. 1-6.

[10] M. A. Abu and Mohamad Yusri Yacob, "Development and simulation of an agriculture control system using fuzzy logic method and Visual Basic environment," *2013 International Conference on Robotics, Biomimetics, Intelligent Computational Systems*, Jogjakarta, 2013, pp. 135-142.

Active Vibration Control of Flexible Beam using Piezoelectric Elements

Zul Fahmi Bin Khamiti
Faculty of Electrical Engineering
Universiti Teknologi Malaysia
Johor Bahru, Malaysia.
famyzul2947@gmail.com

Zaharuddin Mohamed
Department of Control and Mechatronics Engineering
Faculty of Electrical Engineering
Universiti Teknologi Malaysia
Johor Bahru, Malaysia.
zahar@fke.utm.my

Abstract*— Vibration suppression of a flexible beam systems using piezoelectric elements is reviewed in this article. The smart structure system consists of a beam as the host structure and the piezoelectric elements as the actuation and sensing elements. An experimental set-up has been developed to obtain the active vibration suppression of the smart beam. The set-up consists of a smart cantilever beam, data acquisition system and MATLAB based controller. PID controller is used in this experiment to control the flexible beam to ensure it move to the exact desired angle using the closed-loop PID encoder feedback. The PID controller also used for reducing the deflection and vibration of the flexible beam by using the piezoelectric feedback.

I. INTRODUCTION

Vibration is a mechanical phenomenon whereby oscillations occur about an equilibrium point. Vibration can be desirable and also be undesirable depends on the systems. Unfortunately, vibration was considered undesirable in many applications because produce an unwanted outcome. The presence of vibrations also can cause structural or mechanical failures to machine or to the structure itself. These vibrations also may cause discomfort to human and in worst case, can cause death.

The vibration in a flexible structure is considered undesirable and need to be controlled. For the vibration control of a flexible structure, obviously the need to suppress all the oscillation that faced by the structure. Control has been of great interest since many applications that related to the flexible structures such as high speed robots, requiring low weight, lower energy consumption, ease for handling and also safer operation due to reduced inertia [1]. Control of a flexible structures has become broadly field of research among the researchers since past few decades. Usually, the experimental validation and implementation of vibration controls have relied mainly on the use of proof mass actuator, brushless motors and also viscous dampers but recently, piezoelectric elements has been widely used because of their properties of materials have a lot of advantages if compared to the others [2-4].

Two major approaches which is active control and passive control have been accepted broadly [5]. These approaches can be found in many thesis, journal and also books that related to the vibration controls. In the passive method, vibrations of the structure is damped using passive dampers or materials with significant viscoelasticity [6]. This method of vibration control will increase the total weight of structure considerably but is best for high frequency applications. Then, the active vibration control was introduced by the researchers to overcome the weakness of the passive control method. The active vibration control is a method that integrates sensors and actuators with the flexible structures, operated by a suitable control scheme. For this active vibration control, it is very important issue in selecting the suitable sensors and actuators [7].

Among the different types of transducers, distributed piezoelectric elements (sensor and actuator) received the most attention among the researches because of certain features such as less weight, high bandwidth, low cost, its dynamic effects, low maintenance and also easy for bonding with the flexible structures [8,9]. This piezoelectric elements also has the capability of a wide frequency range of control. The use of this piezoelectric transducers has given rise to new approaches in the active control of flexible structures.

Although the piezoelectric elements shows superiority in control of flexible structures which their distributed nature for control the flexible structure systems, this issue is not well addressed yet in designing the control systems due to analytical complexity. Therefore, this cause raising in interest of question in term of sizing, shaping and also the suitable placement of piezoelectric elements to achieve an optimal control systems. Despite some of the results in these control systems, there is still a need for experiment and research for a more reliable dynamic model and easy to design. Also the need for efficient controller for real implementation. In addition, there is still need for optimization of shape and placement of the piezoelectric elements in the active vibration control of flexible structures.

II. SMART STRUCTURE PRINCIPLE

A. Smart Structure

Smart structure can be defined as a structure that integrated with smart materials which are sensors and actuators with a control function to perform a desired behaviour. A smart structure has the capability to respond to a changing of external environment such as shape change in order to control the internal environment such as structure failure or damage [10]. This smart structure basically involves four key elements which are sensors, actuators, control strategies and power conditioning electronics [11].

Most of the applications of smart structures are in the field of active control of flexible structures because flexible structures are distributed parameter systems which naturally allow their integration with distributed sensors and actuators. In the following section some of the advantages of piezoelectric sensors and actuators in active control of flexible structures are presented.

B. Smart Structures with Piezoelectric Transducers

Some of the features that make piezoelectric transducers most popular smart materials in the area of smart materials and structure and widely used in active vibration control of flexible structure are:

- They can be bonded onto or embedded within the structure members and not require support structure.
- They are commercially available.
- They have fast response with high bandwidth.
- The dynamic of the direct contact type of distributed piezoelectric transducers allow a wide frequency range of control.
- They can be distributed along a structure without greatly increasing the mass or changing the passive dynamics properties.
- The nature of distributed piezoelectric actuator allows continuously varying force actuation along the length of the structure.

C. Smart Structures with Integrated Piezoelectric Elements

The developments in piezoelectric materials have motivated many researchers to work in the field of smart structures. A smart structure that has been integrated with the piezoelectric elements can smartly sense the external disturbance and respond to that with active control in real time to maintain the operation requirements [12]. Depending on the characteristics of the smart structures involved and the expected operating conditions, the selection of the sensors and actuators vary considerably.

Typical smart structure sensors used in discrete or distributed locations to measure the performance of the system comprise fibre optics, piezoelectric ceramics and polymers, the actuators used in the smart materials technologies include applications of piezoelectric ceramics, piezoelectric polymers (PVDF), electrostrictive (ES) and magnetostrictive (MS) materials and piezofibres. Their reliability, near linear response with applied voltage, exhibiting excellent response to the applied electric field over very large range of frequencies and their low cost make piezoelectric the most widely preferred one as collocated sensor and actuator pair. Therefore, this project is mainly consider the application of piezoelectric sensors and actuators in the purpose of active vibration control of a flexible beam.

III. EXPERIMENTAL SETUP

A. The Smart Beam System

Figure 1 shows the experimental setup of the experiment. The flexible beam is attached at one end and the system is attached to a motor. The piezoelectric elements is attached near the end of the flexible beam as in Figure 2 because at that point, the bending of the flexible beam is at the most. The signal from the piezoelectric sensor is amplified first electronically before transfer it to the NI DAQ card, then the control scheme is implemented using the MATLAB software.

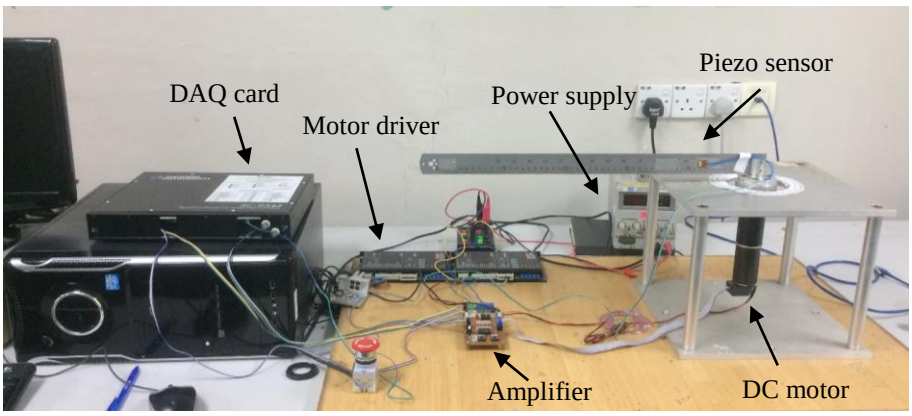

Figure 1 : The complete smart beam systems

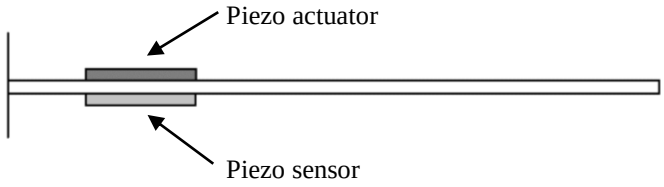

Figure 2 : Piezoelectric sensor and actuator placement

B. Simulink Design with PID Controller

Figure 3 shows the open-loop of the system to move the flexible beam system to desired angle and Figure 4 shows the closed-loop of the system with addition of PID controller. The PID controller is chosen in this experiment since it is the common controller and easy implementation. In addition, the PID controller also provides better robust stability. The PID controller is used to control the flexible beam to ensure it move to the exact desired angle using the closed-loop PID encoder feedback. The PID controller also used for reducing the deflection and vibration of the flexible beam by using the piezoelectric sensor feedback in this experiment.

The *P* (proportional) gain is used to amplify the feedback signal (error). The speed of the control system response increase proportionally with the *P* (proportional) gain. However, if the *P* (proportional) gain is too big, the system will become unstable. The *I* (integral) component sums the error terms over the time. The integral response will continue increase over the time unless the error is zero. So, the *I* (integral) gain is used for eliminating the steady-state error. Lastly, the *D* (derivative) gain is used to decrease the overshoot and reduce oscillation at the endpoint.

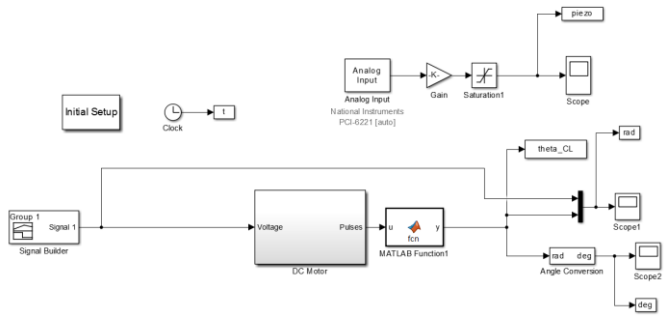

Figure 3 : Simulink block of the open loop system

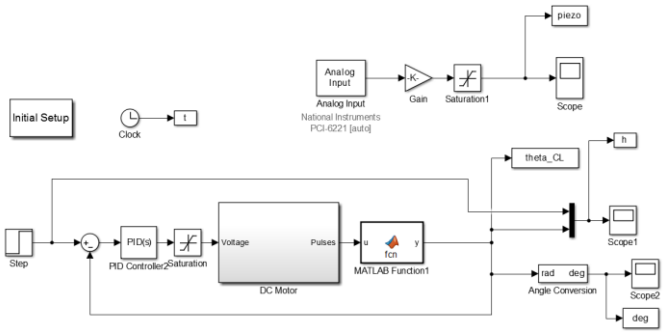

Figure 4 : Simulink block of the closed-loop system with PID controller

C. PID Controller Tuning

The PID controller must be tuned in order to get an efficient control of the system. Because of the widespread use of PID control, it is highly desirable to have efficient manual and automatic methods of tuning the controllers. A good insight into PID tuning is also useful in developing more schemes for automatic tuning and loop assessment.

In this experiment, the PID controller was tuned by using Ziegler-Nichols tuning method. This tuning method was developed by John G. Ziegler and Nathaniel B. Nichols [13]. The tuning process is performed by set the *I* (integral) and *D* (derivative) gains to zero. Then the *P* (proportional) gain, K_p is increased (from zero) until it reaches the ultimate gain K_u, at which the output of the control loop has stable and consistent oscillations. The value of K_u and the oscillation period T_u that obtained from the process are used to set the value of *P*, *I* and *D* gains depends on the type of the controller used. Since this experiment used the PID controller, the value of *P*, *I* and *D* is calculated using the formula that listed on Table 1. These 3 parameters are used to establish the correction $u(t)$ from the error $e(t)$ via the equation:

$$u(t) = K_p\left(e(t) + \frac{1}{T_i}\int_0^t e(\tau)d\tau + T_d\frac{de(t)}{dt}\right)$$

Table 1 : Ziegler-Nichols Tuning Rule Based on Critical Gain K_p and Critical Period T_u

Control Type	K_p	K_i	K_d
P	$0.50K_u$	-	-
PI	$0.45K_u$	$\frac{1.2K_p}{T_u}$	-
PID	$0.6K_u$	$\frac{2K_p}{T_u}$	$\frac{K_pT_u}{8}$

Through the tuning process, the output of the control loop has stable and have the consistent oscillations as in Figure 5 when K_p is set to 27. From the graph, the oscillation period, T_u is 0.128s. Then, by using formula in Table 1 for PID control type, the parameters were obtain as :

$$K_p = 16.2$$
$$K_i = 253.13$$
$$K_d = 0.26$$

Then, all the parameters were substitute back into the Simulink and slightly tuned to get the best performance of vibration control. Figure 6 shows the value of encoder reading for the open loop system and Figure 7 shows the value of encoder reading for the close-loop system of the flexible beam. We can see the difference of response of desired angle when we add the PID controller into the system.

Figure 8 shows the deflection rate of the flexible beam system without the piezoelectric feedback and Figure 9 shows the deflection rate of the flexible beam system with piezoelectric element. We can clearly see that the settling time is reduced from 2.2s to 0.85s. The piezoelectric elements feedback with help of PID control successfully reduced the settling time of the vibration on the flexible beam.

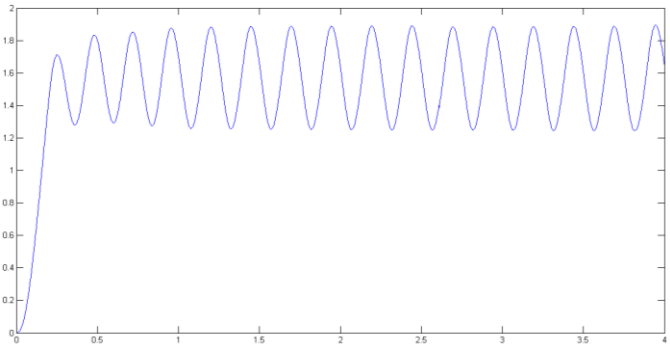

Figure 5 : Output graph of the closed-loop system with stable and consistent oscillation

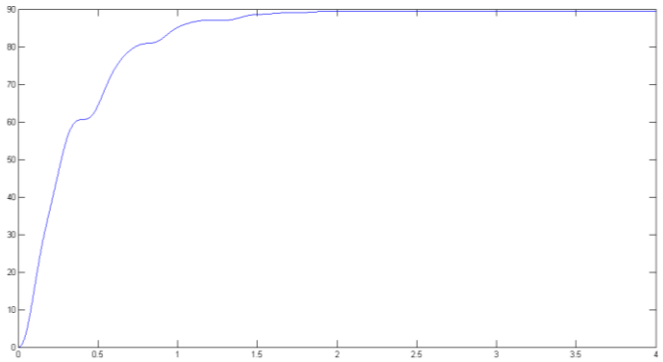

Figure 6 : Encoder reading in open loop system

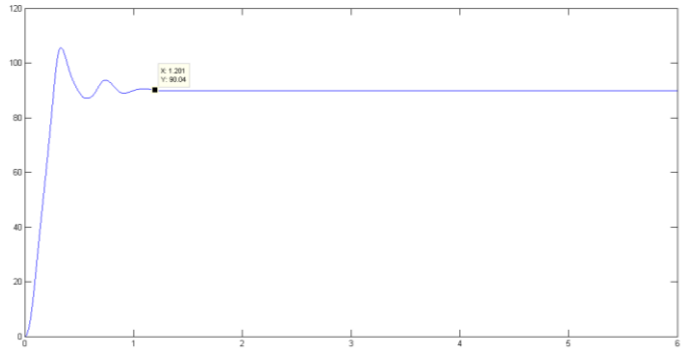

Figure 7 : Encoder reading in close-loop system

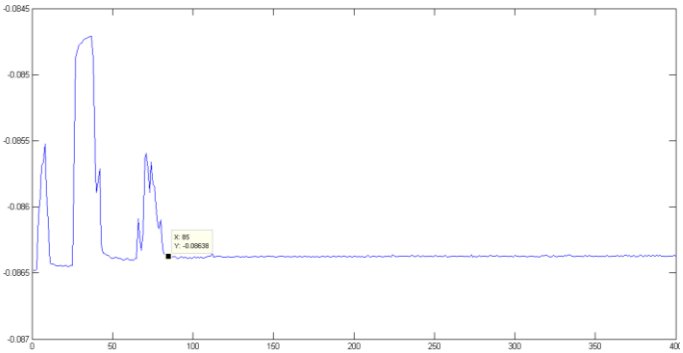

Figure 8 : Deflection rate of the flexible beam system without implementation of piezoelectric feedback

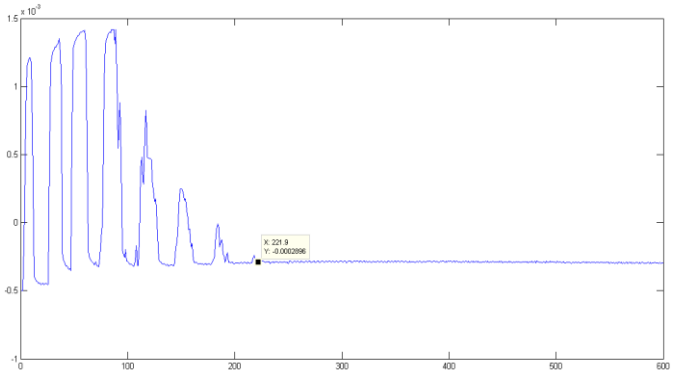

Figure 9 : Deflection rate of the flexible beam system with implementation of piezoelectric feedback

IV. CONCLUSION

In a nutshell, a PID controller with encoder feedback has been successfully designed to get the exact angle of position of the flexible beam system. The PID controller also implemented for the vibration control of the flexible beam system. All the objective in this experiment has been achieved and proved by the results in this experiment. This experiment also can be said successful because the vibration of the flexible beam has been reduced from 2.2s settling time to 0.85s settling time.

V. REFERENCE

[1] Khot, S. M., et al. "Active vibration control of cantilever beam by using PID based output feedback controller." *Journal of Vibration and Control*, 18(3), 2012, 366-372.

[2] Darivandi Shoushtari, Neda. "Optimal Active Control of Flexible Structures Applying Piezoelectric Actuators.", 2013.

[3] Junfeng Hu and Guiyang Xu. "Vibration control of piezoelectric flexible structure using robust control methodology." *Journal of Theoretical and Applied Information Technology*, 51(2), 2013.

[4] W. J. Manning, Andrew R. Plummer and M. C. Levesley. "Vibration control of a flexible beam with integrated actuators and sensors." *Smart Materials and Structures*, 9(6), 2000, 932.

[5] Leleu, Sylvaine, Hisham Abou-Kandil, and Yvan Bonnassieux. "Piezoelectric actuators and sensors location for active control of flexible structures." *Instrumentation and Measurement Technology Conference, 2000. IMTC 2000. Proceedings of the 17th IEEE*, Vol. 2, 2000.

[6] G. Song, V. Sethi, and H-N. Li. "Vibration control of civil structures using piezoceramic smart materials: A review." *Engineering Structures* 28(11), 2006, 1513-1524.

[7] Kumar, K. Ramesh, and S. Narayanan. "Active vibration control of beams with optimal placement of piezoelectric sensor/actuator pairs." *Smart Materials and Structures*, 17(5), 2008, 055008.

[8] I. Bruant, et al. "Active control of beam structures with piezoelectric actuators and sensors: modeling and simulation." *Smart Materials and Structures*, 10(2), 2001, 404.

[9] K. Kumar, Ramesh, and S. Narayanan. "The optimal location of piezoelectric actuators and sensors for vibration control of plates." *Smart Materials and Structures*, 16(6), 2007, 2680.

[10] [27] I. Chopra, "Review of state of art of smart structures and integrated systems", *AIAA journal*, 40(11), 2002, 2145-2187.

[11] Gupta, Vivek, Manu Sharma, and Nagesh Thakur. "Optimization criteria for optimal placement of piezoelectric sensors and actuators on a smart structure: a technical review." *Journal of Intelligent Material Systems and Structures*. 21(12), 2010, 1227-1243.

[12] M. Sahin, F. M. Karadal, Y. Yaman, O. F. Kircali, V. Nalbantoglu, F.D. Ulker and T. Caliskan, "Smart structures and their applications on active vibration control: Studies in the Department of Aerospace Engineering, METU", *Journal of Electroceramics*, 20(3-4), 2008, 167-174.

[13] Åström, Karl Johan, and Tore Hägglund. "Revisiting the Ziegler–Nichols step response method for PID control." *Journal of process control*, 14(6), 2004, 635-650.

Quadcopter Based Transporter

Mohammad Khairul bin Tajudin
Faculty of Electrical Engineering
Universiti Teknologi Malaysia
Johor Bahru, Malaysia.
Khairultajudin13@gmail.com

Mohamad Amir bin Shamsudin
Department of Control & Mechatronics Engineering
Faculty of Electrical Engineering
Universiti Teknologi Malaysia
Johor Bahru, Malaysia.
amirshamsudin@utm.my

***Abstract*— the purpose of this project is to design a scale down quadcopter based vehicle that can emulate quadcopter based transporter. The project will develop the mechanism to work as a transporter to carry the item. There is several online delivery issues that happen to customer such as failed to arrive when promised, had problems with delivery of their item, and human labor during the delivery process. Human still have a problem to transfer their item to the customer in effective ways. In industrial robotic revolution nowadays, the use of robotic in industry has become the first choice to improve the quality of their services or product. To solve this problem, Unmanned Aerial Vehicle (UAV) is a feasible solution to improve the delivery services by providing the quadcopter as a transporter. These features include the fact that they are maneuverable, can still be over a given point in space and able to carry additional equipment or load. Quadcopter was implementing by asymmetrical model instead of symmetrical model that really common nowadays. The proposed model should be able to lift up the load and able to transfer it to the specific position. The research can be further prototyped to practically have a system for delivery services for the online shop company.**

I. INTRODUCTION

Based in definition by techtarget.com website, a drone in a technological context is formally known as unmanned aerial vehicles (UAV) and essentially, a drone is a flying robot. The aircrafts may be remotely controlled or can fly autonomously through software-controlled flight plans in their embedded systems working in conjunction with onboard sensors [1].

According to Commercial UAV News article, Ian Smith state that, it is always interesting to discover what led people to careers in the drone industry. Whether it was a previous position that had something to do with similar technology, or if it just stemmed from something else that something more primal that had been with them since they were younger [2].

Quadcopter is a type of multi-rotors helicopter that has four numbers of rotors that give it the thrust it needs to move. They are divided to two sets of identical, fixed pitch propellers- two spin clockwise and the other two, counter-clockwise. The control of the craft is achieved by using remote control transmitters to change the speed of the rotors.

There was too much decision to be made by the pilot. The only solution to that is with the help of electronic controller and sensors and that is why the electronic parts of the quadcopter are as important as the mechanical parts. The harmony collaboration of mechanical and electronic part made navigating the quadcopter much easier. Thanks to the rapid development of computers microelectronics technology that made quadcopter as a reliable rotorcraft.

Quadcopters also usually has a simple and symmetrical shape as it is where most components will be mounted to and where the center of gravity supposed to be. However, there are several problems associated with using this type of construction. The main problem is calculation of the effective control of quadcopters [3]. To solve this problem, asymmetric model has been proposed. This asymmetric model will consider a model with such precision that necessary for the implementation of complex maneuvers that require high control precision [3]. The scale of a quadcopter is often determined by the diagonal measurement in millimeters from motor to motor through the center of the frame [4].

II. LITERATURE REVIEW

A. Modelling of a Quadcopter

There are several methods to do the mathematical approach to model the kinematics and dynamics of a quadcopter. According to the majority of the papers written, the traditional way of modelling a quadcopter is by using the Euler angles method. It is a method introduced by Leonhard Euler that uses three angles to describe the orientation of a rigid body in 3-dimensional space. Andrew Gibiansky, a software and robotics engineer used Euler Angle ZYZ in his approach to model a quadcopter according to his journal [5]. He claimed that his quadcopter's mathematical modelling to be highly simplified as there are a number of ignored advanced effects that contribute to the dynamics of the quadcopter to be highly nonlinear. His derivation of quadcopter's equations motion started with the voltage-torque relation for the brushless motor and then with the quadcopter kinematics and dynamics.

In Figure 1, he starts deriving quadcopter dynamics by introducing the two frames in which will operate. The inertial frame is defined by the ground, with gravity pointing in the negative z direction. The body frame is defined by the orientation of the quadcopter, with the rotor axes pointing in the positive z direction and the arms pointing in the x and y directions [5].

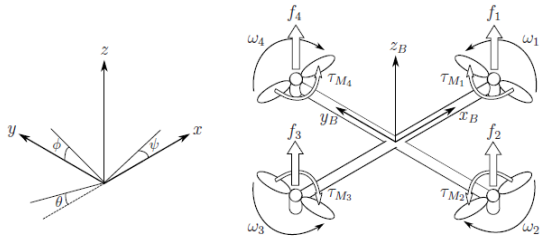

Fig. 1. Dynamic of quadcopter model

Aerodynamical effects such as flapping blade and non-zero free stream velocity are also ignored and replaced by a linear drag force representing air friction in all directions to complete his version of mathematical modelling of a quadcopter. An Italian hardware engineer, Tommaso Bresciani, has his own version of quadcopter model [6]. He mentioned that he used Newton-Euler method to describe the quadcopter's orientation, which is actually the derivation from Euler Angler. In classical mechanics, the Newton-Euler equations describe the combined translational and rotational dynamics of a rigid body.

New asymmetric model of quad copters is proposed in this project, it having the biggest number of perspectives. However, the efficiency of this model will not be improved if it uses the control algorithm for a symmetric or linear model [3]. Therefore, it is necessary to analyze the control methods for this model. New mathematical model of quadcopters and analyze the algorithms and principles of control for various kinds of trajectories, maneuvers, and conditions. The mathematical model has to take into account the asymmetry of the design and the effects of external influences [3].

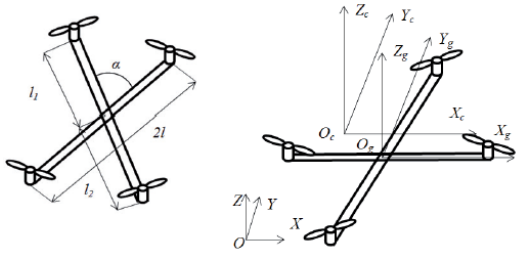

Fig. 2. New assymmetric quadcopter model

Based on Figure 2, quadcopter moves relative to the fixed inertial coordinate system (ICS) (oXYZ). Axis 0x 0y and 0z form an orthogonal right-handed coordinate system. Axis 0z is in the opposite direction to the vector of gravity. Introduce two auxiliary coordinate systems (CS). The coordinate system Oc Xc Yc Zc is related to the center of mass of quadcopters (CSM), and the coordinate system Og Xg Yg Zg associated with the quadcopters geometric center (CSG).

The axes of the coordinate system are parallel to the axes of the inertial coordinate system. The quadcopter related with the right movable orthogonal coordinate system oc Xp Yp Zp (MCS). MCS starts at the center of mass of quadcopters. The angular position of a quadcopter is defined in MCS by

The center of mass of a quadcopter is defined by vector X = (x, y, z) in ICS. The linear velocity vector of a quadcopter is defined as Vc = (vxc, vyc, vzc) and the angular velocity vector as W = (p, q, r) in CSM.

Euler angles η = (φ, θ, ψ): (1)

Roll φ, Pitch θ and Yaw ψ.

- Axis Oc xp is connected with one of the arms of a quadcopter,
- Axis Oc yp lies in the plane of a quadcopter,
- Axis Oc zp is upwardly directed relative to a quadcopter.

The center of mass of a quadcopter is defined by vector X = (x, y, z) in ICS. The linear velocity vector of a quadcopter is defined as Vc = (vxc, vyc, vzc) and the angular velocity vector as W = (p, q, r) in CSM.

Most manufacturers simplify their tasks by developing symmetry with respect to frame design. This greatly simplifies the mathematical description of the motion of quadcopters, but on the other hand, it is necessary to use additional equipment to comply with such symmetry. Manufactured devices differ significantly since the center of gravity with geometric center and the arm with the motors may be positioned at any angle relative to each other [3].

Propose model of quadcopters has the center of gravity structure shifted. One of the arms is also shifted relative to the geometric center of quadcopters and rotated at an angle, generally not a right angle, relative to the other arm. By refer to Figure 2, *l* is the distance from the edge of the second platform to the intersection with the center of the first platform,

$$l1 + l2 = 2l \quad (2)$$

l1 is the distance from the edge of the platform to the center of the motor. In Figure 2.1.2, a dotted line shows a quadcopter symmetric model. The main elements of quadcopters are the basic platform, two arms, four motors, unit with electrical system and accessories [3].

III. METHODOLOGY

A. *Flowchart of the Project*

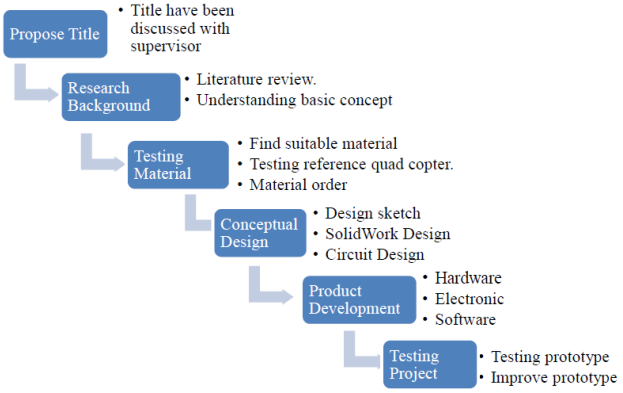

Fig. 3. Flowchart for the project

B. *Basic of Quadcopter*

Basically a Quadcopter is a quadrotor helicopter that is lifted and propelled by four rotors. Unlike helicopters they use symmetrically pitched blades. Control of vehicle motion is achieved by altering the pitch or rotation rate of one or more rotor discs, thereby changing its torque load and thrust characteristics [7].

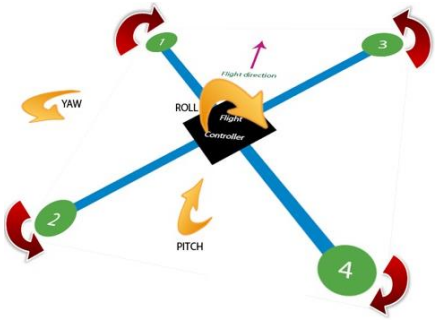

Fig. 4. Rotation for each motor

As shown in Figure 4, Motors 1 and Motor 4 rotate in clockwise (CW) direction while Motor 3 and Motor 2 rotate counter-clockwise (CCW) thus are creating a downward thrust which lifts the quad. By varying the speed of the 4 rotors, it can make the various movements are possible. There are three important terms that is, Yaw, Roll and Pitch which must have to clear concept of it before understanding the quad's movement [7].

- Roll - Angle of the multirotor describes how the craft is tilted side to side. Rotation about the roll axis is like tilting the head towards one of the shoulders. Rolling the multirotor causes it to move sideways [8].
- Pitch - Angle of the multirotor describes how the craft is tilted forwards or backwards. Rotation about the pitch axis is like tilting the head in order to look up or down. Pitching the multirotor causes it to move forwards or backwards [8].
- Yaw - Angle of the multirotor describes its bearing, or, in other words, rotation of the craft as it stays level to the ground. Rotation about the yaw axis is like rotate the head left and right [8].

C. *Hardware Development*

Motor is the most important part for the mechanical part of quadcopter. There are several steps to choose the best motor according to the model and uses of quadcopter.

First thing that need to consider is total weight ratio. It is the approximate weight estimation can be done by considering all the components of the device including the weight of the prospective electronic component that might be using [9].

Next is motor efficiency. Efficient motor is how longer it likely to fly. That means more the thrust produced by the motor as compared to the power utilized the smoother and longer will be quadcopter flight. If the motor is move with higher revolution per minute (RPM), the efficiency will be slightly reduced. In nutshell, it entirely depends on the mode of use [9].

Besides that, the pole of motor also needs to be considered. Quadcopter motors with a higher pole count will require more voltage during its flight, but produce a greater torque but with these conditions come the lower RPM of the motors [9]. On the other hand, motor with a lower pole count for achieving a higher RPM. But these devices will then require smaller blades, coming with a smaller torque or lift off the ground [9].

The last consideration for the motor is the KV value. The higher pole count, the lower will be the KV value. By KV, it basically refers to a constant RPM of the motor when a potential difference of 1 volt is applied across the motor. When the KV value decreases, there is an immediate increase in the torque produced by the motor. This would mean higher acceleration and a more powerful lift [9].

The other of the quadcopter is propeller. Propeller needs an equal numbers of CW and CCW propellers. There are two type of propeller that should come in pair form. This will ensure that the copter will not spin around. Propellers generate thrust by spinning and moving air. The more air it can move, the more thrust it will generate.

In this project, quadcopter use the larger type of propellers, it would be generating more thrust, higher acceleration and more stable flights [9]. Based on the theory, it should be able to carry heavy equipment and are best suited for delivery purpose. Propellers with larger diameters produce more thrust and thus can alter the thrust to weight ratio of the motor compare to the smaller diameter propellers that will generate less thrust [9].

The last part and also the most crucial element for this project is body frame. Size of frame of quadcopter can be estimate by sort of motor that should use. This is because frame size limits propeller size, and propeller size limits motor size and KV [10].

Frame Size ➡ Propeller ➡ Motor Size ➡ KV Value

Table 1 shows that, the simplified example to choose suitable motor and propeller based on frame size. Frame size is referring to wheelbase or diagonal motor to motor distance [10].

TABLE I. MOTOR SELECTION BASED ON FRAME SIZE

Frame Size	**Hardware Specification**		
	Propeller Size	***Motor Size***	***KV Value***
<150mm	<3”	<1306	>3000
180mm	4”	1806	2600
210mm	5”	2204-2206	2300-2600
250mm	6”	2204-2208	2000-2300
350mm	7”	2208	1600

The best quality materials for quadcopter is are fiberglass, carbon fiber and aluminum, but the most important thing is how well the frame is designed, not always the materials it is made out of [25]

D. Electronic Development

The brushless motors are normally in 3 phases, direct supply of DC power will not turn the motors on. By using Electronic Speed Controllers (ESC), it will generate three high frequency signals with different but controllable phases continually to keep the motor turning. The ESC is also able to source a lot of current as the motors can draw a lot of power.

The ESC is an inexpensive motor controller board that has a battery input and a three phase output for the motor. Each ESC is controlled independently by a Pulse Position Modulation (PPM) signal. For quadcopter, it is recommended the controller should support high enough frequency signal, so the motor speeds can be adjusted quick enough for optimal stability.

When selecting a suitable ESC, the most important factor is the source current. It should always choose an ESC with at least 10 A or more in sourcing current as what your motor will require. Another important factor is the programming facilities, which means in some ESC, it allowed using different signals frequency range. This is especially useful for custom controller board [11].

A multicopter control board is the essential part of your multicopter. It is the heart of the quadcopter and controls the motor independently and corrects for equal balancing. In this project, the quadcopter use Arducopter board that already has all necessary component for the quadcopter.

A GPS module measures quadcopter location by measuring how long a signal takes to travel from a satellite. A GPS module is also able to give an estimation of quadcopter altitude. The main feature used by the GPS module is that quadcopter can autonomously fly to way-points and it can potentially fly on its own from takeoff to landing [12].

E. Programming Development

Programming is the crucial part that needs to tackle as finish the hardware and electronic development. Programming is depends on what board controller it is. In this project, the quadcopter use an Arducopter controller boards that using ATmega as microcontroller. The software that suitable for that purpose is using Mission Planner.

For the testing purpose, such as rotor testing, in this project, the quadcopter only using the Arduino Nano board and Arduino IDE software.

Mission Planner will work as a ground station that typically a software application, running on a ground-based computer, which communicates with the quadcopter via wireless telemetry. It displays real-time data on the quadcopter's performance and position. It will show many of the same instruments that prototype would have if it were flying a real plane. It also can be used to control a quadcopter in flight, uploading new mission commands and setting parameters. It is often also use to monitor the live video stream from a quadcopter's cameras [13].

IV. RESULT AND DISCUSSION

A. Phase I

Solidwork design is use for the first phase in this project. Based on the design on Figure 5, the model and the mechanism can be decided and implement it into the prototype.

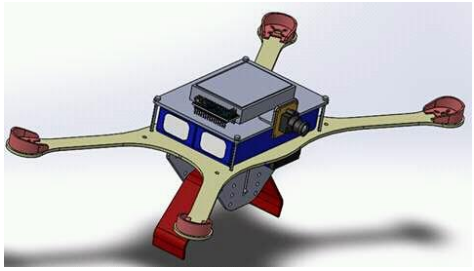

Fig. 5. Solidwork design for the draft planning

This design use asymmetrical model approach to be test in the real design. All the important part of mechanical will be assemble to view how the design will be made. In this phase, the design only for the draft and will be improve by the next phase to see it function well or not.

For the prototype, the frame of the quadcopter was using acrylic material. The reason is to make the frame lighter. From the design, the acrylic was cut using laser cuter machine to make it have shape and follow the design. The motor and propeller or known as rotor and ESC is attached on the frame to test the functionality of each material and to measure the effectiveness of the frame as shown in Figure 6.

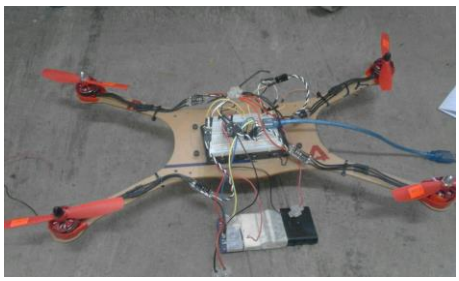

Fig. 6. Prototype of quadcopter in Phase I

The testing process only using the Arduino Nano and simple code to drive the motor was uploaded to the board. From the result, all the motor is move in clockwise direction. To make the quadcopter lift, the direction for motors 1 and motor 4 must be rotate in clockwise direction while motor 3 and motor 2 must rotate in counter-clockwise. To solve this problem, the polarity of the ESC in motor 2 and motor 3 must be change. After the change, the direction of each motor was finally following the desire direction.

Another problem that has been face in this phase is the ability the frame to support the motor movement. When the rotor is move and produces the thrust, the arm of the frame cannot withstand with the larger force and will be crash if the more impact happens to it. To improve this design, the project has to move to Phase II.

B. *Phase II*

In Phase II, the frame of the quadcopter has been support by the aluminum material that attach at the top and bottom of the quadcopter's arm as shown in Figure 7.

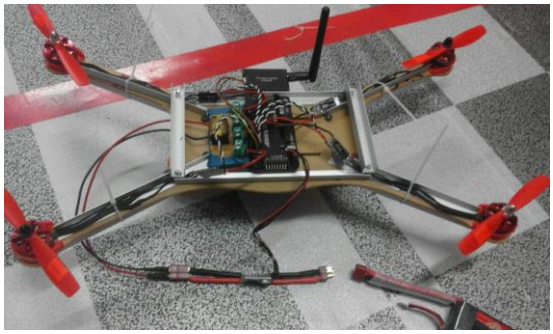

Fig. 7. Quadcopter frame with the support

In the beginning, support for the frame is using aluminum flat bar and attach directly on each arm. The result is, the arm is stronger and cannot be bending. Unfortunately, when the arm is support by this flat bar, the weight of the quadcopter has been increase. It has made the quadcopter difficult to lift.

To reduce the weight and the same time to make the support for the arm, the project was decided to use aluminum angle bar as replacement for the aluminum flat bar. Aluminum angle bar has an "L" shape and when it attach to the arm, the arm was difficult to bend because of the "L" shape on the angle bar. It provide more effective support compare to flat bar and it more light compare to aluminum flat bar. To make the support stronger, the "U" shape angle bar is use at the bottom of the arm. Same as "L" shape, this angle bar also can help the arm to avoid from bend and crash during the flight.

Support on the arm part only is not enough because all the force from the arm will transfer to the center body and also can make the body easy to crash is a lot of force extract to it. To solve this problem, all the arm has been combine and connect together with another angle bar on the body frame. From the testing, the body might be able to overcome the force from the rotor well and more safety to flight.

Next step for the project is to attach the gripper to the quadcopter. To achieve the objective to carry the load and transfer it from one place to place, the quadcopter using the gripper to hold the item while move to the desire destination.

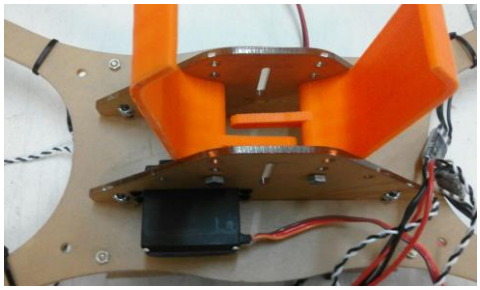

Fig. 8. Rotation for each motor

Based on Figure 8, gripper mechanism was made by the servo and 3d printing gripper. For the prototype, the size of the item is not really consider and it is depends on the limitation of the gripper.

C. *Phase III*

When the most important part, which is mechanical part has been solve, the project then proceed to the electronic and programming part in Phase III.

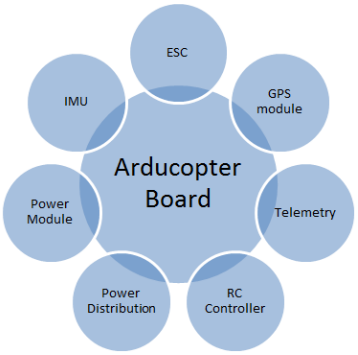

Fig. 9. Electronic component for the quadcopter

By refer to the Figure 9, the entire component has been connected to the flight controller. Arducopter already has a built in IMU on it and the quadcopter only need to assign the value for each parameter of the component by using Mission Planner software.

The problem that faces during the electronic development is the placement for each of the component. To avoid the unnecessary accident for the board and wiring, the placement for the component has been design as shown in Figure 10.

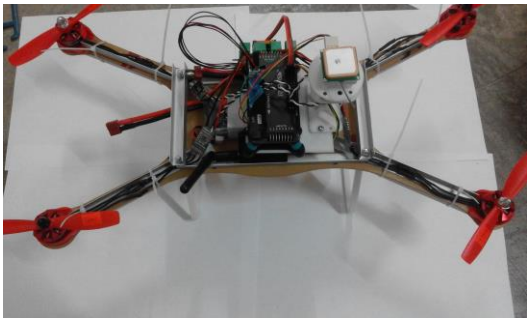

Fig. 10. Fully assemble for quadcopter.

D. *Phase IV*

Since all is complete for mechanical and electronic, the project then proceeds to programming part. The programming will become easy because the software is already build, that is Mission planner. Using Mission planner, the model of quadcopter and the firmware for it model has already set. The user only needs to setup and change some of the parameter based on the objective of the quadcopter.

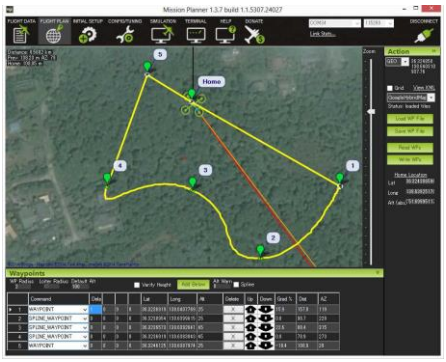

Fig. 11. Assign the waypoint for the quadcopter using Mission Planner

V. CONCLUSION

This project showed that the mechanism of the quadcopter work as important thing to be consider. All the material that choose to build a quadcopter is crucial and any of error that happen need to be aware. Quadcopter also need to consider the weight that will be carrying other than itself.

There are other few things that need to consideration such as body frame material, type of motor and propeller and how to use the software provided in most effective way. This is vital process before development of system is running. The expected outcomes of the proposed model are might be able to lift the load and carry it the desire place.

REFERENCES

[1] Jeremiah Karpowicz, Exploring the Present and Future of the Drone Industry". Commercial UAV News. December 13 2016. [Online]. Available: http://www.expouav.com/news/latest/exploring-present-future-drone-industry/. [Accessed: December 20, 2016].

[2] What is drone (unmanned aerial vehicle, UAV)? - Definition from WhatIs.com". IoT Agenda. [Online]. Available: http://internetofthingsagenda.techtarget.com /definition/drone [Accessed: November 28, 2016]

[3] Beniak, R., & Gudzenko, O. (2016). Control Methods Design For a Model of Asymmertrical Quadrocopter. Journal of Automation, Mobile Robotics & Intelligent Systems, 10(2).

[4] Malloy Hoverbike. The official website of The Hoverbike. [Online]. Available: http://www.hover-bike.com/ [Accessed: September 25, 2016]

[5] Gibiansky, A. (2010). Quadcopter Dynamics, Simulation, and Control.

[6] Bresciani, T. (2008). Modelling, identification and control of a quadrotor helicopter. MSc Theses.

[7] Quadcopter Basic [Online]. Available: https://creativentechno.wordpress.com /2012/06/13/quadcopter-basics/ [Accessed: December 21, 2016]

[8] The Physic of Quadcopter Flight? [Online]. Available: http://blacktieaerial.com/the-physics-of-quadcopter-flight/ [Accessed: December 20, 2016]

[9] Quadcopter Motor: Understanding The Driving force of The Drones? [Online]. Available: http://mydronelab.com/accessories/quadcopter-motors.html [Accessed: December 21, 2016]

[10] How to choose Motor and Propeller for Quadcopter? [Online]. Available: https://oscarliang.com/quadcopter-motor-propeller/ [Accessed: November 9, 2016]

[11] How to Pick The Best Multirotor Frame?. [Online]. Available: http://myfirstdrone.com/tutorials/best-multirotor-frame/ Accessed: November 10, 2016]

[12] What to consider when buying a ESC for your multirotor? [Online]. Available: http://www.dronetrest.com/t/what-to-consider-when-buying-a-esc-for-your-multirotor/1305 [Accessed: November 10, 2016]

[13] Ardupilot Community. The official website of Arducopter. [Online]. Available: http://ardupilot.org/copter/index.html [Accessed: April 15, 2017]

Modeling and Sway Control of a Double-Pendulum Overhead Crane System

Tan Ying Jian
Faculty of Electrical Engineering
Universiti Teknologi Malaysia
Johor Bahru, Malaysia.
yingjian1992@gmail.com

Zaharuddin Mohamed
Faculty of Electrical Engineering
Universiti Teknologi Malaysia
Johor Bahru, Malaysia.
zahar@utm.my

***Abstract*— A Crane system is very important in industries as the system is used to handle heavy load in the industry. In a manufacturing plant, an overhead crane system is used to transport a load from one place to another. A double-pendulum type overhead crane system is very difficult to control and it is always suffer from payload sway and double-pendulum dynamics. These affect the system performance and the safety of the operation. This project focus on the modeling and sway control of a double-pendulum overhead crane system. The mathematical model of a double-pendulum overhead crane system is obtained through Euler-Lagrange methods. The mathematical modelling is then verified through simulation and experiment. The simulation is carried out using the Simulink block diagram in MATLAB whereas the experiment is carried out using a laboratory overhead crane. Upon obtaining an accurate dynamic model of the double-pendulum overhead crane system, controllers based on input shaping are designed to improve the system performance. Input shaping is proposed in this project.**

Keywords—Overhead crane; Double-Pendulum; Control; Modeling

I. INTRODUCTION

A. Introduction to Overhead Crane System

Crane systems are commonly found in industries such as construction sites, manufacturing plants, warehouses, nuclear plants and harbour plants to handle heavy loads [1-6]. The crane system help the industry to transport heavy loads from one place to another place. A tower crane, an overhead crane and a harbour crane are amongst the famous cranes used by the industry. These cranes can be categorised based on their dynamic properties and coordinate system [7].

The tower crane is mainly used in a construction site. For the crane, cylindrical coordinate system is used to describe the coordinate and the motion of the payload during operation. The load is supported by a cable and the cart moves by the trolley along the jib arm [7]. The overhead crane system use Cartesian space to describe the position and the motion of the system. The motion of the crane is perpendicular to the cart or trolley [7]. On the other hand, the harbour crane used a spherical coordinate to describe the coordinate and motion of the system. The payload is supported by the suspension. A harbour crane is normally placed on a base for easier change of workspace [7].

Amongst all the cranes mentioned, the overhead crane system is the most used by crane industries especially in a manufacturing plant. The overhead crane system is capable in moving the heavy load in the industry from one location to another. The system needs to operate at a very fast, precise and accurate manner as the efficiency is very important to the industry. Most of the overhead crane systems used by the industry is a double-pendulum overhead crane system as shown in Fig. 1 In a double-pendulum overhead crane system, the system is equipped with a hook and a payload attach to it. The operation of the overhead crane system become challenging due to the existing of the dynamic behaviour of the double-pendulum overhead crane system.

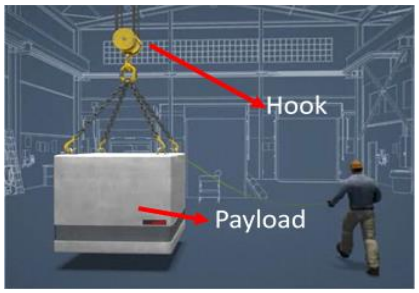

Fig. 1. A double-pendulum overhead crane system

Many previous researches carried out on the overhead crane system based on the assumption that the system is a single-pendulum model which does not always hold true. In certain cases, the hook mass cannot be ignored. When the hook cannot be ignored, a double-pendulum type system is created [8]. Unlike a single-pendulum type overhead crane, which only consist payload sway, a double-pendulum type system need to consider the payload sway as well as the hook sway. Hence, a double-pendulum type overhead crane system is more difficult to control as compared to a single-pendulum type overhead crane system. Besides, obtaining a fast, precise and accurate double-pendulum overhead crane system in positioning the load with minimum payload sway become challenging due to the complexity and dynamic behavior of the double-pendulum overhead crane system.

The objectives of this research are:

- To obtain a mathematical model of a double-pendulum overhead crane system.
- To verify the accuracy of the dynamic model through experiment

- To design a suitable controller for the double-pendulum overhead crane system to reduce payload sway and double-pendulum dynamics.

II. LITERATURE REVIEW

The overhead crane system used by most of the industry is a double-pendulum type overhead crane system with a hook and payload attach it. The overhead crane system needs to operate at a very fast, precise and accurate manner in positioning the load because efficiency is very important to all the industries. However, a double-pendulum type overhead crane systems suffered from payload oscillations [1-2,8-10,5-7,9-12] and double-pendulum dynamics [1-2,5-9,12,14-15].

The payload oscillation degrades the efficiency of the operation. It causes the difficulty for the operators to manipulate the payloads faster and accurately [1-2,8-9]. The operation takes a longer time to settle down and this increase the completion time.

The hook mass used in the overhead crane system cannot be less than the payload mass as if the payload is too heavy, the string will tend to break. In order to avoid this problem, a larger hook mass is used. However, double-pendulum dynamics with high sway will be created when the system has a larger hook mass as compared to payload mass [3-4]. The double-pendulum dynamic will affect the safety [13] of the operators since most of the crane systems are control by operators.

A. Control of a Double-Pendulum Overhead System

1) Feedforward Control

In feedforward control, the control variable adjustment is based on the knowledge about the system especially the mathematical model of the system. All the system variables as well as the disturbance need to be understood before a feedforward control system can be designed. The system will only react based on the established feedforward system because feedback signal is not based on the error of the system. Fig. 2 shows the block diagram of a feedforward control of a system.

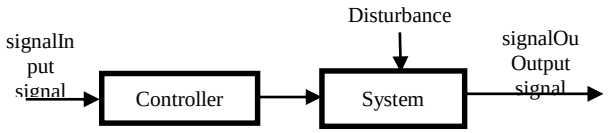

Fig. 2. Feedforward control system

Input shaping [1,9,14,16-18] is the most famous method used by the researchers. Input shaping does not require feedback from the system and it is established based the estimated natural frequencies and the damping ratio of the system [5,16-18]. Input shaping helps to filter out unwanted signal such as the vibration and the command generated by operators [1,5,17-18]. This will reduce the payload sway of the system and also reduce the completion time of a task [1]. There are also several researches using Zero Vibration (ZV), Zero Vibration Derivative (ZVD), Zero Vibration Derivative Derivative (ZVDD) and Specified Insensitivity (SI) [5] shapers as control methods to solve the payload sway and double-pendulum dynamics.

Since there is no feedback is required from the system, camera or sensor is not required during the implementation of feedforward control system in the overhead crane system. Hence, it is cheap to implement [12]. Input shaping is not a feedback system; therefore, it is compatible with the human operators [1,5,17-18]. The major drawback of feedforward control is that it is unable to handle the modelling errors, external disturbances and unexpected vibration from the dynamic behavior of a double-pendulum overhead crane system [6].

2) Feedback Control

Feedback control system takes the output response such as the hook and payload sway into consideration to adjust its performance to meet the system requirement. Hence, an additional sensor device such as sensor or camera is required to obtain the payload sway of the system. With the reading of hook and payload sway as the feedback of the system, a closed-loop feedback control system can be established. Amongst the feedback controller, Proportional-Derivative(PD) controller [1] and fuzzy logic controller [8] are commonly used. A study shows that the use of PD controller is able to improve the performance of an overhead crane system by 66% [1]. Apart from PD controller, fuzzy logic controller is also introduced to the overhead crane system to improve system performance. In fuzzy logic control, single-input-rule modules (SIRMs) was introduced. SIRMs employs genetic algorithm to tune the parameters of the overhead crane system [8]. Fig. 3 shows the block diagram of a feedback control system.

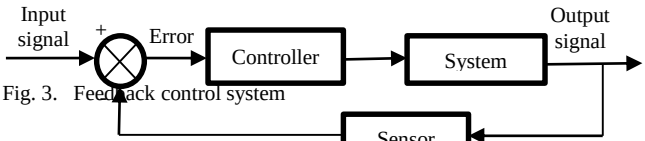

Fig. 3. Feedback control system

III. RESEARCH METHODOLOGY

A. Experimental Overhead Crane System

Fig. 4 shows an overhead crane system manufactured by INTECO that is used in this project. The overhead crane system is a 3D crane with a dimension of length, width and height of 1.0 m. The system is equipped with angle sensor, position sensor, motor drive and power amplifier.

Fig. 4. An Overhead crane system by INTECO

Fig. 5 shows the position sensor of the overhead crane system. The position sensor is actually an incremental encoder. When the cart start moving, the incremental encoder will start to count, the readings from the encoder will be converted into cart position of the system. Fig. 6 shows the cart and angle sensors of the overhead crane system. The angle sensor is positioned

directly below the cart of the overhead crane system. The angle sensor measures the hook sway of the system. Fig. 7 shows the power amplifier for the overhead crane system while Fig. 8 shows the motor drive of the system. The power amplifier will amplifier the signal obtained from the Simulink in MATLAB and send it to the motor drive of the system to move the cart. The system is integrated with MATLAB. All the settings can be configured using MATLAB. Fig. 9 shows the MATLAB user interface provided by INTECO.

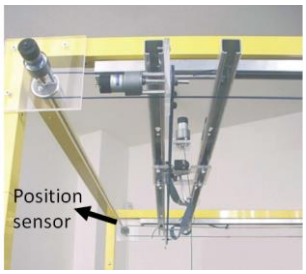

Fig. 5. Position sensor of overhead crane system

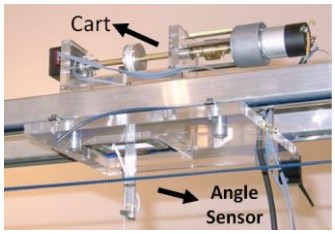

Fig. 6. Cart and angle sensor of overhead crane system

Fig. 7. Power amplifier of the system

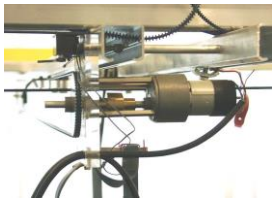

Fig. 8. Motor drive of the overhead crane system

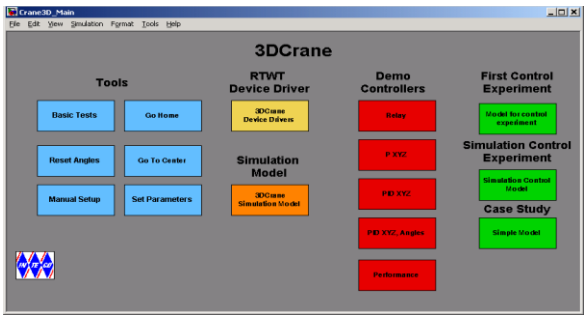

Fig. 9. User interface of the system in MATLAB

B. *Mathematical Modeling*

Fig. 10 shows the schematic diagram of a double-pendulum overhead crane system. The system is driven by a force, F by motor drive and with a frictional force, f_x opposed the motion of the crane. The crane consists of cart, hook and a payload. The payload is attached to the hook as shown in . The cart mass of the system is given by the symbol m, while the hook mass and the payload mass are given as m_1 and m_2 respectively. L_1 indicates the cable length of hook while L_2 indicates the cable length of the payload. There are three outputs response of the system which are the cart position, hook angle and payload angle. The symbols for the output response of the system are given as cart position x, hook sway, θ_1 and payload sway, θ_2.

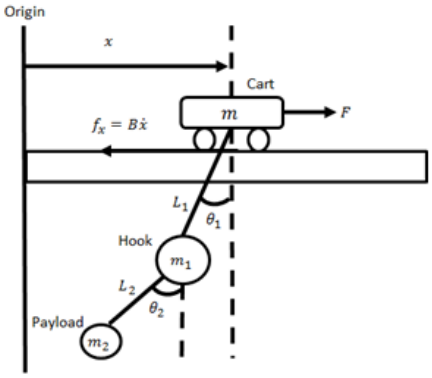

Fig. 10. Schematic diagram of a double-pendulum overhead crane system

There are several assumptions that have been made during the mathematical modelling of a double-pendulum overhead crane system. First of all, the hook and the payload are assumed to be a mass-point. Besides, the cable for the hook and payload is assumed to be massless and inflexible. The elongation of the cables during the motion of the cable is neglected.

The dynamic model of the double-pendulum overhead system is obtained through the Euler-Lagrange method. The Euler-Lagrange method involves the total kinetic energy and total potential energy of the system. Euler-Lagrange equation is given as:

$$L_a = K - P \tag{1}$$

$$\frac{d}{dt}\left(\frac{\partial L_a}{\partial \dot{q}}\right) - \frac{\partial L_a}{\partial \dot{q}} = T_i \tag{2}$$

where
L_a is the Lagrangian function,
K is the total kinetic energy of the system,
P is the potential energy of the system,
q_i is the generalised coordinate of the system,
T_i is the resultant force acting on the cart

Through equations (1) and (2), the mathematical equation is derived as shown below:

$$(m + m_1 + m_2)\ddot{x} + (m_1 + m_2)(L_1\ddot{\theta}_1 \cos\theta_1) - (m_1 + m_2)\left(L_1\dot{\theta_1}^2 sin\theta_1\right) + m_2 L_2 \dot{\theta_2}^2 \sin\theta_2 - \tag{3}$$

$$(m + m_1 + m_2)\dot{x} + (m_1 + m_2)\left(L_1\dot{\theta}_1 \cos\theta_1\right) + m_2 L_2 \dot{\theta}_2 \cos\theta_2 = F - f_x$$

$$(m_1 + m_2)\left(L_1\ddot{x}\cos\theta_1 + {L_1}^2\ddot{\theta}_1\right) + m_2 L_1 L_2 \ddot{\theta}_2 \cos(\theta_1 - \theta_3) + m_2 L_1 L_2 {\dot{\theta}_2}^2 \sin(\theta_1 - \theta_2) + (m_1 + m_2)(g L_1 \sin\theta_1) = 0 \quad (4)$$

$$m_2 {L_2}^2 \ddot{\theta}_2 + m_2 L_1 L_2 \ddot{\theta}_1 \cos(\theta_1 - \theta_2) - m_2 L_1 L_2 {\dot{\theta}_1}^2 \sin(\theta_1 - \theta_2) + m_2 L_2 \ddot{x} cos\theta_2 + m_2 g L_2 \sin\theta_2 = 0 \quad (5)$$

C. Controller

In this project, input shaping is chosen as the control scheme for the double-pendulum overhead crane system. Input shaping is a control technique which involve the convolution of the input signal with the impulse signal to create a shaped input signal. The shaped signal is implemented based on the natural frequency, ω_n the damping ratio, ζ of the system. The convolution of the input signal with the impulse signal will cancel out the residue vibration of the double-pendulum overhead crane system. Hence, the hook and payload sway will be reduced from this system. ZVDD input shaper is proposed in this project. ZVDD is a four-impulse signal which is capable to cancel out the residue vibration of the hook and payload. The natural frequency, ω_n can be obtained through Fast Fourier Transform (FFT) while the damping ratio, ζ can be obtained by using the Curve Fitting Toolbox (cftool) inside MALTAB. The amplitude of the and the time location of the ZVDD impulse signal can be calculate based on the following formula:

$$A_0 = \frac{1}{1+3K+3K^2+K^3}, \quad A_1 = \frac{3K}{1+3K+3K^2+K^3}$$
$$A_2 = \frac{3K^2}{1+3K+3K^2+K^3}, \quad A_3 = \frac{K^3}{1+3K+3K^2+K^3} \quad (6)$$

$$t_0 = 0, \quad t_1 = \frac{\pi}{\omega_d}, t_2 = \frac{2\pi}{\omega_d}, t_3 = \frac{3\pi}{\omega_d} \quad (7)$$

where, $K = e^{-\frac{\zeta\pi}{\sqrt{1-\zeta^2}}}$ and $\omega_d = \omega_n\sqrt{1-\zeta^2}$

D. System Parameter

TABLE I shows the system parameters that are used throughout the project. FFT and Curve Fitting Toolbox is carried out for the hook sway, θ_1 to find out the natural frequency, ω_n and the damping ratio, ζ of the system. Fig. 11 shows the single-sided magnitude spectrum of hook sway in frequency domain.

TABLE I. SYSTEM PARAMETERS

Label	Descriptions	Values
m	Cart mass	1.155 kg
m_1	Hook mass	0.200 kg
m_2	Payload mass	0.100 kg
L_1	Hook length	0.400 m
L_2	Payload length	0.200 m
B	Coefficient of friction between cart and surface	100 kgs^{-1}/m
g	Gravitational force	9.81 m/s^2

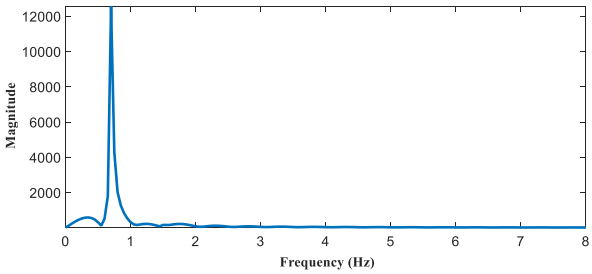

Fig. 11. Single-sided Magnitude Spectrum of Hook Sway

Therefore, the natural frequency of the system is $\omega_n = 2\pi(0.7076) = 4.466$ rad/s and the damping ratio, ζ=0.01389. From equation (6) and (7), the amplitude and time location of impulse signal of the ZVDD are obtained as:

$$\begin{bmatrix} A_i \\ t_i \end{bmatrix} = \begin{bmatrix} 0.1334 & 0.3830 & 0.3666 & 0.1170 \\ 0 & 0.7035 & 1.4070 & 2.1105 \end{bmatrix}$$

IV. Result and Discussion

This section provides a detail analysis on the results obtained from both the simulation and experiment. The first section will focus on the verification of the accuracy of the dynamic model of the double-pendulum overhead crane system between the simulation and experiment. The first section also verifies the accuracy of the dynamic model after the implementation of ZVDD shaper. The second section provides the analysis on the system performance after the implementation of ZVDD shaper. It will analyse the impact of the ZVDD shaper on the experimental double-pendulum overhead crane system. Fig. 12 shows the input signal and the shaped input signal for both simulation and experiment.

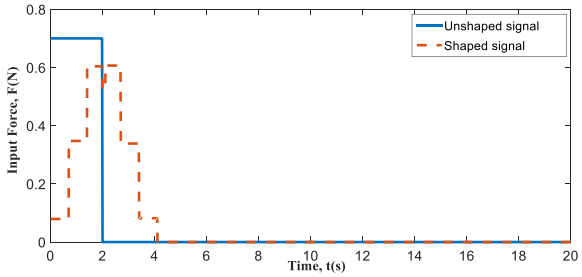

Fig. 12. Input signal and the shaped input signal of the system

A. Model Verification

1) Open Loop

Fig. 13 shows the cart displacement for both simulation and experiment. Fig. 14 shows the hook sway for both simulation and experiment. Payload sway is absent because INTECO 3D crane system does not have sensor to detect the changes in payload sway. Both Fig. 13 and Fig. 14 show that the simulation result are almost the same as the experimental result. It indicated that the accuracy of the model obtained in this paper is highly acceptable. The maximum cart displacement and the hook sway are tabulated in TABLE II.

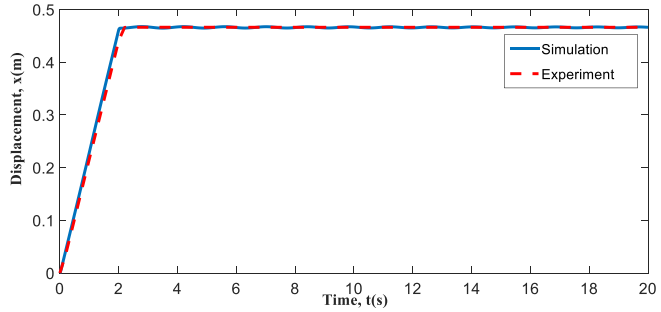

Fig. 13. Cart displacement for both simulation and experiment

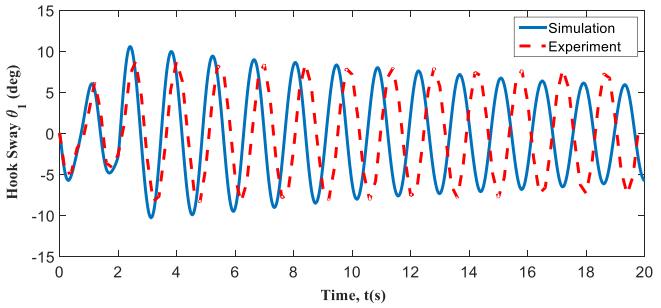

Fig. 14. Hook sway for both simulation and experiment

TABLE II. SIMULATION AND EXPERIMENT RESULTS

	Maximum cart displacement, x(m)	**Maximum hook sway, θ_1(deg)**
Simulation	0.4675	10.6675
Experiment	0.4663	8.879

B. ZVDD shaper

Fig. 15 shows the cart displacement for the simulation and experiment after the implementation of ZVDD shaper whereas Fig. 16 shows the hook sway for the simulation and hook sway after the implementation of ZVDD shaper. Comparing Fig. 15 to Fig. 13, it shows that the maximum cart displacement reduced after the implementation of ZVDD input shaper. Besides, Fig. 16 and Fig. 14 also shows that the hook sway for both simulation and experiment is reduced significantly after the implementation of ZVDD shaper. The maximum cart displacement and hook sway are recorded in TABLE III. Both the simulation and experimental result showing the same characteristics before and after the implementation of ZVDD input shaper. Therefore, we can conclude that dynamic model that obtained in this project is highly accurate.

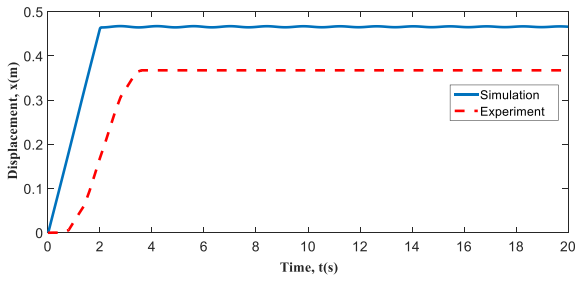

Fig. 15. Cart displacement for simulation and experiment with ZVDD shaper

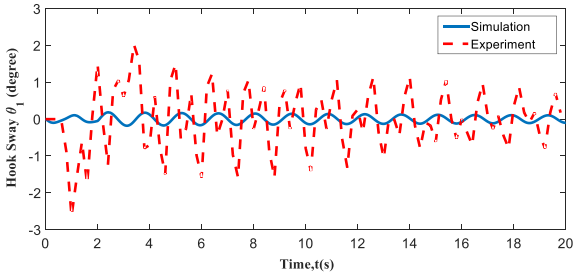

Fig. 16. Hook sway for simulation and experiment with ZVDD shaper

TABLE III. CART DISPLACEMENT AND HOOK SWAY WITH ZVDD SHAPER

	Maximum cart displacement, x(m)	**Maximum hook sway, θ_1(deg)**
Simulation	0.4568	1.7803
Experiment	0.3676	2.022

Fig. 17 shows the experimental results of cart displacement in open loop and ZVDD control system. It indicates that the maximum cart displacement had been reduced after the implementation of ZVDD. The time to reach the maximum cart displacement had been increased as well. This can due to the fact that input signal had been shaped, and some energy had been lost. This causes the maximum cart displacement is reduced. Fig. 18 shows that the hook sway had been reduced significant and the hook sway is approximate equal zero. The hook sway of the system had been eliminated. All the results are tabulated in TABLE IV.

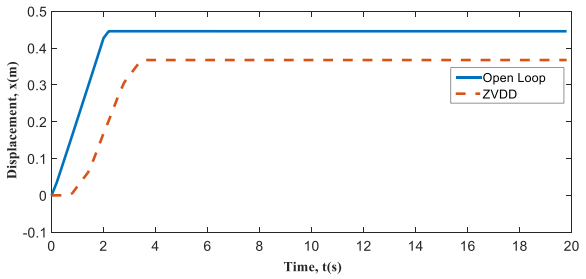

Fig. 17. Cart displacement in open loop system and ZVDD shaper system

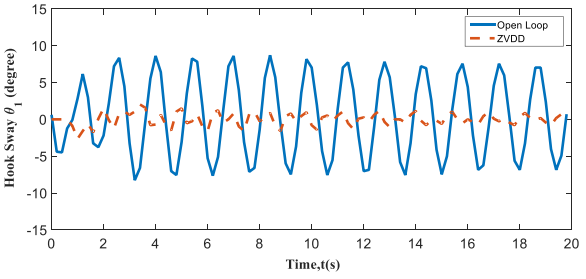

Fig. 18. Hook sway in open loop and ZVDD shaper system

TABLE IV. SYSTEM PERFORMANCE COMPARISON

	Maximum cart displacement, x (m)	**Maximum hook sway, θ_1 (deg)**
Open loop	0.4663	8.879
ZVDD	0.3676	2.022

V. CONCLUSION

As a conclusion, the dynamic model of the double-pendulum overhead crane system had been verified and it is highly accurate. The implementation of ZVDD as input shaper has successfully eliminate the hook and payload sway as well as the double-pendulum dynamics.

REFERENCE

[1] A. Karajgikar, J. Vaughan., W. Singhose, "Double-pendulum crane operator performance comparing PD-feedback control and input shaping," Eccomas Thematic Conference, Brussels, Belgium, 4-7 July 2011

[2] D. Qian, S. Tong., B. Yang, S. Lee, "Design of simultaneous input-shaping-based SI", Technical Sciences, 2015

[3] Guo Weiping, Liu Diantong, Yi Jianqiang and Zhao Dongbin, "Passivity-based-control for double-pendulum-type overhead cranes," 2004 IEEE Region 10 Conference TENCON 2004., 2004, pp. 546-549 Vol. 4

[4] M. Kenison, W. Singhose, "Input Shaper Design for Double-Pendulum Planar Gantry Cranes," Proceedings of the 1999 IEEE International Conference on Control Applications, Hawai'I, USA, August 22-27, 1999, pp.539-544

[5] J. Vaughan, E. Maleki and W. Singhose, "Advantages of using command shaping over feedback for crane control," Proceedings of the 2010 American Control Conference, Baltimore, MD, 2010, pp. 2308-2313.

[6] Zhang, M., et al., "Adaptive tracking control for double-pendulum overhead cranes subject to tracking error limitation, parametric uncertainties and external disturbances." Mechanical Systems and Signal Processing, 2016. 76–77: p. 15-32.

[7] J. Vaughan, D. Kim and W. Singhose, "Control of Tower Cranes With Double-Pendulum Payload Dynamics," in IEEE Transactions on Control Systems Technology, vol. 18, no. 6, pp.1345-1358, Nov.2010.

[8] Qian, D., S. Tong, and S. Lee, "Fuzzy-Logic-based control of payloads subjected to double-pendulum motion in overhead cranes." Automation in Construction, 2016. 65: p. 133-143.

[9] [9] Kim, D. and W. Singhose, "Performance studies of human operators driving double-pendulum bridge cranes." Control Engineering Practice, 2010. 18(6): p. 567-576.

[10] M. A. Ahmad, R. M. T. Raja Ismail, M. S. Ramli and N. Hambali, "Investigations of NCTF with input shaping for sway control of a double-pendulum-type overhead crane," 2010 2nd International Conference on Advanced Computer Control, Shenyang, 2010, pp. 456-461

[11] Huang, J., Z. Liang, and Q. Zang, "Dynamics and swing control of double-pendulum bridge cranes with distributed-mass beams." Mechanical Systems and Signal Processing, 2015. 54–55: p. 357-366.

[12] W. Singhose, D. Kim, and M. Kenison, "Input Shaping Control of Double-Pendulum Bridge Crane Oscillations." Journal of Dynamic Systems, Measurement, and Control, 2008. 130(3): p. 034504-034504.

[13] O'Connor, W. and Habibi, H., "Gantry crane control of a double-pendulum, distributed-mass load, using mechanical wave concepts", Mechanical Science, 4, 251-261, 2013.

[14] D. Kim and W. Singhose, "Reduction of Double-Pendulum Bridge Crane Oscillations", The 8th International Conference on Motion and Vibration Control (MOVIC 2006), KAIST, Daejeon, Korea, August 27 - 30, 2006, pp.300 -305

[15] W. E. Singhose and S. T. Towell, "Double-pendulum gantry crane dynamics and control," Proceedings of the 1998 IEEE International Conference on Control Applications (Cat. No.98CH36104), Trieste, 1998, pp. 1205-1209 vol.2.

[16] Kyung-Tae Hong, Chang-Do Huh, Keum-Shik Hong, "Command Shaping Control for Limiting The Transient Sway Angle of Crane System." International Journal of Control, Automation and Systems, Vol. 1, No.1 , March 2003, pp.43-52

[17] M. A. Ahmad, R. M. T. R. Ismail, M. S. Ramli, A. N. K. Nasir and N. Hambali, "Feed-forward Techniques for Sway Suppression in a Double-Pendulum-Type Overhead Crane," 2009 International Conference on Computer Technology and Development, Kota Kinabalu, 2009, pp. 173-178.

[18] M. A. Ahmad, R. M. T. Raja Ismail, M. S. Ramli and N. Hambali, "Comparative assessment of feed-forward schemes with NCTF for sway and trajectory control of a DPTOC," 2010 International Conference on Intelligent and Advanced Systems, Kuala Lumpur, Malaysia, 2010, pp. 1-6.

[19] M. Adeli, H. Zarabadipour, S. H. Zarabadi and M. A. Shoorehdeli, "Anti-swing control for a double-pendulum-type overhead crane via parallel distributed fuzzy LQR controller combined with genetic fuzzy rule set selection," 2011 IEEE International Conference on Control System, Computing and Engineering, Penang, 2011, pp. 306-311.

[20] E. Maleki, W. Singhose and S. Srinivasan, "Positioning and control of boom crane luffing with double-pendulum payloads," 2010 IEEE International Conference on Control Applications, Yokohama, 2010, pp. 1319-1324.

Smart Home Security System with Iot

Muhammad Nasrullah Bin Mustaffar
Faculty of Electrical Engineering
Universiti Teknologi Malaysia
Johor Bahru, Malaysia.
nasrullahmus94@yahoo.com

Norhaliza Abdul Wahab
Department of Control and Mechatronic Engineering
Universiti Teknologi Malaysia
Johor Bahru, Malaysia.
aliza@utm.my

***Abstract*—This paper presents a smart home security system that have been integrated with IoT applications to make the system easily access from anywhere as long as internet connection is there. Home security become more crucial in our lives as the possibilities of intrusion increase day by day. The method for this home security system are using magnetic contact door and IR as the sensor to detect any breaches and activate the system with locking the door using solenoid lock. Buzzer and the RGB led are used to alert the user and surrounding neighbors. Internet apps is used to activate the system and give alert if any door has been breaches. Hardware of this system are Arduino Mega 2560 and ESP 8266 as the microcontroller. Arduino IDE also used for the programming of this security system.**

Keywords—microcontroller, smart home, security, quality of edutainment

I. INTRODUCTION

Smart Home Security system can also be known as the intelligent security system which can help reduce the intrusion that had been increased every day. Nowadays, the security system is very important to protect our family and help reduce the crime rates. Different home use different automation security system as long as they can provide safety to the owner, efficient and convenient [1]. Some of the security system, they use security officers to guard the house, alarm to alert the user and the thief, monitoring system using CCTV and much more with the new production of electronic hardware and software. Home need to be monitored at all times from the theft as the rate of crime involving robbery and murder are increasing recently. So, home monitoring system should be improved and upgraded to be more efficient to reduce crime rate.

Various method can be integrated to improve the smart home security system than only security monitoring and the using of security officers to guard the house. Unfortunately, both these methods are less reliable, wasteful and not suitable as our era become more modern. All of the system need to work more effective by giving user advantage to monitor their home even not at their home. In other words, manual method is no longer reliable and need to change to the automated system that give the user to monitor the system. This automated system may help prevent human error and save more resources to help improve other system to make the home more modern and friendly to the user[2].

Automated security system provides extra layer of the security by using user authentication to avoid break-ins in the house and track the intruder movement. Sensor-based system such as IR sensor is used to detect any movement across the house. Alarm module is used to improve the system security of each home from the intruder.

In this project, the objectives are:

i. To develop the home security system with IoT applications built in the system.
ii. To design a system that can be easily maintenance and monitored.
iii. To develop efficient system by reducing the cost installation and maintenance.
iv. To expose this advance security system with IoT integrated in the system for the use to use in their daily life.

The scope of the project will make the security system portable and can be control by smartphones with internet. This system also can detect any intruder in the house and alert the user by alarm and notifications. Hardware of this system is using Arduino MEGA 2560 as the microcontroller of the system. The system will be used when user went hometown or not in the house.

II. LITERATURE REVIEW

In understanding the concept of the security system. This literature review will explain a few projects that are related with this project especially their methods and implementation.

A. The Internet of Things in Home Security System: An Overview

In this project, the home security system is integrated with IoT applications where any objects such as smartphones, Internet TVs, sensors and actuators are connected to the Internet where the devices are intelligently linked together enabling new forms of communication between things and people, and between things themselves [3]. Different devices and the hardware such as home security, sensors, appliances and system are now being connected to the internet so that it can be controlled remotely using the smartphones. Not only the devices

can be controlled but home security system also can be continuously monitored for maintaining the security of the house [4].

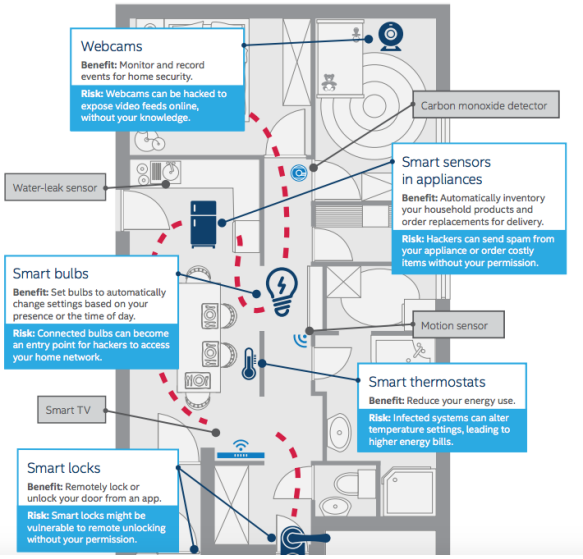

Figure 1: Smart Home Security with IoT.

One of the popular apps to control and monitor the devices in the home is Blynk apps. Another one is Tago.io. So as long as there is internet connection, user can control their devices such as sensor and also monitor their system remotely at the smartphones. This will help the security system become more efficient and user will always be updated and alert if anything happen to their home.

B. *Infrared (IR) sensors for detection*

The security system will use this infrared to detect mid-range obstacle and distance measurement for alert the user whereabouts of the intruder inside the house as in Figure 2.

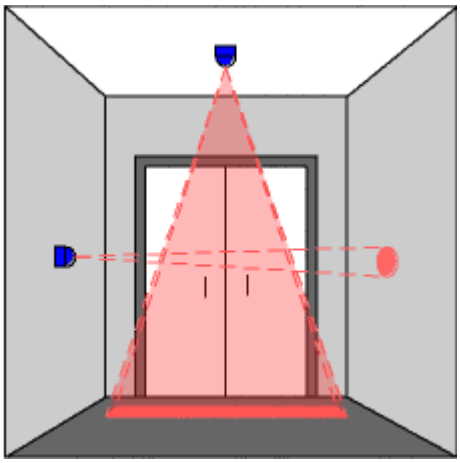

Figure 2: Infrared for intruder detection.

This infrared sensor uses transmitter and receiver to send the wave or transmission and from that, the intruder will be detected if the come into the wave range of the sensor. This infrared sensor works based on the detection of a specific light of wavelength in the range of 760nm (IR spectrum), which the wave been emitted from the IR Emitter Diode(LED). The distance will then be measured by the intensity of the received light. For this infrared sensor, color of the obstacle can also influences the measurement distance. Figure 3 will show the working principle of the infrared sensor[5].

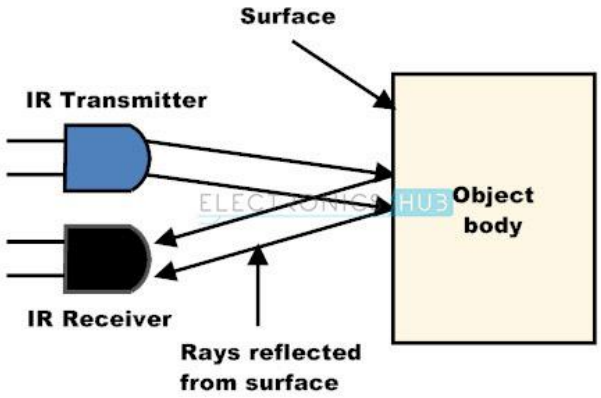

Figure 3: The working principle of Infrared Sensor

C. *Magnetic Contact Door*

This magnetic contact door will act as sensor to detect if the door or window has been opened and breached or not. This sensor also known as reed switch where the switch will be open when magnet moves away. Normally the circuit is closed because of the magnet pull the switch together. Figure 4 will show the diagram of the magnetic contact door.

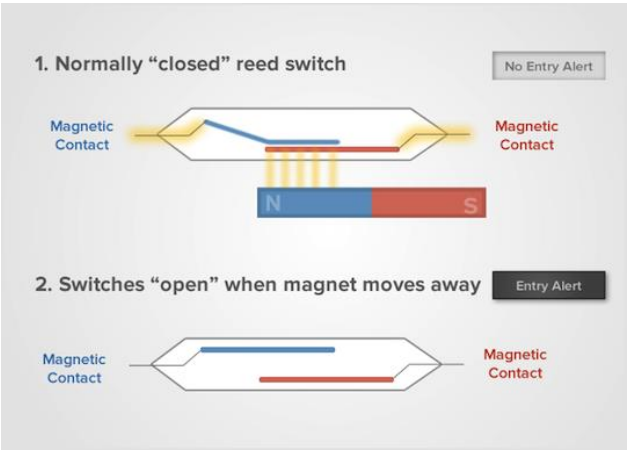

Figure 4: Magnetic Contact Door.

In addition, when the intruder open the window or door, the alarm will be on and the user will be alerted by smartphones. The system also will be on with the lock at the door. The system will not shut down even the door is closed back[6].

III. METHODOLOGY

This chapter, will show the methods and approaches that will be used to design and construct the smart home security system. The core parts of components to construct this project divided into three parts that are the mechanical hardware and electronic circuit, software development and integration of hardware with software. The Arduino microcontroller, DC 12V solenoid lock, ir sensor, magnetic contact door, alarm system and electronics circuit are classified on the hardware part. Besides, the software development will be used Arduino IDE to program the microcontroller. Lastly, the hardware and software need to be integrated which mean that the security system will work efficiently. Figure 5 shows general flowchart of the system.

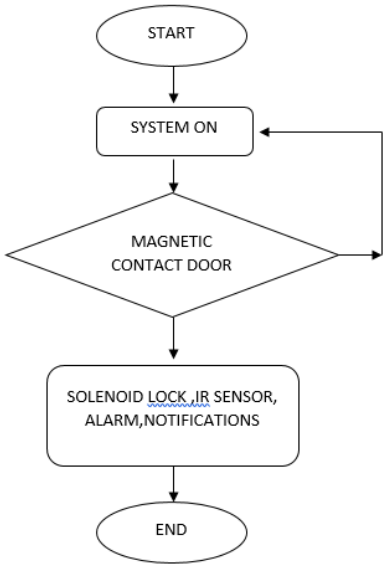

Figure 5: General Flowchart of The System.

A. *Research Design and Procedure*

The design of this project is being construct before making any step forward in building the system. It is to give some ideas on what will be the best and affordable system to all the user. It is very important to make the design of the project workflow to making it more efficient and properly.

Figure 6: Block Diagram

B. *Microcontroller*

For this security system, the microcontroller that been used are Arduino MEGA 2560 and ESP8266. This ESP8266 will be the medium to connect the Arduino with smartphone through internet. For the hardware such as infrared sensor, magnetic contact door, solenoid lock and alarm will be control by Arduino MEGA 2560. The Arduino will sent the data to the ESP8266 that then sent to the smartphones to alert the user or can be monitor by the user.

IV. RESULT AND DISCUSSION

In this section, result from the security system is shown in the truth table below. The system will only trigger if the user on using the smartphone. So the sensor will not be working if the user does not on the system. This will give advantage as only the user can access the system without being hack physically by intruder. The user can monitor the system using the application and use their own id as in programmed. The magnetic door contact will trigger the system to show that the home has been breach and will lock the home in a few second after that. This will on the solenoid lock and lock the house to trap the intruder inside it giving polices or officers to come to the house and arrest them. The alarm will be trigger and alert surrounding people too. So this system will make the intruder have no escape plan because they are trapped inside the house with no hostage.

SYSTEM	MAGNETIC DOOR CONTACT (FRONT)	MAGNETIC DOOR CONTACT (BACK)	ALARM	IR SENSOR(1)	IR SENSOR(2)	IR SENSOR(3)
ON	ON	OFF	ON	ON	ON	ON
ON	OFF	ON	ON	ON	ON	ON
ON	ON	ON	ON	ON	ON	ON
OFF	OFF	OFF	OFF	OFF	OFF	OFF

Figure 7 Truth Table of the Security System.

V. CONCLUSION

This smart home security system was very successful in the system meet all the requirement and can reduce the crime rate. It also meets the required capabilities and objectives as been targeted. The hardware and programming parts is achieving satisfaction level and for the future improvement it is recommended to have an PIR sensor to make sure the sensitivity and range more better and have built in camera to monitor inside the house. Thus, it will become more secure and efficient security system.

REFERENCES

[1] Cyril Jose, A. and Malekian, R. (2015) Smart Home Automation Security: A Literature Review. Smart Computing Re

[2] Bangali, J. and Shaligram, A. (2013) Design and Implementation of Security Systems for Smart Home Based on GSM Technology. International Journal of Smart Home, 7, 201-208. http://dx.doi.org/10.14257/ijsh.2013.7.6.19

[3] G. Kortuem, F. Kawsar, D. Fitton, and V. Sundramoorthy, "Smart objects as building blocks for the internet of things," *Internet Computing, IEEE,* vol. 14, pp. 44-51, 2010.

[4] C.-H. Chen, C.-C. Gao, and J.-J. Chen, "Intelligent Home Energy Conservation System Based On WSN," presented at the International Conference on Electrical, Electronics and Civil Engineering, Pattaya, 2011. Done

[5] M.R. Yaacob, N.S.N. Anwar, A.M. Kassim, 2012, ACEEE International Journal on Electrical and Power Engineering , Vol.3, No.2.Giaimo, C. (2017). Door Sensor Secrets: What They Are, How They Work & 6 Unexpected Uses. [online] SimpliSafe Blog.

Smart Walking Cane

Suhaizadiana binti Ismail
Faculty of Electrical Engineering
Universiti Teknologi Malaysia
Johor Bahru, Malaysia.
dianayana300@gmail.com

Sallehuddin bin Ibrahim
Department of Control and Mechatronic Engineering
Faculty of Electrical Engineering
Universiti Teknologi Malaysia
Johor Bahru, Malaysia.
sallehuddin@utm.my

Abstract*—Commonly, blind people who, having lack in visual perception due to physiological or neurological problem used a simple mechanical device which called blind stick to help them to live their daily life without fully rely on others. However, these blind sticks have several limitations where it can be improved. This paper proposes an improvement of traditional blind stick with three main parts which are obstacles sensor, water sensor and real time monitoring using Global Positioning System (GPS). In order to identify the presence of obstacles, two ultrasonic sensors are used mounted on the top and below the stick. The water sensor is used to detect the presence group of water before users step on it. Meanwhile, the real time monitoring system used to enable the guardian to monitor and know about the current location of blind people from far by receiving messages from GSM module about the latitude and longitude of the their current location.

Keywords— Obstacles sensor; Water sensor; Real time monitoring

I. INTRODUCTION

Blindness is the inability of people to distinguish darkness from bright light in either eye. There are various scales that have been developed to describe the extent of vision loss and define blindness. In the National Eye Survey Malaysia conducted in 1996, the prevalence of visual impairment in Malaysia was found to be 2.71%, which was higher in rural areas (2.87%) than in urban areas (2.54%). In 2010, the Welfare Department accounted that about 64,000 registered blind people and the estimated amount were 4 to 5 times higher [1]. In this world, we cannot deny that vision is one of the most important parts in our body. Without vision, we might undergo various problems including navigation in order to move from one place to another. Human without vision nowadays will fully depend on external existence around them which can be provided by human's arm, trained dog and white walking cane. As they cannot frequently depend on human's arm, they tend to use trained dogs in order to move [2]. Master will feel the attitude of his dog and analyse the situation and immediately give appropriate orders. But, not all can afford to have this trained dog because it is too costly.

Besides, there is white walking cane where it is a simple and light mechanical device which helps user to detect the static and dynamic object, holes as well as uneven surface [3]. Still, this white walking cane has several drawback where the training skills is needed for people who using it for the first time. In addition, the range of motion for them also limited as they still having difficulty to acquire the environmental information even with the help of the walking cane. In addition, this cane also does not protect user from obstacle near to head area.

Thus, by considering all the drawbacks, a smart walking cane is implemented to modify the existing walking cane in order to improve visually impairs people mobility. The walking cane will aided with obstacle detection, water detection for muddy areas and real time monitoring. The main objective of this project is to provide overall measures artificial vision and knee-above obstacle-detection which will help smooth movement from one location to another. In addition, this smart walking cane also will equip with real time monitoring via Global Positioning System (GPS). Nevertheless, the target of this project is also to develop a low cost, sturdy and robust walking cane.

II. METHODOLOGY

A. General construction

The walking stick is made up from PVC with handle where it is light in weight and simple. Fig. 1 shows the stick used in developing the smart walking cane. The estimated height of this stick is about 100 cm in length where it is suitable for average human height.

Fig. 1: Walking stick for blind

B. Project overview

This project involved both hardware and software. In hardware, there are six components are used such as arduino UNO, ultrasonic sensors, vibrator, buzzer, GPS and GSM module. The arduino UNO is used as microcontroller for overall system such as obstacles detection and real time monitoring. In order to sense the obstacles, ultrasonic sensors are used together with vibrator as indicator. Buzzer is used in water sensor and acts as an alarm that alert user when the present of water is detected. Next, GPS module is working together with GSM module in providing a real time monitoring for guardian. As for software part, it involved the coding and programming of arduino UNO for both obstacles detection and the real time monitoring.

The proposed system consists of three main units which are water sensor unit, obstacles detection unit and GPS tracker unit.

a. Water sensor unit

This unit is designed to avoid user from getting wet by alarm them with beeping sound from buzzer as indicator. This unit involved several components such as 220 kilo ohm resistor, 0.01 microfarad ceramic capacitor, 1 microfarad electrolyte capacitor, IC 555 and a buzzer. Fig. 2 show component that involved in water sensor unit:

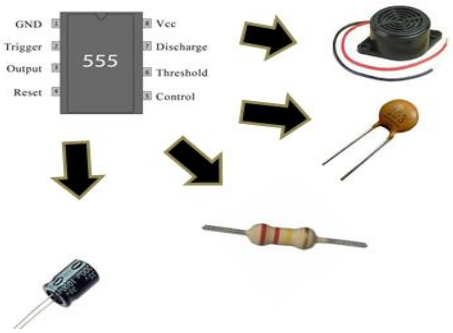

Fig. 2: Component involved in water sensor unit

b. Obstacles detection unit

This unit aims for enable the blind people to walk freely and smoothly without having worried of bumping into any kind of obstruction or obstacles present in their path.

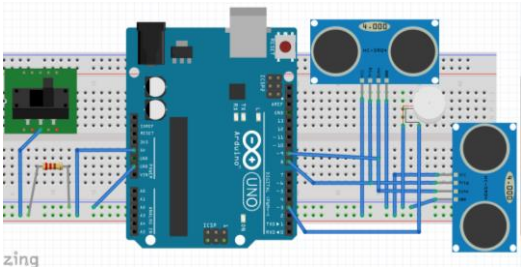

Fig. 3: Overall connection of obstacles detection unit

Fig. 3 shows the overall connection of obstacles detection unit. There are two HC-SR04 ultrasonic sensors with 4 pin which are VCC, GND, Echo and Trig which located both above and below knee to detect the obstacles. As shown is figure above, Echo and Trig pin for both ultrasonic sensors are connected to pin 9 and pin 8 of arduino UNO. This sensor uses sonar to determine the distance to an object. It is non-contact type sensor with high accuracy and stable reading. It can detect up to 400 centimetres range. This unit will alarm user by mini vibration motor where it producing vibration according to voltage supplied. This unit also equipped with slide switch. Users need to slide it to power up and power off when the stick not in used in order to save the power usage.is not in use.

c. Real time monitoring unit

This real time monitoring unit mainly designed for the blind guardian to monitor and know the current location of the blind people from far. The GPS module works together with GSM module and provide the latitude and longitude of current location through message.

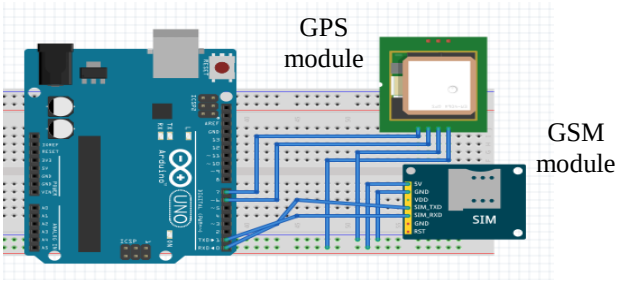

Fig. 4: Connection of real time monitoring unit

Fig. 4 shows the connection of real time monitoring system. The type GPS module used is SKM53 Skylab where it has 4 pins which are VSS, GND, TX and RX. While, type of GSM used is sim900a with 4 pins which are VCC, GND, 5VT which is TX and 5VR which is RX. Both modules are powered up by arduino UNO. TX and RX of GPS module are connected to pin 6 and 7 respectively while TX and RX of GSM module are connected to RX and TX of the arduino UNO.

This smart walking cane is not only focused on adult, but it is also can be used for children who having visual impaired since childhood. As for parents who having children with visual impairments, they must be worried about their child whereabouts whenever they are working. This real time monitoring will decrease the worries as they can know the exact location and monitor them even from far. Besides, this unit also can be used for blind people for them to know their current location from latitude and longitude receives from message. They can use blind short message service (sms) reader application to read the message.

III. RESULT AND DISCUSSION

A. *Water sensor*

The development of water sensor is for the blind people to avoid from stepping on the water. As the transmitter and receiver of sensor touched the water, the indicator used which is buzzer produce beeping sound to alert the users.

B. *Obstacles detection*

The two HC-SR04 ultrasonic sensors are used to detect the present of object around user. Once the sensors detect any object that might disturb or interrupt the smoothness movement of users the mini vibrating motor will vibrate.

As the ultrasonic sensors are use sonar to determine the distance of object, the trigger pin that connected to pin 8 of arduino UNO will send the ultrasound at 40 kilohertz. The ultrasound will bounced back as it hit the object and generate an echo. The distance can be determined by:

$$\text{Distance} = (\text{duration}/2)/29.1 \quad (1)$$

TABLE I: RESULT OF ACTUAL DISTANCE AND DETECTED DISTANCE (SENSOR 1)

	1	2	3	4	5	6	7	8	9	10	11
Actual Distance (cm)	0	5	10	15	20	25	30	35	40	45	50
Detected Distance (cm)	0	5	9	15	19	25	29	33	40	44	48

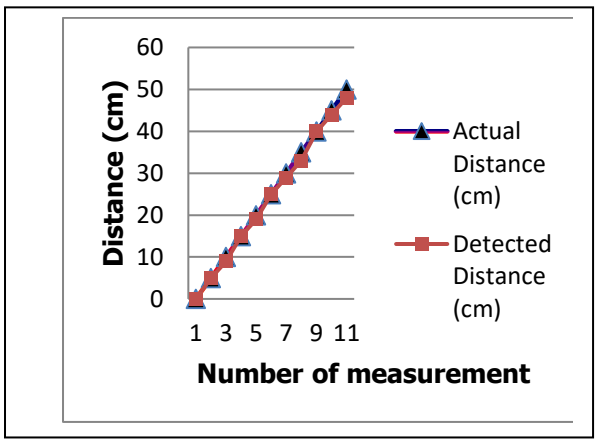

Fig. 5: Actual distance versus Detected distance (Sensor 1)

TABLE II: RESULT OF ACTUAL DISTANCE AND DETECTED DISTANCE (SENSOR 2)

	1	2	3	4	5	6	7	8	9	10	11
Actual Distance (cm)	0	5	10	15	20	25	30	35	40	45	50
Detected Distance (cm)	0	6	8	15	20	24	29	33	39	45	48

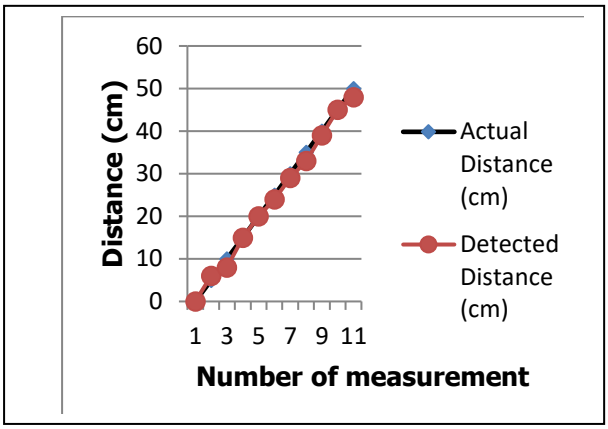

Fig. 6: Actual distance versus Detected distance (Sensor 2)

Table I and fig. 5 shows the differences between actual measurements and detected distance between the obstacles and ultrasonic sensor for above knee (sensor 1) while table II and fig. 6 for below knee (sensor 2). The average error for sensor 1 is 0.73 while for sensor 2 is 1.00. Hence, it can be said that the distance detected by the sensors are reliable.

C. *Real time monitoring*

When users move from one location to another, the GPS module will update the latitude and longitude of the current location and automatically sensing message to guardian and users phone number as shown in fig. 7. Guardian can check the location by entering the latitude and longitude received into Google Map or Google Earth as shown in fig. 8. Fig. 9 shows the blind short message service (sms) reader application where blind people can know about their current location from the latitude and longitude received from GSM module. This application will read message when users press the screen.

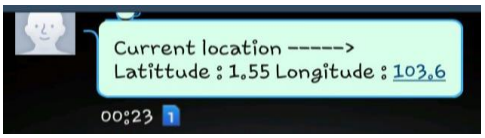

Fig 7: The latitude and longitude

Fig 8: User current location

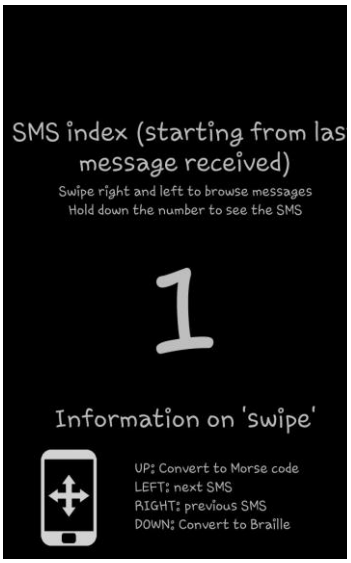

Fig 9: Blind short message service (sms) reader

IV. CONCLUSION

The main objective of this project is to develop an affordable knee-above obstacle-detection and warning system of smart walking cane, which will help smooth movement from one location to another. With the help of two ultrasonic sensors that mounted above and below the knee level and the GPS module, all of three objectives were successfully achieved. The ultrasonic sensors were able to detect obstacles accurately and the vibrator vibrates successfully as both ultrasonic sensors detected the obstacles. Next, the water sensor was worked successfully as the buzzer used produced buzz sound that alert user about the presence of the water. In addition, from the experimental results, the GSM module was accurately sending the latitude and longitude through message to the guardian as the GPS module successfully updating the information about current location. Users also can turn off the overall system as the device is not in use.

REFERENCES

[1] Zainal M, Masran L, Ropilah AR. Blindness and visual impairment amongst rural Malays in Kuala Selangor, Selangor. Med J Malaysia 1998;53:46–9.
[2] Liyana binti Ramli (2011). Development of An Electronic Walking Stick For The Visually Impaired With Z-Axis Detection, Bachelor Degree Universiti Teknologi Malaysia, Skudai.
[3] Shruit and Prof. A., 2011. Smart stick for Blind: Obstacle Detection, Artificial vision and Real-time assistance via GPS.
[4] Ivanov, R. Real-time GPS track simplification algorithm for outdoor navigation of visually impaired. Journal of Network and Computer Applications, 2012, Elsevier. 35(5): 1559–156.
[5] Anon, n.d. Electronic Walking Stick for the Blind, s.l.: s.n.
[6] Jayant Sakhardande, Pratik Pattanayak, and Mita Bhowmick, Smart Cane Assisted Mobility For The Visually Impaired. International Journal of Scientific & Engineering Research. Mumbai, India. April, 2013.
[7] Park, J., Je, Y., Lee, H. and Moon, W. Design of an ultrasonic sensor for measuring distance and detecting obstacles. Ultrasonics, 2010. 50(3): 340–346.
[8] Mannucci, A., Wilson, B., Yuan, D., Ho, C., Lindqwister, U. and Runge, T. A global mapping technique for GPS-derived ionospheric total electron content measurements. Radio science, 1998. 33(3): 565–582.
[9] Kasemsuppakorn, P. and Karimi, H. A. A pedestrian network construction algorithm based on multiple GPS traces. Transportation research part C: emerging technologies, 2013. 26: 285–300.
[10] Potamianos, G., Neti, C., Luettin, J. and Matthews, I. Audio-visual automatic speech recognition: An overview. Issues in visual and audio-visual speech processing, 2004. 22: 23.
[11] Hersh, M. and Johnson, M. A. Assistive technology for visually impaired andblind people. Springer. 2010.
[12] Tielsch, J. M., Javitt, J. C., Coleman, A., Katz, J. and Sommer, A. The prevalence of blindness and visual impairment among nursing home residents in Baltimore. New England Journal of Medicine, 1995. 332(18): 1205–1209
[13] Misra, P. and Enge, P. Global Positioning System: Signals, Measurements and Performance Second Edition. Massachusetts: Ganga-Jamuna Press. 2006.
[14] Prattico, F., Cera, C. and Petroni, F. A new hybrid infrared-ultrasonic electronic travel aids for blind people. Sensors and Actuators A: Physical, 2013. 201: 363–370
[15] Warren, J.-D., Adams, J. and Molle, H. Arduino for Robotics. Springer. 2011
[16] Batarseh, B. and McFadyen. An Ultrasonic Ranging System for the Blind Mississippi State University; 1997. 411-413.

Robot Gripper and Machine Vision for Electronic Component Pick and Place

Mohamad Nasrul bin Mohd Izazi
Faculty of Electrical Engineering
Universiti Teknologi Malaysia
Johor Bahru, Malaysia.
Email: mnasrul9@live.utm.my

Ir. Dr. Kumeresan A/l A.danapalasingam
Department of Control and Mechatronic Engineering
Faculty of Electrical Engineering
Universiti Teknologi Malaysia
Johor Bahru, Malaysia.
Email: kumeresan@utm.my

***Abstract*—The number of machine vision technology has rise in its application in the modern era. In robotics, machine vision increase the flexibility of the robot program by providing various information through images. This paper is directed in application of machine vision in automation technology which is electronic component pick and place system. In the project, machine vision system is used to detect the desired component and extract its 2-dimensional coordinates. A cropping technique and circular Hough transform method is utilized in this project for object detection.**

Keywords—machine vision; image processing; robot arm; object coordinates

I. INTRODUCTION

Machine vision or Image Processing is a fast-developed field and getting more attention in today's technologies. Many developers currently replacing physical sensors with machine vision systems. Moreover, industries are increasing its automation replacing human as machine vision increases the capabilities of robot in handling task.

Machines and robots are introduced in order to increase the production rates and reducing the needs of skillful human resources [1]. Thus, the robot needs to have higher level of skills from human at performing the task. Originally, robot is designed and programmed for static situations. They cannot adapt to a new situation which are not introduced in its program due to its limitation of robot's sense. The robot is confined in a working area with a small variance of interaction with its surrounding [2]. There should be no human interference within its working space as its operation could be deadly. In order to fulfil the industrial demand, these robots need to be designed to have the ability to cope with dynamic environment and could withstand extreme conditions. Thus, using machine vision which serves as additional feedbacks to the robots, expand the robot capabilities and having a more flexible program.

This paper described and explain a project that carried out to build an automatic electronic component pick and place system with the help of machine vision system. The application will be focused on the accuracy in position detection as well as correct orientation of product. Any error in these two elements will cause the electronic component to be mishandled. There are two objectives to be achieved in this project. The first objective is to design and develop a mechanical system for electronic component pick and place application. The second objective is to integrate a computer vision system to enhance the electronic component pick and place operation in a PCB assembly line.

In machine vision, various method and algorithm has been developed. Some are developed to detect a specific object such as openCV face detection library and others are made to be flexible, where the image of any object can be trained to act as reference for object detection. The method presented in [3] incorporates a good illumination technique into the system to enhance detection. Using 'dark field' lighting arrangement to increase the contrast between object and background and eradicate shadowing problems. In order to reduce the noise effect in the image, 5 frames of image are digitized and averaged together before going through further process. Then local thresholding operation and morphological edge detection algorithm are used to detect the object presented on the image. Any object that does not pass a set of determined criteria is then rejected. This method seems to be a reliable method for grouped and small object detection. Works done in [4] mentioned image distortion as one of the factors that contribute to errors in the obtained result. To tackle this problem, the author making use of MATLAB camera calibration functions to determine the intrinsic and extrinsic parameters of the camera. These parameters are then used to correct the distortion in the taken image. Thus, making detection more precise and accurate specially when dealing with pixel coordinates.

The effectiveness of the pick and place system not only depend in the accuracy of image processing but also depends on the developed robot arm. The angle produced in each joint of robot arm must be accurate to ensure that the end effecter positioned on the correct location. The basic theory to achieve a correct end factor positioning in robot arm movement is inverse kinematic. Inverse kinematic does not take account of dynamics and trajectories of robot making it easy to be implemented in the developed robot arm. Related works has been seen incorporates machine vision into robot arm joint angle control [5]. Specific robot arm joint is marked and recognized using color recognition algorithm. These joints are kept track throughout the operation using a dedicated set of mathematical equations.

In this project, the developed system will handle a designated capacitor, an electrolyte type with the diameter of 1cm. This

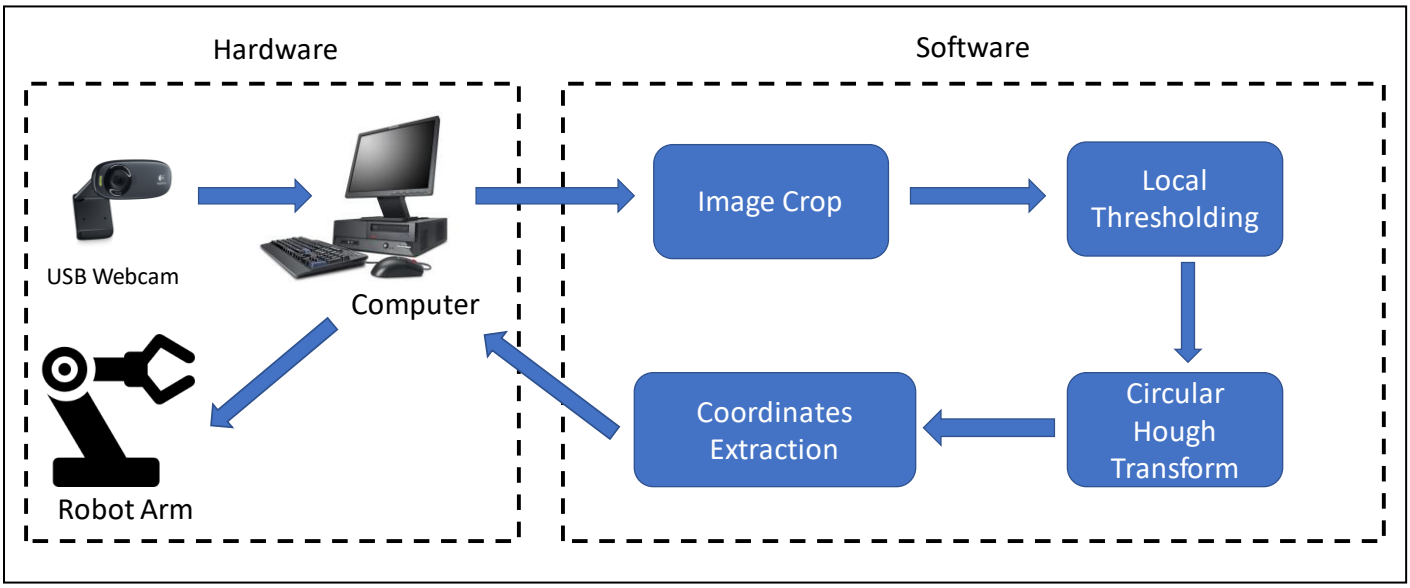

Figure 1. Block Diagram of the system's operation.

capacitor is originally located on the product feeder at the beginning of operation. The location doesn't have to be constant, it can be anywhere as long as it is within the camera visibility range. This is where machine vision takes place, detecting and extracting the coordinate information of the capacitor for further operation. The image of the capacitor is taken from a USB webcam camera. The image is processed using MATLAB software in a series of image processing algorithm such as image cropping, image thresholding and Hough transform. The pixel coordinates of the object are determined and then transformed into the world coordinates before transferred to robot arm controller through serial communication. The robot arm then picks the capacitor and place it at preprogrammed location. The system operation can be summarized in figure 1.

II. Machine Vision Program Flow

The objective of machine vision in this project is to locate the position of capacitor in the workspace. Thus, the camera is placed on top of the workspace capturing the plan view in term of x and y coordinates axis. Raw images are captured and going through a series of stages as described in figure 2

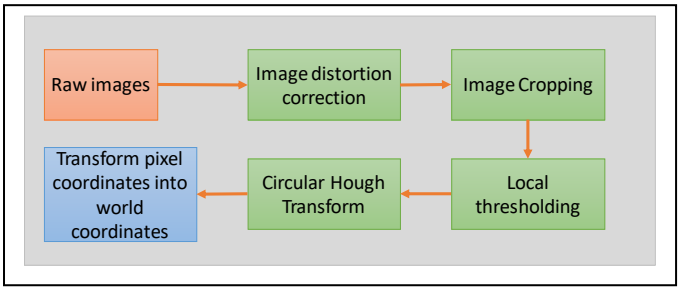

Fig2. Stages of image processing flow to locate object.

A. Camera Calibration

In context of three-dimensional(3D) machine vision, camera calibration is the process of determining the internal camera geometric and optical characteristic (intrinsic parameters) and/or the 3D position and orientation of the camera frame relative to a certain world coordinate (extrinsic parameter) [6]. Camera calibration is done in this work to remove error cause by lens distortion. In calibration process, 12 parameters identified that affect the camera output, 6 of which from inside components while the other 6 are relate to external. External elements include translation vector and rotation matrix of camera's origin relative to global coordinate while internal elements length of the focus, image center's position and lens distortion factors [4]. This calibration process is carried once.

B. Image Cropping

Image cropping is the process of selecting a range of pixel coordinates and discarding the rest. The purpose of image cropping in this project is to ensure that only the image of object within the pickup space are processed. This stage is also important to ensure that the conversion of object pixel coordinates into world coordinates is accurate and consistent.

Before cropping process begin, four parameters need to be determined which are the first point image pixel, the second point image pixel, the width and length of the box constructed by these two points. These parameters can be illustrated in figure 3. Using geometric transformation, the image pixel of the first point is stored as (0,0) pixel coordinates and the rest of the selected image pixel will follow accordingly while unselected pixel data will be erased. This produced a smaller image pixel size compared to the original image captured. Using the following equation, the image pixel is transformed into the world coordinates.

$$Yworld = k \times Ypixel \quad (1)$$

$$Xworld = l \times Xpixel \quad (2)$$

where

$$k = pickupspaceheight/pixelheight$$

$$l = pickupspacewidth/pixelwidth$$

These equations only determine the two-dimensional(2D) coordinates system of X and Y. The term height is referring to the Y coordinate axis while the term width is referring to the Z coordinate axis.

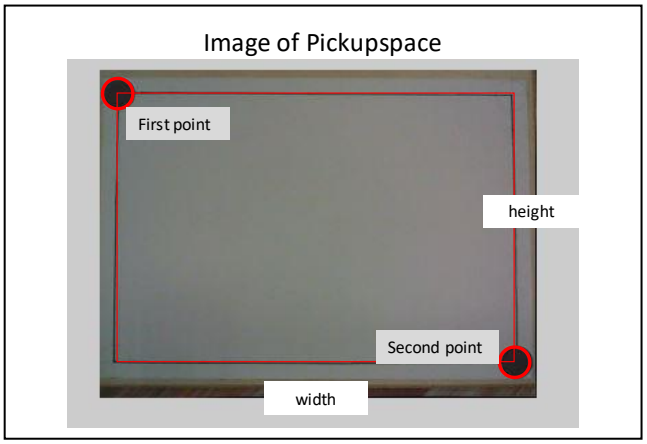

Fig3. The two points determining the height and width of product pickup space.

C. Circular Hough Transform

The Hough Transform (HT), according to [7] can be described as the integral of a function that represents the data points with respect to a kernel function that is define implicitly through the selection of a shape parameterization and parameter-space quantization. The purpose of Hough Transform is to find imperfect instances of objects within a certain class of shapes by a voting procedure.

Originally, Hough Transform is used to detect line in an image but later its application expands into detecting various shapes and its position. In this project, Hough Transform is used to detect circular image in the binary image. It also provide the pixel coordinates of the center of the circular image.

III. ROBOTARM MECHANISM

Robot arm is a type of programmable mechanical manipulator, with similar function to a human arm. The arm consists of multiple rotational actuator that act as joints to position its link to a certain angle that combine to produced desired end effecter positioning and trajectory. A typical robot arm usually designed to represent human arm which has three joints, the shoulder, elbow and the wrist.

A robot end effecter is a device through which a robot interact with the surrounding environment through method of grasping, lifting and manipulating the workpieces [8]. As robot gripper is less adaptable than human hands, the robot gripper should be designed specifically for a certain application. In the market, robot gripper can be categorized into two; Industrial use and Hobby or leisure use[9]. [7]. Industrial robot grippers are more complex in design where the functionality of the gripper must be high, mechanically robust and stable [10, 11]. On the other hand, robot grippers used by hobbyists are simple in design and mechanical movement. In this project, a gripper is built as the robot arm end effecter to lift the capacitor.

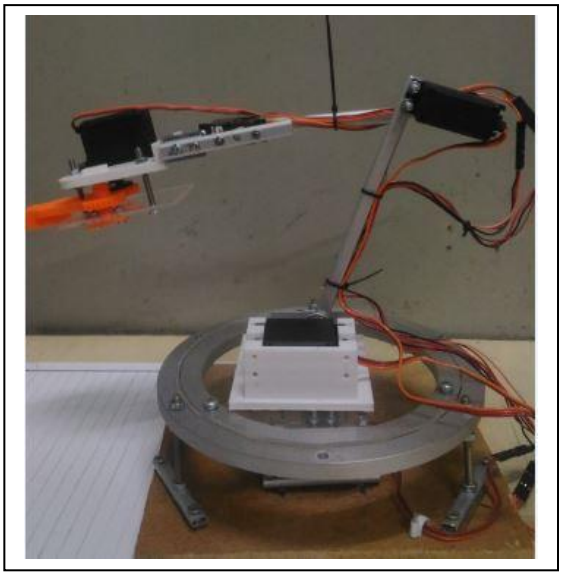

Fig4. Developed Robot Arm.

A. Inverse Kinematic

Inverse kinematic is a problem of determining the angle of robot joints based on the desired coordinates of end effecter. It is more difficult than the forward kinematic problem. To solve the inverse kinematic problem, there are several ways such as kinematic decoupling technique and geometrical method. To Consider the following figure:

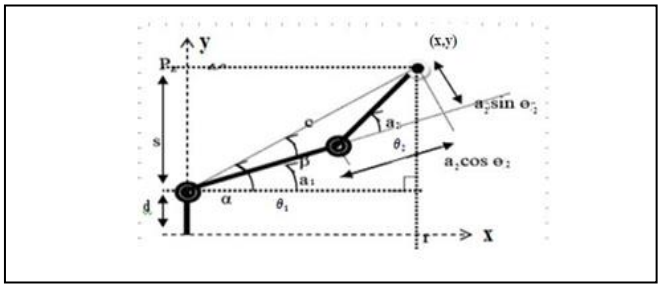

Fig5. Side view of two degree of freedom robot manipulator.

Figure5 is a robot manipulator with 2 degree of freedom in which there exist 2 angles to be determine. By using geometric approach, the following functions are derived:

$$\theta_2 = = atan(D, \pm\sqrt{1 - D^2}) \quad (3)$$

$$\theta_1 = a\ tan2(r, s) - a\tan 2\,(a_1, (a_2 \times D), a_2 \times (\pm\sqrt{1 - D^2} \quad (4)$$

Geometric approach requires an arctangent function in to evaluate the angle θ for -π ≤ θ ≤ π , in which returns $tan^{-1}(\frac{x}{y})$ adjusted to appropriate quadrant. The funtion atan2(x,y) is defined as follows:

$$\theta = a\tan 2(x,y) = \begin{cases} 0° \le \theta \le 90° \ for + x \ and + y \\ 90° \le \theta \le 180° \ for - x \ and + y \\ -180° \le \theta \le -90° \ for - x \ and - y \\ -90° \le \theta \le 0° \ for + x \ and - y \end{cases} \quad (5)$$

By using these formula, the joint angle θ_1 and θ_2 can be determine by subtituting the value of the end-affector point coordinates (x, y) into the equation.

B. Workspace of Robot Arm

The working environment in which the robot arm operates and interact is called workspace. The project workspace consists of a robot arm, product feeder, camera and a container for product placing. The layout of the workspace is illustrated in figure 5.

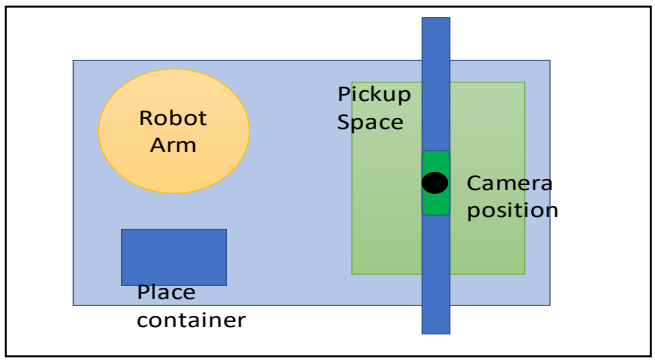

Fig5. Layout of the project workspace.

IV. Position Detection Accuracy Experiment

This experiment is a test to determine the accuracy of the developed machine vision program in detecting the object location on a two-dimensional space of x and y. A camera is installed 43cm above the pickup space. A pin is used as the object to be detect by the system. The image captured by the webcam can be seen in figure 3.

Again, the cropping technique is used in this experiment to increase the accuracy of the system in correlating the pixel space and the world space. Equation (1) and (2) are utilized in this experiment. The measured space height and width are 23.8cm and 35.1 cm respectively with measurement equipment sensitivity of 0.05cm. A set of ten test is carried out and the result is presented in table 1. Bear in mind that the measured position represents the center location of the pin measured using equipment while detected position represents location calculated by machine vision system. This experiment is carried out under fluorescent light with uniform intensity. The error generated by machine vision system is calculated using the following equation.

$$\text{Error} = \text{Measured Position} - \text{Detected position} \quad (6)$$

TABLE I. Result of The Experiment

Test No.	Measured Position (cm)		Detected position (cm)		Error, E (cm)	
	x	*y*	*x*	*y*	*x*	*y*
1	5.90	3.95	5.70	3.87	0.20	0.08
2	23.00	6.00	23.3	5.94	-0.30	0.06
3	13.60	9.00	13.60	9.08	0.00	-0.08
4	19.60	11.00	19.80	11.22	-0.2	-0.22
5	21.60	14.00	21.84	14.28	-0.24	-0.08
6	27.80	20.00	27.64	20.43	0.16	-0.43
7	33.00	22.00	33.51	22.47	-0.51	-0.47
8	5.95	17.5	5.67	17.56	0.28	-0.06
9	30.55	3.05	30.97	2.87	-0.42	0.18
10	1.35	13.00	1.02	13.30	0.33	-0.30

Mean error generated in x and y position for this experiment can be calculated as the following:

$$\bar{E} = \frac{1}{n}\sum_{i=1}^{n} |E| \quad (6)$$

Where $\bar{E}$ is the mean error and n is the number of test carried. The calculated mean error in X position is 0.0264cm while the calculated mean error in Y position is 0.196cm.

These errors can be caused by several factors. The first factor is the flaw in the image cropping technique used. This technique requires that the orientation of the workspace must be correct in which each line present must be parallel with the image frame. If there is any angular displaced between them, the cropped image will contain error in its width and height parameters. The second factor would be the error in camera orientation which are not parallel to the captured space. The other factors would be light disturbance, inaccurate camera calibration and inconsistency in measurement.

V. Conclusion

In conclusion, the desired pick and place electronic component system is successfully built. The develop machine vision program is reliable enough to provide information of the located object for pickup. The challenge lies in the kinematic of the robot arm. As the sensitivity of the joint angle is only 1 degree, the error in end effecter positioning increase as the object is further away from the robot arm center location.

References

[1] Ribeiro, A.F., Machine vision for industry. 1996.

[2] Heyer, C. Human-robot interaction and future industrial robotics applications. in 2010 IEEE/RSJ International Conference on Intelligent Robots and Systems. 2010.

[3] Jones, P., et al., Integration of image analysis and robotics into a fully automated colony picking and plate handling system. Nucleic Acids Research, 1992. 20(17): p. 4599-4606.

[4] Hosseininia, S.J., K. Khalili, and S.M. Emam, Flexible Automation in Porcelain Edge Polishing Using Machine Vision. Procedia Technology, 2016. 22: p. 562-569.

[5] Szabo, R. and A. Gontean, Robotic Arm Control Algorithm Based on Stereo Vision Using RoboRealm Vision. Advances in Electrical and Computer Engineering, 2015. 15(2): p. 65-74.

[6] Tsai, R., A versatile camera calibration technique for high-accuracy 3D machine vision metrology using off-the-shelf TV cameras and lenses. IEEE Journal on Robotics and Automation, 1987. 3(4): p. 323-344.

[7] Princen, J., J. Illingworth, and J. Kittler, A formal definition of the Hough transform: Properties and relationships. Journal of Mathematical Imaging and Vision, 1992. 1(2): p. 153-168.

[8] Osman, D.J.H.S., Brief Notes On Robotics. 4 ed. 2009, Univesiti Teknologi Malaysia: Fakulti Kejuruteraan Elektrik.

[9] Fuster, G., Gripper design and development for a modular robot. 2015.

[10] Bolboe, M. and I. Staretu. Antropomorphic gripper with two symmetrical fingers, designed for industrial robots. in Robotics in Alpe-Adria-Danube Region (RAAD), 2014 23rd International Conference on. 2014. IEEE.

[11] Honarpardaz, M., et al., Finger design automation for industrial robot grippers: A review. Robotics and Autonomous Systems, 2017. 87: p. 104-119.

Semi-Autonomous Direct Seeding Mobile Robot for Paddy Field

Muhamad Shafiq bin Ali, Johari Halim Shah Osman
Faculty of Electrical Engineering
Universiti Teknologi Malaysia
Johor Bahru, Johor
m.shafiqali94@gmail.com, johari@fke.utm.my

***Abstract*—Semi-Autonomous Direct Seeding Mobile Robot is used to perform seeding process in paddy field. This mobile robot was designed to replace the traditional method of seeding process. Then, this mobile robot can move automatically or can be controlled manually by using radio frequency remote control. In automatic mode, this mobile robot uses ultrasonic sensor to detect the obstacles. However, for manual mode, the microcontroller of the mobile robot communicates with the remote control by using radio frequency receiver and transmitter.**

Keywords—autonomous; seeding; mobile; robot; automatic; manual; microcontroller

I. INTRODUCTION

Nowadays many sectors used mobile robot to assist their works. In agriculture, mobile robots are used for many reasons. Farmers usually use mobile robot to replace human task suck as spraying, picking fruit, pruning and weeding. Basically, there are two ways to plant rice which are direct seeding method and planting method [1]. In direct seeding method, farmer will place the seeds directly onto the soil surface [2]. Based on Lembaga Kemajuan Pertanian Muda (MADA), this method increased rapidly in Muda area (Perlis and Kedah) since 1980. Planting method means planting with the use of paddy plants. Firstly, the seeds are placed on nursery area. After 9 to 16 days, pre-grown seedlings or paddy plants are moved to the crop area by using manpower or transplanter. In this project, direct seeding method has been chosen because this method has some advantages compare to planting method. Firstly, in direct seeding method, the plants are mature 7 to 10 days earlier compare to transplanted plants. Secondly, many farmers still prefer this method compare to planting method because of low cost and lack of labor. Then, plant by using transplanter only focused on wide areas of paddy fields.

II. LITERATURE REVIEW

Literature review is a research from existing or previous project. The purpose is to find information and idea on how to design this mobile robot. Hence, this chapter will give information about the previous mobile robot and it structure.

A. A Six-Wheeled Omnidirectional Autonomous Mobile Robot [3]

This is the first example of the existing mobile robot in industries. Six-Wheeled Omnidirectional Autonomous Mobile Robot is a mobile robot that built for unmanned ground vehicles application such as military, agriculture and civilian transportation. The advantage of this robot is it has "smart wheels" which mean each tyre can move independently. This mobile robot used GPS to control its path. Then, this mobile robot also has the ability to avoid the obstacles.

B. Tracked Robot for Search and Rescue in Nuclear Power Plant [4]

This mobile robot was built to do some special operations during a nuclear accident. Therefore, this mobile robot has different specialty compare to ordinary robot. This mobile was built to withstand some worst scenario such as hot temperature, high radiation and high pressure. The robot also has the ability to climb the stair because this robot used tracked tires system. Then, wireless remote control is used to control this mobile robot. After that, this mobile robot also attached with video monitoring system to capture the image during rescue operation.

C. Mobile Robot System for Marking Process in Liquefied Natural Gas (LNG) Cargo Tanks [5]

Every LNG cargo tanks should be insulated. However, the process to mark the positions of bolts and line for insulations panels will take time. So, a mobile robot with 3-wheel driving system was built. This robot has ability to climb up the vertical walls because it has magnet under its frame. Then, the robot used GPS 3D coordinates to navigate.

D. Autonomous Christmas Tree Weeder [6]

The autonomous Christmas tree weeder (ACW) is used to control grass and weeds between Christmas trees. This mobile robot is fully controlled by using computer. The man-machine interfaces of a standard ride-on lawn mower were removed and replaced with linear actuators. CPUrunning Simulink from Matlab was used to control the vehicle functions. Basically ACW used GPS for primary navigation because the trees are small and there is a clear view of the sky. However, one problem faced by ACW was to detect trees location before it

can start, so position of each tree was surveyed and geo referenced manually with a Real Time Kinematic (RTK) GPS.

E. Autonomous Robotic Vehicle for Greenhouse Spraying [7]

This mobile robot was design with a six wheeler differential steering base. The function of this robot is to carry spraying system such as sprayer tank, boom and pump. This robot is moving by using DC motors that connected to the wheels. Then, ultrasonic sensor is used to control the left and the right of the motor by giving the range information.

F. Tree-Climbing Robot for Invasive Insect Detection [8]

Tree-Climbing Robot for Invasive Insect Detection is a robot that built to carry a single camera for image processing. This robot has 4 or 6 legs to give this robot ability for climbing and walking. Three servos motor were attached on each leg of the robot. This robot also designed to rotate around the three to acquire images from multiple viewpoints.

G. Vision based Guidance Line Extraction for Autonomous Weed Control Robot in Paddy Field [9]

Autonomous Weed Control Robot mobile robot is used to remove weeds between rice rows. This process is important to increase crop yield. This robot is equipped with vision camera to extract image of rice rows. Then, this rice row is used as a guidance line. This robot also used a screw type of wheel instead of commonly used wheels for many reasons. The first one is to remove weeds automatically when this robot starts to move. The second reason is to increase the performance of this mobile robot so that this mobile do not do not stuck in the mud.

H. The Control System Design of Automatic Weeding Robot Based on Visual Navigation [10]

This robot used image processing to control the automatic navigation. The robot used crop rows as guidance. This robot will move along the row and remove the weeds by using stamping mechanism that place at the side of this robot. Then, this robot was equipped with continuous track instead of wheels. When changing to another row, this robot will turn easily and do not destruct the crops in paddy fields.

I. Paddy Weeding Robot [11]

This robot was design to adapt in the Korean paddy fields. The robot is used rotating weeper to remove the weeds. A motor is used to rotate the weeper. The weeper is designed to kill the weeds but at the same do not affect the rice.

III. SYSTEM DESIGN

Semi-Autonomous Direct Seeding Mobile Robot was designed to perform a seeding process in Malaysian paddy field. A system for seeding process was built on this mobile robot. This mobile robot has the special ability to move in the mud and it can carry heavy load on its back.

The process to build Semi-Autonomous Direct Seeding Mobile Robot can be divided into two parts which are mechanical part and electronic part.

A. Mechanical Part

This mobile robot was designed to perform seeding process in paddy field. Hence, the most important part on this mobile robot is the seeding mechanism. Firstly, four cylinders were placed under the seed containers. All of the cylinders were connected to a high torque 12V DC motor. When the cylinder is rotating, the holes on its surface will bring the seeds downward onto the soil.

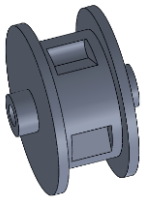

Figure 1: Design of the rotating cylinder

The body of this mobile robot was built by using aluminium L bar while the seed containers were built by using acrylic. Then, the front wheels were designed like in Figure 2 to make sure that this mobile robot does not get stuck in the mud. The wheels were connected directly to the 12V power window motors. Power window was used because it can produce high torque to drive this mobile robot.

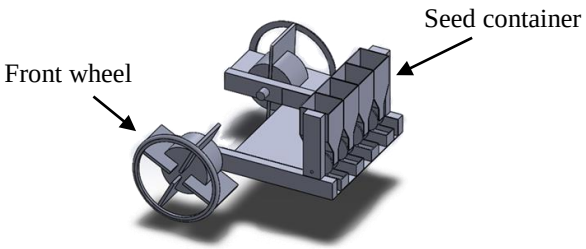

Figure 2: Design of Semi-Autonomous Direct Seeding Mobile Robot by using CAD

Figure 3: Semi-Autonomous Direct Seeding Mobile Robot

B. Electronic Part

In electronic part, a circuit connection was designed to connect the microcontroller to the sensor and actuators. The microcontroller used in this project is ATmega328P.

Basically, this mobile robot has two main modes which is manual mode; secondly is automatic mode. In manual mode, user can control this mobile robot manually by using radio

frequency remote control. A pair of 315MHz radio frequency receiver and transmitter were used to communicate between the remote control and the microcontroller.

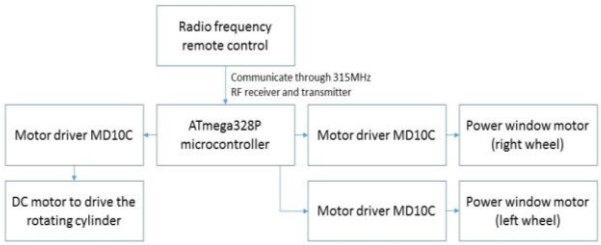

Figure 4: Block diagram of circuit connection for manual mode

Ultrasonic sensor was used in automatic mode. When the sensor detects the obstacle, it will send signal to the microcontroller.

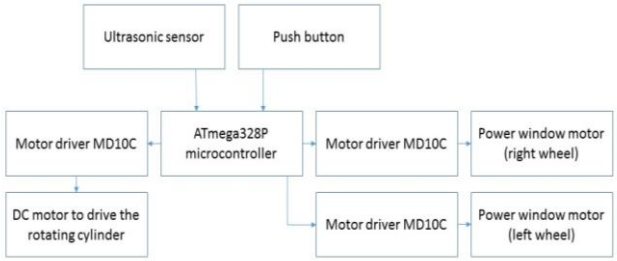

Figure 5: Block diagram of circuit connection for automatic mode

A push button that works as an additional sensor was placed at the front of the mobile robot to create a zig zag movement like in Figure 6. Table 1 shows the truth table for the mobile robot movement.

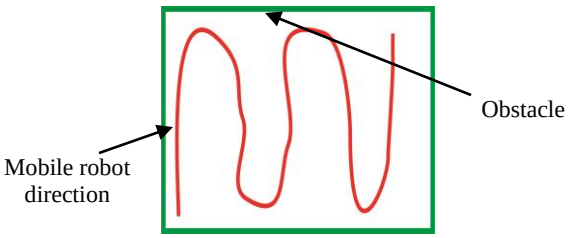

Figure 6: Zig zag movement of the mobile robot

TABLE 1
TRUTH TABLE FOR THE MOBILE ROBOT MOVEMENT

Condition		Mobile Robot Movement
Sensor	**Push Button**	
High	High	Turn right
High	Low	Turn left
Low	Don't care	Move forward

IV. EXPERIMENT

An experiment has been conducted to test the maximum load that this mobile robot can carry. This experiment is important to make sure that this mobile robot does not get stuck in the mud during the direct seeding process. Firstly, the Pulse Width Modulation (PWM) of the motor driver was set to maximum speed. Four different load were placed on the mobile robot. Then, the time taken for the mobile robot to travel in 5 meter was measured.

TABLE 2
MOBILE ROBOT CONDITION WITH DIFFERENT LOAD

Load (kg)	Time taken (s)	Mobile Robot Condition
10	3.11	Moving with high speed
20	3.30	Moving with medium speed
30	4.06	Moving with low speed
40	5.25	Mobile robot move very slow

From the experiment, this mobile robot can support the load up to the 40kg. However, the speed of this mobile robot reduced slightly when the load more than 30kg. Based on the experiment, the ideal load for the mobile robot is less than 20kg. This is because this mobile robot also need some power to drive it through a muddy surface.

V. RESULTS AND DISCUSSION

The main objective of this project is to design and build a prototype of direct seeding mobile robot. Figure 7 shows the flow chart of the complete operation for this mobile robot.

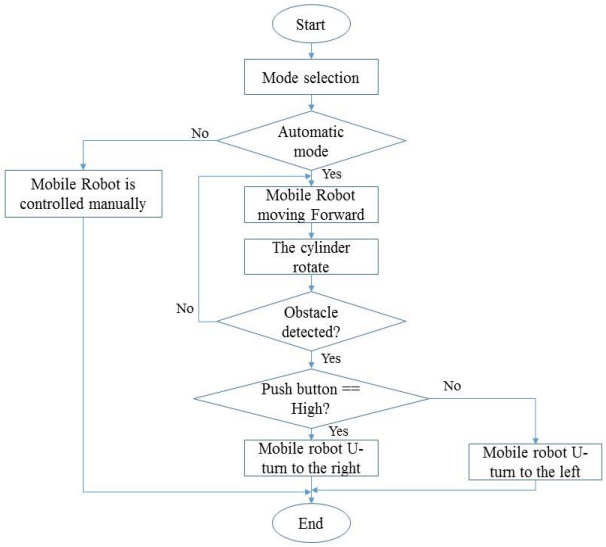

Figure 7: Flow chart for the mobile robot operation

A. *Mobile Robot Fuctionality*

After testing this mobile robot, all of the electronic components can run properly. In automatic mode, the mobile robot can detect the obstacle in front of it. While, in manual mode the mobile robot can successfully communicate with the radio frequency remote. However, there is a limitation in this mode which is the communication between the mobile robot and the remote control must be in range of 100-meter radius.

B. *Direct Seeding Mechanism*

By using traditional method, there is greater crop competition because rice plants are close to each other. In traditional method, farmers usually used their hand to spread the seeds. Hence, more seeds are required because there is

inconsistency during the seed's spreading process. Figure 8 show illustration of seeds distribution by using traditional method.

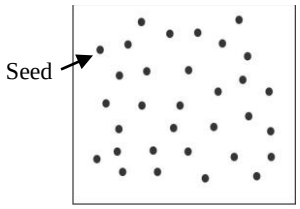

Figure 8: The illustration of seeds distribution in traditional method

To solve the problems in traditional method, the paddies are planted in rows. The seed container was designed to have some space between each other. When the mobile robot is moving, the cylinder that placed under the seed container will bring the seeds downward in a row.

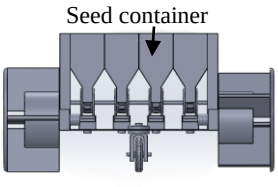

Figure 9: The seed containers were designed to have some space between each other

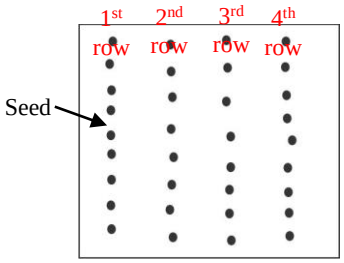

Figure 10: The illustration of seeds distribution by using Direct Seeding Mobile Robot

CONCLUSION

This paper proposed a solution on direct seeding process in paddy field. An automated direct seeding mechanism was designed to replace the traditional method. Then, the mobile robot also designed to adapt with Malaysian paddy field. For conclusion, the following objectives must be fulfilled to make this project success. The first objective of this project is to investigate and study about direct seeding methods in paddy field. After fulfilled the first objective, a prototype of an autonomous direct seeding mobile robot that uses Arduino Uno as microcontroller was developed. Then, the last objective is to design suitable mechanism for direct seeding method to implement on the mobile robot.

ACKNOWLEDGMENT

The author gratefully acknowledges the support from Faculty of Electrical Engineering, Universiti Teknologi Malaysia.

REFERENCES

[1] Akhgari, H. (2011). Assessment of Direct Seeded and Transplanting Methods of Rice Cultivars in the Northern Part of Iran. African Journal Of Agricultural Reseearch, 6(31).

[2] "Laman Web Rasmi Lembaga Kemajuan Pertanian Muda". Mada.gov.my. N.p., 2016. Web. 12 Dec. 2016.

[3] Flann, N., & Moore, K. (2000). A Six-wheeled Omnidirectional Autonomous Mobile Robot. IEEE Control Systems Magazine, 20(6), 53-66.

[4] Dong, P., Wang, X., Xing, H., Liu, Y., & Zhang, M. (2016). Design and Control of a Tracked Tobot for Search and Rescue in Nuclear Power Plant. 2016 International Conference on Advanced Robotics and Mechatronics (ICARM).

[5] Song, S., Choi, D., Hur, J., Lee, M., Park, Y. J., & Kim, J. (2009, August). Development and application of Mobile Robot system for Marking Process in LNGC cargo tanks. In ICCAS-SICE, 2009 (pp. 2636-2638). IEEE.

[6] Blackmore, S., Have, H., Shariff, R., & Noguchi, N. (2005). Mobile Robots for Tree Care. Frutic05: Information and Technologies for Sustainable Fruit and Vegetable Production, 12-16.

[7] Singh, S., Burks, T., & Lee, W. S. (2004). Autonomous robotic vehicle for greenhouse spraying. In 2004 ASAE Annual Meeting (p. 1). American Society of Agricultural and Biological Engineers

[8] Babu, B. P. W., Read, E. T., & Gennert, M. A. (2012). A Tree-Climbing Robot for Invasive Insect Detection.

[9] Choi, K. H., Han, S. K., Park, K. H., Kim, K. S., & Kim, S. (2015, December). Vision based guidance line extraction for autonomous weed control robot in paddy field. In 2015 IEEE International Conference on Robotics and Biomimetics (ROBIO) (pp. 831-836). IEEE.

[10] Qin, C., Du, Q., Tian, L., & Huang, X. (2012, December). The control system design of automatic weeding robot based on visual navigation. In Robotics and Biomimetics (ROBIO), 2012 IEEE International Conference on (pp. 956-961). IEEE.

[11] Yoon, B., & Kim, S. (2013, October). Design of paddy weeding robot. In Robotics (ISR), 2013 44th International Symposium on (pp. 1-2). IEEE.

Ammonia Detection System using Integrated Microfluidic-Microneedle

Khairul Akmal Muslimin
Faculty of Electrical Engineering
Universiti Teknologi Malaysia
Johor Bahru, Malaysia.
khalifahakmal94@gmail.com

Mohd Ridzuan Ahmad
Department of Control and Mechatronics (CMED)
Faculty of Electrical Engineering
Universiti Teknologi Malaysia
Johor Bahru, Malaysia.
ridzuan@fke.utm.my

***Abstract*—The purpose of this project is to develop a device that able to conserve the safe ammonia level in water reservoir. An Ammonia Detection System by using an Integrated Microfluidic-Microneedle enable to log data of ammonia level in time altogether to give prompt action as early detection system towards the ammonia contamination. This project describes the system in detail from conceptual idea to design an electrical approach to tackle this vital problem since the existing approach applied in industry is time consuming and manually operated. Since capacitance is differed by element and its concentration, hence a liquid capacitance detector is built to measure the capacitance of liquid. The device works by inserting the sample of liquid into the device to be tested. Then, the microcontroller (Arduino UNO) sources AC voltage to generate constant currents that flows through the liquid sample via a pair of electrodes. As a result the capacitance of the liquid can be measured and displayed on the LCD. These readings is then translated by comparing them with part per million (ppm) reading of several ammonia concentration in several water sample, thus a boundary can be made so that ammonia level in water is according to water quality standard. If the ammonia is above the allowable limit, a prompt message will be sent by application via cloud that is controlled by ESP8266 which can be accessed by monitoring devices. Every reading taken will be recorded in real time monitoring and all data will be logged for minimizing the probability of losing data.**

***Index Term*—Ammonia Detection System; Liquid Capacitance Detector; Data Logger; Real Monitoring; Cloud.**

I. INTRODUCTION

This project focuses on the water quality monitoring system, more specifically ammonia level monitoring. The crucial part of this project is to develop a system that monitor ammonia level in water source by using electrical and electrochemical approach [1].

Basically, this device monitor and detect the ammonia level that beyond its par so that early action can be taken when being prompted.

Thus, the development of this device could be divided into three parts; the first part is verifying the existing liquid capacitance detector to justify this electrical approach can relate to differences in ammonia level [2]. The second part is developing data logging system to record and log data taken by liquid capacitance detector in time. The third part would be the virtual monitoring via Cloud and push notification as early prompt action when ammonia level is beyond its safe par.

II. LITERATURE REVIEW

There are many methods or devices have been existed and used to detect the quality of water or contamination of water.

The most popular device to ammonia detection is Hach DR900 Colorimeter, one of a product from Hach Company. This colorimeter has been equipped by multiple sensor to measure the complex parameters that related to water quality monitoring, i.e. ammonium sallicate and aluminum sulphate [3]. DR900 Colorimeter is the high water quality sensing platform that give the precise and detailed part per million (ppm) data through detection of colour of water and its colour intensity. It is a need of using the appropriate reagent to get the matched parameter that desired. Applications of this device are suitable for detecting the complex molecules that is exist along the water treatment process. The water quality parameters that can be measured from this device are intensity of ammonia, aluminum, sulphur and carbon in water.

Another example is SmartTROLL Multiparameter Handheld System is allowed to collect data on water quality parameters based on Android or iOS mobile device. The parameters that can be sensed by using this system are pH, dissolved oxygen (DO), oxidation-reduction potential (ORP), water level and pressure, salinity, total dissolved solids, resistivity, density, air and water temperature and barometric pressure [4]. It is has features such as instant data-sharing, real-time data, site tagging with photos and GPS coordinates, field-replaceable sensor and auto-calibration functions.

There is one method that is practically used but somehow time consuming. Swimming Behavioural Spectrometer (SBS)

method is the method to detect the pollution of water through the behaviour of the protozoa in water called genus *Tetrahymena*. The pollution can be determined by comparing the movement of protozoa in control and the movement of protozoa in the sampling water that allow the digital camera along specialized software which stored over 50 behaviour of protozoan in 3D motion [5]. The problem of water will be indicated if any other movement which are not programmed.

There are very few device that focused on ammonia contamination, somehow most of them are using chemical approach. Instead, every devices have their own advantages and limitation. The biggest limitation that reduce effectiveness of water quality monitoring is time-consuming due to chemical reaction, use of effective reagent and others [6]. This review towards the existing ammonia detection system using understandable and not complex approach leads to the development of this project.

III. PROJECT METHODOLOGY

To develop the whole ammonia detection system using integrated microfluidic-microneedle, the basic thing need to concern is the system as real monitoring and early detection system. Therefore, the system has microcontroller that control the whole system, sensor to measure input parameter and flash disk or cloud for output data storage.

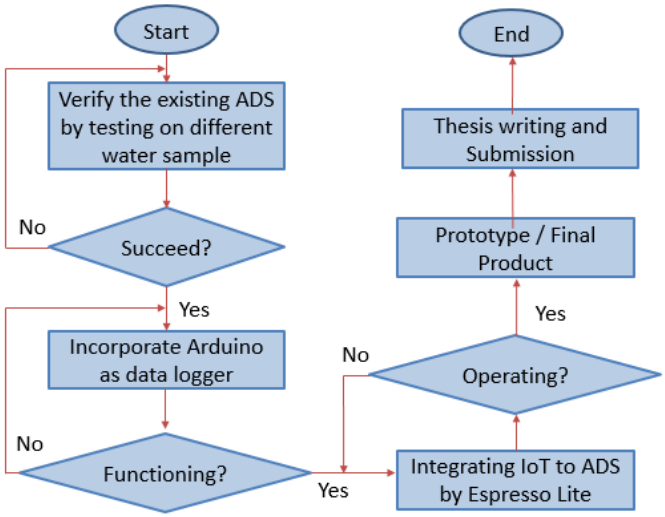

Fig. 1. Flowgraph of the project

A. Integrated Microfluidic- Microneedle

To develop an integrated of a microneedle with microfluidic, a suitable material and technique had been used. This integrated mechanism was called as microfluidic capacitance [7] and its function was acted as a sensor to sense the sample of various type of liquid.

To fabricate the microfluidic, Measure the mass of PDMS and curing agent at a w/w ratio of 10:1 which is for 10 grams of PDMS and 1 gram of curing agent, then mixed them. Spin the mixture until they are mixed well. The PDMS is then placed in a refrigerator to remove air bubbles. It takes approximately 2 hour to remove all the air bubbles. The PDMS poured onto the mold and left at room temperature for one days to cure. Cut the PDMS followed the size are needed [8][9].

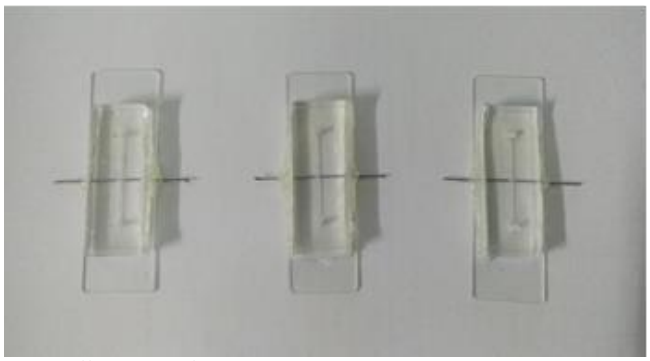

Fig. 2. Different size of microneedles integrated to PDMS-molded-microfluidic

To integrate PDMS, clean the PDMS and glass strip with a small amount of ethanol. Place the PDMS and glass strip in oxygen plasma machine with several setup; plasma pump down to 290.2A, gas stabilize to S:2 and A:4, plasma times to 25 seconds, plasma purge to S:20 and A:18. Bring out the PDMS and glass strip from the machine [10][11]. Attach them perfectly with microneedle for 5 minutes. Test an integration of microfluidic-microneedle with inserting liquid.

B. Liquid Capacitance Detector

Whenever the water sample pass through the gap made by microneedle, the liquid capacitance can be measured via the flow between a pair of electrodes inside [12]. The receiving data of capacitance measurement of sample had been modulated by electronic circuit module and Arduino Uno to monitor the result at LCD. After being calibrated, the device is freely to be used.

In ensuring the result can get perfectly and smoothly, shrink a deionizer water onto the device to clean up the channel of an integrated of microfluidic-microneedle. Blow the channel of an integrated of microfluidic-microneedle with air compressor to remove a deionizer water. Shrink the sample that will be measured and read the result on LCD. Record the results [13].

C. Data Logging System

Data logger is a feature added into the system to record and log data. Serial communication between Arduino UNO and real time clock (RTC) DS1305 altogether with memory card module [14]. RTC DS1305 is acts as real clock, while memory card module is a slot that enable memory card or flash card inserted to write and log the data in specific file [15].

RTC DS1305 need serial data input (SDA) and serial clock input (SCL) onto analog pin in Arduino, pin A4 and A5 respectively. Meanwhile, the serial peripheral interface (SPI) technique is used to Arduino microcontroller (master) to send

data to its peripheral, memory card module (slave) by SS, MOSI, MISO and SCK accordingly [16].

D. Real Monitoring Via Cloud

The existing system can be monitored virtually however giving the real time data. Serial UART pin 0 (RXD) and pin 1 (TXD) in Arduino microcontroller is connected serially to ESP8266 module to get full control of the system as long as connected to Internet [17].

Blynk Apps, an application that is used, acting as the global user interface (GUI) that enable user to monitor the system virtually [18]. It is as easy as drag and drop to have the system with interactive interface. The widget in this application in not only enable monitoring data by graph, moreover push notification can be set whenever interrupt is introduced. For this system, the interrupt will be the boundary is capacitance reading for the safe ammonia level. Whenever system is interrupted, the push notification will be sent to user showing that the ammonia level is beyond its level [19].

E. Circuit Implementation

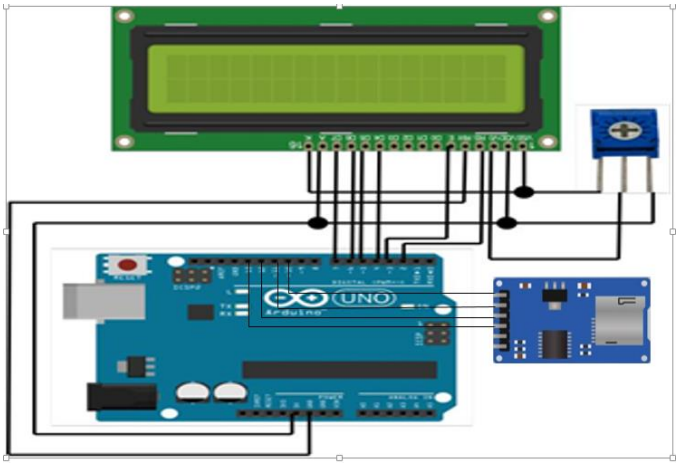

Fig. 3. Circuit diagram of the device

For the whole picture in this device as shown in Figure 3, the Arduino UNO is the microcontroller that process all the program. For analog input, pins A0 and A1 are connected to the integrated microfluidic-microneedle that act as sensor. The analog serial pins A4 and A5 are connected to RTC DS1307 that acts real time clock.

The Serial UART pins (pins 0 and 1) acts as serial write that send data translated earlier to ESP8266 module. The digital I/O pin 2 until pin 7 is connected to LCD to display the capacitance reading. The SPI pins (pin 10 until pin 13) are connected to memory card module as master-slave communication.

All the modules including LCD, RTC DS1307, ESP8266 module and memory card module are operating by connecting them to the same node of supplied voltage (Vcc) and ground (GND). To make them portable, external power supply (9V battery) is connected to input voltage pin and ground pin in Arduino UNO [20].

IV. RESULT AND ANALYSIS

A. Ammonia Level in Water and Capacitance Relationship

An experiment was conducted to find the relationship between these ppm and capacitance parameter. As the result, a capacitance reading can be obtained as the boundary limit to ensure the safe ammonia level in water source by relating to its ppm reading.

Different volume of ammonia solution is diluted into fixed amount of 400mL of different water sample – deionized water, tap water and raw water, in order to obtain their capacitance and ppm reading, hence those parameter reading will show their relationship.

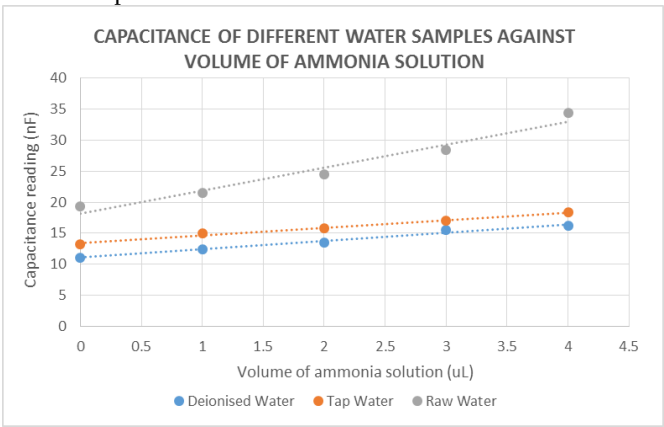

Fig. 4. Capacitance reading towards different concentration of ammonia solution in various water samples. Blue, red and green lines represent capacitance reading of deionized water, tap water and raw water respectively, passing through integrated microfluidic-microneedle.

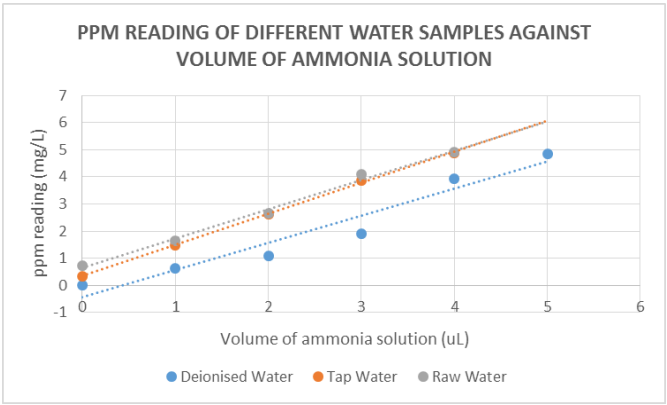

Fig. 5. Part per million (ppm) reading towards different concentration of ammonia solution in various water samples. Blue, red and green lines represent ppm reading of deionized water, tap water and raw water respectively, passing through integrated microfluidic-microneedle

From the Figure 4 and Figure 5, capacitance and ppm reading are directly proportional to concentration of ammonia solution in all water sample and consequence increase raw

water followed by tap water and then deionized water. Those readings have a significant relationship is caused by the particle content in the water sample that increase due to ammonia concentration and water purity.

Parameter	Singkatan	Unit	Air Mentah	Air Bersih/ Terawat
Total Coliform	TC	mg/L	5000	0
E-Coli	E-Coli	mg/L	5000	0
Ammonia	NH3-N	mg/L	<1.5	<1.5
Chemical Oxygen Demand	COD	mg/L	10	0
Biological Oxygen Demand	BOD	mg/L	6	0
Kekeruhan	NTU	NTU	<1000	<5000

Fig. 6. Various parameter limit in water quality standard. Ammonia ppm reading must less than 1.5 L, so it is safe to be consumed [21].

To verify their relationship further, a parameter for water quality standard is taken as the boundary limit as shown in Figure 6.

For an example, since the ammonia level must be less than ppm reading of 1.5 mg/L, it will give the sign that volume of ammonia solution that is safe to be in treated water is 1.0uL. Thus, the capacitance of 15.00nF must be set as boundary limit so that the water is safe to be consumed

B. Data Logging System and Real Time Data

As the capacitance reading displayed by LCD is temporary and continuously overwritten, data logger is a solution to minimize the data from lost. The RTC DS1307 is the real time clock that oscillated by crystal oscillator connected. As the result, every oscillation will read the current data to be written by sentence.

Every sentence of data will be logged in flash disk. The data can be extracted from flash disk that slotted in the memory card slot as .TXT file and then ready to further analyzed into form of file, such as .CSV file for the better analysis.

C. Real Time Monitoring via Cloud

Every output data obtained will be displayed by Blynk Apps. The widget in this application in not only enable monitoring data by graph, moreover push notification can be set whenever interrupt is introduced. Whenever output data obtained by the system is sent to Blynk cloud, the data is sent to the project that have the unique ID. The graph widget will show the current reading recorded in field but is just displayed through mobile phone screen as shown in Figure 7.

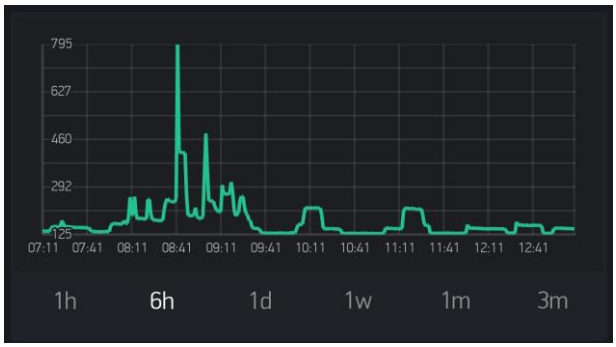

Fig. 7. Graph widget shown by Blynk Apps

For this project, the interrupt will be the boundary is capacitance reading for the safe ammonia level. Whenever system is interrupted, the push notification will be sent to user showing that the ammonia level is beyond its level. It is indicated by push notification widget in this application.

V. CONCLUSION

At the end of this project, the ammonia detection system using integrated microfluidic-microneedle is verified as a way of electrical approach toward ammonia contamination. Even though this device is applying the fundamental knowledge of monitoring system, it able to demonstrate the use of channeling data and early detection system well.

However, there are limitation of this device to be furthered. Firstly, calculation made by Arduino program is bundled, not as smooth as multimeter reading. Secondly, dielectric constant of samples had been used may be different from the literature review. Thirdly, others parameter such as pH, conductivity, and level of oxidation did not be counted in this experiment.

REFERENCES

[1] "Basic Circuit Analysis," *Electric Power Systems*, pp. 30–48, Jun. 2006.

[2] M. A. Misrun, "Liquid Detection System using Integrated Microneedle-Microfluidic," thesis, 2016..

[3] Hach, "*DR900 Handheld Colorimeter : Technical Guide,"* H. S. Inc., ed. USA, 2013

[4] Libelium, "*Smart Water : Technical Guide*," L. C. D. S.L, Ed., ed. Spain, 2016

[5] J. Firooz, "*SMARTROLL™ MP Handheld Instrument*," I.-S. Inc., Ed., ed. USA, 2013

[6] S. Ng, "*Monitoring and Detection Methods of Water Pollution*.," in *Environmental Biotechnology Monitoring & Detecting water pollution*, ed, 2012

[7] S. D. Minteer, *Microfluidic techniques: reviews and protocols*. Totowa, NJ: Humana Press, 2006..

[8] B. Wang, J. H. Horton, and R. D. Oleschuk, "Sulfonated-polydimethylsiloxane (PDMS) microdevices with enhanced electroosmotic pumping and stability," *Canadian Journal of Chemistry*, vol. 84, no. 4, pp. 720–729, 2006..

[9] "Microfluidic Interface Provides PDMS Chip Connection," *Product News Network*, 28-Jun-2012..

[10] P. L. Matheson, "Modeling of a poloidally symmetric toroidal field divertor in a reversed-field-pinch plasma machine," thesis, 1989.

[11] D. Amouroux, "Spéciation biogéochimique des éléments traces aux interfaces des environnements aquatiques," thesis, 2006.

[12] A. Trautmann, *Advanced microneedle and microelectrode arrays*. Tönning: Der Andere Verl., 2006..

[13] J. A. Roig, *8051: real time clock*. 2002..

[14] M. A. Mazidi, S. Naimi, and S. Naimi, *The AVR microcontroller and embedded systems: using Assembly and C*. Boston: Prentice Hall, 2011.

[15] M. Evans, J. Noble, and J. Hochenbaum, *Arduino in action*. SHelter Island, N.Y: Manning, 2013.

[16] C. Doukas, *Arduino, Sensors, and the Cloud*. Sted: APress, 2012..

[17] C. Webb, *Interrupt-: critical making for contemporary conditions*. 2015..

[18] *LCD: liquid crystal display, 1995*. Tokyo: Optrex Corp., 1995.

[19] T. O'Neill and J. Williams, *Arduino*. Ann Arbor, MI: Cherry Lake Publishing, 2014.

[20] M. Schmidt, *Arduino: a quick-start guide*. Dallas, TX: Pragmatic Bookshelf, 2015..

[21] Ministry of Health Malaysia: *10th Malaysia plan (2011-2015)*. Kuala Lumpur: Ministry of Health. 2011.

Listening Device for Locating Underground Water Leakage in Residential Area

Muhammad Anugerah Affendi Bin Saliman
Faculty of Electrical Engineering
Universiti Teknologi Malaysia
Johor Bahru, Malaysia.
anugerahaffendi@ymail.com

Abdul Rashid Bin Husain
Department of Control and Mechatronic
Faculty of Electrical Engineering
Universiti Teknologi Malaysia
Johor Bahru, Malaysia.
rashid@fke.utm.my

***Abstract*— Leakage in water distribution system especially at residential area is one of the big issues that continuously happened in worldwide and cause too many losses to the water companies and also their customers. Regarding to this issue, there are too many researches related to the methods developed for controlling the water leakage either detection on the hotspot of the leakage or detection from the comparison data of water level current consume and future. The purpose of this project is to trace the underground water leakage by using the vibration detector device in acoustic method. Generally, water leakage will produce some noise of vibration and the wave will propagate along the soil. The data acquisition is performed by conducting one experiment which is the pipeline was designed by using two sizes of UPVC pipes, 20mm and 25mm diameter with some broken part to represent as a leakage. In order to check the ability of the device sensor, the experiment was repeated with buried the pipeline in different depth between 0.1 to 0.4m and finally the data will be compared. The data were displayed via the IOT system to easier the user used the device. The results have shown that the depth and size of pipeline influence the detection of leaks. The device is more accurate and only suitable for small pipeline with high pressure of water flow. Conclusions, the device made is really function to detect the water leakage but still need improvement to make it function well and better.**

Keywords*— *water leakage; pipeline; vibrations; piezoelectric; IOT system

I. INTRODUCTION

Water leak management is a big issue and growing concern around the world and cannot be solved until now, also give a trouble and impact especially to the user. Almost every piping system around the world have a water loss problem and the most common reason is leakage in water distribution systems such as at the valve, service connection, transmission pipes and mostly in distribution pipes [1]. Every second of leakage will make losses for certain industrial such as water supply industry that has to supply purified water at high cost to the consumer if many water leaks occur in their piping system. The estimation of water loss in Asia, is about 29 billion cubic per meter and its equal to $9 billion per year (Asian Development Bank) [2]. However, it has not just affected to economic issues presented by water companies, but it is also an ecological, sustainability, risk on health due to unclean water and safety issues [3].

There are several factors that cause the buried pipe leak and technically include horribly pipe connections, poor quality of workmanship, corrosion inside and outside pipe or mechanical damage caused by pressure from the traffic [3]. Besides that, disaster occurred on the piping system also give an impact to the pipes such as ground movement, flood, landslides, and others. Other factors are high water pressure in the pipe, damage due to excavation in construction activity, pipe age, and ground conditions [3]. In many countries, usually type of pipe use is cast iron or asbestos cement and mainly ductile iron, polyethylene (PE) in older water distribution, while for newer system, they are using polyvinyl chloride (PVC) especially in secondary networks and connection from the treatment plant to the consumer [6].

In order to avoid water loss through bursts and leaks in water distribution systems, new and more efficient methodologies are required and detections of water leaks can be improved if leaks can be detected early and effectively [7]. However, the current solution nowadays in industries always has limitations with several factors. According to the past review paper from R. Ben-Mansour, 2012, the effectiveness underground leak detection depends on the experiences of operator conduct the devices, place or ground condition and time operation used [4] [5] [8]. This paper will emphasize the relationships between the vibration effect of a pipe leak at the ground surface and their wave propagation. The technique will be focusing on an acoustic method which is using vibration sensor (piezoelectric).

II. LITERATURE REVIEW

A. Non Acoustic Methods for Water Leak Detection Methods

1) Ground Penetrating Radar: Ground penetrating radar, GPR is a technique which uses high resolution geophysical process based on changing in the electromagnetic pulses in the microwave range [9]. These methods have been claimed and explored through several numbers of studies, specifically for detecting the plastic pipe leakage [10] [11] [12] [13]. Principally, the system worked using electromagnetic waves radiate from the transmitting antenna. Buried object or boundaries cause part of the way to bounce back to the receiver. The time lag from the signal transmitted and receive signal from the antenna can be used to determine the deepness, character

and properties of detection material. From the project test result made in literatures before, GPR antenna with low frequency can detect the large object and large debts while high frequency antenna detect small object and small debts. GPR also able to find hidden metallic and non-metallic structures without varying the environment, but with GPR investigations there are limitations depending on the unrestrained and restrained groups of factors, and ground condition, for examples, soil penetration depends on soil type and antenna type [14].

2) Thermography: The principle use of thermography (IR) is detecting the thermal contrasts in soil due to water leaks by using the camera and images [15]. There are several detection methods in thermography process either with physical handheld or sometimes with vehicles and also can attach infrared cameras on a plane. Factors that affect thermal contrast is heat balance of pavement surface and heat of moisture transfer in soil. In addition, several advantages when use thermography, it can use both in a day or night, also faster than others and highly effective for large areas. By the way, from the experiment conducted in literature, the IR camera cannot operate in summer and winter due to the temperature effect [16].

3) Tracer Gas Technique: For tracer gas technique, water leak can detect only by using gas sensor. In the operation process, some non-toxic or any substance that can produce gas such as helium or hydrogen was used. Firstly, the substance is injected into the water pipe. Gas is produced from the reaction of substance and water flow along the pipe to find a leak. The gas escapes at a leak opening and absorb to the pavement. With highly sensitive gas detector use, the leak will be traced.

B. Acoustic Methods for Water Leak Detection Methods

1) Listening Device: Listening device can be found in electrical and mechanical depends on their features. Listening method is also called as locate or pinpoint method [1]. In practice, more user chooses the electrical listening device due to the sensitive sensing element and also it has noise filter and amplifier to control the output. Mostly, they use very high sensitivity mechanisms or ground sensor such as geophone, aqua phones, and listening rods that can detect vibration and sound of water leak. The sensitivity of a piezoelectric sensor (accelerometer) above 1 v/g is the common use and for the geophone is 1mv/pa. The filter was used to make sure only the actual signal of water leak can be detected by the ground sensor. Listening device is commonly used to detect large leaks, especially for the metal pipe system. It is not very suitable for the non-metal pipe unless the high pressure of water in the pipe makes a loud sound and vibration same with the metal pipe. For the survey operation, mostly operator puts the sensor only at convenient fittings, such as valves and fire hydrant. Another way, ground microphones are used to pinpoint leaks in small interval at the location target by listening sound or vibration signal at the ground surface straightly above pipes [20]. However, the effectiveness of this method depends on the surrounding conditions, especially from ambient noise such as traffic and wind, the size of leaks, and the type of pipe. This method is very easy to conduct and straightforward, but the process will take a long time depends on the experiences of the user [17].

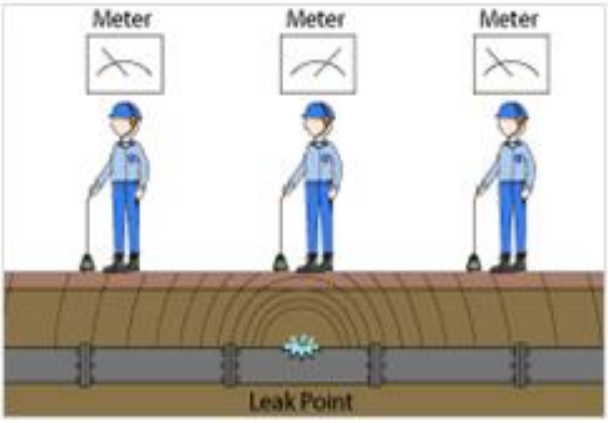

Fig. 1. Acoustic method for water leakage detection [21].

2) Leak noise correlators: These are portable microprocessor-based devices that pinpoint leaks automatically based on the cross-correlation method [18]. A noise correlation works by attaching hydrophone or two vibration sensors normally accelerometer at two points suspected leak and usually at fire hydrant or any point same pipe. This method uses wireless radio transmitter to sense the vibration or the sound frequency signal. By using the simple calculation and also from the relationship between time delays, the propagation of signals, and velocity of signals, the distance of leak from the sensor can be traced [18] [20]. Usually, the engineer will refer to the map or architecture drawing for piping system in that place after they get the actual distance from the sensor point. This is the most technique used to detect leakage, but it only gives a satisfactory results only with metal pipes. For the plastic pipes, this technique can be problematic because of the acoustic signals are generally very low frequency and narrow band. Nevertheless, high energy interferers, the presence of surrounding noise, and signal scattering also will reduce the effectiveness of this method [19].

III. METHODOLOGY

A. Design Flowchart

The Fig. 2 shows the flow of the project starting from the literature review of the previous project, selection of sensor from various type of sensor, selections of amplifier circuit that give high output gain, Wi-Fi and hardware design. After all the assembly part done, testing process was took place. The output result from the testing process is very important to prove that the device is really function or not to detect underground water leakage.

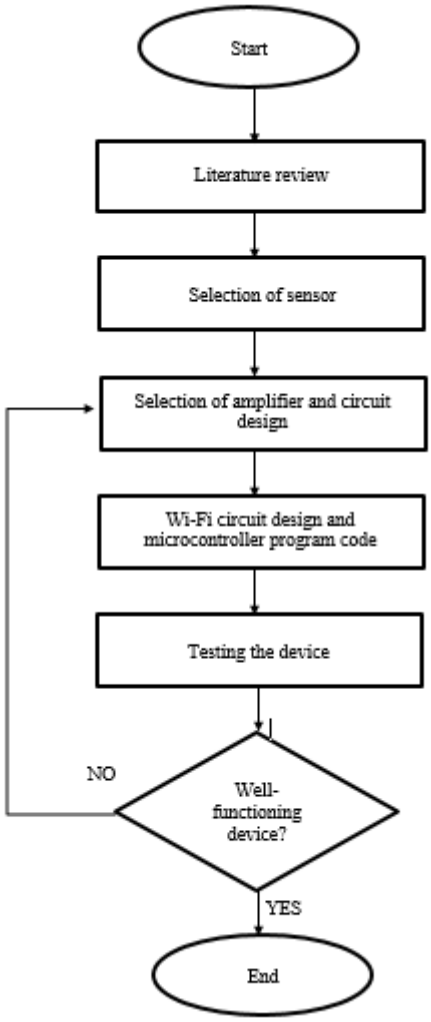

Fig. 2. Flow of project device.

B. *Working Principle*

The Fig. 3 shows how the project runs from the input sensor to the output display. Firstly, when the sensor is placed on the ground surface above the pipe leakage, the small vibration wave signal will be detected. The water leakage is detected by using the vibration sensor (piezoelectric). The signal then transfers from the sensor to the amplifier. The purpose of the amplifier is to amplify the signal by using suitable input gain. In order to operate the circuit in the system, supply source was converted from 12v dc to 5v dc by microcontroller and then supply it to the other circuit. All the components involved in the circuit design only have a low rating of current and it is safe to run it for long time operations depending on the capacity of the battery. High input analogue signal creates by amplifier then go to the Arduino Mega microcontroller for data processing. The combination of program code between application and sensor reading was programmed into the Arduino Mega. In this project, IOT system was used to easier the user and also reduce cost. Only by using the connection between Wi-Fi module and smartphone hotspot signal, all of the data required can be transferred to the application in smartphones and the data also can be recorded.

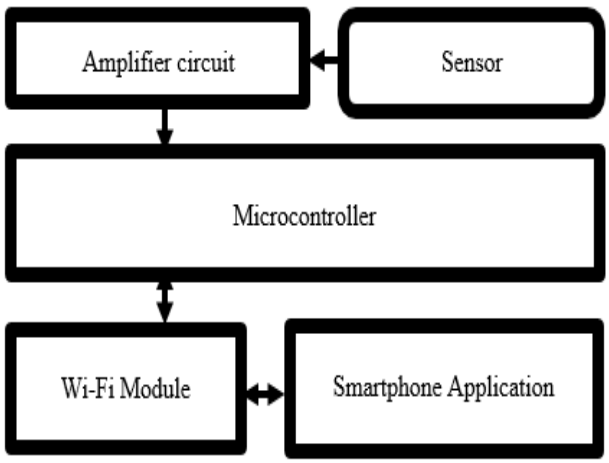

Fig. 3. Flow of project device.

C. *Sensor used*

Piezo ceramic is used in this project due to their characteristic which is full with desired need. Dimension of the sensor is 3.5mm outer diameter, 25mm inner diameter, 0.25mm and 0.51mm thickness. It is a very low rating for the resonant frequency and capacitance which is around 50 HZ to 10 KHz and for sure it can sense very small scale of vibration. The Piezo ceramic disc is a small, inexpensive and a good performance transducer that commonly used in industries for many purposes especially to sense vibrations. Moreover, the sensor can act in both as a sensor and also actuator. It is also omnidirectional which is can absorb or capture noise from all directions and also can be used as a buzzer.

When the sensor receives the vibration from one direction, the vibration reduction system will react and take action to send back the signal to other direction via electric power. The sensor can deliver great noise of vibration quality but need constant vibration to produce a better result wave signal output. This transducer was made from two conducting plates. Following the functional concept of piezo-ceramic disc, the best result or higher output reading of piezo-ceramic sensor only can produce when forcing the higher compress in the middle of piezo-ceramic wafer. In this project, 0.1 gram mass is needed to double increase the reading of frequency due to the leakage vibration produce by UPVC pipe is very small and sometime cannot be read only by using the amplifier circuit. When the vibration is detected, the mass can give an impact to the piezo ceramic wafer by compress it more and make it move harder.

D. *Audio Amplifier*

In this project, the amplifier is used to amplify the signal from the sensor to the microcontroller. Low voltage audio power amplifier LM386 is chosen with gain adjustment from 20 to 200. Voltage gain simply means that voltage out is 200 times than voltage in. To set suitable gain, additional capacitors and resistor was added to their pins as shown in Fig. 4.

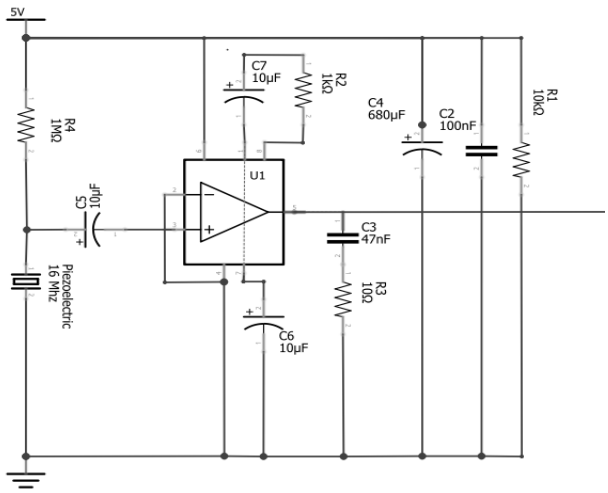

Fig. 4. The arrangement of amplifier circuit.

E. ESP 8266 Wi-Fi module

In this project, the ESP 8266 W Wi-Fi module is used as a communication device between the user and the hardware to display the result by using the application on the smartphone. The ESP 8266 Wi-Fi module is very small and less cost compare to other Wi-Fi shield module. This module also comes from the AT command set firmware and can increase their ability as a Wi-Fi shield offer. This Wi-Fi has capabilities and powerful enough processing and storage to integrate with sensor or any application and also can minimal the runtime process.

F. Structure Design

In order to design the suitable casing for the sensor, it must be considered about the relationship between the sensitivity of the sensor and their vibration effect. The aim is to make sure the sensor can absorb the bigger scale area of vibration with low frequency in multi directional. The material use for the sensor part is (Polyamide) AB which are commonly used in filament form. The material design is solid and high resistance to protect the sensor from damage. There also have a place for O ring rubber behind the sensor to avoid from water flow into it. The base area for the sensor part play as a main role to enable the sensor to detect the water leak. Practically, the wide base will increase the strength of sensitivity to capture the vibration. The shape of the base part also flat and clean to stable the device when places it on the ground surface.

G. Experimental Setup

To achieve the objectives of this project, an experiment was set up to investigate the function of device to sense the underground water leakage along the UPVC pipe. The testing experiment was conducted at PETRONAS Taman Cempaka, Johor Bharu. Some parameters have been set as a variable factor which is the diameter of pipe, the size of hole represented as a broken pipeline and also the depth of buried pipe.

As shown in Fig. 5, this 'L' shape of pipe was developed and represented as a piping line with a leak. The physical design of experiments was based on UPVC pipe with diameter size 20mm and 25mm and there are points in the line which are prepared for the leak sources. The point was created with two different sizes.

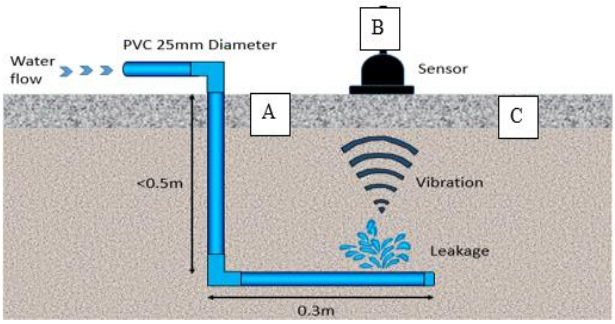

Fig. 5. The pipeline arrangement of the experiment setup.

The depth of pipe buried is changed for every experiment conducted from 0.1m to 0.4m. The data reading was recorded every 3 minutes per experiment. In this case, the target point to take a reading was divided into 3 parts which is A, B and C as shown in Fig. 5. A is a point where the sensor is put before the leak but still above the piping system, B is a straight point from a leak happen to the surface and the last one is a point C which is after the leakage but not in piping way. However, all data is recorded in 1 minute for every step taken at each point.

The starting point of PVC pipe was connected to the water supply with constant normal pressure. When the water source is opened, water flow through the pipe and burst out from the hole. The effect of contacting water with that pressure and the soil will produce some noise of vibrations. The propagation of vibration then spread into the soil and continuously until the wave arrive to the top of the ground surface. The vibration sensor leave on that surface then absorb the vibration and display it on the smartphone.

Fig. 6. The way of device use.

IV. Result And Discussion

In reality of piping system without any leakage, are actually perfectly quiet but still has a noise which is developed from water turbulent flow in pipes. Besides that, it is also effected from the changing pressure of water flow due to different size of piping, pipe junction, pumps, valve, or leaks and simultaneously increase the noise level above the base. However, by ignoring the disturbance from surrounding noise

effect, that turbulent water flow noise can be used as a reference level of noise. Yet, data of the acoustic signature graph shown in figure below are the result of experiment and may be varied from one side to the other depends on the condition of soil, pressure, size of pipes, and also the depth of buried pipe. In focus, the data trying to identify the vibrations of soil affected by the leakage pipe. It can be detected by comparing the data while it increases obviously then the normal condition.

A. Testing on 20mm UPVC Pipe with Small Hole

From the vibration reading in y axis of the graph, it is actually the difference between the peak to peak values from the output waveform. By using the basic digital concept, 0~5v input supply was converted to 4 bits, and it will become in range 0~1023 integer. To identify the amplitude of vibration, the difference between the maximum and minimum of the waveform was taken.

Fig. 7 shows the result from experiments conducted for 20mm diameter of UPVC pipes. It is a summarize graph from 4 experiments conducted in different depth. The arrangement of graph shows the increasing of the depth. Highest reading is the result from 0.1m depth and the lower is 0.4m reading. From the observations, the leak signals are correctly detected and the sensitivity is extremely high with a remarkable point of leak. The sound spectral density increase immediately after the water leakage found and it proves that the vibrations at that time is higher due to the water pressure impact to the soil.

When the distance between leak and the sensor is close, the vibration can easily be sense by the sensor because of the amplitude wave propagation of the vibration is still high and less absorbed into the soil. It is different conditions, when the pipe was buried deeper, the journey of vibration energy to go out to the surface become long and at the same time the vibration effect was already absorbed by the soil. Wave propagation between water leak and soil is a complicated phenomenon. In case of UPVC pipe used, the pressure leak is already small instead of using the aluminium or other metal pipe. Because of that, the energy of vibration, then change to very tiny scale of frequency and make a sensor difficult to sense the leak. In addition, by referring to the specifications of the sensor, it is not sensitive enough to sense the small frequency which is < 50 Hz.

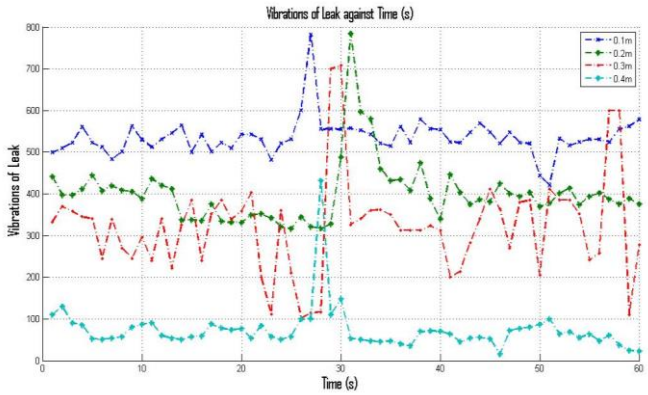

Fig. 7. The combination of data for 20mm UPVC pipe.

B. Testing on 25mm UPVC Pipe with Small Hole

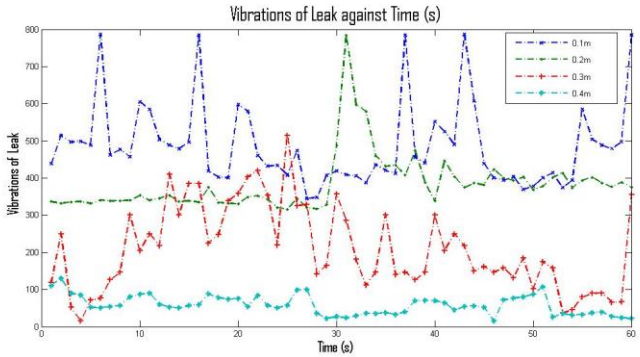

Fig. 8. The combination of data for 25mm UPVC pipe.

The Fig. 8 shows the graph result from the experiment conducted for 25mm diameter UPVC pipe. In general, the result is consistent and the pattern of the graph is quietly the same as the result from the 20mm diameter. However, the data from 25mm pipe is lower than the data from 20mm pipe when compares it at the same depth. It is because, the water pressure produced from the pipe 25mm is lower than 20mm pipe. The data prove that, the pressure of water depending on the size of pipe. When the size of the pipe increase, the water pressure will become decrease and the impact of water leak to the soil will decrease too. Focusing on the Fig. 7 and Fig. 8 for the 0.4m depth, the value of the data is equal to the reference value like no leakage detected. From the observation, the vibrations spread into the surrounding soil before it goes through the sensor.

C. Testing on 20mm UPVC Pipe with Big Hole

The Fig. 9 shows the graph signal for big hole experiment by using 20mm UPVC pipe with depth 0.3m. The red and blue graph shows the reading in point A and C following the experiment setup above. It represents the reference value without leaks. This condition and such levels make a deletion of the vibrations associated with the background noise, thus causing problems to the sensor to detect correctly. The spectral analysis obtained reveals that signals recorded is not from the leak but from the noise surrounding. However, it reveals that, the larger scratch of leak will reduce the collision impact between water and soil to produce the high vibration signal.

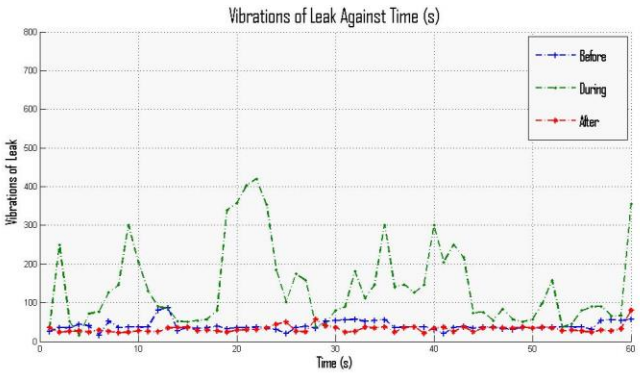

Fig. 9. The data for big hole scratch experiment.

D. Application Software

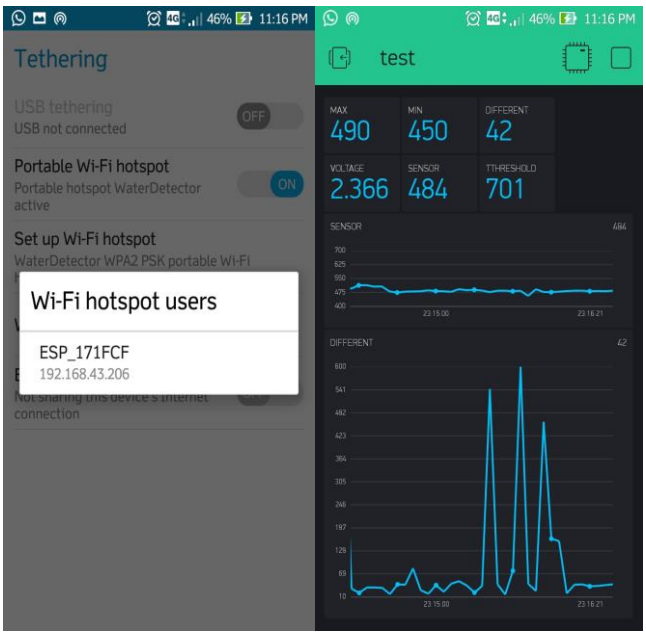

Fig. 10. The data display on Blynk application.

In order to display the result, the Blynk application was used in this project. Blynk is a platform with iOS and Android apps to control many microcontroller such as Raspberry Pi, Arduino and more over that can be related to internet. In project, it is a digital dashboard to build a graphic interface only by dragging and dropping widgets. The Blynk also is one of the famous IOT apps that allow the user to control or monitor something only by using the smartphone. The Fig. 10 above shows how the application runs in this project.

V. Conclusion

In this project, an innovative technique for the acoustic method detection of underground water leaks UPVC pipes was presented. Moreover, the data collection shows the positive result and prove that the water leakage also can be sense from their vibration effect. The effectiveness of the device is depending on several factors and must be avoided from the surrounding noise. The involvement of IOT system also makes a device more function. However, the device should be upgraded in term of type of vibration sensor, the speed of Wi-Fi module, and various the applications in the device system to make it run more smoothly and can be use in the real conditions in industries without failure.

References

[1] A. Cataldo, G. Cannazza, E. De Benedetto and N. Giaquinto, "A New Method for Detecting Leaks in Underground Water Pipelines", *IEEE Sensors Journal*, vol. 12, no. 6, pp. 1660-1667, 2012J. Clerk Maxwell, A Treatise on Electricity and Magnetism, 3rd ed., vol. 2. Oxford: Clarendon, 1892, pp.68-73.

[2] Water Loss Asia 2016: Conference & Exhibition - Home", *Waterlossasia.com*, 2016. [Online]. Available: http://www.waterlossasia.com/. [Accessed: 04- Dec- 2016].K. Elissa, "Title of paper if known," unpublished.

[3] R. Puust, Z. Kapelan, D. Savic and T. Koppel, "A review of methods for leakage management in pipe networks", *Urban Water Journal*, vol. 7, no. 1, pp. 25-45, 2010.

[4] R. Ben-Mansour, M. Habib, A. Khalifa, K. Youcef-Toumi and D. Chatzigeorgiou, "Computational fluid dynamic simulation of small leaks in water pipelines for direct leak pressure transduction", *Computers & Fluids*, vol. 57, pp. 110-123, 2012.

[5] Y. Khulief, A. Khalifa, R. Mansour and M. Habib, "Acoustic Detection of Leaks in Water Pipelines Using Measurements inside Pipe", *Journal of Pipeline Systems Engineering and Practice*, vol. 3, no. 2, pp. 47-54, 2012.

[6] D. Ayala-Cabrera, M. Herrera, J. Izquierdo and R. Pérez-García, "Location of buried plastic pipes using multi-agent support based on GPR images", *Journal of Applied Geophysics*, vol. 75, no. 4, pp. 679-686, 2011.

[7] US20140028459A1 - Method and system for leak detection in a pipe network - Google Patents", *Patents.google.com*, 2016. [Online]. Available: https://patents.google.com/patent/US20140028459A1/en. [Accessed: 01- Dec- 2016].

[8] O. Hunaidi and W. Chu, "Acoustical characteristics of leak signals in plastic water distribution pipes", *Applied Acoustics*, vol. 58, no. 3, pp. 235-254, 1999.

[9] O. Hunaidi, "A new system for locating leaks in urban water distribution pipes", *Management of Environmental Quality: An International Journal*, vol. 17, no. 4, pp. 450-466, 2006.

[10]]Kim SW, Kim SY. Comparison of FMCW and pulse type GPR for water leakage detection. In: Proceedings, IEEE International Geoscience and Remote Sensing Symposium 2005, Seoul, Korea, July 25–29, 2005, vol. 7, p. 4596–9.

[11] Hyun SY, Jo YS, Oh HC, Kim SY, Kim YS. The laboratory scaled-down model of a ground-penetrating radar for leak detection of water pipes. Meas Sci Technol 2007; 18:2791–9.

[12] Bimpas M, Amditis A, Uzunoglu N. Design and implementation of an integrated high resolution imaging ground penetrating radar for water pipeline rehabilitation. Water Resour Manag 2011; 25(4):1239–50.

[13] Bimpas M, Amditis A, Uzunoglu N. Detection of water leaks in supply pipes using continuous wave sensor operating at 2.45 GHz. J Appl Geophys 2010;70(3):226–36.

[14] D. Ayala-Cabrera, M. Herrera, J. Izquierdo and R. Pérez-García, "Location of buried plastic pipes using multi-agent support based on GPR images", *Journal of Applied Geophysics*, vol. 75, no. 4, pp. 679-686, 2011.

[15] R. K. Parida, V. Thyagarajan and S. Menon, "A thermal imaging based wireless sensor network for automatic water leakage detection in distribution pipes," *2013 IEEE International Conference on Electronics, Computing and Communication Technologies*, Bangalore, 2013, pp. 1-6. doi: 10.1109/CONECCT.2013.6469289

[16] M. Fahmy and O. Moselhi, "Automated Detection and Location of Leaks in Water Mains Using Infrared Photography", *Journal of Performance of Constructed Facilities*, vol. 24, no. 3, pp. 242-248, 2010.

[17] A. Cataldo, R. Persico, G. Leucci, E. De Benedetto, G. Cannazza, L. Matera and L. De Giorgi, "Time domain reflectometry, ground penetrating radar and electrical resistivity tomography: A comparative analysis of alternative approaches for leak detection in underground pipes", *NDT & E International*, vol. 62, pp. 14-28, 2014.

[18] J. Yang, Y. Wen, P. Li and X. Wang, "Study on an improved acoustic leak detection method for water distribution systems", *Urban Water Journal*, vol. 10, no. 2, pp. 71-84, 2013.

[19] Y. Gao, M.J. Brennan, P.J. Joseph, J.M. Muggleton, O. Hunaidi On the selection of acoustic/vibration sensors for leak detection in plastic water pipes J Sound Vib, 283 (2005), pp. 927–941

[20] O. Hunaidi, M. Bracken, T. Gambino, and C. Fricke, "Acoustic methods for locating leaks in municipal water pipe networks," in Proc. Int. Conf. Water Demand Manag., Dead Sea, Jordan, 2004, pp. 1–14.

[21] "Water Leak Detection". *UK Leak Detection*. N.p., 2017. Web. 15 May 2017.

Digital Control of Water Level Plant using MyOpenLab Software

Nur Azmah binti Mat Kia
Faculty of Electrical Engineering
Universiti Teknologi Malaysia
Johor Bahru, Malaysia.
azmah2086@gmail.com

Rosbi bin Mamat
Department of Control and Mechatronic Engineering
Faculty of Electrical Engineering
Universiti Teknologi Malaysia
Johor Bahru, Malaysia.
rosbi@utm.my

***Abstract*— This paper present way to evaluate on how to implement digital control by using less expensive software and hardware for teaching, learning, research and real-time implementation. In this project, digital control used both MyOpenLab software and Arduino as data acquisition card (DAQ). MyOpenLab software is the open source software which is free to install and does not required a license. For this project, module G30A, G30B and TY30 is used for prototype. Before digital control system is applied, a few experiment is done such as calibration process and experiment for full open valve condition and half open valve condition. The calibration is done to determine the voltage that is corresponding to the level of water. The experiment for full open valve and half open valve condition is done to determine the transfer function for this system. The transfer function of this system is also used to find the parameter of PI controller. The parameter of PI controller, K_p and T_i is used in MyOpenLab software for digital control system. After the digital control system is applied, the performance of this system is shown in MyOpenLab software at the front panel. From this performance, the characteristic of transient response was determined. It shows that MyOpenLab software can operate same as other software that required license and more expensive to install such as MATLAB and Labview.**

Keywords—MyOpenLab software; digital control; PID controller; Arduino

I. INTRODUCTION

In Malaysia, water treatment plant used SCADA system that consists of PLC (Programmable Logic Controller) to monitor and control this plant. By using SCADA, all the process can be monitored and controlled at control room that is controlled by the person in charge. SCADA stands for Supervisory Control and Data Acquisition that commonly use in an industrial automation control system. SCADA system allows real time data from plant to be accessed from anywhere in the world [1]. The controlling and monitoring water treatment plant can be simulated by using MATLAB and LABVIEW. By using MATLAB software, simulink model can be used to simulate water control level for water treatment plant. However, Labview software uses graphical programming language to control and monitor water treatment plant. This graphical programming language is simple to create and visualize. Both software required specific data acquisition (DAQ) card for simulation.

Therefore, prototyping digital control or computer control in teaching, learning and research required software and hardware. Software that commonly used for digital control system is MATLAB and Labview. This two software also required a specific data acquisition (DAQ) card for communication with hardware system. This software and hardware are expensive because the software required a licence for installing process. So, the problem statement for this paper is to evaluate on how to implement a digital control by using less expensive software and hardware for teaching, learning, research and for real-time digital control implementation. The software and hardware used in this project is MyOpenLab software and Arduino as a data acquisition card (DAQ).

There are three objective for this paper which is to study the effectiveness of using MyOpenLab software for teaching and learning in Digital Control System. The second objective is to implement real time control of PI controller on a water tank level control system and lastly to evaluate the performance of analog PID and digital PID of the level control.

II. LITERATURE REVIEW

A. Overview of Digital Control System

Digital control system used digital signal (instruction) and a digital computer to control the process. However, there are some type of digital control system that require instruction to execute automatically because the control system requires information to do the process.

Fig.1 shows that the general block diagram for digital control system is consist of digital part and analog part. Digital part consist of computer, DAC and ADC while analog part consist of actuator, process and sensor. In digital control system, the analog to digital converter (ADC) used is to convert the analog signal from plant to digital signal before the information is transferred to computer. Meanwhile, the digital to analog converter (DAC) is used to convert digital signal from computer to analog signal to proceed with the process [2].

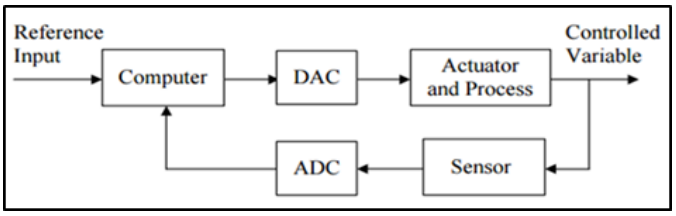

Fig. 1. General Block diagram for digital control system [2].

The advantages of digital control system are less expensive, less noise and flexibility in response to design changes. The digital control system is also used to improve the tracking performance for complex system because it introduce delay in the loop [3].

B. PID Controller

Feedback control is a control mechanism that use information from measurement to continue the process. A PID controller is a feedback control that is widely use in industrial control system and it is the most important ingredient of a distributed control system. PID controller is used for correcting the error between a measured process variable and a desired set point by calculation. PID controller is a combination of three parameters which are proportional controller (K_p), integral controller (K_i) and derivative controller (K_d) [4]. The general equation of PID controller is:

$$G(s) = K_p\left(1 + \frac{1}{T_i s} + T_d s\right) = K_p + \frac{K_i}{s} + K_d s \qquad (1)$$

Each controller have their own characteristic. By using proportional controller, K_p it will reduce the rise time of system but never eliminate the steady state error while integral controller, K_i can eliminate the steady state error but it make transient response become worse. For derivative controller,K_d, it can increase the stability of system, reduce the percent overshoot and improve the transient response but, PI controller is the most common type of controller used in industry.

TABLE I. A PID CONTROLLER IN CLOSED LOOP SYSTEM [4].

Parameter	Rise Time	Overshoot	Settling Time	Steady state error
K_p	Decrease	Increase	Small change	Decrease
K_i	Decrease	Increase	Increase	Decrease significantly
K_d	Minor decrease	Minor decrease	Minor decrease	No effect in theory

C. Ziegler-Nichols method

Ziegler-Nichols method is one of the method for tuning the PID controller. It is used to determine the parameter of proportional controller, integral controller and derivative controller. Ziegler-Nichols method was introduced in 1942 by the employee of Taylor Instrument which is Ziegler and Nichols [5]. There are two methods to identified parameter of PID controller which is bode plot where it is used to determine ultimate gain (K_u) and period (T_u). The other method is based on step response where it need to have transfer function of system [6].

TABLE II. ZIEGLER-NICHOLS SELF OSSILATION METHOD [7].

Controller	K	T_i	T_d	T_p
P	$0.5K_u$			T_u
PI	$0.4K_u$	$0.8T_u$		$1.4T_u$
PID	$0.6K_u$	$0.5T_u$	$0.125T_u$	$0.85T_u$

TABLE III. ZIEGLER-NICHOLS BASED ON STEP ESPONSE [6].

Controller	K_c	T_I	T_D
P-only	$(1/K)(\tau/\theta)$		
PI	$(0.9/K)(\tau/\theta)$	3.3θ	
PID	$(1.2/K)(\tau/\theta)$	2.0θ	0.5θ

D. MyOpenLab Software

MyOpenLab is Java programmed software that was developed for the fast administration [8]. It is an open source software with source code that anyone can inspect, modify and share. This software does not required a licence and free to install. MyOpenLab is a graphical programming language which is a simple program that have been built on to others. MyOpenLab is the alternative and a cheap way compared to Labview as their function is the same. The advantage of MyOpenLab is easy to use, minimal cost (cheap), graphical source code and it is a graphical user interface (GUI).

MyOpenLab software is simple to be used for data analysis and presentation of result through graphs. It also can analyse the performance of the controller to see the differences.

III. METHODOLOGY

This project consist of two important parts which are software and hardware part. For software part, the coding for the system must be developed which is graphical programming language to interface by using data acquisition card (DAQ). After finish the software part, it can be tested with hardware by using module G30A/G30B and water tank (TY30A) to see whether the hardware followed the command that given from software part.

Fig. 2. Project configuration

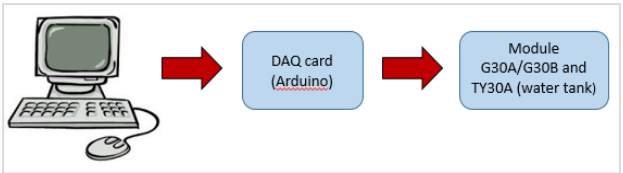

In this project, module G30A,G30B and water tank (TY30) are used as a prototype, arduino is used as a DAQ card and MyOpenLab software is used to control the level of water in TY30. Before using the digital contol, the equipment must be calibrated to make sure the equipment is in a good condition. After that, the experiment is run to find the transfer function of this system used in a digital control by using MyOpenLab

software. It can also identifed the PI controller by using the transfer function of this system.

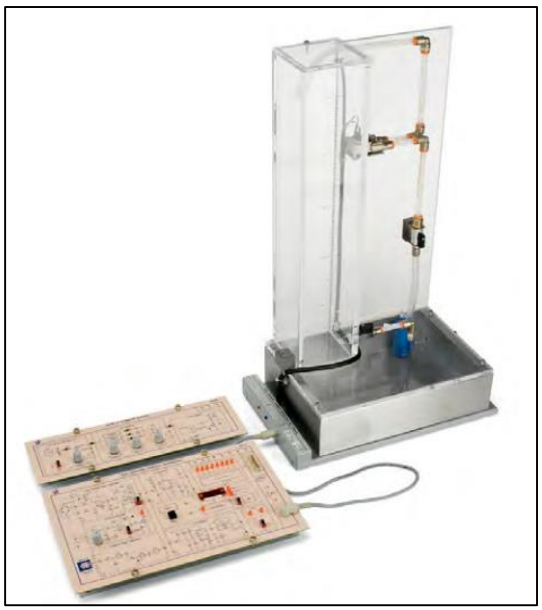

Fig. 3. Module G30A/G30B and TY30

A. *Calibration*

This experiment is done to make sure the equipment is in a good condition and to find the voltage that corresponding to the level of water in TY30. The voltage are measured at terminal 6 of module G30A by using multimeter. The connection for this experiment is shown below:

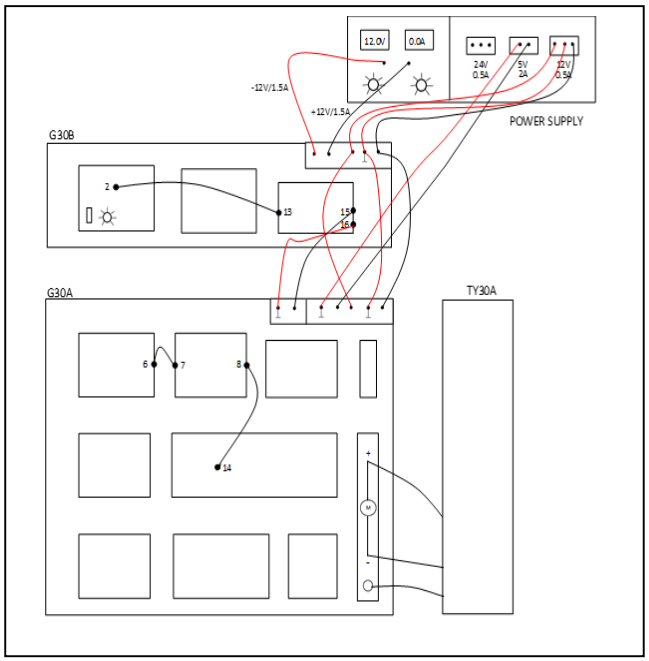

Fig. 4. Connection for calibration process

B. *Experiment for full open valve and half open valve*

The experiment is done to determine the transfer function for this system and parameter of PI controller was identified from the transfer function. The connection for this experiment is the same as the calibration process but in this experiment, the set point and error amplifier block is used (first block in G30B). The knob at this block have to be adjusted to a certain value to pump the water into TY30. When the knob is adjusted to a certain level of water, the reading of voltage is taken for every 15 second before it reached the specified level.

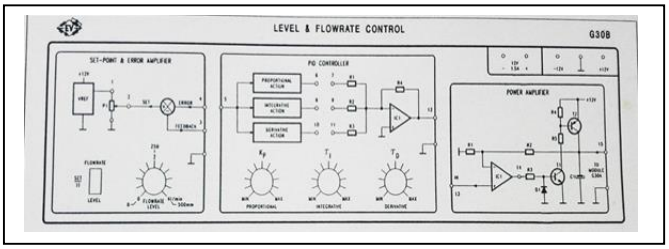

Fig. 5. Block in Module G30B

For full open valve experiment, it is done for the level of water from 100mm to 200mm and 200mm to 300mm while for half open valve it is done for the level of water from 100mm to 200mm, 200mm to 300mm and 300mm to 400mm. This experiment is repeated three time for each level of water and for both experiment.

C. *Data Acquisition Card (DAQ)*

In this project, Arduino is use as data acquisition card because Arduino is less expensive and easy to use. Besides that, it also have firmware which is suitable for a data acquisition card. Firmware is a programming that is written to the flash Read-Only Memory (ROM) that can be erased and rewrite because it is a type of flash memory [9]. The Arduino has been modified by adding a simple circuit to amplify the voltage from 10V to 5V and vice versa. This is because the maximum voltage for input and output of Arduino is 5V.

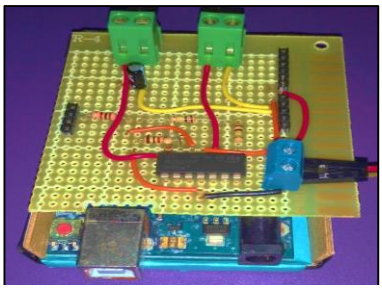

Fig. 6. Connection Arduino with simple circuit

D. *MyOpenLab Software*

In this project, MyOpenLab is used because it is an open source software that do not required licence to install and free. This software are used to control the system and to monitor the performance of this system. For digital control system, the block in G30B that are used is power amplifier block that is

connected with DAC from Arduino. ADC which is also from arduino is connected to the output of the level pressure signal block in G30A.

MyOpenLab software used a graphical programming language to programme the system. Fig.7 is the connection of the system with PI controller that can be executed by Arduino. Fig. 8 shows the front panel in MyOpenLab that can control the set point of the system and show the performance of system.

Fig. 7. Circuit panel in MyOpenLab software

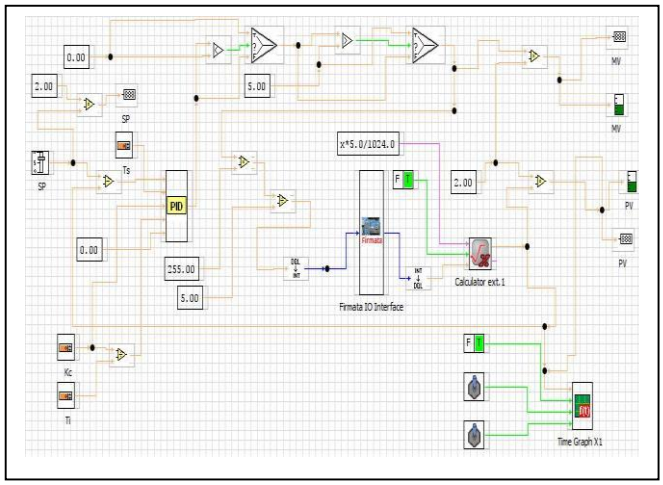

Fig. 8. Front panel in MyOpenLab software

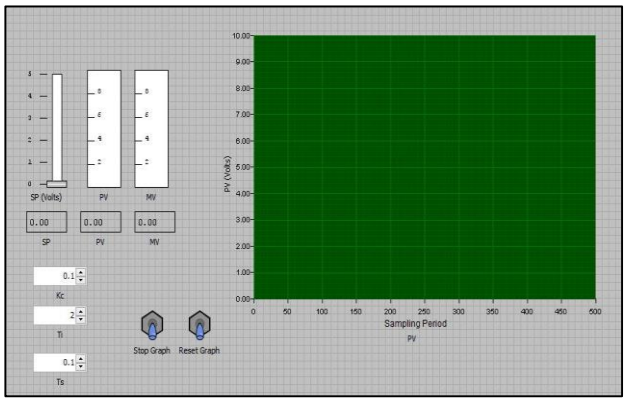

IV. RESULTS AND DISCUSSIONS

A. Calibration process

Form the calibration, the voltage is measured and the corresponding voltage for the certain level of water is determined. When the level of water increased, the output voltage of the sensor also increased. The graph shows the linearity between voltage and level of water.

TABLE IV. TABLE FOR RESULT CALIBRATION

Level(mm)	Voltage(V)
0	-0.01
50	0.69
100	1.53
150	2.37
200	3.20
250	4.03
300	4.85
350	5.68
400	6.50
450	7.33
500	8.12

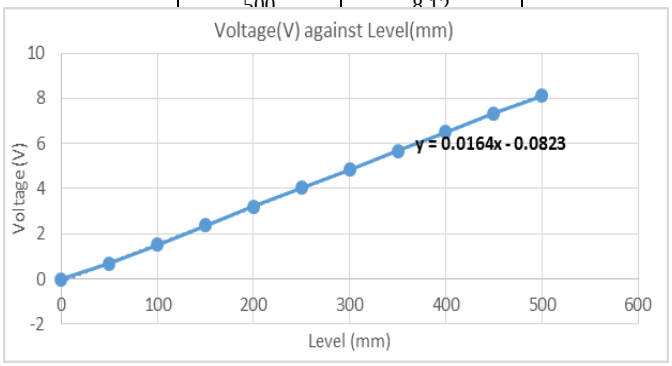

Fig. 9. Graph between voltage and level of water

B. Experiment for full open valve and half open valve.

From this experiment, transfer function for this system was determined by using process reaction curve. To get the transfer function from process reaction curve method, the graph of this system is plotted. For this experiment the dead time was assume as 0.1 second.

1) Full open valve

a) For 100mm to 200mm

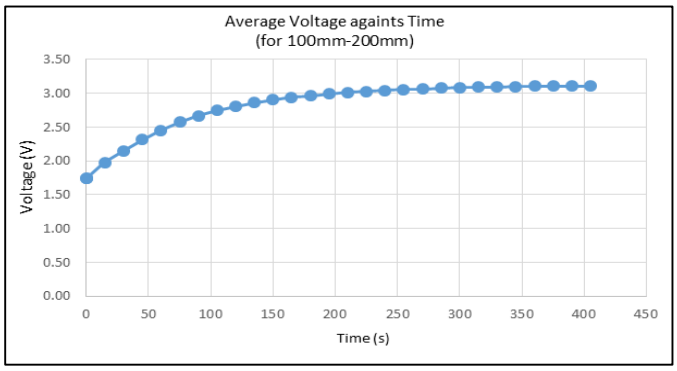

Fig. 10. Graph of average voltage agaisnt time for 100mm-200mm.

The transfer function for this graph is:

$$G(s) = \frac{1.24e^{-0.1s}}{1 + 91.5s} \quad (2)$$

b) For 200mm to 300mm

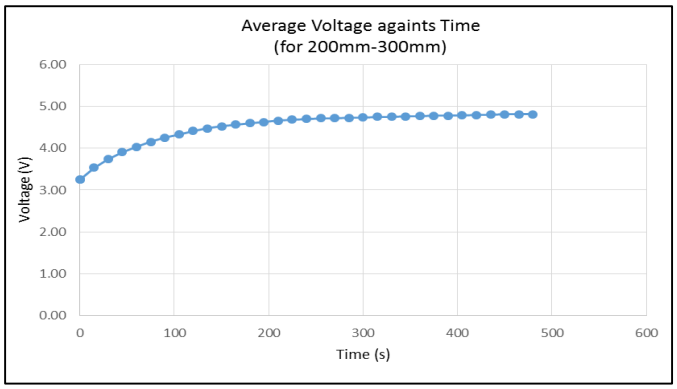

Fig. 11. Graph of avarage of voltage against time for 200mm-300mm.

The transfer function for this graph is:

$$G(s) = \frac{1.51e^{-0.1s}}{1 + 97.5s} \quad (3)$$

From two transfer function determined from this experiment, the average transfer function calculated is:

$$G(s) = \frac{1.375e^{-0.1s}}{1 + 94.5s} \quad (4)$$

According to Fig.10, Fig.11 and average of transfer function, the system is a first order system. In this project, PI controller is used to get a better performance. The parameter of PI controller is determined from transfer function by using Ziegler-Nichols method. However, the dead time is assumed as 10 second to calculate the parameter. Therefore, the value of the parameter is $K_c = 6.1855$ *and* $T_i = 33.3$.

2) Half Open valve

a) For 100mm to 200mm

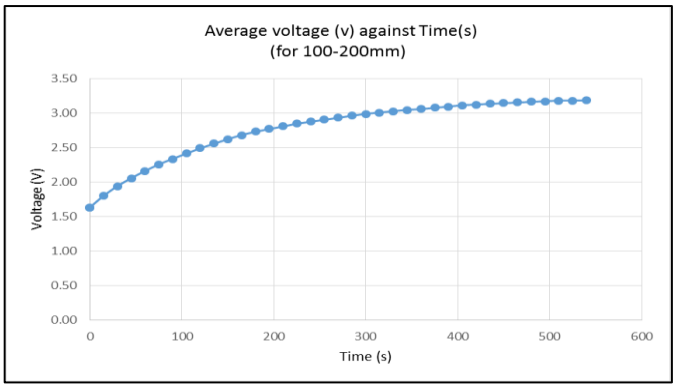

Fig. 12. Graph of average voltage against time for 100mm-200mm

The transfer function from this graph is:

$$G(s) = \frac{4.33e^{-0.1s}}{1 + 180.5s} \quad (5)$$

b) For 200mm to 300mm

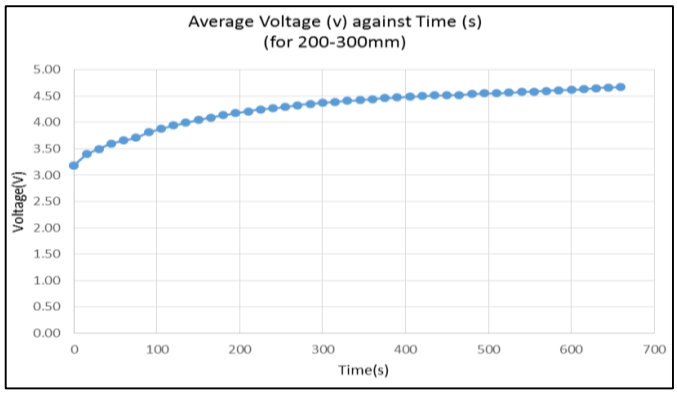

Fig. 13. Graph for average of votage against time for 200mm-300mm.

The transfer function for this graph is:

$$G(s) = \frac{4.35e^{-0.1s}}{1 + 202.5s} \quad (6)$$

c) For 300mm to 400mm

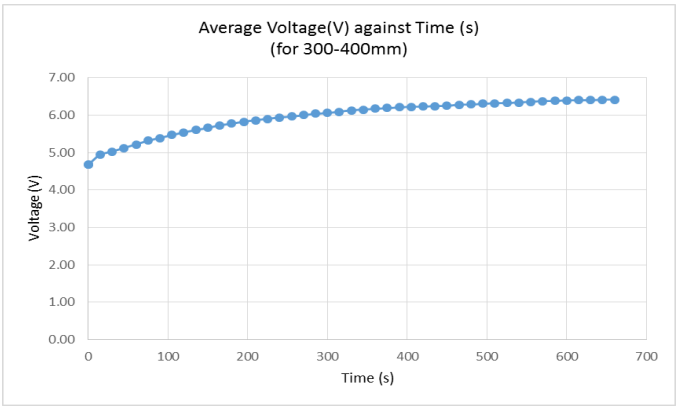

Fig. 14. Graph of average voltage against time for 300mm-400mm

The transfer function from this graph is:

$$G(s) = \frac{4.97e^{-0.1s}}{1 + 202.5s} \quad (7)$$

From these three transfer function for half open valve experiment, the average transfer function calculated for this system is:

$$G(s) = \frac{4.55e^{-0.1s}}{1 + 195.17s} \quad (8)$$

This system is a first order system same like the full open valve experiment. From this transfer function, the parameter of PI controller is also calculated by using Ziegler-Nichols where the parameter are $K_c = 3.8605$ *and* $T_i = 33.3$.

C. MyOpenLab Software

In the MyOpenLab software, the parameter of PI controller that is calculated from the open valve and half open valve experiment is used. The performance of this system has been shown in the front panel of MyOpenLab software.

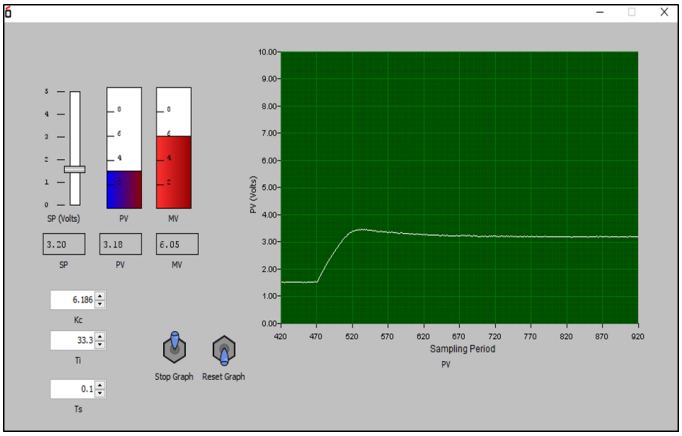

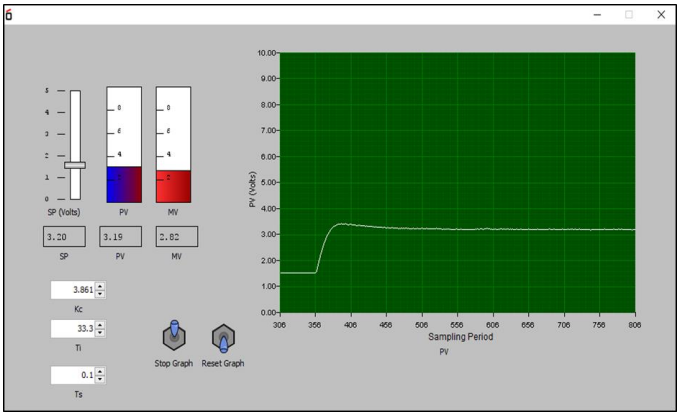

Fig. 15. Full open valve condition for 200mm-300mm

Fig. 16. Half open valve condition for 200mm-300mm

From Fig. 15 and Fig 16. , the percent overshoot, rise time and settling time has been calculated. For full open valve condition, the percent overshoot is 7.69%, rise time is 27 second and the settling time is 210 second while for half open valve condition, the percent overshoot is 4.17%, rise time is 6 second and the settling time is 90 second. It shows that the value of proportional controller, K_c influence the rise time, percent overshoot and settling time.

V. CONCLUSION

In this project, the characteristic of transient response of the system can also be identified from the graph that is displayed inside the front panel in MyOpenLab software. The best system for this experiment is half open valve condition because the settling time is faster than full open valve condition. This project also shows the performance of MyOpenLab software. This software is one of the alternative software that can be used besides MATLAB and LabView. This software is easy to install and simple to be used compared to MATLAB and LabView because there is need a license to install them.

REFERENCES

[1] SCADA systems are the backbone of modern industry (2016). Retrieved November 17, 2016 from Inductive Automation Website, https://inductiveautomation.com/what-is-scada

[2] M. Sami Fadali and Antoni Visioli (2013). Digital Control Engineering Analysis and Design. Elsevier Inc. Waltham, USA.

[3] Norman S. Nise (2006). *Control System Enginnering.* United State, America. John Wiley & Sons, Inc.

[4] Kambiz Arab Tehrani and Augustin Mpanda (2012). *Introduction to PID Controllers - Theory, Tuning and Application to Frontier Areas.* Retrieved November 28, 2016 from Website, http://cdn.intechopen.com/pdfs/29826/intech-pid_control_theory.pdf

[5] Brian R Copeland (2008). *The Design of PID Controllers using Ziegler Nichols Tuning.* Retrieved March 6, 2017 from Website, http://educypedia.karadimov.info/library/Ziegler_Nichols.pdf

[6] *Process Dynamics and Control.* Retrieved March 8, 2017 from Website, http://my.chemeng.queensu.ca/courses/CHEE319/documents/CHEE319_notes_2012_lecture5.pdf

[7] Ulf Holmberg. *PID control - Simple tuning methods.* Retrived March, 8 2017 from website, http://www.hh.se/download/18.7502f6fd13ccb4fa8cb2f6/1360676928481/PID.pdf

[8] André MIGEON and Anne-Elisabeth LENEL. *Modern Sensor Handbook.* Retrieved November 28, 2016 from http://www.iste.co.uk/data/doc_zyxkztsuofok.pdf

[9] Firmware (2016). Retrieved December 5, 2016 from TechTerms Website, http://techterms.com/definition/firmware

Multi-Rate Controller for Networked Multi Agent System (NMAS)

Nurul 'Atikah binti Zakaria
Faculty of Electrical Engineering
Universiti Teknologi Malaysia
Johor Bahru, Malaysia.
nurul.atikah228@gmail.com

Nurul Adilla Binti Mohd Subha
Department of Control and Mechatronics Engineering
Faculty of Electrical Engineering
Universiti Teknologi Malaysia
Johor Bahru, Malaysia.
nuruladilla@utm.my

***Abstract*—The paper discussed about methods used to design the multi-rate controller for networked multi agent system (NMAS). Consensus in NMAS is a system that consists of multiple agents or a group of subsystem which exchange their information through a shared network in order to achieve the consensus value. In industrial practice, most systems are inherently multi-rate systems because of the difference sampling rates employed at every subsystem. In this work, the robust multi-rate PI controller is introduced to minimize the effects of the network-induced delay. The developed strategy is simulated with single-input single-output (SISO) models for two dissimilar agents. The results show significant improvement on the overshoot and settling time compared to the single-rate controller.**

***Index Terms*—Networked Control System (NCS), Multi-Agent System, Network Delay, Proportional Integral(PI).**

I. INTRODUCTION

Networked multi-agent system (NMAS) is a control system structure composed of several agents or a group of subsystem that are physically separated and exchange their information through a shared network [1]. The advantages of the NMAS structure such as higher flexibility and scalability have gained a wide interest from researchers worldwide.

The consensus is defined as agreement. Within the control perspective, consensus represents the cooperative behavior of the NMAS agents to achieve their common goal or consensus value through information exchange under share network communication. The goal can be represented by physical quantities such as angle, temperature, level, velocity, and mass.

In this study, the consensus value is defined as water level of the single tank. This value is also called as external reference input which is determined by the user. This input is connected directly to only one agent (leader) in the NMAS. Other agents need to communicate and exchange their information with the assigned leader in order to update its current state and converge to the consensus value. However, the presence of the network-induced delay inevitably introduces challenges for the agents to reach the consensus.

Proportional-integral (PI) controller is a common and widely used in the industry due to its simplicity and practicality. However, single-rate PI controller may not appropriate to be used for solving the consensus problem with network-induced delay. Therefore, the multi-rate PI controller is proposed to compensate the effects of the network delay and improve the consensus convergence performance.

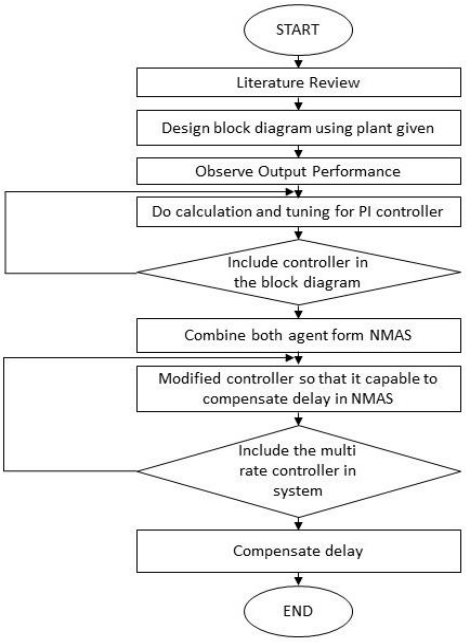

Fig. 1. Research Methodology Flowchart.

II. LITERATURE REVIEW

A. PI Controller

Proportional Integral Derivative (PID) and Proportional Integral (PI) controllers are commonly used in industry and it is a control loop feedback mechanism in control system.

PI controller has its ability to make zero steady state error with a step change [3]. PI and PID controller also widely used in

industry because the parameters need to be tuned is reduce or lower than others [6] - [7].

More recently, there has been a renewed interest in PID control, and the number of publications in the last ten years has overcome the total number of papers published before 1990 [5].

B. Good Gain Method

Good gain method (GGM) is an approach that almost similar with Ziegler's Nichols method [15] – [16]. GGM give more stability and it does not require control loop to get into oscillation during tuning like Ziegler's Nichols. In this project, GGM is used to tune the parameters of PI controller by adjusting the gain until there is show an overshoot and undershoot.

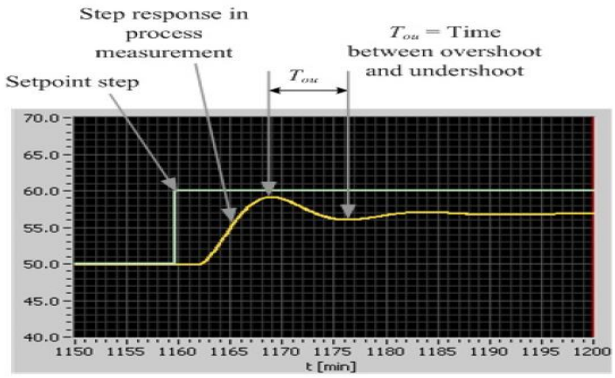

Fig. 2. Good Gain Method. [15] – [17]

C. Robust PI Controller

Robust PI controller is a method which designs the controller to compensate the network-induced delay for non-minimum phase system.

To make a stable system, the desired phase margin and gain margin must be complied. With the presence of network-induced delay, the phase margin will be decreased making the system unstable [17].

III. METHODOLOGY

To design the PI controller for single-rate NMAS agents, the controller parameters are designed based on GGM without considering the network-induced delay as follows:

i. Design Block Diagram: The block diagram is designed using Simulink in MatLab for both agents in separated windows.

ii. Both agents operated with a similar sampling rate. The agents can be represented as $G_1$and G_2 as follows:

$$G_1(z^{-1}) = \frac{0.001703z^{-1} + 0.005419z^{-2}}{1-0.9718z^{-1}-0.025z^{-2}} \quad (1)$$

$$G_2(z^{-1}) = \frac{0.002352z^{-1} + 0.001673z^{-2}}{1-1.646z^{-1}-0.6573z^{-2}} \quad (2)$$

iii. Good gain method is used in order to get the parameters of PI controller for each agent.

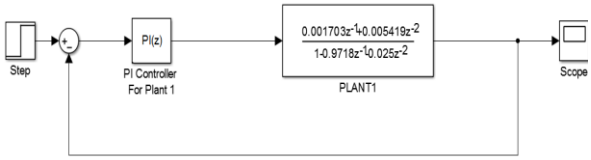

Fig. 3. Simulink block for Agent 1.

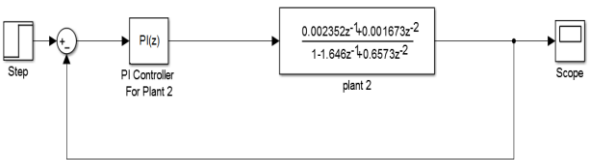

Fig. 4. Simulink block for Agent 2

iv. The PI for both agents are obtained using equation in [16] as follows:

$$T_i = 1.5T_{ou} \quad (3)$$

$$K_p = 0.8K_{gg} \quad (4)$$

v. The transfer function of PI controller for each agent is obtained using GGM to ensure that the closed-loop agent's system without network delay is stable and they are,

$$G_{c1}(z^{-1}) = \frac{32-26.67}{1-z^{-1}} \quad (5)$$

$$G_{c2}(z^{-1}) = \frac{5.6-5.313}{1-z^{-1}} \quad (6)$$

vi. Then, to develop non-identical NMAS, combine both agents in (1) and (2) and controllers in (5) and (6) into one Simulink block diagram as shown as in Fig. 5.

vii. Run the simulation with single-rate sampling and observe the consensus convergence performance.

viii. Repeat the vii step with network delay. The network delay is represented by the $Z^{-\tau}$ block. Observe the effects of the delay in consensus convergence performance.

ix. Finally, change the single-rate to multi-rate sampling to construct multi-rate NMAS. Then, observed the output response.

x. Repeat step ix with network delay.

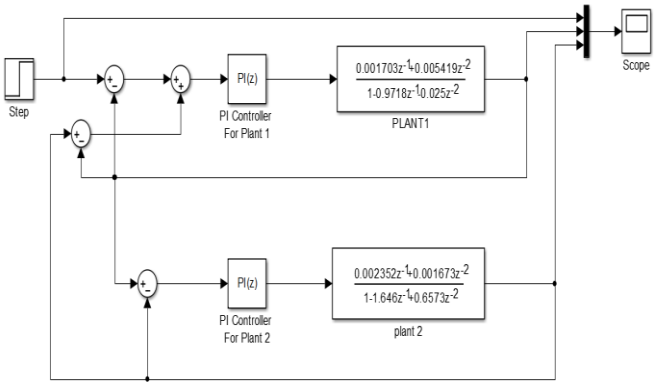

Fig. 5. Simulink block for NMAS without network delay.

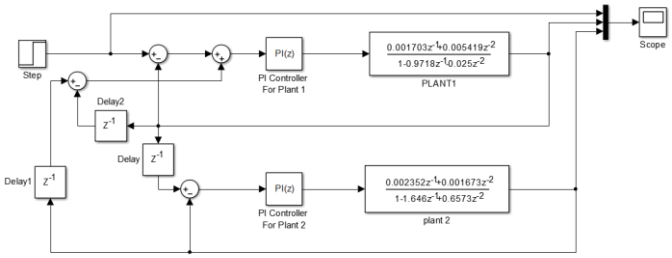

Fig. 6. Simulatink block for NMAS with network delay.

It is expected that multi-rate NMAS with PI controller will degrade the performance obtain in single-rate NMAS with PI controller. Thus, improvement has to be made on the controller to enhance its ability in compensating the network-induced delay in multi-rate NMAS. Thus, multi-rate robust PI controller is proposed.

Robust PID is a method that takes consideration on the frequency domain analysis in control system, which are gain margin, phase margin and frequency [17].

For a high-order non-minimum phase system which contain the time delay element transfer function is as shown [17], so the transfer function for this multi rate NMAS is obtained,

$$G_1(s) = \frac{A_0 s^2 + A_1 s + A_2}{s^3 + A_3 s^2 + A_4 s + A_5} e^{-Ts} \quad (7)$$

$$G_2(s) = \frac{A_0 s + A_1}{s^2 + A_2 s + A_3} e^{-Ts} \quad (8)$$

where T is the time delay of the system [17]. From equation (7) and (8) the PI controller is obtained by using method mention in [17] but used only K_p and K_i . The proposed controller is designed as,

$$G_c(s) = K_p + \frac{K_i}{s} \quad (9)$$

$$G_i(s) = G_c(s) \, . \, G_p(s) = \frac{N(s)}{D(s)} \quad (10)$$

$$F(j\omega) = D(j\omega) + A^{-j\theta} N(j\omega) \quad (11)$$

By solving (11) using (7)-(11), the parameter of robust PI controller can be obtained from frequency domain analysis by setting the desired output specification for the system.

Then, the output response is observed for multi-rate NMAS with network delay. The result is compared and discussed.

IV. Result

In this section, the consensus output performance for non-identical NMAS is presented. Results from both methods PI controller based GGM and robust PI controller are discussed.

A. Good Gain Method

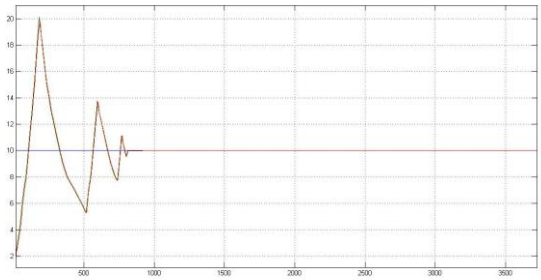

Fig. 7. Single-rate NMAS without network delay.

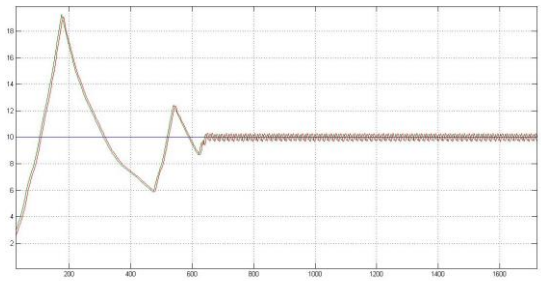

Fig. 8. Single-rate NMAS with network delay

The result for multi-rate NMAS with PI controller based GGM without and with delay can be illustrated in Fig. 7 and 8 respectively.

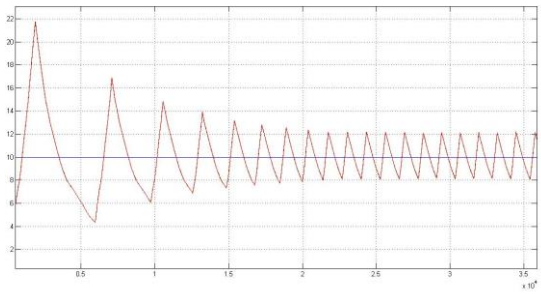

Fig. 9. NMAS Multi-rate without Delay Output.

The result for multi-rate NMAS with robust PI controller can be illustrated in Fig. 6 and 7 respectively.

From Fig. 7 and Fig. 8 it can be concluded that the single-rate NMAS is stable. However, with the presence of network

delay, both agents took a longer time to reach the consensus with small ripples.

For Fig. 9, the multi-rate NMAS is unstable with PI controller based GGM even though the network delay is not considered. This show that the PI controller based GGM is not suitable to be used with multi-rate NMAS.

Therefore, the new controller should be designed in order to minimize the effect of the network delay and has an ability to work with multi-rate NMAS. Thus, robust PI controller is studied and investigated.

B. Robust PID

Using this method, the proposed controller should be able to minimize the effect of the network delay and suitable to be implemented with multi rate NMAS.

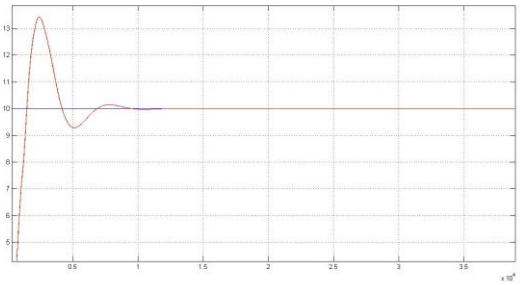

Fig. 10. Expected Response for Robust PI without delay.

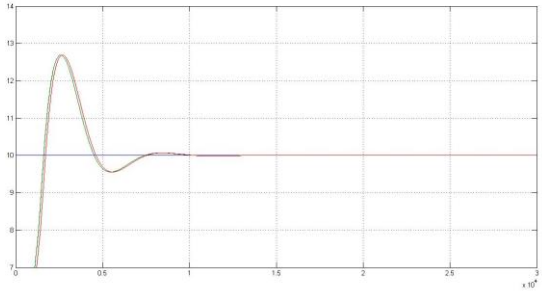

Fig. 11. Expected Response for Robust PI with delay.

V. CONCLUSION

For the conclusion, the proposed robust PI controller has a better performance in solving the consensus problem for multi-rate NMAS. It is also able to minimize the effects of the constant network-induced delay.

ACKNOWLEDGMENT

Thanks to all people who is helping to finish this project and who is always help when there is problem in this project especially to my supervisor, Dr Nurul Adilla Mohd Subha

REFERENCES

[1] N. A. M. Subha and G. P. Liu, "Design and Practical Implementation of External Consensus Protocol for Networked Multiagent Systems with Communication Delays," in IEEE Transactions on Control Systems Technology, vol. 23, no. 2, pp. 619-631, March 2015.

[2] https://en.wikipedia.org/wiki/Multi-agent_system

[3] S. Singh. Dr. Pandey, Dipraj “Design of PI Controller to Minimize the Speed Error of DC Servo Motor.” International Journal of Science & Technology Research, vol. 1, 2012.

[4] J. C. Basilio and S. R. Matos, "Design of PI and PID controllers with transient performance specification," in IEEE Transactions on Education, vol. 45, no. 4, pp. 364-370, Nov 2002.

[5] J. G. Ziegler and N. B. Nichols, “Optimal settings for automatic controllers,”Trans. ASME, vol. 64, pp. 759–768, 1942.

[6] K. J. Astrom and T. Haglund, Automatic Tuning of PID Controllers, 1st ed. Research Triangle Park, NC: Instrum. Soc. Amer., 1988.

[7] K. J. Astrom and T. Haglund, PID Controllers: Theory, Design andTuning, 2nd ed. Research Triangle Park, NC: Instrum. Soc. Amer.,1995.

[8] Á. Cuenca, J. Salt, A. Sala and R. Piza, "A Delay-Dependent Dual-Rate PID Controller Over an Ethernet Network," in IEEE Transactions on Industrial Informatics, vol. 7, no. 1, pp. 18-29, Feb. 2011.

[9] H. B. J. Derbel, "Design of PID controllers for time-delay systems by the pole compensation technique," 2009 6th International Multi-Conference on Systems, Signals and Devices, Djerba, 2009, pp. 1-6

[10] A. Cuenca, J. Salt and V. Casanova, "Multi-rate PID Controller for a Networked Control System," 2007 IEEE International Symposium on Industrial Electronics, Vigo, 2007, pp. 2882-2886

[11] R. Olfati-Saber, J. A. Fax and R. M. Murray, "Consensus and Cooperation in Networked Multi-Agent Systems," in Proceedings of the IEEE, vol. 95, no. 1, pp. 215-233, Jan. 2007.

[12] L. H. Dreinhoefer, "Controller tuning for a slow nonlinear process," in IEEE Control Systems Magazine, vol. 8, no. 2, pp. 56-60, April 1988.

[13] A. Mirzal, "Delay compensation using PID controller and GA," 2013 IEEE International Conference on Control System, Computing and Engineering, Mindeb, 2013, pp. 300-304.

[14] J. Tornero, M. Tomizuka, C. Camina, E. Ballester and R. Piza, "Design of dual-rate PID controllers," Control Applications, 2001. (CCA '01). Proceedings of the 2001 IEEE International Conference on, Mexico City, 2001, pp. 859-865.

[15] F. Haugen, “The Good Gain Method for Simple Experimental Tuning of PI Controllers,” Norwegian Society of Automatic Control, 2012. Modeling, Identification and Control, Vol. 33, No. 4, 2012, pp. 141-152.

[16] F. Haugen, “The Good Gain Method for PI(D) Controller Tuning.” Tech Teach,2010 retrieved from http://techteach.no

[17] D.Pansari, B.Timande, D.Chandrakar, “A Design of Robust PID Controller for Non-Minnimum Network Control System.” in International Journal of Advance in Engineering & Technology, Vol. 5, Issue 1, pp. 486-493, Nov 2012.

Agarwood Grading Estimation using Artificial Neural Network Technique and Carving Automation

Muhammad Syafiq Afif Bin Ishak
Faculty of Electrical Engineering
Universiti Teknologi Malaysia
Johor Bahru, Malaysia.
syafiq0115@gmail.com

Mohd Amri Bin Md Yunus
Department of Control and Mechatronic
Faculty of Electrical Engineering
Universiti Teknologi Malaysia
Johor Bahru, Malaysia.
amri@fke.utm.my

***Abstract*— Agarwood is a fragrant dark resinous wood formed when Aquilaria tress infected with a certain type of mould and appears like wood defects. It a most valuable non-timber product has been traded in international markets because of its distinctive aroma, and can be processed into incense and perfumes. Agarwood grade is determined by wood several characteristics, such as black color intensity, smell, texture and weight through visual inspection. However, this could lead to several problems such as false grading results. Traditionally, the carving process of separation the uninfected Aquilaria wood that lacks of the dark resinous accomplished by using simple tools like knife and chisel. Hence, an expert worker is required to complete the task. In this paper, the Artificial Neural Network (ANN) technique is used to classify the Agarwood based on the features extraction from Gabor Filter and percentage of black color estimation. At first, the images of seven groups of wood defects or knots are identified: dry, decayed, edge, encased, horn, leaf, and sound defect with total sample of 410 knots. Then, these images of knots are matched into three grade groups of Agarwood. Next, the experimental results show the Agarwood can be classified into three grades groups based on knot and black intensity. A set of selected images of knots were used as trace pattern and carved on pieces of wood blocks by using a Computer Numerical Control (CNC) machine where the total time taken for each carving process was calculated. For each image, two Gabor Filter features and percentage of black color were used as ANN inputs. In conclusion the total accuracy of the experiments is 98% and the total time of carving is increased with the increased of grade group number.**

Keywords*— *Articial Neural Network (ANN); Agarwood grading system; Computer Numerical Control (CNC) machine

I. INTRODUCTION

In Malaysia, Agarwood is known as Depu, Gaharu or Cendana [1]. Otherwise, it also known as Agarwood or Eagleswood (British), Agar (India), Aloeswood (Bible), Adlerholz (German), Ahalim (Hebrew), Bais d'angle (Perancis), Ch'en Hsiang (China), Chan Krasna (Kemboja), Ghara (New Guinea), Ingkaras or Kaju Alim or Tanduk (Indonesia), Jin-ko (Jepun), Mai Kritsana (Thailand), Mai Ketsana (Laos), Ogoru (Assamese), Oud (Arab), Poa D'aquila (Portugis), Tengala (Brunei), and Tram Hurong (Vietnam) [1-5]. Agarwood is a fragrant wood that is usually derived from the infected timber of the genus Aquilaria Thymelaeceae or locally known as Karas [4, 6] and often occurs as dark coloured patches or streaks in the tree [5]. Karas or Aquilaria is the tree that will produce Agarwood. Meanwhile, Agarwood refers to products or goods resulting from physical injury and mechanical either naturally or man-made which is bacteria injection or inculated [1]. There are 28 species of Aquilaria found in the world [7]. Mainly, in Malaysia only 5 species of Aquilaria can be found which is Aquilaria Beccariana, Aquilaria Hirta, Aquilaria Malaccensis, Aquilaria Microcarpa, and Aquilaria Rostrata [1, 7]. But, there are also introduced new species in Malaysia which are Aquilaria Sinensis, Aquilaria Crassna and Aquilaria Crassna-Hybri [1]. Agarwood is an important non-timber forest product. Agriculturalist sees the plantation of Agarwood as a green 'gold mine' of the future, if there is a breakthrough in processing technology.

Agarwood is consumed for three main purposes which are medicine, perfume, and incense [3-5, 8]. For thousand years, Agarwood has been used for medicinal purpose and continues to be used in Ayurvedic, Tibetan, and traditional East Asian medicine [3]. It is used for treating pleurisy, asthma, rheumatism and jaundice. It is also known to be beneficial to the liver, lungs and stomach. Agarwood is used as incense in Buddhist, Muslims and Hindus religious ceremonies [8]. Both Agarwood smoke and oil are normally used as perfume in the Middle East [3]. Agarwood has become the most valuable non-timber forest product traded in the international market [8]. These species have been listed under Appendix II for Convention on International Trade in Endangered Species of Wild Fauna and Flora (CITES). CITIES aims to ensure that the trade is well-regulated, and that it proceeds under a system of permits based on conditions of legality and sustainability [6].

Agarwood are produced in three forms, namely woodchips, sawdust and oil. The higher-grade Agarwood are sold in the marketing chain with minimal processing. Meanwhile, the lower grade Agarwood are processed into oil through distillation. However, the manual carving process of getting a valuable core of Agarwood required experienced. The uninfected part of the wood is removed to ensure that the wood is categorized as a better grade and hence higher prices [8]. This process only required simple tools such as knife and chisel.

This paper discuss the development of a system for grading the Agarwoood using Artificial Neural Network (ANN) technique and the implementation of carving automation by Computer Numerical Control (CNC) machine for valuable core acquisition of Agarwood.

The rest of this paper organized as follow. In section II, the literature review on basic principle of Artificial Neural Network and Agarwood grading system are discussed. In section III, the methodology of this research is explained. Section IV discusses the result obtained from the experiments. In section V, the conclusion is expounded.

II. Literature Review

A. Basic Principle of Artificial Neural Network

The idea of neural network development was established based on biological neuron. The human brain is comprised of a network of neurons that are coupled with receptors (dendrites) and effectors (axons). A neural network is a highly-interconnected processing elements of large number of sample [9, 10]. A biological neuron is shown in Fig. 1. By analogy from [11], the output processing element (axon) branches out and become the input to many other processing elements. These signals pass through connection weights (synaptic junction) that correspond to the synaptic strength of the neural connection. The input signal to a processing element are conditioned by the connection weights prior to being summed by the processing element.

Fig. 2 illustrates the artificial neural that similar function as compared to biological neuron. The processing elements joined together to form an appropriate network with adjustable weighting function for each input. This processing element is organized in a sequence of layer. Each layer is connected to each other. Commonly, there are three or more layers. These layers are an input layer, an output layer and hidden layer. An ANN can be used to solve classification, clustering and regression of related problems [9, 11].

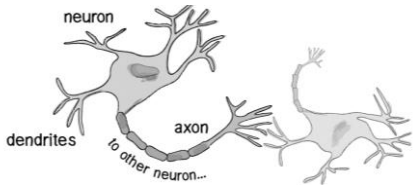

Fig. 1. The depiction of a biological neuron.

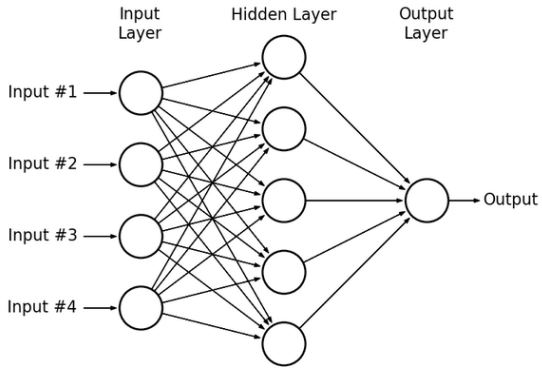

Fig. 2. A generic ANN structure.

B. Agarwood Grading System

In common Agarwood is graded in grade A, grade B, grade C and Grade D. The grading system varies in different countries. The process of grading is depending on the intensity of black color, smell, texture and weight of Agarwood. These are the characteristics used by a human expert to grade any Agarwood. Moreover, there is no international and unified standard for Agarwood until now.

Forest Department of Peninsular Malaysia (FDPM) has introduced their grading system which is based on the color of Agarwood resin and their potential end use [7]. This grading system is represented in Table I. Another grading system was introduced by Mazlan and Dahlan (2010) [12]. This system is divided into nine grades. In grade A and B, it has a subgrade which is break down into A1 to A10 and B1 to B10. This grading system is summarized in Table II.

TABLE I. AGARWOOD GRADING SYSTEM BY FDPM

Grade	Resin color	Potential used
Super A	All color with attractive shape	Decoration or esthetical value
A	Black or shiny black	Aromatherapy or burnt for fragrance
B	Brown or dark brown	Aromatherapy or burnt for fragrance
C	Whitish or yellowish	Essential oil.

TABLE II. AGARWOOD GRADE FOUND IN MALAYSIA MARKET

Grade	Resin coverage on the surface	Resin color	Wood shape
Super king	Entire	Total black and shiny	Solid wood chunks (500g to 3kg)
Triple king	Entire	Total black and shiny	Solid wood chunks (200g to 500g)
Double super	90%	Less black and shiny	Solid wood chunks (50g to 200g)
Super	80%	Black and greyish	Solid wood chunks of mixed sizes
A (A1-A10)	Entire	Black turning into grey	Solid wood chunks of mixed sizes
AB	Entire	Black turning into brown	Solid wood chunks of mixed sizes
B (B1-B10)	Entire	Black turning into brown	Solid wood chunks of mixed sizes
C	50%	Grey	Varies in shapes and sizes
D	Entire	Grey and whitish	Varies in shapes and sizes

III. Research Methodology

A. Project Overview

This study covers both simulation and hardware works. Where the simulation parts are MATLAB software for ANN and thresholding technique, while Inkscape software for getting *gcode*. Then, hardware part is CNC machine for automation carving process. The general block diagram for this project is shows in Fig. 3.

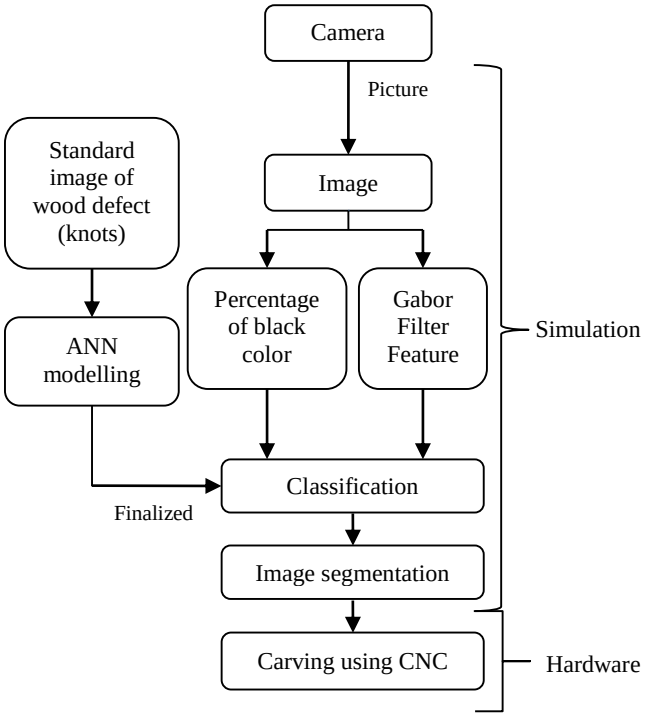

Fig. 3. The project flow of this study.

After the process of ANN modelling using the standard picture of wood is taken before carving. Then, the picture is converted into grey color ad 32x32 pixel size format. The image is also transformed by Gabor Filter for two features of mean and standard deviation. The grade estimation can be obtained from the ANN classification model which was estimated based on standard images of wood defects (knots), and matched it with appropriate Agarwood grade group member. After the grade is estimated, the image is segmented through thresholding technique into wanted and unwanted parts in the image segmentation process. Then, Inskscape software is used to get the *gcode* for CNC machine. Lastly the process of carving utilized SpectraLight Machining Center. From the thresholded image, the CNC is automatically operated to remove unwanted parts which marked as blacked part of the final image.

B. Sample Preparation for ANN

The sample of wood defect is taken form the University of Oulu Wood and Knot Database [13]. The defect on each sample is perceived as knots of wood. This knot consists of seven group which are decayed knot, dry knot, edge knot, encased knot, horn knot, leaf knot and sound knot. Fig. 4 shows the difference shapes of knots used in this project. These knots will categorize into three grade which are grade 1, grade 2 and grade 3. Table III shows the grading system for this project. This categorization is based on the shape and intensity of black color of the knot. To match the defects level with Agarwood group grade: grade 1 is the good grade, grade 2 the is moderate grade and grade is the lower grade.

TABLE III. SAMPLE DATA

Grade	Type of knot	No of sample
1	Encased	49
2	Horn and edge	90
3	Dry, decayed, leaf and sound	271

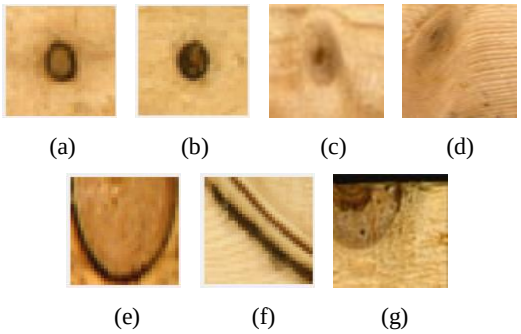

Fig. 4. (a) dry knot; (b) decayed knot; (c) sound knot; (d) leaf knot; (e) encased knot; (f) horn knot; (g) edge knot

C. Features Extraction

The features used are texture features extracted from knot image using a Gabor filter bank and also the percentage of the black color of knot. The Gabor filters are 2D selective band pass filter which is frequency and orientation sensitive respectively [14]. Basically, using this filter, the filtered image is dilated, translated and rotated with regard to each other [14]. The mathematical definition is

$$G_{f,\theta}(x,y) = exp\left[\sqrt{-1}(xfcos\theta + yfcos\theta) - \frac{f^2(x^2+y^2)}{2\sigma^2}\right] \quad (1)$$

Where x and y are the pixel coordinate of the image. f is the central frequency of the band pass. θ is the orientation of the filter and σ is the bandwidth. θ is varying to look for texture oriented in a particular direction. While, varying σ to change the support of the basis or the size of the image region being analyzed.

Basically, each image is converted to grayscale and normalized to size 32 x 32 pixels. A set of Gabor filter is utilized with six frequencies (0°, 30°, 60°, 90°, 120°, 150°) and six orientations (2.828, 5.657, 11.314, 22.627, 45.255, 90.51). The image is converted with these set filter bank. The result is 36 filtered images. This will give a difference information for each image corresponding to the orientation and frequency. Then, the output image is linked together by row to build a features vector of dimension 1024 x 36.

Meanwhile, the percentage black color of image is taken from this mathematical expression:

$$\%Black = \left(\frac{1-a}{b}\right) * 100 \quad (2)$$

Where a is the number of non-zero matrix and b is the number of array elements. Therefore, mean, standard deviation and percentage black color of each image are extracted and fed to the ANN classification.

D. Features Selection

Features selection can expand the generalization, so avoid the problem of dimensionality and diminish the computational requirement of the classifier [14]. This is a process of selecting or removing the number of features based on the data from features while maintaining or improving the classification accuracy. In this study, the features selection by considering the values of mean and standard deviation extracted from Gabor Filter and percentage of black color. Some part of the data is removed after it was determined as outliers.

E. Artificial Neural Network (ANN) Classification Model

This study utilized try and error method and resulted in a three-layer ANN model structure. Fig. 5 shows the architecture of a three-layers ANN. The dataset splited into three parts which is 70% of dataset is for training, 20% of dataset for testing and 10 % of dataset for validation. These parts are selected randomly from the original whole set of data.

The initialization of weight is selected form non-zero value between interval of [-1,1]. But this initialize value need to re-select and go through the same training to reach global minima. During the training session, the weight is updated from train dataset then applying validation dataset to avoid over-fitting. For stopping citeria, the number of neuron in hidden layer will varied until achieved Mean Squared Error (MSE) approximately to 0.01 without disturbing the performance.

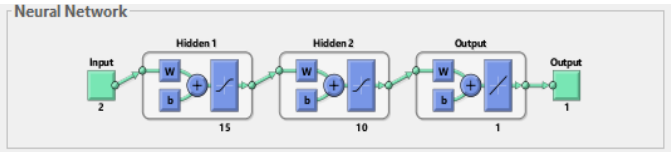

Fig. 5. Three-layer ANN.

F. Input for ANN

There are three inputs for Artificial Neural Network. Two inputs are from the extracted features of Gabor Filter output and one input from the total percentage of black color. These inputs are means, standard deviation and percentage black color of the sample. For this study, the total number of sample is 410. Each sample has values of means, standard deviation and percentage of black color.

G. Hidden Layer and Node for ANN

Usually, the neural network is made up of one or more neurons layer interconnected between input layer, hidden layer and output layer. Depending on the design structure of network, each layer has the number of nodes connected to other nodes in the other layer. The propagation of information flow in single direction from input to the neurons output layer in the network training.

Inputs are received by the input layer, which performs as a data distribution center and fans out the inputs to the first hidden layer. Each hidden layer will first activate and transform the data before propagating them to the next layer. This process is repeated through each hidden layer until finally all of the outputs from the last hidden layer will be reunited in the output layer to produce the network outputs. For this study, the three Multi-Layer Propagates is used using the trial and error approach.

H. Threshold

Each image will go through thresholding in order to differentiate between the wanted and unwanted parts. In this process, image will be converted to black and white where black is unwanted part and white is wanted part. The threshold weight range on the scale between 0 to 1. Each threshold weight will produce different coverage of blacked area of the image.

I. Computer Numerical Control (CNC) Machine

The type of CNC machine utilized in this study is SpectraLight 0200 Machining Center as shows in Fig. 6. This machine is used for carving process in acquiring valuable Agarwood core. This machine is a three-axis milling machine that can be run directly from computer and accepts standard EIA RS-274D G&M code programming. The work area is limited to 13 inches x 2.75 inches (330mm x 70mm). It can travel about 8.5 inches (216mm) along X-axis, 4.5 inches (114mm) along Y-axis and 5.5 inches (140mm) along Z-axis. For this project, the *gcode* for CNC machine is taken form Inkscape software.

Fig. 6. SpectraLight 0200 Machining Center.

IV. Result And Discussion

This experiment was implemented in MATLAB R2016a and computer Lenovo Ideapad z585 with a processor of AMD A6-4400M APU with a Radeon HD Graphics of 2.70 GHz and a 4 GB RAM. The separation of group for grading system is based on the percentage of black color and shape for each wood knots. By using the Eq. 2, the percentage of black color of dataset can be categorized into three groups with specific knots corresponding to the mean and standard deviation. The results are shown in the Table IV. The input data for classification is represented in three-dimension graph in Fig. 7.

TABLE IV. CLASSIFICATION BASED ON PERCENTAGE OF BLACK COLOR

Grade	Type of knot	Percentage of black color (%)
1	Encased	51-100
2	Horn and edge	31-50
3	Dry, sound, decayed and leaf	0 -30

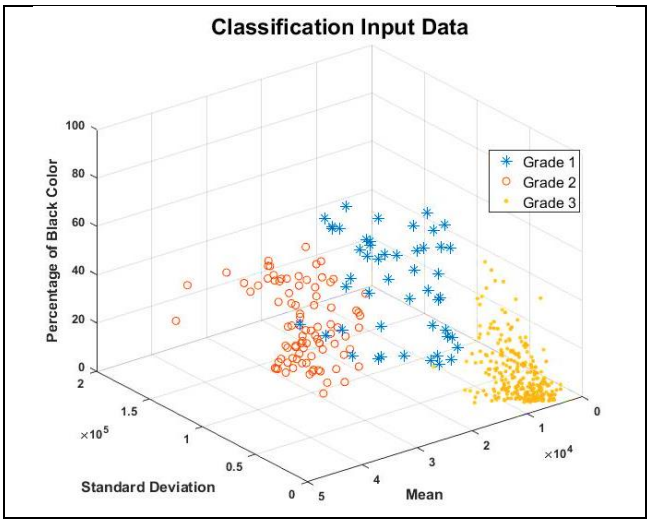

Fig. 7. Three-dimension classification input data.

For ANN, the experiment was carried out by varying the number of neurons in both hidden layers. First experiment involved varying the number of neurons in the first hidden layer but fixing the number of neurons in second layer. Second experiment involved varying the number of neurons in the second hidden layer but fixing the number of neurons in the first layer. Both experiments were tested on the same dataset of training, validation and testing. The activation function is sigmoidal with scalar output 0 (false) and 1 (true). The result for the the first and second experiments are shown in Table V and VI, respectively.

For Table V, the testing accuracy is increased every time when the number of neurons in the hidden layer 1 is increased. But at 16 neurons, the accuracy is slightly decreased. From Table VI, the testing accuracy is increased when the number of neurons in the hidden layer 2 is increased but slightly decreased when the total number of neurons reached 11. Overfitting of data had caused the decreased in the accuracy. Therefore, the results shown that the best ANN structure is with three input neurons, 15 first hidden layer neurons and 10 second hidden layer neurons. There are 3 out of 85 number of sample error classifications for this testing accuracy where the dataset was selected randomly. The final ANN model structure applied for this experiment is shown in Fig. 8.

TABLE V. RESULT FOR VARYING NUMBER OF NEURONS IN FIRST HIDDEN LAYER

Network Structure			Mean Squared Error	Clustering Accuracy (%)	
Input	*Hidden 1*	*Hidden 2*		*Training*	*Testing*
3	9	5	0.01	100	92.41
3	10	5	0.01	100	95.78
3	11	5	0.01	100	96.72
3	12	5	0.01	100	97.33
3	13	5	0.01	100	97.51
3	14	5	0.01	100	98.11
3	15	5	0.01	100	98.21
3	16	5	0.01	100	97.46

TABLE VI. RESULT FOR VARYING NUMBER OF NEURONS IN SECOND HIDDEN LAYER

Network Structure			Mean Squared Error	Clustering Accuracy (%)	
Input	*Hidden 1*	*Hidden 2*		*Training*	*Testing*
3	15	6	0.01	100	93.12
3	15	7	0.01	100	94.03
3	15	8	0.01	100	96.30
3	15	9	0.01	100	98.50
3	15	10	0.01	100	98.54
3	15	11	0.01	100	97.91

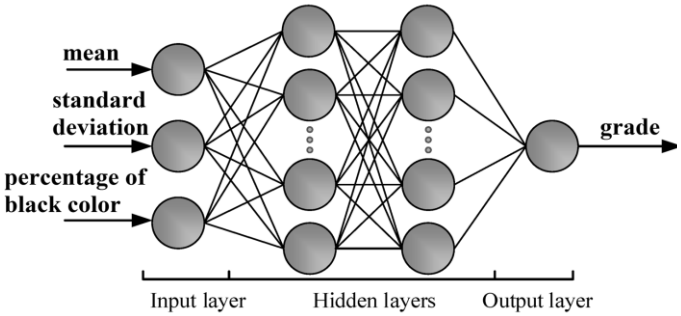

Fig. 8. ANN structure used

The carving process was carried out by SpectraLight 0200 Machining Center using cylinder drill with diameter size of 3.175 mm. The test sample was prepared using regular wood with dimension of 8cm x 6cm and thickness of 2cm. The size of working area is set to 6cm x 6cm. The results of carving process are shown in the Table VII. The result for sample after carving 1mm depth shown in Fig. 9.

The results in table VII show that the removed wood weight and time taken are increasing with the increasing number of grade. But, the removed wood weight depends on the covered black areas of Agarwood. If the total black area is large, the removed wood weight is less. This also will effect the total time taken to complete the carving process. From this experiment, the carving process can be accomplished by using CNC machine to minimize the total time taken to complete the process.

TABLE VII. RESULT FOR CARVING EXPERIMENT

Sample type	Depth drill	Weight removed	Time taken
Grade 1	1mm	0.84g	4m 35s
Grade 2	1mm	0.91g	5m 44s
Grade 3	1mm	1.05g	6m 55s

Fig. 9. Sample result after carving 1mm depth.

V. CONCLUSION

In this paper, a three-layer Artificial Neural Network is utilized, built from 3 number of input neurons, 15 number of first hidden layer neurons, 10 number of second hidden layer neurons and 1 output. The inputs were extracted from Gabor filter (mean and standard deviation) and percentage of black color. The data was classified into three grades based on percentage of black color and wood knots. The results of ANN are satisfied with an accuracy 98.54%. The carving process was accomplished by using a CNC machine. The removed wood weight is proportional to the blacked area. The time taken to complete also depends on the covered black area of and complexity of the shape.

REFERENCES

[1] I. Muhammad, "Cabaran dan Halatuju Perladangan Karas di Malaysia," *Bengkel Gaharu Sesi I-2014, Fakulti Perhutanan, Universiti Putra Malaysia, 43400 UPM Serdang, Selangor, Malaysia* 10 Mac 2014.

[2] A. Barden, N. A. Anak, T. Muliken, and M. Song, "Heart of the Matter: Gaharu and Trade and CITES Implementation for Aquilaria malaccensis," *TRAFFIC*, 2001.

[3] A. Abdullah, N. K. N. Ismail, T. A. A. Kadir, J. M. Zain, N. A. Jusoh, and N. M. Ali, "Agar Wood Grade Determination System Using Image Processing," 2007.

[4] L. S. L. Chua, "Agarwood (Aquilaria malaccensis) in Malaysia," *Forest Research Institute Malaysia*, 2008.

[5] Y. Nik Yasmin, "Comparison of chemical profiles of selected gaharu oils from Peninsular Malaysia," *Malaysian Journal of Analytical Sciences*, vol. 12, pp. 338-340, 2008.

[6] L. T. Wyn and N. A. Anak, "WOOD FOR THE TREES: A REVIEW OF THE AGARWOOD (GAHARU) TRADE IN," 2010.

[7] *Manual Penggredan Gaharu Jabatan Perhutanan Semenanjung Malaysia*. Malaysia: Alamedia Sdn. Bhd., 2015.

[8] H. F. Lim, M. P. Mamat, and Y. S. Chang, "Production, use and trade of gaharu in Peninsular Malaysia," 2007.

[9] R. E. Uhrig, "Introduction to artificial neural networks," in *Industrial Electronics, Control, and Instrumentation, 1995., Proceedings of the 1995 IEEE IECON 21st International Conference on*, 1995, pp. 33-37 vol.1.

[10] D. Qi, P. Zhang, and L. Yu, "Study on wood defect detection based on artificial neural network," in *2008 IEEE Conference on Cybernetics and Intelligent Systems*, 2008, pp. 951-956.

[11] A. Dongare, R. Kharde, and A. D. Kachare, "Introduction to artificial neural network," *International Journal of Engineering and Innovative Technology (IJEIT)*, vol. 2, pp. 189-193, 2012.

[12] M. Mazlan and T. Dahlan, *Pengredan dan Pemprosesan Gaharu. Selangor: Seminar Kebangsaan dan Pameran Gaharu*, 2010.

[13] (September). *University of Oulu Wood and Knot Database*. Available: http://www.ee.oulu.fi/research/ imag/knots/KNOTS/

[14] A. Marcano-Cedeño, J. Quintanilla-Domínguez, and D. Andina, "Wood defects classification using Artificial Metaplasticity neural network," in *2009 35th Annual Conference of IEEE Industrial Electronics*, 2009, pp. 3422-3427.

Energy Scavenging from Waste Heat of Home Refrigerator

Nur Afni Izyani Zainuddin
Faculty of Electrical Engineering
Universiti Teknologi Malaysia
Johor Bahru, Malaysia.
afniizyani94@gmail.com

Herman Wahid
Department of Control and Mechatronic Engineering
Faculty of Electrical Engineering
Universiti Teknologi Malaysia
Johor Bahru, Malaysia.
herman@utm.my

***Abstract*—In recent years, the environmental issues such as emissions and global warming are due to the limiting factor of the energy resources .Extensive researches on new technologies of power generation are currently ongoing. Thermoelectric power generators (TEG) have emerged as another promising green technology due to their diverse advantages. A TEG is usually having two junctions incorporating different metals or alloys. If heat is introduced to a circuit at the junction of two different conductors, a current will be generated. In this project, a prototype of TEG system will be designed to prove that it can generate electricity using waste heat. The goal of this project is to propose a solution for harvesting waste heat from refrigerator's compressor unit. Thermoelectric cooling module (TEC), a sensor module based on the principle of Seebeck effect is used to achieve the project aim. Heat sinks and aluminum are attached to TEC module to maximize the temperature difference. The output voltages may need to be amplified and regulated with suitable conditioning circuits. These output voltages are expected could be used for charging the low-powered portable gadgets such as mobile phone and tablet.**

Keywords—Thermoelectric generator; Thermoelectric cooler; Seebeck effect

I. INTRODUCTION

In our daily life, we will definitely be using electricity no matter in any aspect of usage. Electricity has benefited not only to humans but also to the development of a country. In many countries, electricity is mainly generated by burning fossil fuels such as natural gas, oil and coal. Now, after more than 200 years of using it, this type of energy sources has dwindled. One of the best solutions to reduce the use of fossil fuels in generating electricity is by using thermoelectric generator. Besides that, waste from the combustion process can be recycled through the thermoelectric generator. The thermoelectric power generation is based on the Seebeck Effect. Statistic shows that only 34% of the energy becomes useful energy and the rest 66% are contribute to energy loss or waste heat. In order to reduce waste heat, thermoelectric generator (TEG) is one of the alternative solutions to produce energy from waste heat. For this project, heat energy will be harvested from the compressor of refrigerator and the voltage generated from waste heat could be used to charge low-power portable gadgets (e.g.: mobile phone).

The operation of home appliances produce waste heat and it is a loss that can lead to greenhouse effect. Generation of energy from waste heat by using thermoelectric effect is a promising solution. However, suitable power conditioning circuit needs to be designed as thermoelectric generator will produce fluctuated output voltage with very low output power/current for limited temperature deviation.

The specific objectives of this project are to study the available energy harvesting technologies which focusing on waste heat based sources, through literature studies, to study the generation of regulated voltages using TEG module on refrigerator compressor and to design energy storage system, using suitable circuitries design and to analyze the designed model for its performance, reliability, energy efficiency and capability of being used practically as portable charger.

This paper is organized as follows: in Section I, an introduction along with the problem statement and objectives was addressed. Section II describes the literature review related to the project. In addition, Section III explained the project methodology to develop the proposed system. In the last two sections, results and analysis were tabulated and discussed followed by the conclusion section.

II. LITERATURE REVIEW

Literature review was carried out right through the whole project to increase the knowledge and skills needed to complete this project. The main sources for this project are previous related projects, research thesis, journals, and articles which are mostly obtained from online database provided by UTM and UTM library.

A. Electrical Energy Scavenging From Waste Heat

Whenever a work is done, small to large amounts of thermal energy is intemperate into air, which if converted back to electric energy may serve useful purpose [3]. Harvesting energy from previously unemployed ambient sources can play important role in saving energy and reducing the dependency to primary power sources (AC power or battery) of an electronic system [4].

B. Energy Harvesting Using Thermoelectric Modules

The design of a thermoelectric generator (TEG) unit (see Fig. 1) as a solid state device using Seebeck effect of converting heat energy into electricity is dependent on the correct thermal gradient across the thermoelectric modules for the optimal operation of these modules [5]. Thermoelectric power

generators deal with a rare and attractive back-up compare to conventional batteries due to its waste heat energy harvesting potentials. It is particularly suited for many low power and portable electronics such as for supporting unattended sensors and wireless devices [3].

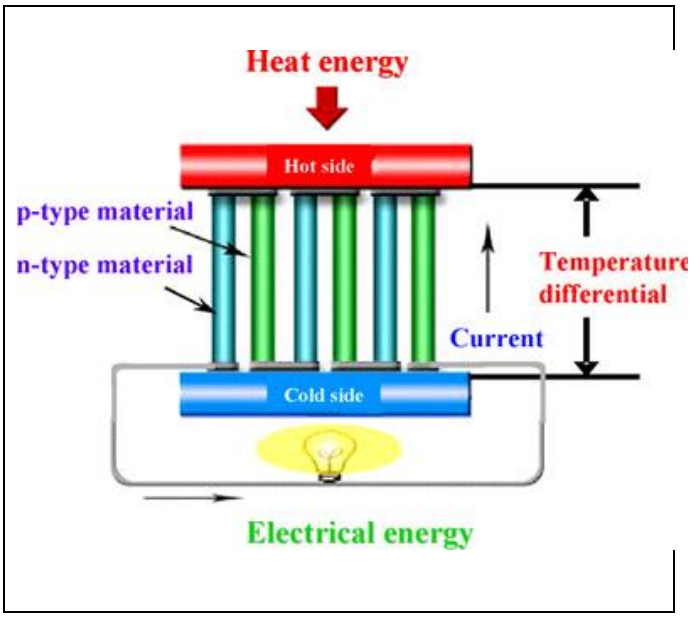

Fig. 1. Thermoelectric generator (TEG)

C. Seebeck Effect

The Seebeck effect is the conversion of temperature differences directly into electricity and is named after the Baltic German physicist Thomas Johann Seebeck. Seebeck, in 1821, discovered that a compass needle would be deflected by a closed loop formed by two different metals joined in two places, with a temperature difference between the junctions. The Seebeck effect is a classic example of an electromotive force (emf) and leads to measurable currents or voltages in the same way as any other emf [7].

D. Physical Parameters of Thermoelectric

Three parameters are considered in the classification of thermoelectric materials: electrical conductivity σ, thermal conductivity λ, and the Seebeck coefficient, α. Electrical conductivity is given as the product of the concentration and the mobility of charge carriers. It is high with metals, very low with insulators, with an intermediate position taken by semiconductors. The three parameters mentioned above depending on carrier concentration (see Fig. 2) form the essential part of it. There are two components of the thermal conductivity: lattice vibration and the electronic part. The latter also increases with carrier concentration and typically contributes about one third to the thermal conductivity. The maximum of the quantity A2σ (the numerator of the equation for the figure of merit) falls into the realm of semiconductors (see Fig. 2). Consequently, semiconductors have been the materials of choice for further development of thermoelectric devices. Thermoelectric devices have been further classified with respect to the temperature ranges over which they can be usefully employed [8].

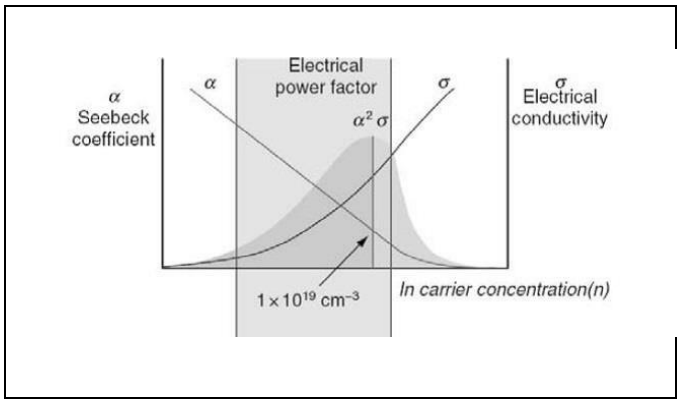

Fig. 2. Dependence of electrical conductivity, Seebeck coefficient, power factor and electrical conductivity on concentration of free carriers [7]

III. Project Methodology

In this project of energy scavenging from refrigerator waste heat, there are several things that need to be covered under the project scope. The scope consists of hardware and software elements. The hardware elements include thermoelectric cooling module (TEC 12710), heat sinks, aluminum plates, operational amplifiers (LM358), capacitor bank, arduino UNO and LCD display. On the other hand, the software elements involve Matlab to simulate the design circuit and Arduino software for display programming.

A. Project Design

Based on the Seebeck principles of thermocouple, a small electrical energy is produced (in millivolts) when there are temperature differences between hot and cold side of TEC modules. Hence, the output voltages may need to be amplified and regulated with suitable conditioning circuits. These output voltages are expected could be used for charging the low-powered portable gadgets such as mobile phone and tablet. As shown in Fig. 3, the project design shows from the harvesting process of TEC modules, the amplification process at the conditioning circuit, storage of amplified voltage to the USB head as the output to charge the low-powered portable gadgets.

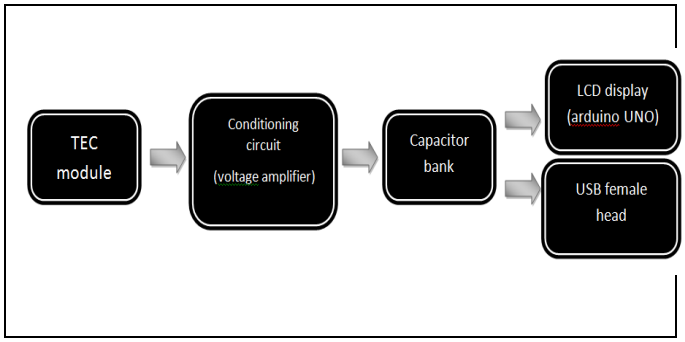

Fig. 3. Project design

LM358 is chosen as the voltage amplifier because this device consist of high gain frequency compensated operational amplifiers and it also have two independent operational amplifiers in one chip. Since the voltage output is fluctuated, a storage need to store the fluctuate voltage. Then the voltage stored can be adjusted it output from the storage for charging

low-power portable gadgets. Fig. 4 shows the design of TEC module.

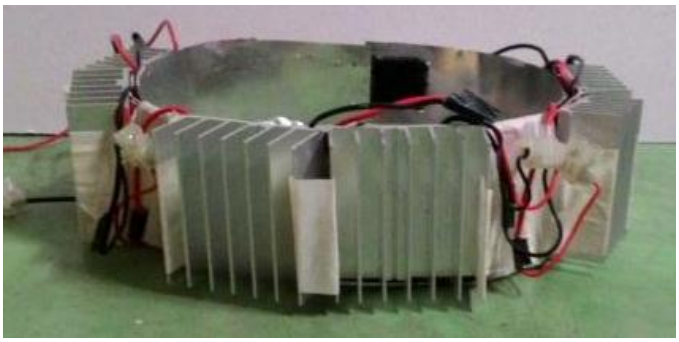

Fig. 4. Design of TEC module

B. Operational Framework

The heat waste first harvested and collected from the refrigerator compressor. Then, the waste heat is converted into electrical energy using TEC module. Voltage output generated pass through conditioning circuit, voltage amplifier. Amplified output voltage then stored into capacitor bank before being use as portable charger. LCD display will indicate the voltage reading and whether the USB is charging (see Fig. 5).

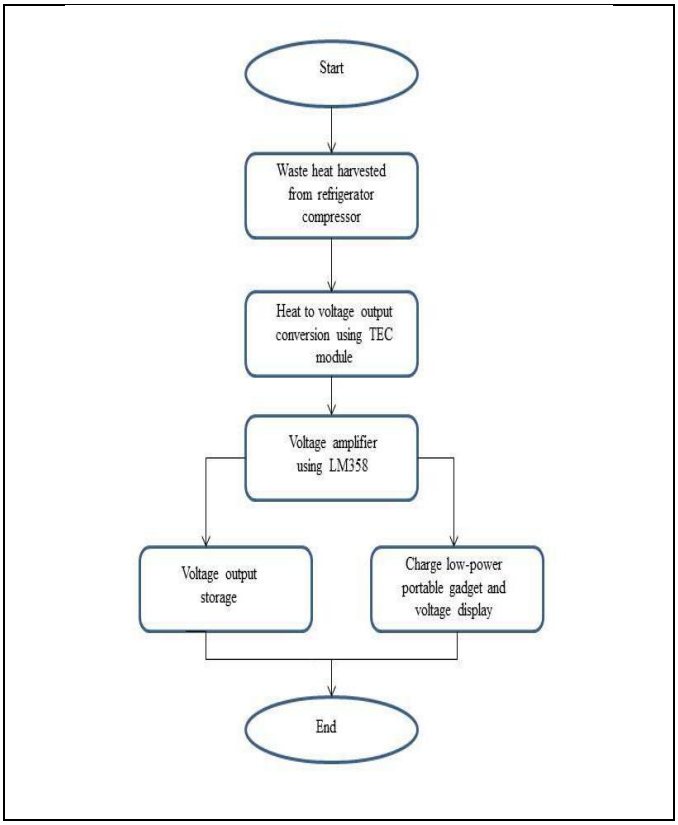

Fig. 5. Project flowchart

IV. Result & Analysis

At the end of this project there are four expected outcome that need to be accomplished. First expectation from this project is, available energy harvesting technology which focusing on waste heat based source such as TEG will harvest and collect heat waste from refrigerator compressor. Second, the collected waste heat to generation of regulated voltages conversion using TEG module. Next, a conditioning circuit is required to amplify the generated voltage and suitable circuitries design as energy storage system to achieve desired voltage output. Lastly, the designed model capability of being used practically as portable charger.

A. Generation of voltage produced by TEC modules

Table I shows the output voltages along with the temperature difference between hot side and cold side of six TEC modules with heat sink attached to the refrigerator compressor. The table also shown the temperature of the hot side and cold side of six TEC modules.

TABLE I. Results for TEC Module with Heat Sink (Raw Output)

Hot side temperature (°C)	Cold side temperature (°C)	Temperature difference (°C)	Output voltage (V)
52.00	33.00	19.00	0.43
51.80	33.00	18.80	0.45
53.80	34.00	19.80	0.44
54.00	34.00	20.00	0.49
54.00	34.00	20.00	0.48
55.00	34.00	21.00	0.52

B. Generation of voltage produced by TEC modules after amplification

Table II shows the output voltages along with the temperature difference between hot side and cold side of six TEC modules with heat sink once amplifier circuit attached to the refrigerator compressor. The table also shown the temperature of the hot side and cold side of six TEC modules

TABLE II. Results for TEC Module with Heat Sink and Amplifier (Amplified Output)

Hot side temperature (°C)	Cold side temperature (°C)	Temperature difference (°C)	Output voltage (V)
47.90	33.00	14.90	4.23
51.20	35.00	16.20	4.58
50.10	34.00	16.10	4.57
50.80	34.00	16.80	4.60
50.80	34.00	16.80	4.73
51.90	34.00	17.90	4.97

From Table II, the average voltage output produced by six TEC modules after amplified is 4.61V which is higher than the voltage output from six TEC modules without amplification.

This amplified voltage is tested to charge the low-portable gadget that is mobile phone. The mobile phone was successfully charged with the amplified voltage.

This experiment conducted with random opening of the refrigerator door. The act of opening the refrigerator door will lead to higher voltage. This is because the act of opening the door of refrigerator will turn on the refrigerator compressor. When the temperature inside the refrigerator is not reached its target, the compressor will turn on and cooling the temperature inside refrigerator until it achieved its target. This will lead to higher temperature differences between the hot side and cold side of TEC modules and higher voltage output.

V. CONCLUSION

This project was able to achieve the objective to amplify the voltage produced from TEC modules and charging mobile phone.

The prototype of energy harvesting system from home refrigerator compressor has been successfully developed to achieve the three objectives which are to study the available energy harvesting technologies which focusing on waste heat based sources, through literature studies, to study the generation of regulated voltages using TEG module on refrigerator compressor and to design energy storage system, using suitable circuitries design and to analyze the designed model for its performance, reliability, energy efficiency and capability of being used practically as portable charger.

This prototype of energy harvesting successfully harvest the waste heat from home refrigerator compressor. TEC module can be used to harvest the waste heat but it needs amplifier circuit to amplify the voltage produce from the TEC module. Voltage output from this energy harvesting system can be used to charge low-power portable gadgets.

VI. ACKNOWLEDGEMENT

At the very beginning I would like to express my deepest gratitude to almighty Allah for giving me the strength and the composure to complete my final year project 1 and prepare this report within the scheduled time. Not to forget, the continuous support and courage from my family that keeps me going. Bearing in mind previous I am using this opportunity to express my deepest gratitude and special thanks to my supervisor, Dr. Herman bin Wahid who in spite of being extraordinarily busy with his duties, took time out to hear, guide and keep me on the correct path and allowing me to carry out my project. I express my deepest thanks to him for taking part in giving necessary advices and guidance throughout this semester. I choose this moment to acknowledge his contribution gratefully. I expose myself to independent learning skill. Based on this project, I have a deep knowledge of energy scavenging from home refrigerator waste heat using Thermoelectric Cooling module.

REFERENCES

[1] BCS “Engineering Scoping Study” 2006, pp 4

[2] Dhafer Abdulameer Shnawah, Mohamed Hamid Elsheikh, Mohd Faizul Mohd Sabri, Masjuki Haji Hassan, Mohamed Bashir Ali Bashir, Mahazani Mohamad and Suhana Binti Mohd Said “A review on thermoelectric renewable energy: Principle parameters that affect their performance ” University of Malaya, 2013, pp 2 – 37

[3] Zhou, Y., S. Paul, and S. Bhunia. Harvesting wasted heat in a microprocessor using thermoelectric generators: modeling, analysis and measurement. in Proceedings of the conference on Design, automation and test in Europe. 2008. ACM.

[4] Chen, W.-H., C.-Y. Liao, and C.-I. Hung, A numerical study on the performance of miniature thermoelectric cooler affected by Thomson effect. Applied Energy, 2012. 89(1): p. 464-473.

[5] Ando, O., et al., Acquisition and Monitoring System for TEG Characterization. International Journal of Distributed Sensor Networks, 2014.

[6] Electric Power Generated from Waste Heat, National Institute of Advanced Industrial Science and Technology (AIST), http://www.aist.go.jp/aist_e/latest_research/2005/20050617/20050617.html, 2005

[7] G. Min, “Thermoelectrics Handbook, Macro to Nano”, Thermoelectric Module Design Theories, CRC Press, 2006, pp 41

[8] Andreas Bitschi “Modelling of thermoelectric devices for electric power generation” Technical University of Vienna, 2009

[9] A.Jacks delightus peter, Balaji.D, D.Gowrishankar “Waste heat energy harvesting using thermo electric generator” Hindustan University, Chennai, 2013

[10] Z.B. Tang a, Y.D.Deng a, C.Q.Su a, W.W.Shuai a, C.J.Xie” A Research On Thermoelectric Generator's Electrical Performance Under Temperature Mismatch Conditions For Automotive Waste Heat Recovery System” Wuhan University of Technology, China, 2015

[11] Vargas-Almeida, A., M.A. Olivares-Robles, and P. Camacho-Medina, Thermoelectric System in Different Thermal and Electrical Configurations: Its Impact in the Figure of Merit. Entropy, 2013. 15(6): p. 2162-2180.

[12] Wang, C.-C., C.-I. Hung, and W.-H. Chen, Design of heat sink for improving the performance of thermoelectric generator using two-stage optimization. Energy, 2012. 39(1): p. 236-245.

[13] Patronis, Gene (1987). "Amplifiers". In Glen Ballou. Handbook for Sound Engineers: The New Audio Cyclopedia. Howard W. Sams & Co. p. 493. ISBN 0-672-21983-2.

[14] "Understanding Amplifier Operating "Classes"". electronicdesign.com. Retrieved 2016-06-20.

[15] Robert Boylestad and Louis Nashelsky (1996). Electronic Devices and Circuit Theory, 7th Edition. Prentice Hall College Division. ISBN 978-0-13-375734-7.

[16] Deshpande, R.P. (2014). Capacitors. McGraw-Hill. ISBN 9780071848565.

[17] Dorf, Richard C.; Svoboda, James A. (2001). Introduction to Electric Circuits (5th ed.). New York: John Wiley & Sons. ISBN 9780471386896.

[18] Ulaby, Fawwaz Tayssir (1999). Fundamentals of Applied Electromagnetics. Upper Saddle River, New Jersey: Prentice Hall. ISBN 9780130115546.

[19] "Power Supply Glossary". Aegis Power Systems, Inc. Aegis Power Systems, Inc. Retrieved 15 September 2014.

[20] Kordyban, T., 1998, Hot air rises and heat sinks – Everything you know about cooling electronics is wrong, ASME Press, NY.

[21] M. R. Hajmohammadi, V. Alizadeh Abianeh, M. Moezzinajafabadi and M. Daneshi, Fork-shaped highly conductive pathways for maximum cooling in a heat generating piece, Applied Thermal Engineering, 61 (2013) 228–235.

[22] Bulusu, A. Walker and D. G , “Review of electronic transport models for thermoelectric materials” , 2008

[23] Tritt, Terry, M. Subramanian, M. A. “Thermoelectric Materials, Phenomena, and Applications” , 2011

[24] Neeharika Naik-Dhungel “Waste Heat Streams Classified by Temperature” , 2012

[25] D.A.Reay “Heat Recovery Systems” E & F.N.Span, 1979

Magnet Engine Free Energy Generator

Siti Amirah Binti Ramli
Faculty of Electrical Engineering
Universiti Teknologi Malaysia
Johor Bahru, Malaysia.
Email: miraramli7@gmail.com

Dr. Anita Binti Ahmad
Department of Control and Mechatronics
Faculty of Electrical Engineering
Universiti Teknologi Malaysia
Johor Bahru, Malaysia.
Email: anita@fke.utm.my

***Abstract*—This paper describes a research into an innovation by testing the practicable and viability of the system which is by using water pump in an aquarium to turn on the light in the aquarium. A 12 volt direct current CPU cooling fan is used as the turbine and motor to produce voltage to light up the bulb inside the aquarium. The CPU cooling fan construction consist of brush-less direct current motor which is, it is low torque characteristic motor, long operating life and has rugged construction. The water flow from the pump in the aquarium fall onto the blade of the fan and it will start to rotate. The flowing water must be in specified height to ensure that the blade can rotate very fast and produce constant rotating speed as well as constant output voltage. There is magnet at the center of the fan around the blade and as the commutator inside the fan start to rotate as for the brush-less direct current motor will start to create flux around the magnet. The rotating conductor will cut the flux lines and convert that cutted flux lines into output voltage. Then, an amplifier is used to compare the output voltage from the fan into the amplifier and power up the voltage booster module. The voltage booster connected to the load. As the first segment is completed, the amplifier will be integrated with the DC to DC voltage booster to increase the voltage up to the usable output value. Hence, the output value will be able to power up the load within the range of the resultant voltage produced by the DC to DC voltage booster.**

Keywords—aquarium; water pump; CPU cooling fan; amplifier; DC to DC voltage booster.

I. INTRODUCTION

Nowadays, the cost of energy is continually increasing while environmental concerns are increasing as well as many businesses are turning to green technology to save long-term costs and take advantage of green marketing. Innovation will be needed to manage the trend of rising energy costs in the future and address environmental concerns [1]. This study tests the feasibility of an idea by using an aquarium water pump and CPU cooling fan to produce an output value for low consumption electrical load. Electricity is a crucial and important for human to survive and keep on living. Electricity can be considered as a very efficient way of energy consumption in part because it is weightless as well as easy to distribute. The CPU cooling fan has been used in this system because it has axial flow fan shape which it is rotating in a common unrestricted air space. The axial flow fans come in many variations that all have one thing in common which is they rotate about their axis and they move a column of air parallel to that axis [2]. At the point where electricity generates, it is a renewable form of energy as well as a clean one. The generator can be implemented by using a mini fan or blade which the certain amount of water at a certain height flow onto the blade to make it continuously rotating and will produce voltage and current. The output voltage and current can be the new supply and sources for low power consumption electrical load.

II. LITERATURE REVIEW

The reason why the hydro-generator more favorable because it is a clean source of energy and will last longer which mean it can be used for a long time period. The dynamic head (H), amount of water flowing (Q) and the efficiency of the generator give a crucial influences towards the performance of the system. It is important to know the power potential of a river where the flow, Q of the river is the amount of time (in m3 or litters) that passes in a certain amount of time across a section of the river also it is necessary to know the flow in the river and the available head which is head is the vertical difference in levels (m) through which water falls down [3] .This available power will be converted by the hydro turbine into mechanical power.

The ship propellers are one of the free-form surfaces, such blades are design individually for each application and the various parameters controlling the performances must be considered so the design approach is important [4]. In this paper, the blade design is based on the medial representation of the blades, medial surface with profile curves attached to it. By using suitable parameterization, the B-spline surfaces able to describe the pressure and the suction size of the blade, the design of blades for hydroelectric turbines and ship propellers follows the classical approach. First, the medial surface is designed using the conformal mapping of the projected streamlines. Second, the profile curves are added to the medial surface. The resulting surface is given by a medial surface and profiles attached to it.

The modeling consists of a variable speed micro-hydro turbine coupled to a permanent magnet synchronous generator and connected to the electric grid through an advanced power conditioning system [5]. The stator windings of the system are connected to the next level, which is composed of a three-phase rectifier bridge, a DC-DC converter and a DC-AC power inverter. The generator will spin the

turbine and create pressure in the water.The water will flow out from the water outlet pipe and flowing into the blade as the blade continue to rotate, the electricity will be generated as the electrical circuit will be connected to the water pump block.

A simple dc motor usually consist of a rotor and stator and both of them usually were made up of ferromagnetic and the fin will act as a generator or the motor [6]. The disc shaped magnets are placed in such a way that all the north poles and south poles are facing at the same directions so both of the magnetic field repel each other which cause the fins to move. As the fin or the blades are rotating, it will cut the flux line and electricity will be produce as follow the Faraday's Law [6, 7].

In a simple motor, magnetic field generated by the coils generally Cu and Al where these motors continuously need electrical supply to produce magnetic field and there will be a huge amount of losses occur.

According to Donald Lee Smith, the basic unit of electricity is electrons. Electrons are defined as being the practical source of electrical and magnetic energy and now it is universally accepted that the electron exists and one of the sources of electrical energy. When the electron is agitated, it produce magnetic and negative electrical energy and physics still cannot explain why the electron remains intact and is not diminished by the energy it release [8].

Upon the encountering a moving magnetic field spins, it giving off an electric impulse. Therefore, magnetic and electric are two sides of the same coin. When it is done consecutively, each cycle pushes current forward while pulling electron into the system where the electrons are obtained from earth and air grounding [9]. Useful electrical energy is obtained directly from electron spin induced by incoming magnetic wave or indirectly through mechanical exchange as in dynamo type devices. Simply put, electron spin converts from magnetic to electrical energy and vice versa. The Magnetic Wave which is Faraday's Action at a Distance allows energy activation transfer to remote points of usage. The method of capture and use of this energy is optional, and therefore it is cost a function of Human Stupidity.

III. METHODOLOGY

The water flow from the water pump in the aquarium will help the blade to rotate. The rate of flow of the water is a crucial factor to maintain the rotation of the blade as a turbine. The head measurement, the rate of the water flow and the position of blade influence the speed of the rotation as the first step in determining the hydro power potential of a water source is to measure the flow rate [10]. Since this project focus on the small scale generator in the aquarium, the distance of the blade and the flow of water are easy to be measured because it located just in a small range. As the blade is rotating, the working principle for the blade obey the faraday's law principle which is when the blade is rotating, a moving conductor cut the lines of force or flux of a constant magnetic field and produced a induced voltage in it. Hence, the changing magnetic flux inside a loop made from a conductor material will also induce a voltage and current in the loop [6]. Then, the output voltage from the blade connected into the voltage amplifier circuit. The instrument amplifier circuit was used to amplify the output voltage which is this circuit is very suitable to used when dealing with very small voltage as stated, instrumentation amplifiers are important integrated circuits when dealing with low voltage situations [11]. Then, the resultant output voltage will be used to power up any small power consumption electrical load, for example Light Emitting Diode (LED).

A. *The Block Diagram*

The working principle of the system is that once the blade is rotating, the BLDC motor inside the housing of the blade will rotate and created flux lines which is there was permanent magnet around the rotor to create rotor flux and the energized stator windings create electromagnet poles. The BLDC motor is a synchronous motor with permanent magnets on the rotor which is the moving part and windings on the stator, the fix part. Then, the rotation of the motor able to produce output voltage and the amplifier circuit was used to compare the output voltage from the BLDC motor inside the blade. From the amplifier circuit, the output voltage was feed into the DC to DC 5 V voltage booster module which is the voltage from the amplifier was able to be boost up to 5 V. Then, the resultant voltage was used for the low power consumption electrical load, such as LED.

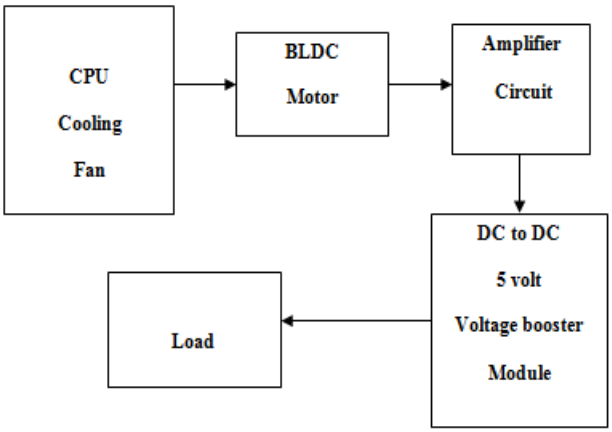

Fig 1: The block diagram

B. *CPU Cooling Fan*

The properties of the blade which act as the turbine and the generator is very important as the speed of rotation influence the output voltage for this system. The axial flow fan was used and there are many variations of axial flow fans, all of which have their own performance characteristics. There were three basic types of fans which are propeller fans, tube axial fans and vane axial fans [2]. However, for this project, the blade just focus on propeller fan which is an axial flow fan moves air or gas parallel to the axis of rotation, by comparison, a centrifugal or radial flow fan moves air perpendicular to the axis of rotation. Axial flow fans are better suited for low-resistance, high-flow applications, whereas centrifugal flow fans apply to high-pressure resistance, low-flow conditions [12].Water had been used instead air and gas and as the result, the rotation of

the blade was smooth and the speed of rotation had been measured. For this project, the propeller or blade for the generator was using the blade from CPU cooling fan as can be seen in Fig 2. From the Fig 2**,** the blade is very suitable to be used as the design already fulfill and custom-made by the manufacturer. The advantages of this type of cooling fan are high quality stable balance work, high speed and large air flow, low noise, high efficiency and have long life expectancy.

Fig 2: CPU cooling fan

C. Brush-Less Direct Current (BLDC)

DC motors have commutator and brushes as shown in Fig 3. While this function of commutator and brushes were implemented by the solid state switches, the maintenance free motor were realized this motor is known as Brushless DC motor(BLDCM) [13]. Fig 3 showed that there was permanent magnet around the rotor to create rotor flux and the energized stator windings create electromagnet poles. The BLDC motor is a synchronous motor with permanent magnets on the rotor which is the moving part and windings on the stator, the fix part. The rotor is attracted by the energized stator phase as in Fig 3. By using the appropriate sequence to supply the stator phases, a rotating field on the stator is created and maintained result in an action of the rotor chasing after the electromagnet poles on the stator is the fundamental action used in synchronous permanent magnet motors. The lead between the rotor and the rotating field must be controlled to produce torque and this synchronization implies knowledge of the rotor position [14].

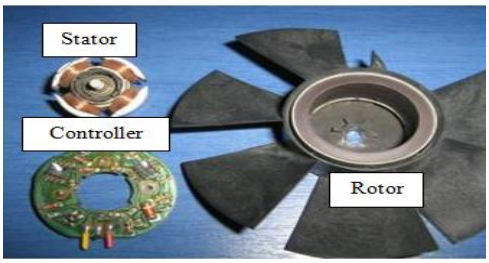

Fig 3: The cross-sectional inside the fan

D. Instrumentation Amplifier

Instrumentation amplifiers are important integrated circuits when dealing with low voltage situations which, an instrumentation amplifier is an integrated circuit (IC) that is used to amplify a signal [15]. This type of amplifier is in the differential amplifier family because it amplifies the difference between two inputs. The importance of an instrumentation amplifier is that it can reduce unwanted noise that is picked up by the circuit. The ability to reject noise or unwanted signals common to all IC pins is called the common-mode rejection ratio (CMRR). Instrumentation amplifiers are very useful due to their high CMRR[16]. Other characteristics, such as high open loop gain, low DC offset and low drift; make this IC very important in circuit design. The calculation for the suitable value of resistors had been done to get the suitable amount of output voltage to power up the voltage booster module. As shown in Fig 4, the schematic diagram for the system and all the calculation that required in this circuit. This instrumentation amplifier need to use seven resistors and the suitable resistor value must be determined by using the equation based on the circuit that had been chosen.

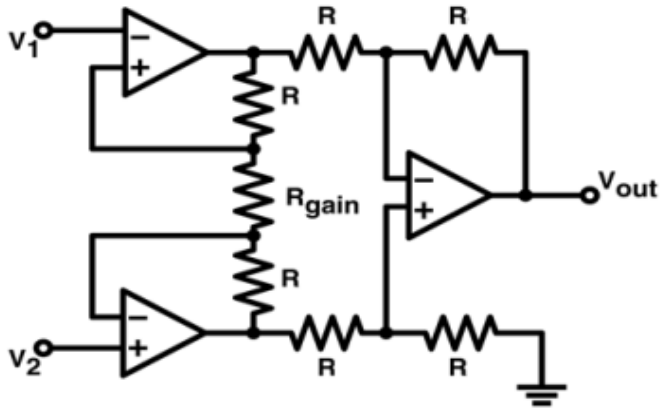

Fig 4: Schematic of Instrumentation amplifier

The design of instrumentation amplifier involves three Op-amps with two of them used in non-inverting amplifier configuration and the other in differential amplifier configuration[17]. Instrumentation amplifiers are unique in the fact that resistor values can be selected so that only one resistor will dictate the overall gain [10]. The KCL method had been used to get the equation of the op-amp. The calculation for the circuit as follows:

Let R5 = R6, R2 = R4 and R1 = R3, the equation became:
V out= (V1-V2)(R2/R1)(1+2R5/RG) (1)

As R2 = R4 = R1 = R3 = R5 = R6 = R, the equation became:
V out = (V1 -V2) (1+2R/RG) (2)
The minimum output voltage for the CPU cooling fan is 0.3mV, so:

Let V1 = 0 V,
Let V2 = 0.63 V
Let R = 98 kΩ,
Let RG = 50 kΩ,
From equation 2,
V out = (0 – 0.63) (1+2(98k)/50k)

V out = 2.46 V.

The calculation is just a reference to determine the suitable value of resistors to be used in designing the circuit. The voltage amplifier was used because it has the concept of gain which is the RG is the value for Gain Resistor needed for this system and 50 KΩ resistor had been used to help boost the voltage in the gain of 2, based on the Table 2.2. The instrument amplifier need to use separated power supply which is the 1.5 V battery used to ensure the LM 324N can be operated. The output from the fan is 0.63 V which will not able to operate the voltage booster module and it needed another system to be integrated with between the outputs from the propeller with the voltage booster module. The amplifier was used because it is able to compare the output voltage from the fan into the amplifier to get the resultant amplified output voltage.

E. DC-DC Voltage Booster Module

The DC-DC Voltage Booster Module was used as the input for the output of the amplifier. The input from any DC voltage of 1 V~5 V, output 5 V DC voltage is stable, high conversion efficiency, up to 96%,ultra-small size, and installed in a variety of small equipment. As the voltage booster module get the input, the resultant output can be used to power up the load, for example then LED because LED only consume low power of electricity as compared to the others within the 5 V output value.Table I show the characteristic of the module.

TABLE I: 5 V VOLTAGE BOOSTER MODULE PARAMETER

Parameter	Description
Input voltage	1 v to 5 v
Output voltage	5 v
Output current	500 mA
Dimension	17.55 mm x 25.22 mm x 5.85 mm

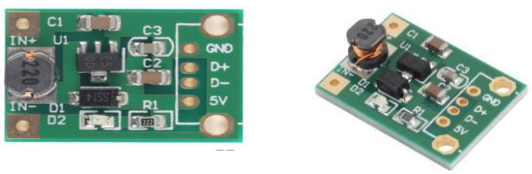

Fig 5: 5 V voltage booster module

IV. RESULT AND DISCUSSION

The output value for the system had been showed in Table II. The testing for the system had been done to monitor the performance of the system. The output current was able to be boost up until 5 V and the load as LEDs can be light up by using the system.

TABLE II: RESULT OF THE SYSTEM

Height (cm)	Speed (RPM)	Output Voltage (V)	Output current (mA)
2	0	0	0
4	0	0	0
6	36.8	0.02	0.01
8	101.0	0.16	0.35
10	121.1	0.18	0.42
12	237.8	0.21	0.52
14	254.1	0.24	0.60
16	257.6	0.27	0.65
18	260.8	0.29	0.72
20	267.7	0.31	0.83
22	267.6	0.35	0.89
24	269.6	0.37	1.67
26	275.4	0.38	2.56
28	279.7	0.40	4.72
30	280.1	0.41	5.48
32	287.6	0.46	6.40
34	299.6	0.51	6.54
36	306.4	0.57	6.92
38	320.1	0.61	7.20
40	327.4	0.63	7.80

From the Fig 6, the height of the water source influences the speed of the rotation. The graph clearly shows that when the height is 40 cm above the CPU cooling fan, the speed can reach up to 320 RPM. However, if the height is 2 cm and 4 cm above the propeller, the speed remains at 0 RPM because the blade was not able to move.

The conclusion that can be made is if the distance of the head is increasing, then the speeds of the rotation also increase. The graph linearly increases characteristic performance of the height of the water source against the speed of rotation.

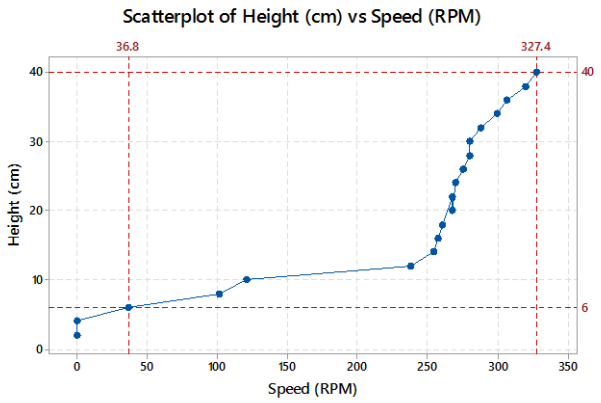

Fig 6: Graph of height of the water source (cm) against the speed of rotation (RPM).

From the Fig 7, the speed of the rotation influences the output voltage from the propeller. The graph clearly shows that when the speed is 327.4 RPM, the output value was 0.63 V. However, if the speed is 36.8 RPM, the output voltage only up to 0.02 V.

The conclusion that can be made is if the speed is increasing, then the output voltages also increase. The graph show the linearly increase characteristic performance of the speed of the rotation against the output voltage in the system.

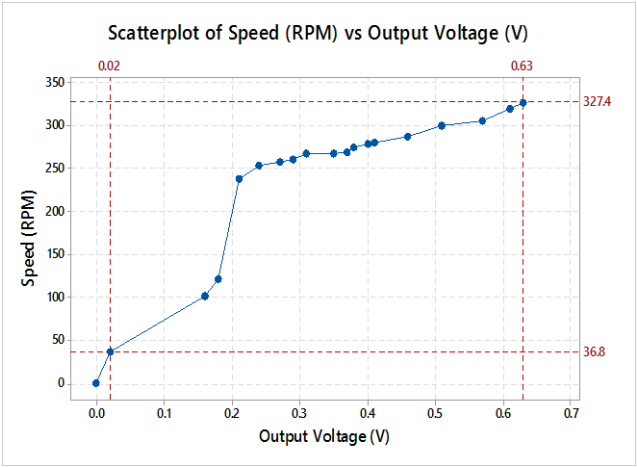

Fig7: Graph of speed of rotation (RPM) against Output voltage (V)

From the Fig 8, the speed of the rotation influences the output current from the propeller. The graph clearly showed that when the speed is 324.7 RPM, the output value is 7.80 mA. However, if the speed is 36.8 RPM, the output voltage only up to 0.01 mA.

The conclusion that can be made is if the speed is increasing, then the output voltages also increase. The graph show the linearly increase characteristic performance of the speed of the rotation against the output voltage in the system.

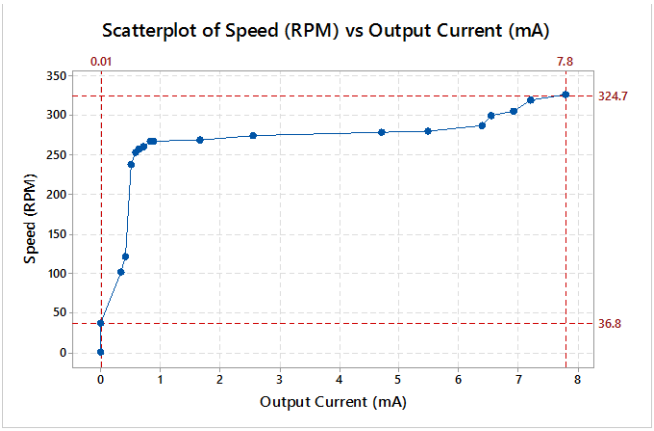

Fig 8: Graph of speed of rotation (RPM) against Output Current (mA)

V. Limitation and Recommendation

Every system has its own weaknesses and limitation. As for this system, the output value only can be boost up to 5 V and suitable to be apply for small bulbs and LEDs. So, the system can be boost up to high value voltage and current if there is a suitable and future development for the circuit to interface with the voltage booster module. So, this system can be implemented for more huge scale of application such as for the houses lighting system.

VI. Conclusion

In this project, by integrating the concept of voltage amplifier and current booster, the achievable output value able to power up the small consumption electrical load which is LEDs that widely used in the aquarium lighting system. Even though the output value from the system is small but it is still can be improve with the same concept and method.

References

[1]. Komgrich Prakobtham, K.W., *Innovation of Hydro Power Generator from Waste Energy to Green Marketing.* International Journal of Business and Social Science 2012. **Vol. 3** (No. 15; August 2012): p. 8.

[2]. ENGINEERING, F., *Fan Performance Characteristics of Axial Fans*, Engineering, Editor. 2000, Information and Recommendations for the Engineer FE-2300: Twin City Fan Companies, Ltd.

[3]. Ogochukwu, E.S., *Design and installation of a mini hydro electric power plant.* Scholarly Journal of Engineering Research Vol. 1(1), pp. 11-15,, April 2012.

[4]. M. Rossgatterera, B.J.u., M. Kapla, G. Della Vecchiab, *Medial design of blades for hydroelectric turbines and ship propellers.* March 15, 2012.

[5]. Marquez J.L, M.M.G., Pacas J.M, *Modelling and simulation of micro-hydro power plants for applications in distributed generation.* 2009: p. 13-64.

[6]. Himank Pratap Sigh, H.U., Utkarsh Srivastava,Om Prakash Yadav, *Free Energy Genarator.* International Advanced Research Journal

in Science, Engineering and Technology(IARJSET), 2015. **2**(1): p. 334.
[7]. Mayank Grover, B.L.K., Isaac Ramalla, *The Free Energy Generator.* Scientific and Research Publications, 2014. **4**(12): p. 4.
[8]. loxtronix, *An introduction to Motor and Generator*. 2010: p. 30.
[9]. Kelly, P.J., *A Practical Guide to Free Energy Devices.* 2002: p. 123.
[10]. Bauer, J., *Design of an Instrumentation Amplifier*. 2015.
[11]. Kunwor, A., *Technical Specifications of Micro Hydropower System Design and its Implementation Feasibility Analysis and Design of Lamaya Khola Micro Hydro Power Plant.* Förnamn Efternamn Bachelor's Degree Thesis Industrial Management, 2012(2012).
[12] Hudson, *The Basics of AXIAL FLOW FANS*. Auto-Variable, Combin-Aire, Exact-A-Pitch, Fin-Fan, Heatflo, Hy-Fin, Solo Aire, Split-Flo, Stac-Flo, Steamflo, Thermflo, Tuf-Edge, Tuf-Lite and Tuf-Lite II are registered trademarks of Hudson Products Corporation. 2000, Houston, Texas 77036-3321
[13] Halavadia Akash Natvarlal, P.M.J.M., *Speed Control of Brushless DC Motor: A Review*. AIJRSTEM 15-310; © 2015, AIJRSTEM All Rights Reserved, 2015: p. 25
[14] Ashwini M. Welekar, A.A.A., *Development of Brushless DC Motor Drive.* IOSR Journal of Electrical and Electronics Engineering (IOSR-JEEE), 2014: p. 18.
[15] Davis, B., *Should I Turn My Fish Aquarium Light Off at Night?* 2015.
[16] Kerszenbaum, G.K.a.I., *PRINCIPLES OF OPERATION OF SYNCHRONOUS MACHINES.* 2004: p. 31.
[17] Wordpress. *Instrumentation amplifier design and applications ECE Tutorials*. 2017 [cited 2017 5 May]; Available from: http://ecetutorials.com/analogelectronics/instrumentationamplifier/.

ISBN 978-967-0194-93-6

UTM
UNIVERSITI TEKNOLOGI MALAYSIA

Faculty of
Electrical Engineering